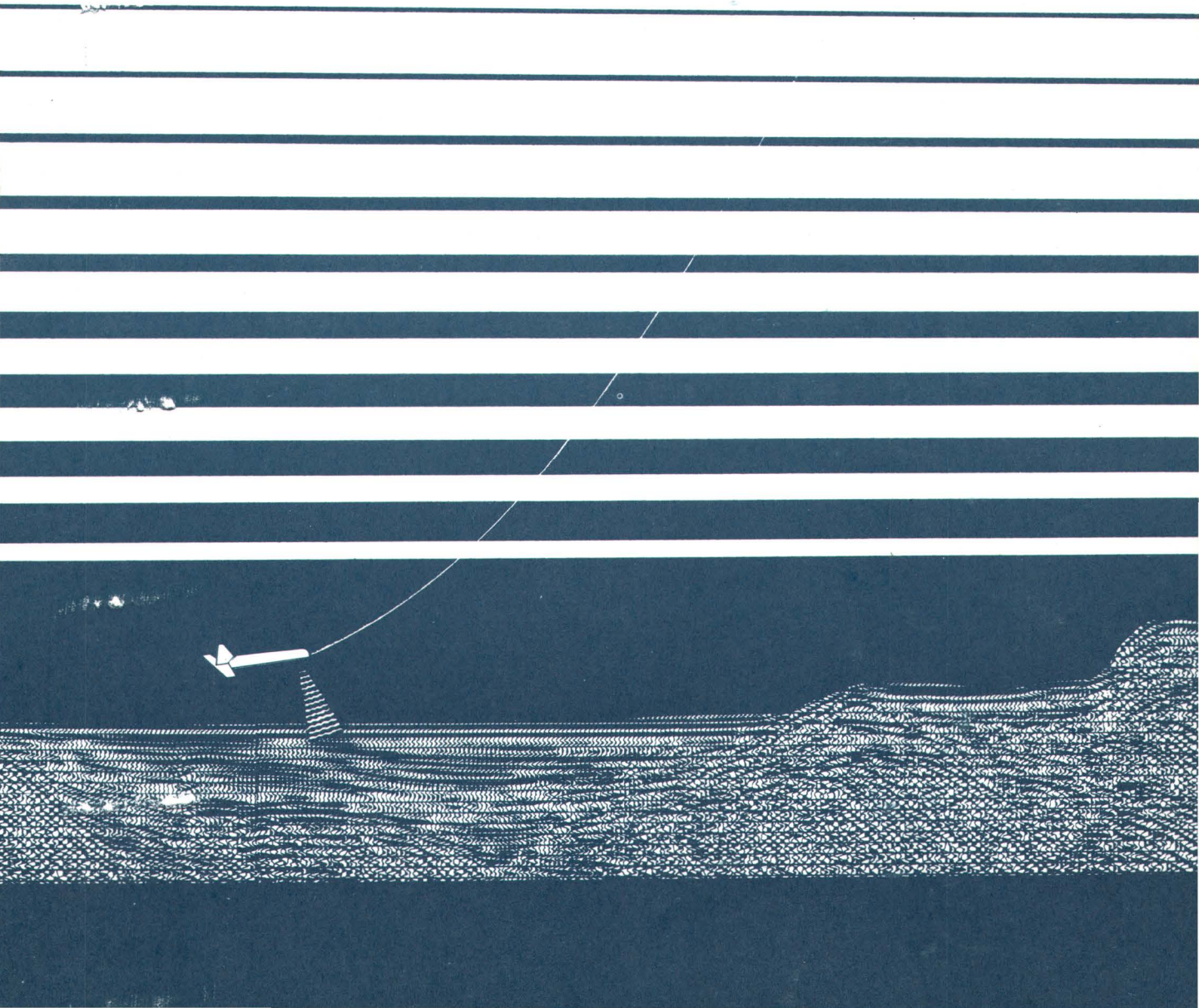


U. S. GEOLOGICAL SURVEY

Highlights in Marine Research



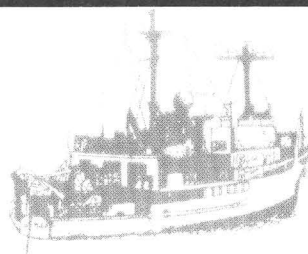
USGS CIRCULAR 938



U. S. GEOLOGICAL SURVEY

Highlights in Marine Research

Samuel H. Clarke, editor



USGS CIRCULAR 938

Department of the Interior
WILLIAM P. CLARK, *Secretary*



U.S. Geological Survey
Dallas L. Peck, *Director*

Library of Congress Cataloging in Publication Data

Highlights in marine research of the U.S. Geological Survey.

(U.S. Geological Survey Circular 938)

Supt. of Docs. no.: I 19.4/2:938

1. Submarine geology--Addresses, essays, lectures. 2. Geology--Pacific coast (United States and Canada)--Addresses, essays, lectures. 3. Geology--Atlantic coast (U.S.). 4. Geological Survey (U.S.). I. Clarke, Samuel Harvey. II. Series: United States. Geological Survey. Circular 938.

QE39.H54 1984

551.46'08

84-600204

*Free on application to Distribution Branch, Text Products Section,
U.S. Geological Survey, 604 South Pickett Street, Alexandria, VA 22304*

Contents

Foreword.....	IV
Dallas L. Peck, Director, U.S. Geological Survey	
Highlights in Marine Research of the U.S. Geological Survey.....	1
Samuel H. Clarke, editor	
Sixty Million Years of Growth Along the Oregon Continental Margin	9
Parke D. Snavely, Jr.	
New England Nearshore Geology Project: Glacial and Postglacial Geology of the Inner Continental Shelf... ..	19
Sally W. Needell and Robert N. Oldale	
Basins Beneath the Bering Sea Shelf	31
Michael S. Marlow	
Hydrocarbon- and Mineral-Resource Investigations in the Southwest Pacific	37
Florence L. Wong, H. Gary Greene, and the scientific staff of the 1982 CCOP/SOPAC cruise	
The Juan de Fuca Ridge Metallogensis Program	49
William R. Normark, Janet L. Morton, and Randolph A. Koski	
Submerged Sand Resources of Puerto Rico.....	57
Rafael W. Rodriguez	
The Submarine Landslide of 1980 off Northern California	65
Michael E. Field	
Undercurrents and Nearshore Erosion During Storms	73
Asbury H. Sallenger, Jr.	
Environmental Monitoring on Georges Bank: Trace-Metal Analysis of Bottom Sediment	81
Michael H. Bothner	
Significance of Long-Term Variations in Estuarine Benthos	91
Frederic H. Nichols	
Gray Whales, Tillers of the Sea Floor.....	99
C. Hans Nelson and Kirk R. Johnson	
The Georges Bank Border Dispute	109
John S. Schlee	
Principles and Applications of Marine Gravity Surveys.....	115
Jonathan R. Childs	
Program EEZ-SCAN: A Reconnaissance View of the Western U.S. Exclusive Economic Zone	125
James V. Gardner	
Abstracts of selected papers submitted for publication from January 1, 1980, to December 31, 1983.....	133



Foreword

By

Dallas L. Peck, Director, U.S. Geological Survey

The reports and abstracts in this volume illustrate the breadth and depth of U.S. Geological Survey (USGS) research in marine geology. The mission of the USGS's marine program is to provide information on the geology of the continental margins and adjacent ocean basins of the United States and, where it is of interest to the U.S. Government, remote, deep-sea, and foreign areas.

We conduct these studies on land as well as at sea, for the shoreline—normally considered to delineate the marine realm—is a boundary that changes over time and thus is of little geologic significance. Shorelines migrate depending on the amount of water in the oceans, which in turn varies as the polar icecaps advance and retreat, and on the volume of the ocean basins, which changes as ocean ridges warm and swell, or cool and subside. Moreover, continental margins are uplifted as migrating crustal plates converge and collide. A more fundamental geologic boundary between the continental and oceanic realms lies at water depths of 3,000-5,000 meters, near the base of the Continental Slope, where basement rocks of continental affinity are juxtaposed with rocks of oceanic composition.

The marine research program within the USGS is a youthful one, less than 25 years old. At first, during the 1950's, USGS marine scientists assisted other Federal agencies with their studies. Not until 1962 did the USGS marine research program have its inception. At that time, efforts were initiated cooperatively with the Woods Hole Oceanographic Institution (WHOI) to make a comprehensive geologic survey of the shallow structures and sediment of the U.S. Atlantic Continental Shelf. This work resulted in the creation of a USGS office at Woods Hole, Massachusetts, staffed jointly by USGS and WHOI geologists; this office subsequently became the Branch of Atlantic Marine Geology and has been independent of WHOI since 1970. In 1966, the Branch of Pacific Marine Geology was formed in Menlo Park, California, with studies focused largely on the mapping of the then newly discovered structural basins (subsequently shown to have hydrocarbon potential) beneath the Bering and Chukchi Seas, locating sedimentary heavy-metal deposits along the Pacific margin, and evaluating offshore hazards associated with the siting of nuclear powerplants and oil-drilling platforms in southern California. This branch took the lead role in the study of the massive 1969 Santa Barbara Channel blowout and oilspill, and in studies of the geologic framework of the southern California Continental Borderland. Eventually, in 1969, a third office was formed in Corpus Christi, Texas, with work focused on the characterization of geologic structures and nearshore geologic processes in the Gulf of Mexico region; this office was later incorporated into the Branch of Atlantic Marine Geology.

The oil crisis of the 1970's, and consequent efforts by the Federal Government to lease for petroleum exploration up to 10 million acres/year of offshore lands, required a major effort on the part of the USGS marine geology program to explore and map our continental margins. Our professional and support staff and research facilities grew correspondingly, and

many significant contributions resulted from this period of accelerated scientific effort. Previously unknown sedimentary basins having hydrocarbon potential were discovered off the Atlantic coast and off Alaska, and the geology and the geologic evolution of these offshore regions and of the U.S. Pacific margin were discussed in numerous reports and publications. Efforts were made to identify and characterize sedimentary, tectonic, and, in the Arctic, ice-related processes that could affect offshore structures, to study the dispersal and potential effects of pollutants in the marine environment, and to better understand the sedimentary and tectonic processes that contribute to the formation of sedimentary basins and to petroleum migration and entrapment. The data from these investigations were placed in the public domain and have been used extensively by colleagues in private industry, as well as by our scientists.

Reorganization within the Department of the Interior in 1982 and establishment of an Exclusive Economic Zone in 1983 brought major changes to our marine geology program. By extending the jurisdiction of the United States to 200 nautical miles offshore of the United States and its territories, the U.S. marine domain now encompasses 3.9 billion acres (four times the ocean area before the proclamation). Within this vast underwater domain lie resources of immense importance to the Nation: an estimated 35 percent of the economically recoverable oil and gas yet to be found in the United States; such strategic metals as cobalt, manganese, and nickel in sea-floor crusts and nodules; massive sulfide deposits actively forming today on ridge crests; and major concentrations of heavy minerals in nearshore sand bodies. Along with immense potential for increasing our domestic resource base, exploration of the seabed provides an exciting scientific frontier. The USGS has taken an aggressive role in establishing a national program that includes academia, industry, and several other Federal agencies, to assess the energy and mineral resources of this new territory.

A joint project with the Institute of Oceanographic Sciences of the United Kingdom, to acquire images off the west coast by using their GLORIA wide-swath side-scan-sonar system, has significantly improved our knowledge of submarine-canyon morphology and other structural and geomorphic elements. This information, coupled with information from the U.S. National Oceanic and Atmospheric Administration's Seabeam and Swath Survey Systems, will provide the bathymetric data needed to construct base maps of the sea floor for marine geologists. New programs focusing on the mineral resources of the U.S. Exclusive Economic Zone include studies to map and determine the origins of cobalt-enriched manganese crusts on the flanks of islands and seamounts in the Central Pacific, of polymetallic sulfides on the spreading-ridge crest seaward of Oregon, and of ferromanganese nodules and pavements off Florida. Other new programs include the production of a series of maps describing the geology and geohazards of the U.S. Atlantic and Pacific margins. Geophysical and sampling surveys are evaluating the petroleum potential of offshore regions of the south Pacific and the framework geology of parts of the Antarctic continental margin. We are confident that these programs, together with our mandate to explore the resource potential of the recently established U.S. Exclusive Economic Zone, will ensure that our research, through the next decade and beyond, will be as scientifically diverse, productive, and exciting as ever.



GLORIA launch, offshore California

Highlights in Marine Research of the U.S. Geological Survey

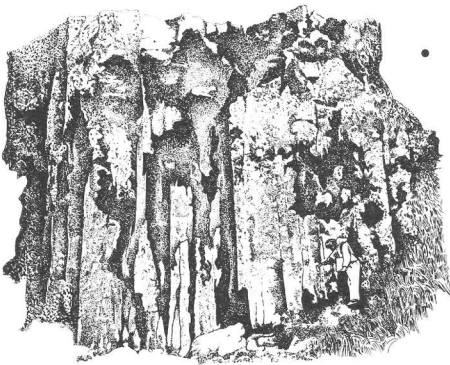
Samuel H. Clarke, editor

Recent years have seen enormous advances in our knowledge of the Earth's principal remaining geographic frontier—its ocean basins. Indeed, a prominent marine scientist and author recently stated that almost everything we know about the geology of the oceans has been discovered during the past 30 years. This revolution, still in its infancy, is largely the result of geophysical studies and deep-sea drilling programs that have documented evidence of sea-floor spreading, the creation of new crust at midoceanic spreading centers, and the migration, collision, and destruction of great plates of crustal material, and that have given rise to the unifying concept of global plate tectonics. An integral part of this revolution has been the development of sophisticated instruments and analytical techniques that, for the first time, have provided the capability to identify and, in many cases, to measure geologic processes that hitherto were understood only in the most general terms.

In addition to the scientific perspectives gained, the potential economic rewards of this work are staggering. For example, 35 percent of remaining economically recoverable hydrocarbon resources are thought to lie within our offshore domains; recent discoveries of sulfide deposits containing zinc, copper, and other heavy metals associated with midoceanic spreading centers (1978) and of cobalt-rich manganese crusts on some island flanks and seamounts of the Pacific Ocean (1982) have rekindled interest in sea-floor hard-mineral exploration and exploitation; manganese nodules containing nickel, copper, cobalt, iron, and other metals and placer deposits of heavy minerals form other potentially exploitable offshore resources; and offshore sand and gravel deposits, though less exotic, nonetheless provide materials vital for construction in some parts of the world. Apart from evaluating resource potential, this work includes new techniques for mapping our continental margins that promise to reshape the contours of existing bathymetric charts as well as to revitalize our concepts of geologic processes that operate on our continental shelves and slopes.

Marine research by the USGS has firmly established its position in the forefront of the advance on this last geographic frontier. Our major resource in this quest is a research and technical staff that has an exceptional breadth and depth of expertise and interest, imagination, and innovative research skills. This staff consists of approximately 100 professional scientists, assisted in their data collection, reduction, and analysis by a support group of technicians and junior geologists. A well-trained staff of electronic and mechanical engineers is responsible for design and maintenance of the wide spectrum of sophisticated equipment necessary for modern data acquisition and processing. The wide scope of scientific and technical endeavors carried on collectively by this group is reflected in the reports and abstracts contained in this volume.

- Petroleum and natural gas are generally found trapped within thick accumulations of sedimentary rock in ancient basins of continental regions, including the submerged margins of continents. Snavely's summary in this volume is based on long-term study of the Oregon continental margin, including onland mapping, offshore geophysical profiling, and deep-test-well data; it traces the geologic evolution of a region characterized by a history of episodic plate convergence and continental growth by accretion that has added an area equal to about 30 percent of the breadth of present-day Oregon. While this study is aimed at unraveling the complex history of the Pacific margin of western North America, it will also help target areas for offshore oil and gas exploration; further, it may aid in estimations of the size and recurrence interval of potential earthquakes in western Oregon and Washington.
- In New England, Needell and Oldale have used offshore geophysical and geological investigations in combination with onshore studies to contribute to knowledge of the geologic history, resource potential, and geologic hazards of parts of the New England inner shelf. Their summary here describes the Quaternary paleogeographic evolution of this region and summarizes recent project findings, which include correlation of late Quaternary glacial deposits and identification of major glacial events in southern New England, the history of local Holocene sea-level change, and evidence of rapid postglacial crustal uplift in the western Gulf of Maine.
- Long-term geophysical and sampling studies of the Bering Sea shelf, described by Marlow, indicate that this region, encompassing nearly 2 million square kilometers, is underlain by large sedimentary basins having hydrocarbon potential. Four of these basins are to be leased by the U.S. Government for oil and gas development. Lease sales for oil and gas development in Norton and St. George basins have been completed, although exploration has been delayed in court. The 1984 lease sale conducted for the Navarin Basin, discovered by USGS scientists in 1970, netted the Government more than \$630 million. Additional lease sales and further hydrocarbon studies extending into deeper water areas of the Bering Sea are planned, as are surveys of potential strategic and precious metals, such as gold, titanium, tin, chromium, and platinum, known to be concentrated by waves and currents as placer deposits in shallow parts of the inner Bering Sea shelf. Other work in this region is directed at mapping recently identified zones of gas hydrates present as icelike "clathrate" compounds in deep-sea sediment and at determining whether these zones could represent a future hydrocarbon resource.
- In 1982, the USGS research vessel *S. P. Lee* conducted geophysical surveys and sampling in waters off the Southwest Pacific Island nations of Tonga, Fiji, Vanuatu, the Solomon Islands, and Papua New Guinea under a tripartite agreement involving Australia, New Zealand, and the United States, in association with the United Nations-sponsored Committee for Co-ordination of Joint Prospecting for Mineral Resources in South Pacific Offshore Areas (CCOP/SOPAC). These studies of crustal dynamics, geologic



framework, and depositional history were to assess hydrocarbon and mineral-resource potential and geologic hazards to development in this region of small, newly independent nations in which even a small oil or gas discovery could have a substantial economic effect. Initial results of this cruise, reported by Wong, Greene, and others, suggest that a hydrocarbon potential may exist in parts of the Southwest Pacific; additional work in this region, coupled with studies of the geologic framework of the Ross Sea and offshore Wilkesland of the Antarctic continental margin, are to be conducted in 1984.

- The discovery along some oceanic spreading ridges of submarine volcanic hot springs associated with newly forming metallic sulfide deposits and a hitherto unknown benthic fauna is perhaps the most exciting event of the past decade in marine science. The study of these deposits, rich in copper, zinc, silver, and, to a lesser extent, gold, iron, cadmium, and germanium, is important because of the obvious mineral potential they hold and because it may enable us to better target for mineral exploration remnants of ancient spreading-ridge systems that have become incorporated into continental terranes by plate migration. The present efforts of USGS marine scientists, involved in these studies virtually since their inception, are focused along the Juan de Fuca Ridge, about 500 km off the Oregon coast; the geologic and geochemical results from sampling and photographic studies of the volcanic and hydrothermal deposits on the ridge crest are described here by Normark, Morton, and Koski. Further study to determine the extent and composition of these deposits and to reach a better understanding of how they formed is planned using the combined techniques of coring and photography from a surface vessel, in tandem with detailed mapping and sampling from a manned submersible vehicle. Still other study efforts are underway to map, determine the origin, and evaluate the resource potential of (1) 1- to 5-cm-thick encrustations rich in cobalt, manganese, iron, and nickel that occur at depths of 800 to 2,500 m on some submerged mountains (seamounts), oceanic plateaus, and submarine slopes of the central Pacific, and (2) ferromanganese nodules, golfball- to grapefruit-size black spheres rich in the same metals as the encrustations, that are abundant at depths of about 5,000 m in the central Pacific and of about 800 m on the Blake Plateau in the Atlantic Ocean off Florida.
- The USGS has an ongoing program to locate and evaluate sand and gravel—a less obvious, yet vital resource—on our continental shelves. For example, in Puerto Rico the construction industry is facing a crisis unless a major new supply of sand and gravel is located within the near future. The wholesale removal of sand from dunes and beaches in past years resulted in the deterioration of beaches on an island having a major tourist industry; moreover, it rendered beach and dune areas susceptible to erosion by storm waves, thereby causing damage to ocean-front structures. Rodriguez describes a joint effort by the USGS and the Department of Natural Resources of the Commonwealth of

Puerto Rico to map and evaluate offshore sand bodies whose exploitation would not have adverse environmental effects. This work, still in progress, has to date been successful in locating sand deposits estimated to be worth \$2.6 million and able to supply the needs of Puerto Rico's construction industry for 25 years.

- Concurrently with investigations directed at understanding the geologic framework and evolution of the U.S. continental margin and the distribution, composition, and mode of formation of offshore mineral deposits, the USGS conducts studies pertinent to the understanding of potential geohazards, such as earthquake faults and submarine sediment mass movement, seabed erosion and deposition, and ice gouging in Arctic regions, as well as studies of the effects of man's activities on the marine environment. For example, Field describes the investigation of a submarine landslide associated with a magnitude 7 earthquake occurring 40 km offshore northern California. In his study, previously surveyed seismic-reflection tracklines were resurveyed using side-scan sonar and seismic-reflection equipment a short time after the earthquake, and sea-floor changes attributable to the earthquake were mapped and described in detail. This zone of sea-floor failure covers an area of 20 to 40 km² and occurs on very low slopes (approx. 0.25°), a finding especially significant to planners in that it shows that moderate to steep slopes and thick accumulations of sediment are not requisite to such failures. Many potential sites of failure exist in seismically active areas elsewhere along the California coast, and much larger earthquakes centered closer to shore are likely in this region. It is also noteworthy that many of the features mapped are ephemeral owing to the action of waves and currents, and so may go unrecognized in conventional geohazard surveys.
- Sediment transport in the coastal zone may have a profound effect on manmade structures and vice versa; moreover, the failure to adequately plan for these effects can be disastrous. The cost of damage to coastal structures in California resulting from the winter storms of 1983 exceeded \$100 million, some of this the result of offshore transport of sand with consequent erosion of the shore-face by storm waves. Using a device Sallenger developed to obtain bottom profile and current information during storms, he was able to collect data showing that during storm conditions undercurrents, offshore-directed currents near the seabed that were previously considered unimportant, may make a major contribution to offshore sediment transport. From such knowledge his continuing work aims to predict amounts and rates of nearshore erosion during varying conditions of wind and surf, information important in coastal planning and development.
- Another major area of geoenvironmental research concerns assessment of the dispersal paths and effects of potentially toxic effluents on the marine environment. Probably no controversies have been more heated than those related to offshore-drilling activities, especially the effects of oil and drilling wastes on our fisheries. Exploratory drilling on the rich Georges Bank fishing

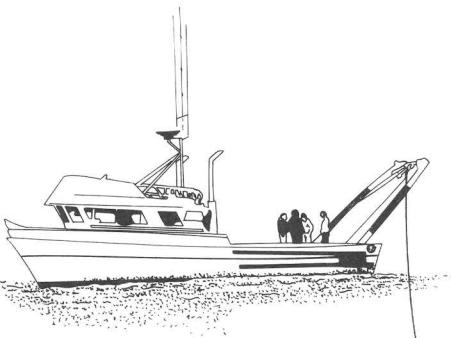


grounds was delayed in court until 1981, when a Biological Task Force was established with USGS participation to recommend studies to evaluate the effects of drilling and provide early warning of adverse effects on benthic communities, those most likely to be exposed to drilling wastes. Extensive and systematic programs, described by Bothner, for sampling sediment and benthic biota during the time period 1981-84 were established to study the composition and amount of drilling discharge and to learn where and in what concentrations these materials accumulate and what changes in benthic populations can be attributed to drilling activities. These programs will produce what is probably the most comprehensive set of environmental data ever obtained from a marine area potentially affected by offshore drilling during and after petroleum exploration. First-year results of this study have revealed no adverse effect on benthic communities due to exploratory drilling, even in areas adjacent to drilling rigs. Samples collected during subsequent years of study are being analyzed and will provide important baseline information with which to assess any future changes.

- Benthic animals, because they live in and feed from water and bottom sediment that may contain potentially toxic wastes, commonly are studied to assess human impact on the environment, notably impact on water quality. A fundamental assumption in the use of benthic populations as indicators of environmental change is that they are relatively stable in composition and number. This assumption is brought into question, however, by long-term USGS research on San Francisco Bay fauna, discussed here by Nichols, that shows populations to be profoundly affected, temporally and spatially, by a complex interplay of natural factors, such as the change of seasons, climatic perturbations, floods, and others that influence water temperature, salinity, turbidity, and nutrient levels, and the competition between species in their quest for a niche in the environment. Benthic populations may be much less stable than was previously thought, and naturally occurring short-term population variations must be taken into account in studies using these populations as indicators of long-term, human-induced changes in the environment if such studies are to be valid. This, in turn, requires studies of long duration and the acquisition of very long term data sets.
- As a byproduct of a geologic survey of the Chirikov Basin of the northeastern Bering Sea, Nelson and Johnson were able to study the feeding range and food resources utilized by the gray whale population on their Arctic summer feeding grounds, information vital to sound ecologic decisionmaking. In the process of ingesting amphipods, small burrowing crustaceans, gray whales leave distinctive sea-floor feeding pits that can be mapped on side-scan sonographs. From this investigation, the authors were able to estimate the extent and intensity of gray-whale feeding and, by extension, the total food resources utilized by these whales in this region, one of their principal feeding grounds. Clearly, an event such as an oil or toxic-waste spill or the mining of sand that disturbs the substrate could have a profound effect on this

gray-whale population.

- Apart from studies of geologic framework and natural resources, geologic processes, and geoenvironmental matters, our research staff provides geologic expertise to a wide variety of other agencies and research groups. For example, USGS scientists contributed to the formulation of the United States claim that Georges Bank, important for its fisheries and mineral potential, is properly a physiographic extension of the U.S. Continental Shelf and should therefore lie within U.S. territorial limits. Schlee here summarizes geologic and oceanographic information that will be important in resolving this boundary dispute with Canada in a case to be presented before the International Court of Justice at The Hague, Netherlands, in 1984.
- Gravity data routinely collected by USGS vessels during geophysical surveys are analyzed and used to prepare gravity-anomaly maps that are useful in interpreting geologic framework and structure. As described by Childs, many such maps have been completed on a regional scale for parts of the U.S. continental margin and, most recently, for parts of the Southwest Pacific Ocean. A high-precision gravity survey, the most extensive yet done in U.S. waters, is being carried out along parts of the continental shelf in cooperation with the U.S. Department of Defense (DOD). Very detailed maps compiled from these data will be of value to the DOD, but also are used by USGS scientists in efforts to locate and evaluate offshore resources.
- Use of advanced technology by USGS personnel to conduct marine geologic investigations is most recently illustrated by work with GLORIA (Geological Long-Ranged Inclined Asdic), described here by Gardner, to map the Pacific Exclusive Economic Zone (EEZ), an area that extends 200 miles seaward from U.S. shores and over which President Reagan has recently declared U.S. sovereign rights and jurisdiction. GLORIA is a sophisticated side-scan-sonar system developed in England that can survey swaths as much as 60 km wide in a single pass. This large swath width, coupled with GLORIA's fast survey speed, allows as much as 27,000 km² per day of reconnaissance-scale sonogram coverage to be obtained. During the summer of 1984 the entire western U.S. EEZ from Canada to Mexico will be surveyed; this program, conducted in cooperation with the Institute of Oceanographic Sciences (U.K.), represents the first use of GLORIA off our Pacific coast. Because this vast area is little known geologically, the GLORIA data will be valuable in determining the presence of as well as the potential for economic resources, including oil and gas, polymetallic sulfides, cobalt-rich crusts, manganese crusts, sand and gravel, and phosphates. Sonograms and interpretations will be compiled and published in atlas form available in 1986.

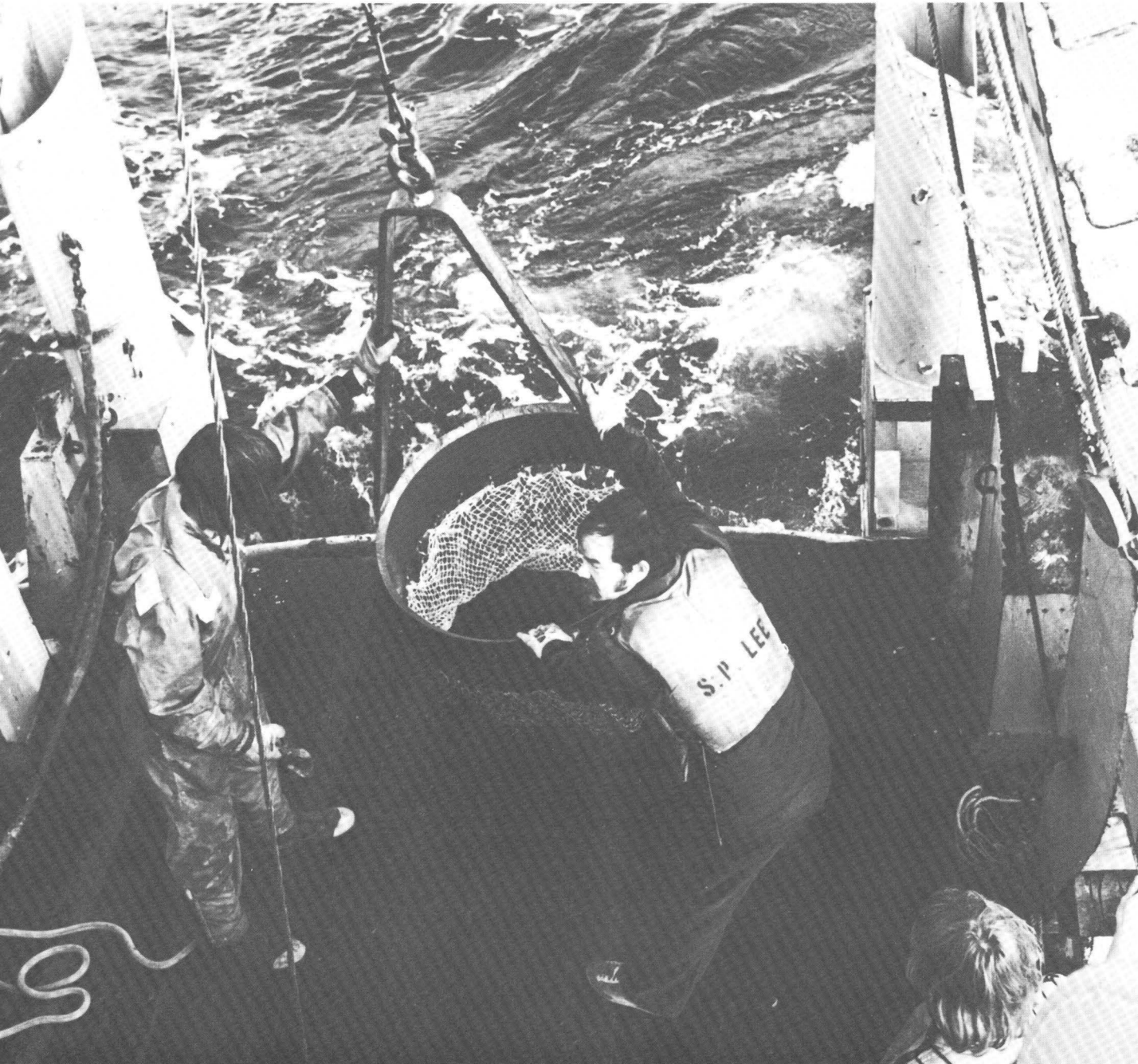


These summaries represent only part of a comprehensive program of research in marine geology, but they provide insight into the scope of the USGS scientific endeavors in this arena. Beyond them lie numerous activities, ranging from the traditional to the exotic and extending from our own shores to remote corners of the globe, that include:

- Compilation and production, for the first time, of a series of adjoining maps at a standard scale depicting the geology and geohazards of the U.S. Atlantic and Pacific continental margins.
- Development and use of the GEOPROBE instrument package to obtain long-term measurements on bottom currents and waves and of sediment erosion and transport in shallow to deep water.
- Study of deep-sea fan morphology and growth, and the relation of these to sea-level change and tectonic history.
- Compilation of a series of continental-margin transects—geologic cross sections depicting major geologic and structural features to a depth of tens of kilometers that extend from the interior of the North American Continent across continental margins into the deep ocean basins.
- Studies of geologic processes peculiar to the Arctic latitudes and their effects on human activities.
- Continuation of long-term studies of the geologic evolution and sea-floor conditions of offshore areas within the U.S. domain.

Throughout the broad ranges of USGS marine research, vitally important geologic information has been gained, and, in some areas of study, great economic rewards have been recognized. Moreover, the sense of excitement and collaboration among marine scientists during this era of discovery provides a solid foundation from which further advances will be made. We anticipate that these advances will hold substantial benefits for both the Nation and the scientific community.





Dredge recovery

Sixty Million Years of Growth Along the Oregon Continental Margin

By Parke D. Snavely, Jr.

Introduction

The sedimentary and volcanic rocks that crop out in the Oregon Coast Range, and those hidden below the sea floor on the adjacent continental shelf and slope, document a nearly complete record of the evolution of this segment of the Pacific Northwest during the past 60 million years (m.y.), practically all of Cenozoic time (table 1). Before 1970, our interpretation of this history was based on classic methods of geologic mapping and long-established geologic concepts. In those days, our mapping stopped when it reached the shoreline, for we had no way of studying rocks beneath the ocean. Knowing that an area essentially equal to the land area of the Coast Range lay seaward of the ephemeral boundary between land and sea, we were eager to learn about the geology in this submarine terrain. We continually found ourselves frustrated in attempts to resolve the geologic history of the region by being able to study the onland area only. In effect, it was like playing cards with only half a deck.

New clues regarding the history of the submerged continental shelf became available after marine geophysical-exploration programs that culminated in the offshore drilling of 10 deep test wells off Oregon and Washington by petroleum companies during the mid-1960's. Offshore seismic-reflection work (deep acoustic soundings that record the structure of rock layers beneath the sea floor) was initiated off Oregon in the early 1970's by the U.S. Geological Survey and geophysicists from Oregon State University. These data have provided us with much of the knowledge required to interpret the history of the Oregon continental margin, particularly in terms of plate-tectonic theory. We now know that the Oregon continental margin represents a zone of convergence, or a subduction zone, between two great plates, the North American continental plate to the east and an oceanic plate to the west which underlies the Pacific Ocean. This oceanic plate, which moves slowly eastward beneath the North American plate at a rate of a few inches per year, has created a broad area of deformation along the Pacific continental margin.

In the late 1970's, we began a program to construct a series of land-sea geologic cross sections and transects that would correlate the onland structure (faults and folds) and stratigraphy (sedimentary- and volcanic-rock units) with those present on the continental shelf and slope off Oregon and Washington. For this chapter, we have selected one of our land-sea geologic cross sections off Oregon (fig. 1) to illustrate the westward growth of the continent throughout the past 60 m.y., a growth equal to about 30 percent of present-day Oregon. This new terrane consists of a montage of various sedimentary- and igneous-rock sequences that were accreted to the Oregon continental margin during episodic interactions between the Pacific and North American plates.

Table 1. Major events and geologic evidence for Tertiary evolution of the Oregon continental margin

Era	Period	Epoch (ages in millions of years)	Major geologic events	Effects and evidence
Cenozoic	Tertiary	60 late Paleocene	1. Highly oblique subduction of the Pacific plate beneath the North American plate, with development of a rift zone along the Oregon and Washington continental margin.	Great volume of oceanic basalt extruded on sea floor along spreading ridge represents the oldest rocks in western Oregon and Washington. Submarine lavas contain interbeds of deep-water sediment.
		~54	2. Construction of Hawaiian-type island chain on oceanic crust; islands were situated adjacent to the continental margin. 3. Downwarping of rift basin.	Subaerial flows and shallow-water coral-bearing sand identify island areas. Interbeds of quartz-rich sand and gravel indicate nearby continental terrane during island eruptions. Widespread deposition of deep-water siltstone and sandstone.
		~52	4. More nearly head-on subduction of the Pacific plate.	Deformation of volcanic and sedimentary rocks by compressive folds and low-angle faults, followed by uplift and erosion to create a regional unconformity.
		~50 Eocene	5. Accretion of the Coast Range to the North American plate; rapid downwarping of marginal basin.	A thick sequence of mildly deformed rhythmically bedded sandstone beds derived from a continental landmass in the present-day Klamath Mountains unconformably overlies and buries volcanic islands and older deformed marine deposits. Widespread deep-water silt overlies this sandstone sequence.
		43	6. Major reorganization between the Pacific and North American plates; northward translation of the Pacific plate along fault A, a strike-slip fault with San Andreas-type movement. 7. Strike-slip movement along fault A between 43 and 37 m.y. ago and extension between the Pacific and North American plates.	Sandstone beds (about 52 m.y. old) west of fault A moved northward at least 200 km to come to rest against 60- to 54-m.y.-old oceanic basalt. Alkalic-basalt flows erupted from several vent areas along deep rift zones east of fault A.
		~37	8. Oblique subduction between the Pacific and North American plates along fault B; deformation of rocks above the downgoing Pacific plate.	Regional unconformity at base of 36-m.y.-old rocks in western Oregon and Washington and adjacent continental shelf. Formation of melange wedge exposed on west side of the Olympic Peninsula.
		36		
		Oligocene	9. Continuous, but episodic, downwarping of deep marginal basin off Oregon; extension between the Pacific and North American plates.	Thick beds of deep-water marine deposits separated by unconformities in deep marginal basin. Igneous events (which include nepheline syenite, camptonite, and gabbro) related to extension occurred 33 and 30 m.y. ago.

Cenozoic	Tertiary	24		
		Miocene		
		~ 12	10. Oblique subduction and episodic downwarping of continental shelf, and concomitant uplift of the Coast Range.	Thick sequence of marine sediment deposited along west flank of the Oregon Coast Range. Basalt flows erupted 16 to 14 m.y. ago are interbedded with sediment.
			11. More nearly head-on subduction between the Pacific and North American plates.	Major regional unconformity at base of 12-m.y.-old marine deposits. Formation of Hoh melange that crops out along west side of the Olympic Peninsula and is penetrated in test wells on the Oregon and Washington Continental Shelf.
		~ 5.0		
	Pliocene			
			12. Oblique subduction accompanied by rapid downwarping of shelf basins and uplift of the Coast Range and Olympic Mountains.	Widespread and thick deep-water marine deposits on the continental shelf; unit coarsened near basin margins along the Coast Range. Deep-water turbidite sand deposited in trench along present-day continental slope and abyssal plain.
	Pleistocene			
			13. Oblique subduction and episodic downwarping of inner- and outer-shelf basins and in trench beneath slope and abyssal plain.	Thick deposits in shelf basins contain several unconformities; sediment is deformed by diapiric structures.
			14. Uplifted and deformed abyssal sediment along the continental slope.	Abyssal sediment uplifted as much as 1,000 m by broad folds and thrust faults. Strata in slope basins formed landward of folds contain several unconformities supporting episodic uplift.
	Holocene			
			15. Episodic oblique subduction and continued deformation of sediment at base of slope and on the shelf.	Thrust faults at base of slope reach within 150 m of the sea floor, indicating movement less than 10,000(?) years old. Faults on shelf offset sea floor, and sediment is deformed by diapiric structure. Nonoccurrence of earthquakes during past 150 years suggests episodic movement along a megathrust at base of slope.

Geologic History

The rocks of the Oregon Coast Range began to form about 60 m.y. ago, when great volumes of basalt were extruded onto the sea floor along a spreading ridge that formed along a rift zone near the continental margin during a period of rapid, strongly oblique subduction of the Pacific plate (fig. 2). A chain of volcanic islands grew on this oceanic crust in much the same way that the Hawaiian Islands have formed. In places, flows and breccia that erupted from these islands were deposited on the adjacent sea floor, where they intertongued with coarse sand and gravel derived from nearby older continental terranes. In submarine basins adjacent to the islands, thin-bedded silt and sand intertongued laterally with volcanic debris derived from the islands. As shown on cross section (fig. 1), these oceanic basalt flows (unit Tev) extend westward onto the continental shelf, where they terminate against fault A.

About 50 m.y. ago, the Coast Range was accreted to the North American Continent. The oblique convergence of the Pacific plate after this period of accretion may have changed to a direction more nearly perpendicular to the coastline, and the older volcanic and sedimentary rocks of the present-day Coast Range were compressively deformed. These highly deformed sedimentary rocks and the volcanic islands were later buried by a 2,000-m-thick sequence of deep-water rhythmically bedded sandstone (unit Te, fig. 1) derived from an adjacent continental landmass that was situated in the present site of the Klamath Mountains (K, fig. 2).

A major reorganization occurred between the Pacific plate and the newly accreted Coast Range terrane about 43 m.y. ago. This change initiated a northward translation of the Pacific plate with respect to the Oregon continental margin along fault A (fig. 1). The sandstone deposits (unit Teu) west of fault A were carried northward at least 200 km from their original site of deposition in northern California and came to rest against the 54- to 60-m.y.-old Coast Range oceanic crust. The major movement on fault A probably occurred between 43 and 37 m.y. ago, as indicated by mildly deformed 36-m.y.-old siltstone strata (unit Toe) that overlap the fault. Between 43 and 12 m.y. ago, several periods of movement undoubtedly occurred on related deep rifts east of fault A along the west flank of the present-day Coast Range. These deep rift zones provided avenues along which magma rose from the mantle to erupt chemically complex volcanic and intrusive rocks during two major periods of activity. Subaerial alkalic-basalt flows, 37 to 42 m.y. old, were erupted from several vent areas near the coast, such as those shown in black (unit Toe) in the middle part of the cross section. Other igneous events related to this period of rifting included the 33-m.y.-old light-gray alkalic intrusive rocks (nepheline syenite) and the dark-gray alkalic rocks (camptonite); 30-m.y.-old widespread thick sills of iron-rich gabbro; and 14- to 16-m.y.-old basalt flows and intrusive rocks (unit Tm, fig. 1; table 1).

Along the Oregon continental margin, during the period 43-12 m.y. ago, regional subsidence and essentially continuous sedimentation occurred in a marginal basin whose axis is on the inner continental shelf (fig. 1). As much as 4,000 m of deep-water sand and silt, together with minor amounts of volcanic rock, accumulated in this basin. This deep-water sediment grades eastward into shallow-water coarse-grained marine strata deposited in small basins situated in structural embayments along the west flank of the present-day Coast Range. For

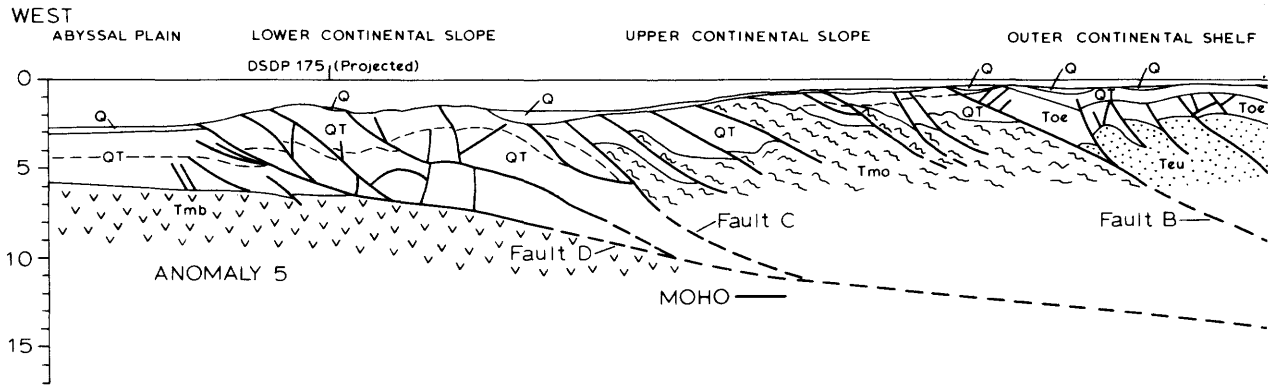
example, unit Tm in the cross section is a coarse-grained sandstone where exposed along the coast; but the contemporaneous unit penetrated in Standard-Union Nautilus well P-0103 is largely fine-grained sandstone and siltstone.

Periods of plate convergence apparently occurred during the time intervals between extension-related igneous events. A major episode of convergence took place about 37 m.y. ago when the Pacific plate plunged beneath the North American plate. This period of plate interaction is marked by a widespread unconformity in western Oregon and Washington and on the adjacent continental shelf. A thick wedge of highly deformed and disrupted sandstone, siltstone, and volcanic rocks along the coast of the Olympic Peninsula in Washington represents a "fossil" subduction zone. This material, "melange" in geologic parlance, was scraped off the downgoing Pacific plate as it moved under the North American plate. Fault B on the cross section (fig. 1) marks the 37-m.y.-old underthrust boundary between the Pacific and North American plates. Part of the sandstone (unit Teu) west of fault A was subducted at that time.

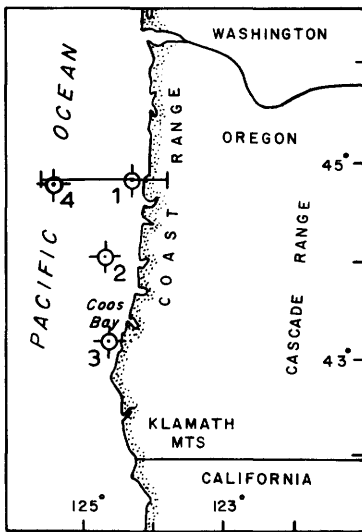
A major period of underthrusting, which occurred about 12 m.y. ago, is recorded by renewed movement on fault B. During this episode, the older strata (units Teu, Toe, fig. 1) west of fault B on the outer and inner parts of the continental shelf were subducted. A widespread unconformity, or time break, at the base of rocks 12 m.y. old on the Oregon and Washington Continental Shelf records regional uplift in response to this period of plate convergence. Strata older than 12 m.y. were folded and uplifted on the continental shelf; later, these strata were truncated by erosion before downwarping and deposition of sediment younger than 12 m.y. The anticlinal fold on the cross section that was tested by Standard-Union Nautilus well P-0103 (fig. 1) was formed during this period of plate convergence.

The structure of the Outer Continental Shelf and upper slope also reflects this 12-m.y.-old period of compressive deformation; this structure consists chiefly of a set of low-angle landward-dipping faults (thrusts) and related folds. The intensely deformed wedge of strata (unit Tmo, fig. 1) between faults B and C on the cross section is interpreted to be material deformed above the Pacific Plate as it underthrust the North American plate. Although there are no drill holes near the line of the cross section to support this interpretation, melange of this age has been penetrated in test wells drilled on the northern Oregon and southern Washington Continental Shelf. Also, melange of the same age as unit Tmo is exposed along the west side of the Olympic Peninsula, where it is called the Hoh Assemblage. The melange (unit Tmo) was deeply buried as it was carried beneath the North American plate and later was uplifted along a series of east-dipping thrust faults between faults B and C (fig. 1). Studies of an inferred correlative melange unit along the Olympic Coast support deep burial for these rocks because organic hydrocarbons in the silt have been "sweated out" to produce the so-called "smell muds" and small gas seeps found in many places along the coast. Microfossils are rare in the melange units because in most places the calcium carbonate in their shells has been dissolved by hot solutions moving through these deeply buried rocks. These solutions also deposited carbonate and zeolite minerals in fractures formed in the rocks when they broke under stress.

The present boundary between the Pacific plate (referred to as the Juan de Fuca plate) and the North American plate is a deformational front at the base of



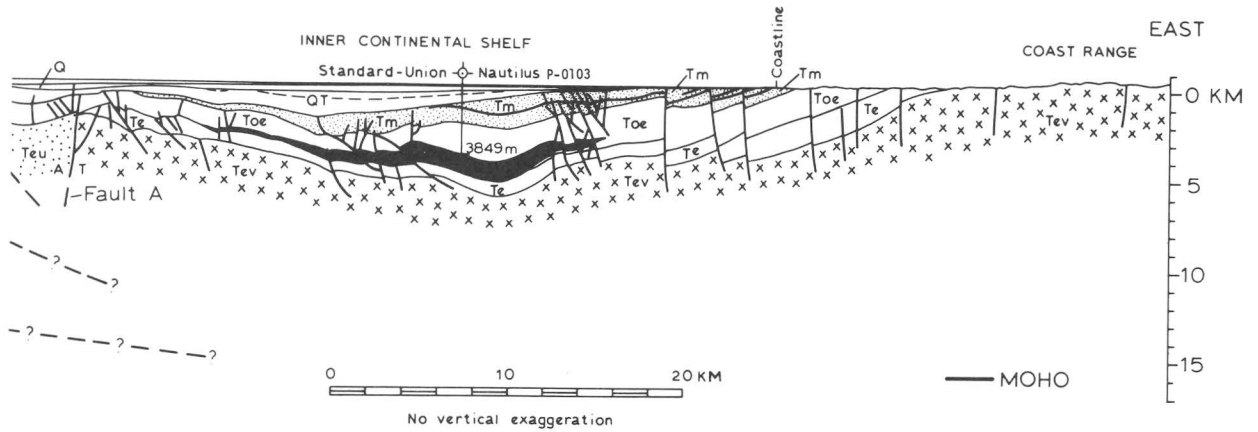
INDEX MAP
(shows line of section)



CORRELATION OF GEOLOGIC UNITS

LOWER SLOPE AND ABYSSAL PLAIN	UPPER SLOPE AND OUTER SHELF	INNER SHELF	ONSHORE	EPOCH
Q	Q	Q	Not shown	Holocene
QT	QT	QT	Not shown	Pleistocene
Tmb				Pliocene
				late
	Tmo			middle
		Tm	Tm	early
				Miocene
				early
	Toe	Toe	Toe	Oligocene
				late
		Te	Te	middle
				early
		Tev	Tev	early
	Teu			late
				Paleocene

Figure 1. Generalized cross section of the central Oregon continental margin, prepared by P. D. Snavely, Jr., H. C. Wagner, and D. L. Lander in 1980. Index map shows locations of cross section and exploratory test wells: (1) Standard-Union Nautilus P-0103, (2) Union Oil Co. Fulmar P-0130, (3) Pan American Oil Co. P-0112, and (4) Deep Sea Drilling Project (DSDP) Site 175.



DESCRIPTION OF GEOLOGIC UNITS

- Q
Silt and sand (Holocene and upper Pleistocene)--marine, semiconsolidated
- QT--
Sandstone and siltstone (Pleistocene, Pliocene, and upper Miocene)--marine, fine-grained; dashed line marks Pleistocene-Pliocene boundary
- ∇Tmb∇
Tholeiitic(?) basalt (upper Miocene)
- Tm
Sandstone and siltstone (middle to lower Miocene)--marine; contains interbedded middle Miocene basalt flows and breccia (black units)
- Tmo
Inferred melange and broken formation (middle Miocene to upper Oligocene marine)
- Toe
Siltstone and mudstone (Oligocene and upper Eocene)--marine; contains minor sandstone and conglomerate and interbedded basalt pillow lava, breccia, and lapilli tuff (black units)
- Te
Turbidite sandstone and siltstone (middle and upper Eocene)--marine
- Teu
Inferred arkosic wacke (Eocene)--marine
- xTevx
Pillow basalt and breccia (middle to lower Eocene)--marine; contains minor siltstone and basaltic sandstone, in part subaerial onshore

the continental slope of Oregon and Washington. This convergent margin is characterized by a broadly folded and thrust-faulted thick sequence of uplifted abyssal (deep water) sediment from less than 1 to about 10 m.y. old. These uplifted and tectonically accreted strata are in the upper plate of a low-angle (less than 5° dip) megathrust (fault D, fig. 1) formed by the subduction of young (about 10 m.y. old) oceanic crust (unit Tmb, fig. 1). Compressive deformation of sediment on the continental slope has created a series of elongate anticlinal ridges. Small basins that lie behind these fold ridges contain a few hundred meters of young bedded sediment which shows several periods of tilting due to episodic uplift of the anticlinal structures; this uplift reflects the periodic nature of underthrusting by the Juan de Fuca plate. Figure 3 shows a typical seismic profile at the base of the slope off the Oregon coast.

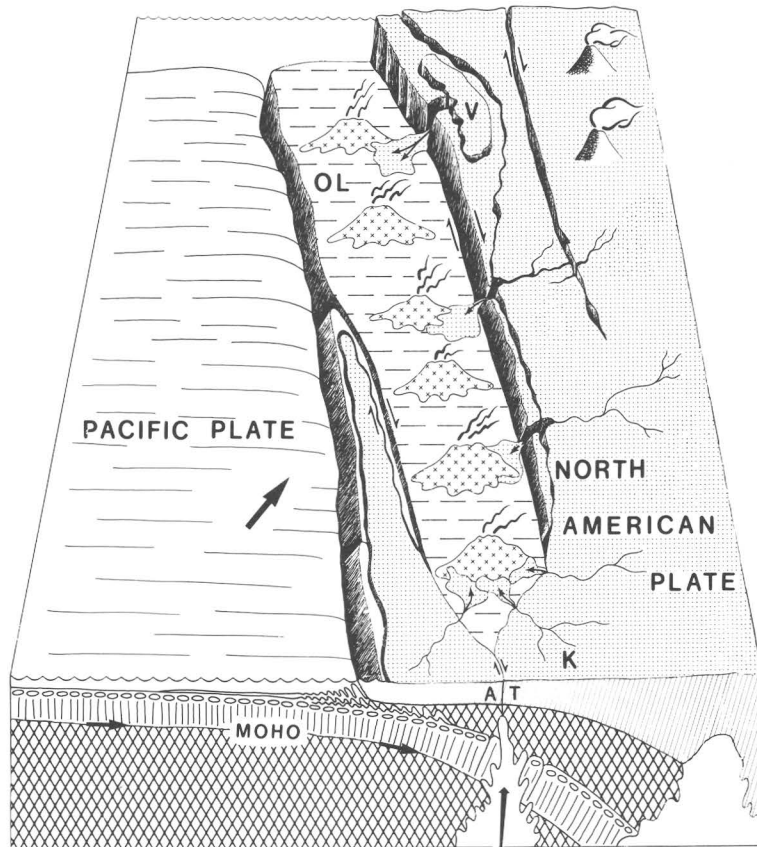


Figure 2. Assumed interarc-rifting model for origin of 50- to 60-m.y.-old oceanic basalt and islands in western Oregon and Washington. Oblique subduction of the Pacific plate creates a deep zone of right-lateral rifting along which basaltic magma rises to the surface and forms a spreading ridge. K, Klamath Mountains; OL, Olympic Mountains; V, Vancouver Island, British Columbia. Moho defines base of oceanic crust of the Pacific plate; slant line pattern denotes continental crust of North American plate. Arrow denotes direction of movement of the Pacific plate relative to the North American plate. Movement on fault in cross section is toward (T) or away from (A) observer.

Summary

Our onshore and offshore studies demonstrate a westward growth of Oregon during the past 60 m.y. by the accretion of terranes along the interface between the Pacific and North American plates. This geologic history adds to our repertoire of scientific knowledge—knowledge that will aid in unraveling the complex history of other regions extending from southern California to southeastern Alaska. Understanding the geologic events during the past 60 m.y. also will assist geologists in their search for new accumulations of oil and gas and in evaluating potential geologic hazards due to earthquakes and landslides.

For example, the studies across the continental slope and abyssal plain indicate that sediment, possibly as young as 10,000 years, has been dramatically uplifted by broad compressive folds and thrust faults above the downgoing oceanic plate. Because recorded earthquake activity (seismicity) along this zone of subduction is very low, we might conclude that the convergence between the giant Pacific (Juan de Fuca) and North American plates is episodic, but inactive at the present time. Our thrust model, therefore, may have significant implications for postulating the size (magnitude) of potential earthquakes in western Oregon and Washington, because strain release along convergent margins elsewhere has generated large earthquakes. Additional geophysical and geologic studies along the base of the slope may help to establish the recurrence interval for major movements along the megathrust and thus increase our ability to predict potential earthquake hazards in western Oregon and Washington.

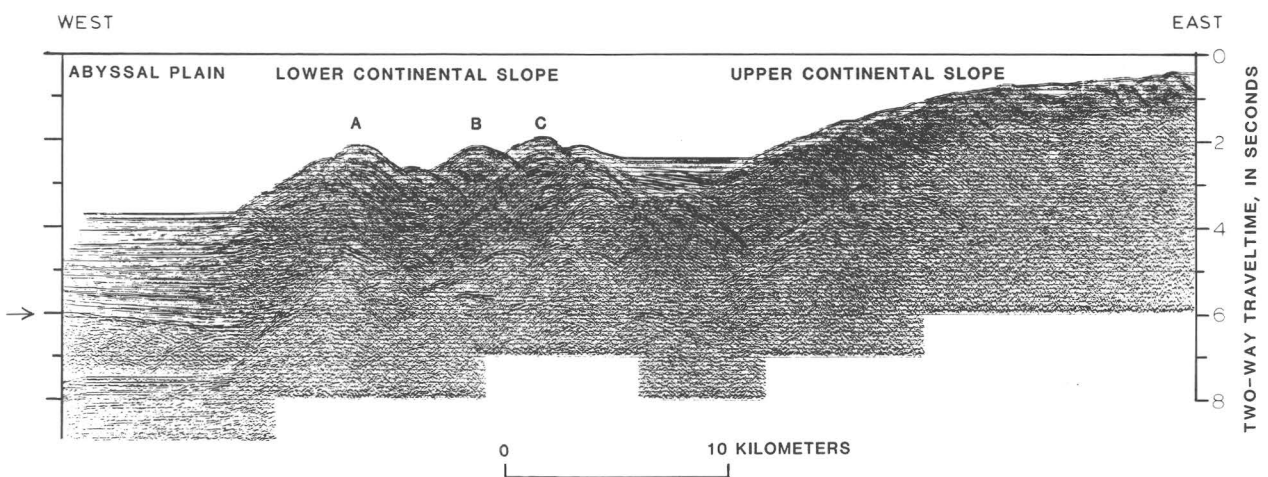
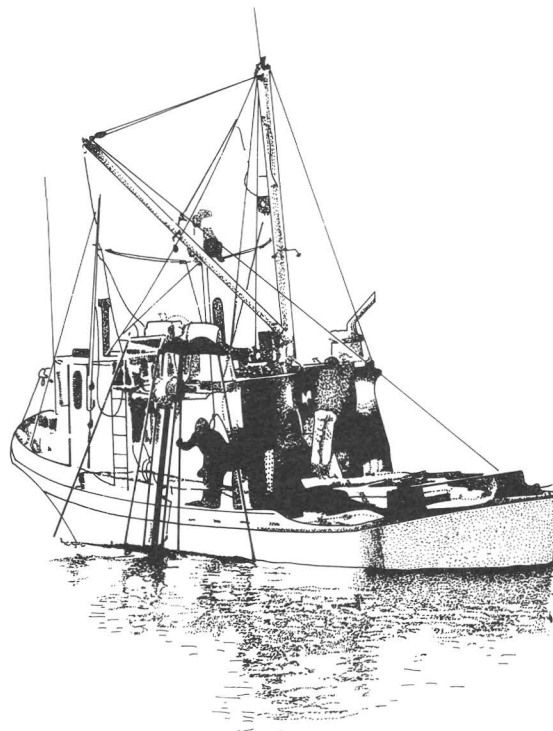


Figure 3. Deformational front at base of the continental slope off central Oregon, as shown on 24-channel seismic-reflection profile obtained by U.S. Geological Survey research vessel *S. P. Lee*. Arrow on left side of profile denotes top of 10-m.y.-old oceanic crust of downgoing Pacific plate. See figure 1 for interpretation. Broad folds A, B, and C are formed by abyssal sediment that has been uplifted about 1,000 m.

We can also apply the underthrust-structural model, with its attendant formation of thick wedges of melange, to the search for oil and gas. New studies of the onshore melange wedges indicate that these rocks, where deeply buried, have reached temperatures high enough to distill off hydrocarbons. The 12,000 barrels of high-quality oil produced from a well drilled along the central Washington coast probably originated from such a melange. Therefore, in the search for oil and gas, new targets might be found in areas where thick melange wedges underlie younger strata that contain structures that could trap the oil and that may hold reservoir sand in which petroleum could accumulate. Melange wedges also may exist far inland, where they have been transported eastward on the subducting oceanic plate, to a position below the 50- to 60-m.y.-old oceanic crust and younger sedimentary rocks of the upper plate. Thus, we might drill through the old oceanic crust in the upper plate and reach the underlying petroliferous melange. Also, oil generated from melange in the lower plate may migrate upward and accumulate in structures formed in rocks of the upper plate.

Thus, our scientific investigations have resulted in models that can be applied to resource exploration and environmental assessment that contribute to the needs of the Nation.



New England Nearshore Geology Project: Glacial and Postglacial Geology of the Inner Continental Shelf

By Sally Needell and Robert Oldale

Introduction

The New England Nearshore Geology Project involves geologic study of the inner continental shelf off New England through offshore investigations (fig. 1) and onland studies related to offshore problems. These studies help to define the sea-floor and subbottom geology and are used to understand the geologic history, resource potential, and geologic hazards of the inner shelf.

The project has produced maps of the sea-floor geology, the thickness and distribution of principal geologic and economic units, and the depth to major erosion surfaces beneath the bottom for coastal New England from New Hampshire to Connecticut (Oldale and O'Hara, 1975; Robb and Oldale, 1977; O'Hara and Oldale, 1980; Needell and others, 1983a; Needell and Lewis, 1984). Special maps have also been produced—for example, geologic-hazard maps and maps showing the locations and thicknesses of potential sand-and-gravel resources. In addition, scientific findings of the project have made major contributions to our understanding of the geologic history of coastal New England and its geologic processes.

Two primary methods are used to study the inner continental shelf—high-resolution seismic-reflection profiling and vibracoring. Seismic-reflection profiling provides continuous images of the subbottom geology; vibracores as much as 12 meters long, which sample the deposits below the bottom, are used to identify the units seen in the seismic profiles and to collect shell and wood that can be radiocarbon dated for establishing chronology.

Acknowledgments

We thank the Massachusetts Department of Public Works, the Connecticut Geological and Natural History Survey' and the University of New Hampshire Geology Department for their cooperation and support.

Geologic Framework

The geology of the New England inner shelf is unique to the east coast of the United States because this region was glaciated during the great ice age (the Pleistocene epoch of the Quaternary period, which began approximately 2 million years ago). Northern North America was covered by glacial ice at least four times during the Pleistocene, and the nearshore geology shows evidence that the ice advanced as far seaward as Long Island, N.Y., Block Island, R.I., Martha's Vineyard, Mass., and Nantucket Island, Mass., during the latest ice advance (between about 25,000 and 13,000 years ago) and during a previous ice advance.

Each advance of the ice was accompanied by a worldwide lowering of sea level and migration of shorelines out onto the continental shelves. The oceans were the source of water for the growth of the ice. As sea level fell, it exposed the nearshore areas to erosion by streams flowing offshore. As the glaciers waned, the sea rose, and bottom sediment was reworked by the wave action of the seas.

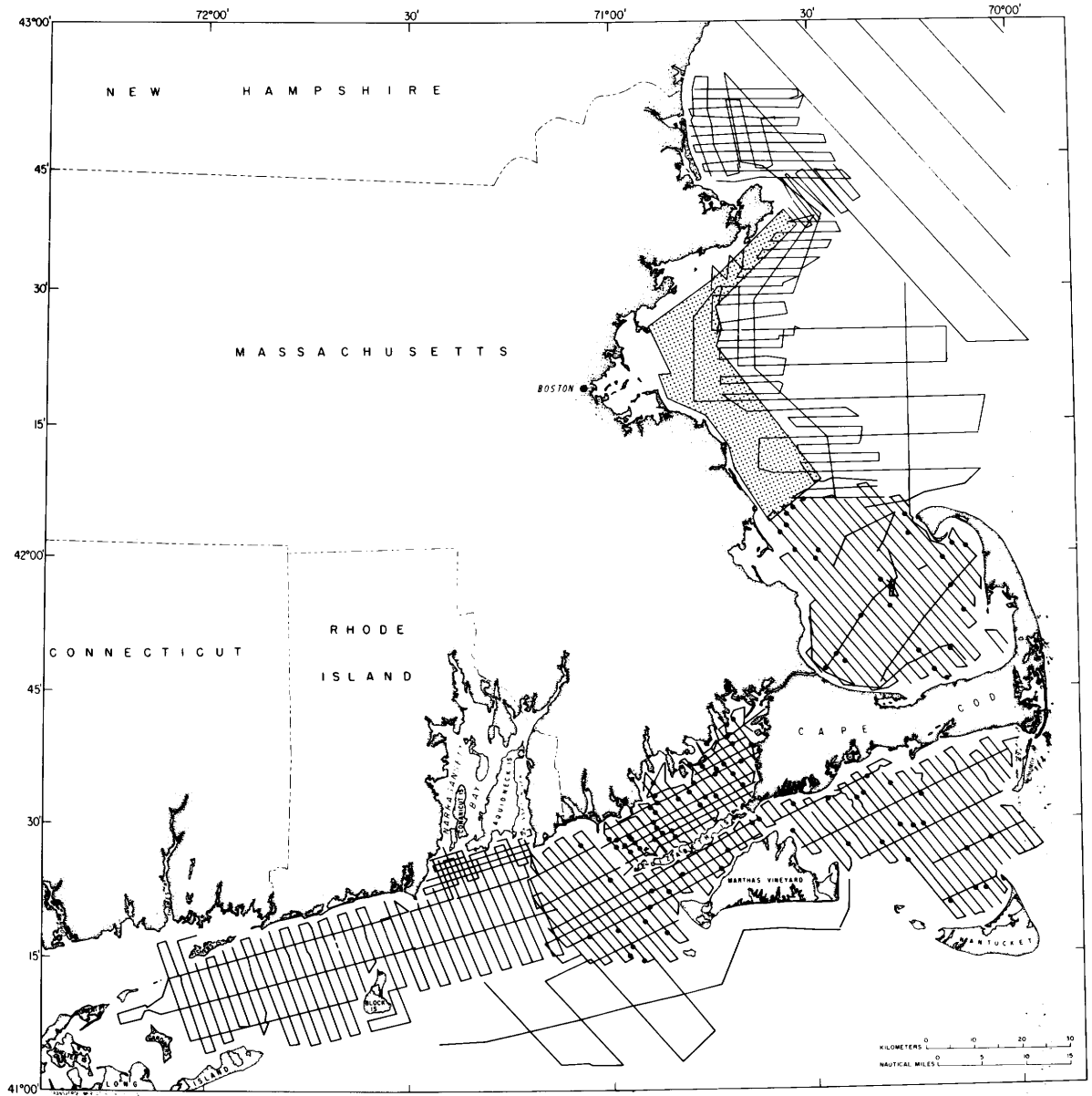


Figure 1. New England region, showing locations of high-resolution seismic tracklines and vibracores (dots). Shaded area east of Boston represents location of seismic survey of the Raytheon Co. for the Massachusetts Department of Natural Resources.

Geologic History

Before glaciation, the landscape was stream dissected, and the present-day major river valleys were in place. The landscape consisted of uplands underlain by igneous and metamorphic rocks of Paleozoic age and lowlands underlain by sedimentary rocks of late Paleozoic or early Mesozoic age. The bedrock surface was overlain by a thick layer of weathered rock or regolith. Near the present-day shore and in the Gulf of Maine, these older rocks were overlain by erosional remnants of coastal-plain rocks of late Mesozoic and Tertiary age. Along the south shore of New England, the north limit of these coastal-plain rocks formed a cuesta with a north-facing escarpment, an eroded cliff. Streams flowed southward across the older bedrock and northward down the escarpment, as tributaries to the main-stream flow along the foot of the escarpment. During Pleistocene time, the regolith was stripped off the bedrock, and the landscape was modified by glacial erosion and deposition. Glacial sediment was deposited in the form of moraine, outwash, lake, and marine deposits. Stratified deposits and till (unsorted rock debris) formed ridges called end moraines. Melt-water streams deposited sand and gravel as valley fill or broad outwash plains sloping away from the ice. Silt and clay were deposited in quiet lake or marine environments. The end moraines on Long Island, Block Island, Martha's Vineyard, and Nantucket Island mark the maximum seaward extent of the ice advance. As the ice retreated from the inner shelf (approx. 18,000 years ago), a readvance of the ice formed an inner line of moraines from Long Island to Fishers Island, N.Y., southern Rhode Island, the Elizabeth Islands south of Buzzards Bay, and Cape Cod, Mass. (fig. 2).

South of Cape Cod, freshwater lakes formed as the ice retreated from its terminal position (Bertoni and others, 1977; Needell and others, 1983b; Needell and Lewis, 1984). Melt water, prevented from draining seaward by end moraines and uplands of coastal-plain strata, formed lakes in the deep valleys and later coalesced to form larger lakes. Eventually these lakes drained, possibly as a result of crustal subsidence and downcutting at the outlets. After drainage of the lakes, glacial and preglacial deposits were eroded by streams that flowed southwestward and southeastward and drained to the sea through Block Channel, between Block Island and Long Island. North of Cape Cod, a large glacial lake formed as the ice retreated from Cape Cod Bay (Oldale, 1976; Oldale, 1982b). From Boston northward, because the crust was depressed below the glacial sea level by ice loading, the sea advanced over the land as the ice retreated. Along this part of New England, glacial-marine deposits are found well inland. Rebound of the crust shortly after ice retreat caused a rapid recession of the shore to a point well below present-day sea level (Oldale and others, 1983). After this lowstand in the Gulf of Maine, the continuing postglacial worldwide rise in sea level submerged the coast to its present point. During submergence, the postglacial valleys were partly filled by stream, freshwater-peat, estuarine, and saltmarsh-peat deposits. Transgressing seas eroded and smoothed the sea floor, and marine sediment accumulated over a wave-cut surface.

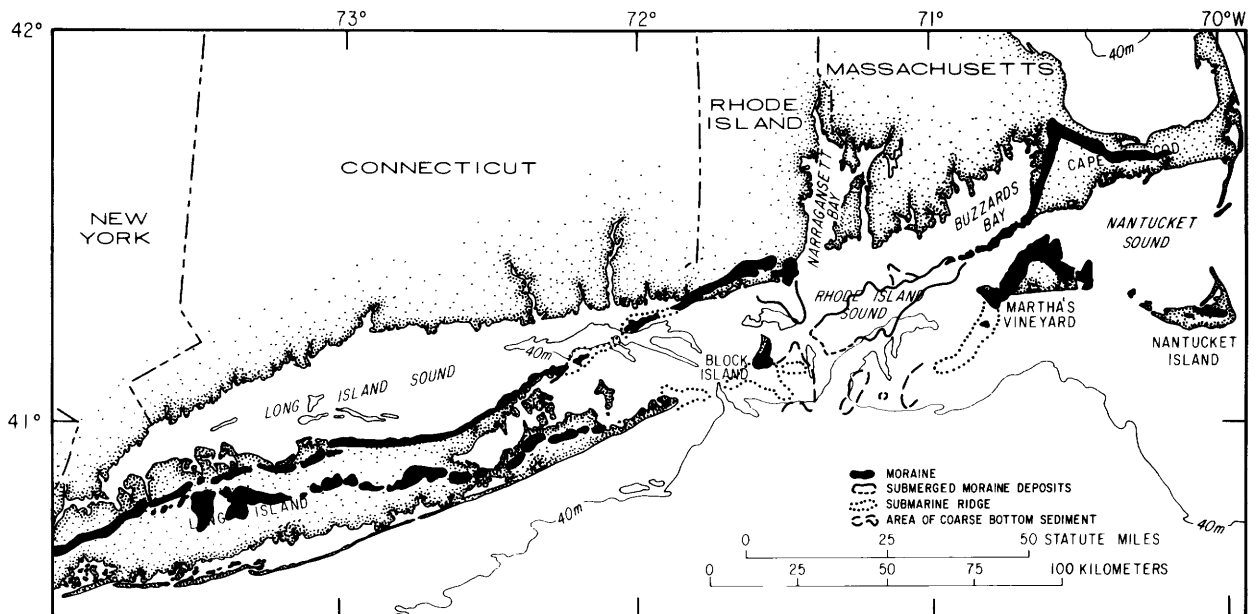


Figure 2. Southern New England region showing coastal end moraines from Long Island, N.Y., to Nantucket Island, Mass., and their offshore extensions.

Scientific Findings

Major accomplishments of the New England Nearshore Geology Project include establishment of a modern geologic column for the glacial and recent deposits of southern New England, identification of major glacial events in the region, a proposed origin for the coastal end moraines, establishment of a local sea-level curve for southern New England for the past 12,000 years, and recognition of rapid postglacial crustal rise in the western Gulf of Maine.

Pleistocene Geology

Detailed studies of important exposures and onland geologic mapping are used to more fully understand the geology of the region. Oldale (1982b) has correlated the late Wisconsinan glacial units (table 1) for Cape Cod and the offshore islands of southeastern Massachusetts. The relative age of the glacial deposits indicates a northward retreat of the last ice, interrupted by readvances to build end moraines, and, in southern New England, the progressive west-to-eastward retreat of separate lobes of glacial ice. Correlations among the Pleistocene de-

Table 1. Correlation chart of the upper Wisconsin glacial deposits of the cape and islands region (from Oldale, 1982b).

Narraganset Bay-Buzzards Bay lobe deposits. Western Cape Cod and Martha's Vineyard		Cape Cod Bay lobe deposits. Inner Cape Cod, Nantucket, and Martha's Vineyard		South Channel lobe deposits Nantucket and outer Cape Cod	
Drift beneath Buzzards Bay	Drift north and west of Buzzards Bay	Drift west shore of Cape Cod Bay		Cape Cod Bay lake deposits	
					Eastham plain deposits
					Truro plain deposits
					Highland plain deposits (?)
				Wellfleet plain deposits	
		Formation of the Billingsgate shoal moraine		Drift beneath Nantucket Sound	
		Barnstable lake deposits			
		Drift beneath Vineyard Sound	Harwich plain deposits		Nauset Heights ice-contact deposits
			Dennis ice-contact deposits		
			Formation of the Sandwich moraine Buzzards Bay outwash deposits		
Buzzards Bay ground moraine deposits					
Formation of the Buzzards Bay moraine	Mashpee and Barnstable plain deposits				
Mashpee plain deposits	Nantucket Sound ice-contact deposits (?)		Nantucket Sound ice-contact deposits(?)		
Nantucket Sound ice-contact deposits(?)					
Martha's Vineyard outwash plain deposits	Martha's Vineyard outwash plain deposits*	Younger Nantucket plain deposits	Quidnet ice-contact deposits(?)		
	Quidnet ice-contact deposits(?)				
	Siasconset outwash deposits	Siasconset outwash deposits (?)			
Formation of the Martha's Vineyard moraine, including the Gay Head moraine, and Squibnocket moraine ~ after Kaye (1964 b)	Formation of the Nantucket moraine and the Martha's Vineyard moraine*				
	Older Nantucket plain deposits	Older Nantucket plain deposits(?)			
	The Woods drift				
	Upper delta sand (?) ~	Upper delta sand (?) ~			

(?) Source uncertain.

* Age relative to the Nantucket drift units unknown.

~ May be early Wisconsin in age.

posits of the Cape and Islands region, southernmost Rhode Island and Connecticut, and Long Island, N.Y., have been revised (table 2) on the basis of recent work in all areas (Oldale, 1982b). Key elements of this revision include the identification of glacial deposits older than the last ice advance on Nantucket Island and Martha's Vineyard, correlation of glacial deposits of the last ice from Long Island to southeastern Massachusetts, and establishing that the two belts of coastal end moraines were formed during the last glaciation.

Pre-Wisconsinan Till and Marine Deposits

Two major glacial events are recognized in the glacial deposits on Nantucket Island, Mass. (Oldale and Eskenasy, 1983). The Sankaty Sand of Nantucket, a marine deposit which represents a highstand of sea level (Oldale, 1982a; Oldale and others, 1982), is underlain and overlain by glacial deposits (fig. 3). The lower part of the Sankaty Sand represents a marine transgression and contains fossils that indicate a marine climate slightly warmer than the present climate on Nantucket. This warm period probably represents the previous interglacial stage, the Sangamonian. The fossils within the upper part of the Sankaty Sand point to a slightly cooler nonglacial marine climate that most likely prevailed later in the Sangamonian. Till beneath the Sankaty Sand is correlated with the lower till of New England; its presence supports the view that the two different tills common in New England represent two glaciations.

Table 2. Tentative correlation of Pleistocene deposits from Nantucket, Martha's Vineyard, and Cape Cod to Long Island, New York (from Oldale, 1982b).

TIME UNITS	LONG ISLAND	RHODE ISLAND and CONNECTICUT	CAPE COD, MARTHA'S VINEYARD, and NANTUCKET
late Wisconsinan	Roslyn till and outwash	New Shoreham drift	All drift on Cape Cod All drift atop the "Montauk till" All drift atop upper Sankaty Sand
middle Wisconsinan	Thrusted oyster reefs, peat deposits, and clay north of the Harbor Hill moraine, Western Long Island	Silts atop Montauk drift	
early Wisconsinan	Manhasset Formation including its Montauk Till Member	Montauk drift	"Montauk till"
earliest Wisconsinan or latest Sangamonian	Tabaccolot fauna on Gardiners Island		Fauna of upper part of Sankaty Sand
Sangamonian	Westhampton Beach fauna Bridgehampton fauna		Fauna of lower part of Sankaty Sand
Illinoian or older			Nebraskan drift Aftonian deposits and Kansan drift. Drift below lower part of Sankaty Sand

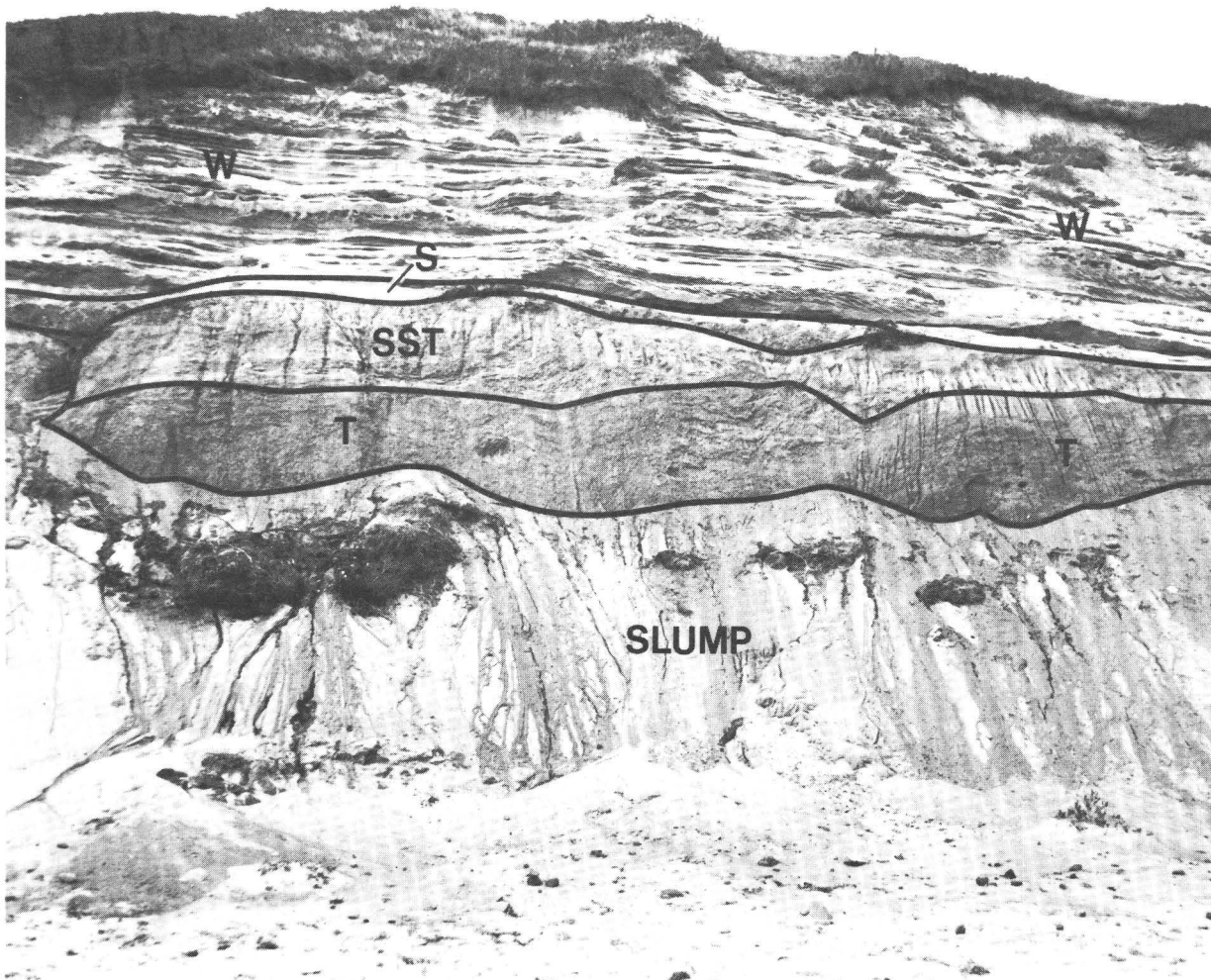


Figure 3. Pre-Wisconsinan till at Sankaty Head, Nantucket Island. S, upper part of Sankaty Sand; SST, layered pre-Wisconsin till; T, pre-Wisconsin till; W, late Wisconsin stratified drift. (Lower part of Sankaty Sand not shown.)

Coastal End Moraines

The coastal end moraines on Cape Cod, Martha's Vineyard, Nantucket Island, and Block Island formed near the end of the last glaciation. These end moraines consist of folded, faulted, and thrust glacial and preglacial deposits and are considered to be the products of vigorously advancing ice fronts (fig. 4A) (Oldale and O'Hare, 1984) rather than of stillstands of the ice margin, that is, ice-front advance balanced by melting (fig. 4B). As the ice margin advanced, detached sheets of glacial and preglacial deposits were displaced forward and upward and beyond the ice margin to form the moraines. Beneath Block Island Sound, for example, vigorously advancing ice, obstructed by preglacial uplands, was diverted into deep valleys and formed end moraines as it thrust glacial and preglacial deposits up and out of the valleys (S. W. Needell and R. S. Lewis, unpub. data, 1983). On Cape Cod and the islands, extensive outwash-plain sediment deposited over and beyond the end moraines by melt-water streams draining stagnant ice is evidence that overall recession of the late Wisconsinan ice was alternately characterized by stagnation and vigorous ice-front advance.

Sea-Level Rise

Radiocarbon dates on shells and freshwater peat sampled from vibracores collected offshore of southeastern Massachusetts provide points for a curve (fig. 5) representing sea-level rise for the past 12,000 years along the south coast of New England (Oldale and O'Hara, 1980). This curve shows that relative sea level was about 70 m below its present level 12,000 years ago and rose at a rate of 1.7 m per 100 years until 10,000 years ago. Between 10,000 and 6,000 years ago, the rate of sea level rise dropped gradually to about 0.3 m per 100 years and remained at that rate until about 2,000 years ago. From then until now, the rate of sea-level rise has been only about 0.1 m per 100 years.

Rapid Crustal Rise, Western Gulf of Maine

North of Boston, Mass., postglacial sea-level history differs from that of southern New England. At 13,000 years ago, the glaciated crust was depressed, and relative sea level stood at its highest point, 32 m above present sea level. Subsequent rebound of the crust as the load of the glacier was removed caused a rapid drop in relative sea level. Based on the identification of a submerged delta of the Merrimack River situated offshore between Cape Ann, Mass., and the New Hampshire state line, Oldale and others (1983) suggested that the postglacial lowstand of sea level reached 47 m below present sea level at 10,500 years ago. A curve (fig. 5) based on the high and low relative sea-level stands and younger radiocarbon ages related to sea-level rise represent the sea-level and crustal-rise history in the western Gulf of Maine. This curve indicates an early postglacial crustal rise of at least 5 m per century for the first 2,000 to 3,000 years following retreat of the ice.

Evidence of Paleo-Indian occupation of the coastal zone in this region has led to speculation as to the impact of crustal rise on the Paleo-Indian environment. On gently sloping (4 m/km) land surfaces, the rate of shoreline regression would have been about 12 m/yr in northeastern Massachusetts and New Hampshire. During such rapid shoreline regression, it is unlikely that barrier beaches, salt marshes, and tidal flats could have developed; indeed, such features are not

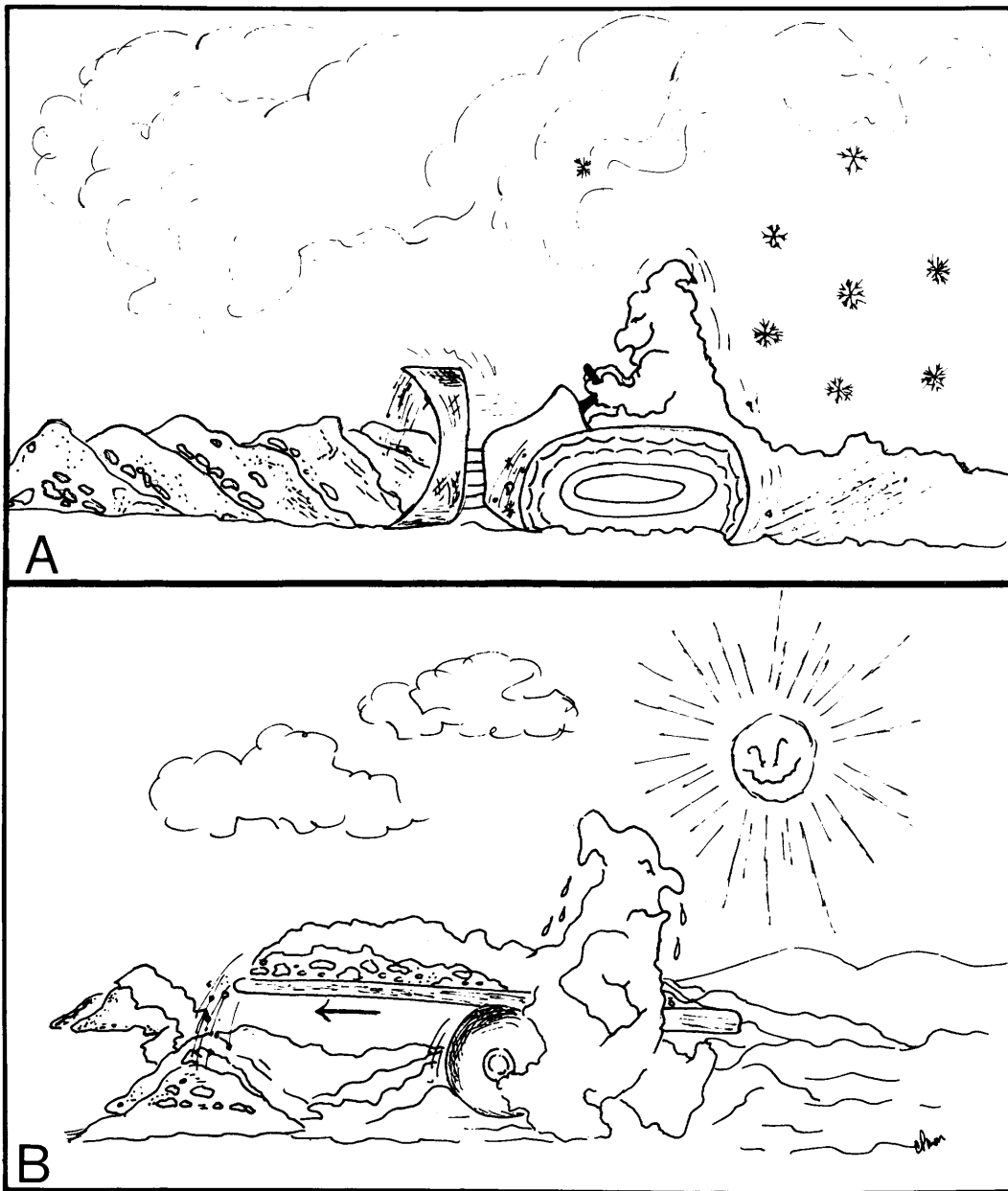


Figure 4. Cartoon representing the formation of coastal end moraines. (A) Thrusting of older glacial deposits by advancing ice front. (B) Ice-front advance balanced by melting to form dump moraine.

presently found in the region above sea level but only below the maximum late glacial shoreline. Without lagoons, salt marshes, or tidal flats, shellfish activity was probably very low. Finfish and marine mammals may have been scarce owing to a deficient food chain. Thus, it is likely that Paleo-Indians living adjacent to the Gulf of Maine relied on nonmarine rather than marine sources of food, and Paleo-Indian sites may be confined to the region landward of the maximum late glacial shoreline or, at least, restricted within the region seaward of that shore.

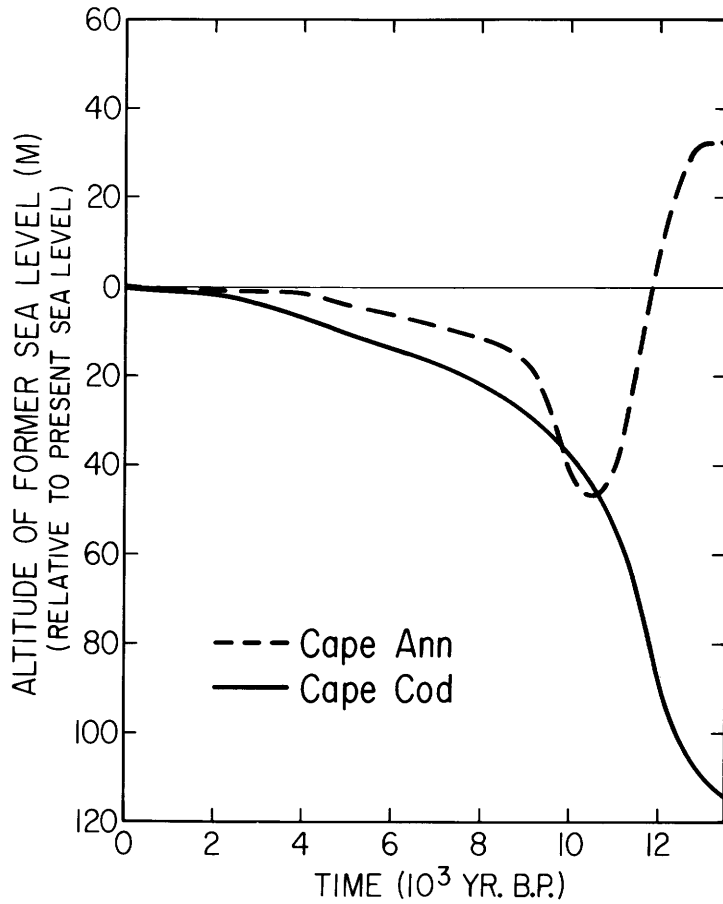


Figure 5. Proposed sea-level curve for southeastern Massachusetts, from radiocarbon-dated shell and peat (solid line) and proposed sea-level curve for period 13,000-5,000 years ago in the western Gulf of Maine (dashed line).

Summary

At present, the New England Nearshore Geology Project involves investigations of coastal New Hampshire, Massachusetts, Rhode Island, and Connecticut. From these investigations, numerous scientific reports and detailed maps of the surface and subsurface geology have been published that provide an understanding of the glacial and postglacial history of the New England inner continental shelf and that identify resource deposits and geologic hazards. Future studies are expected to include nearshore areas of Maine and the coastal States south of Connecticut.

References

- Bertoni, Remo, Dowling, J. J., and Frankel, Larry, 1977, Freshwater-lake sediments beneath Block Island Sound: *Geology*, v. 5, no. 10, p. 631–635.
- Needell, S. W., and Lewis, R. S., 1984, Geology and shallow structure of Block Island Sound, Rhode Island and New York: U.S. Geological Survey Miscellaneous Field Studies Map MF-1621, scale 1:125,000 [in press].
- Needell, S. W., O'Hara, C. J., and Knebel, H. J., 1983a, Geology and shallow structure of Rhode Island Sound, Rhode Island: U.S. Geological Survey Miscellaneous Field Studies Map MF-1537, scale 1:125,000.
- 1983b, Quaternary geology of the Rhode Island inner shelf: *Marine Geology*, v. 53, p. 41–53.
- O'Hara, C. J., and Oldale, R. N., 1980, Maps showing geology and shallow structure of eastern Rhode Island Sound and Vineyard Sound, Massachusetts: U.S. Geological Survey Miscellaneous Field Studies Map MF-1186, 5 sheets, scale 1:125,000.
- Oldale, R. N., 1976, Generalized geologic map of Cape Cod: U.S. Geological Survey Open-File Report 76-765, 23 p., scale 1:125,000.
- 1982a, Photographs of the upper Pleistocene section at Sankaty Head Cliff, Nantucket Island, Massachusetts: U.S. Geological Survey Miscellaneous Field Studies Map MF-1397, 2 sheets.
- 1982b, Pleistocene stratigraphy of Nantucket, Martha's Vineyard, the Elizabeth Islands, and Cape Cod, Massachusetts, *in* Larson, G. J., and Stone, B. D., eds., Late Wisconsinan glaciation of New England: Dubuque, Iowa, Kendall/Hunt, p. 1–34.
- Oldale, R. N., and Eskenasy, D. M., 1983, Regional significance of pre-Wisconsinan till from Nantucket Island, Massachusetts: *Quaternary Research*, v. 19, no. 3, p. 302–311.
- Oldale, R. N., and O'Hara, C. J., 1975, Preliminary report on the geology and sand and gravel resources of Cape Cod Bay, Massachusetts: U.S. Geological Survey Open-File Report 75-112, 2 p.
- 1980, New radiocarbon dates from the inner continental shelf off southeastern Massachusetts and a local sea-level-rise curve for the past 12,000 yr: *Geology*, v. 8, p. 102–106.
- 1984, Glaciotectonic origin of the Massachusetts coastal end moraines and a fluctuating late Wisconsinan ice margin: *Geological Society of America Bulletin*, v. 95, p. 61–74.
- Oldale, R. N., Valentine, P. C., Cronin, T. M., Spiker, E. C., Blackwelder, D. T., Wehmiller, J. F., and Szabo, B. J., 1982, Stratigraphy, structure, absolute age, and paleontology of the upper Pleistocene deposits at Sankaty Head, Nantucket Island, Massachusetts: *Geology*, v. 10, no. 5, p. 246–252.
- Oldale, R. N., Wommack, L. E., and Whitney, A. B., 1983, Evidence for a postglacial low relative sea-level stand in the drowned delta of the Merrimack River, western Gulf of Maine: *Quaternary Research*, v. 19, no. 3, p. 325–336.
- Robb, J. M., and Oldale, R. N., 1977, Preliminary geologic maps, Buzzards Bay, Massachusetts: U.S. Geological Survey Miscellaneous Field Studies Map MF-889, 2 sheets.



Navigation at sea

Basins Beneath the Bering Sea Shelf

By Michael S. Marlow

Introduction

The Bering Sea Shelf out to a depth of 200 m encompasses an area of 1.9 million km², more than twice the area of California, Oregon, and Washington combined (840,000 km², fig. 1). The shelf technically extends around the perimeter of the Bering Sea and includes waters off Soviet Siberia. In this chapter, however, I restrict discussion to the largest shelf area, which extends some 600 km westward from the coast of Alaska. The shelf zone, which I here call Beringia for brevity, is underlain by five large basins filled with sedimentary rocks that are described in table 1 and mapped in figure 2. Except for the Anadyr Basin, these basins are to be leased as part of the U.S. Government's program of offshore oil and gas development.

The Beringian shelf is one of the last unexplored frontier areas on the Outer Continental Shelf (OCS). Favorable economics and advances in the technology for recovery of offshore hydrocarbon deposits has made such frontier shelf areas as the Bering Sea attractive to industry. In these areas, hydrocarbon deposits must be large (at least 500 million barrels) to be commercially attractive.

In this chapter, I briefly review the exploration of the Beringian shelf, describe the major basins beneath this shelf, and set forth the proposed leasing schedule. Finally, I note areas of future exploration in the Bering Sea.

History of Exploration

The first two surveys of the Bering Sea by the USGS were conducted in 1967 and 1968 on U.S. Navy ships in a cooperative program between the USGS and the Department of Defense. Another Bering Sea cruise took place in 1969 on a U.S. Coast Guard vessel and included a brief field excursion to St. Matthew Island, which had not been visited by a geologist since 1911 (fig. 2). These early cruises were voyages of discovery that demonstrated for the first time that the Beringian shelf is underlain by large basins filled with sedimentary strata.

A cooperative venture in 1970, again with the U.S. Navy, that used more powerful geophysical equipment capable of resolving deeper geologic structures resulted in the discovery of the Navarin Basin, one of the largest shelf basins on the Beringian margin (figs. 2, 3). The Navarin Basin, which encompasses 80,000 km², is filled to a depth of 10 to 13 km with sedimentary strata.

In 1971, private U.S. service companies began surveys of the OCS on commission from the oil industry. These surveys confirmed the basin discoveries made by the USGS and sparked industry-wide interest in the Bering Sea. Numerous surveys have been conducted in the Bering Sea since early 1971 by oil companies, and these surveys are continuing to the present during each Arctic field season.

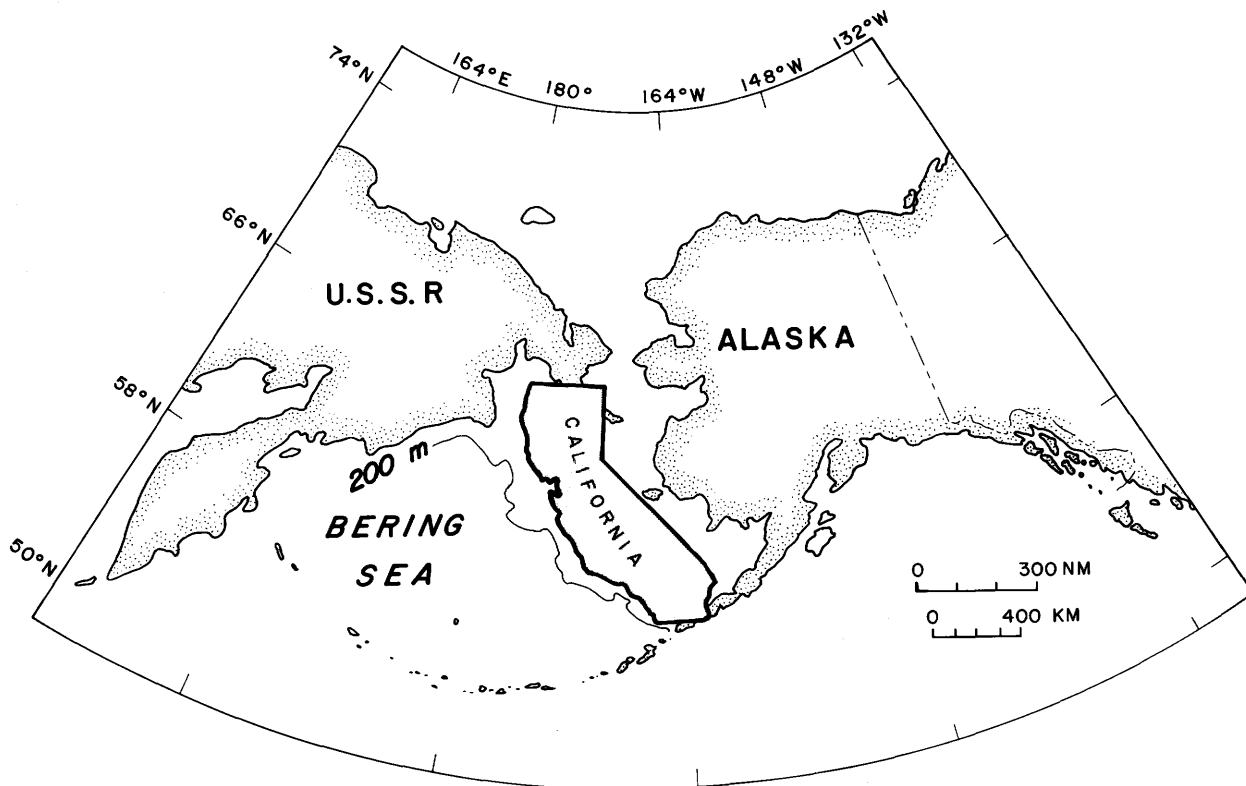


Figure 1. Location map of the Bering Sea, showing area of California for comparison. Albers equal-area projection.

Table 1. Sedimentary basins of the Bering shelf

Basin	Length		Width		Area	
	(km)	(mi)	(km)	(mi)	(km ²)	(mi ²)
Bristol Bay-----	290	(180)	75	(47)	21,750	(8,400)
St. George-----	300	(190)	50	(31)	15,000	(5,800)
Navarin-----	400	(250)	190	(130)	80,000	(31,000)
Anadyr-----	400	(250)	300	(190)	120,000	(46,300)
Norton-----	250	(155)	180	(111)	45,000	(17,400)

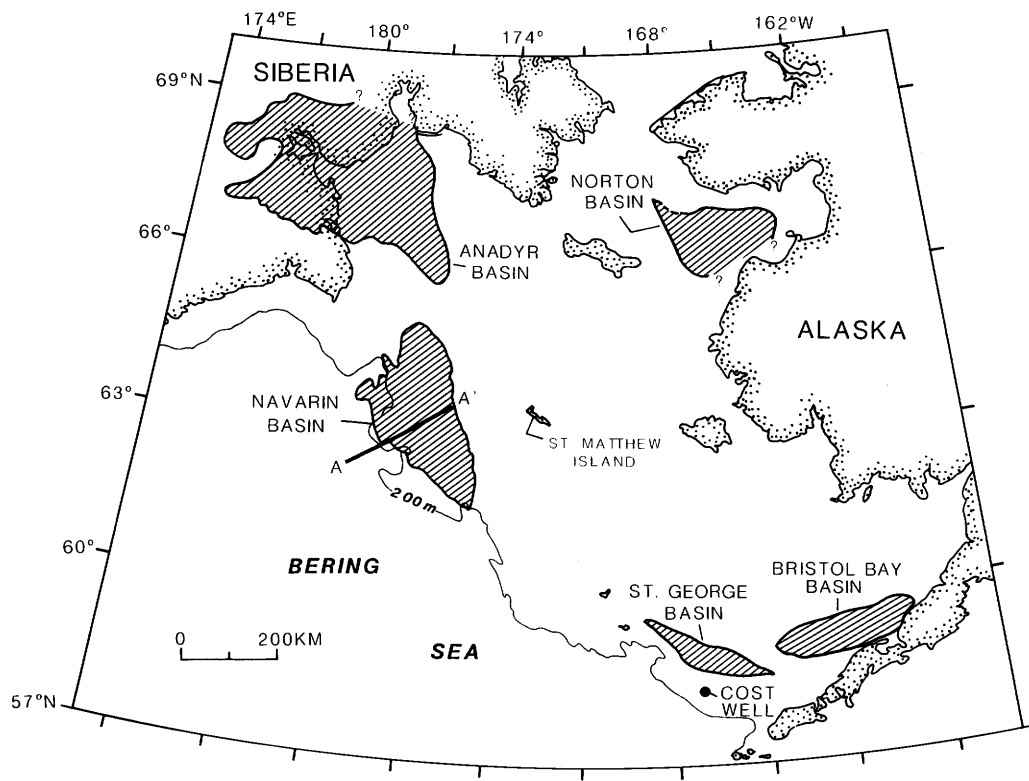


Figure 2. North Pacific region, showing locations of major basins (shaded) beneath the Bering Sea Shelf (table 1). Dot denotes location of COST well drilled near the St. George Basin. Albers equal-area projection.

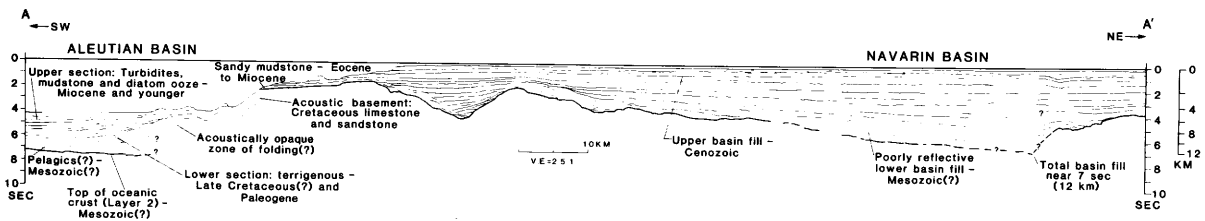


Figure 3. Interpretative drawing of 24-channel seismic reflection profile (A-A') across north Beringian margin. See figure 2 for location.

Sampling of the continental slope adjacent to the Bering Sea shelf began through a cooperative program between the USGS and the University of Washington in 1967. Another USGS sampling expedition was run in 1970 from the U.S. Navy ship *Bartlett*. An extensive sampling program commenced in 1978, using the USGS research vessel *S. P. Lee*, and this program has continued to the present. Results from these sampling programs have radically altered geologic interpretations of the Beringian margin. Alaskan terranes extend beneath the shelf and flank of the southern-shelf basins. Recent geologic hypotheses require large northward motions of fragmental Alaska through geologic time before the amalgamation of these fragments into present-day Alaska. If these hypotheses are correct, then the discovery of extensions of the various Alaskan terranes into the Bering Sea requires that northward motion of Alaska must also include northward motion of large areas of the Bering Sea as excess baggage.

The early sampling work by the USGS prompted a parallel and more extensive program by private industry. The first Continental Offshore Stratigraphic Test (COST) well was drilled near the St. George Basin (fig. 2) by a consortium of oil companies in 1976. Five other COST wells have since been drilled, including one additional well in the Navarin Basin. These wells historically were not drilled on possible resource targets but were intended only to reveal the regional geologic framework of the shelf basins as a guide to finding oil and gas.

Basin Description

Table 1 lists the sizes of the major basins of the Beringian shelf. Detailed descriptions of these basins were given by Marlow and Cooper (1980), Fisher and others (1982), and Marlow and others (1983).

The Bristol Bay, Anadyr, Norton, and Navarin Basins appear to have formed as large downwarps in the Earth's crust. Blocklike structures formed within these basins during downwarping. These structures are buried in places by sedimentary layers, which may form traps for migrating hydrocarbons.

The St. George Basin and the south half of the Navarin Basin are tensional features, formed by pulling-apart of the Earth's crust. Continued subsidence of these basins through geologic time has formed fold structures associated with "growth faults" along the flanks of the basins. These fold structures may also trap economically significant volumes of oil and gas.

The north half of the Navarin Basin is dominated by compressional structures, such as anticlines and domes, which formed when the basin fill was subjected to horizontal compression. Anticlines and domes are classic geologic structures from which most of the world's oil has been produced.

The shelf basins have not been explored directly for hydrocarbons by drilling, and so their hydrocarbon potential remains unknown. The Navarin Basin, however, one of the largest shelf basins, contains many large geologic structures that exhibit geophysical signatures that suggest the presence of hydrocarbons. The onshore part of the nearby Anadyr Basin (fig. 2) has been drilled by the Soviet Union. These wells revealed shows of oil and gas which suggest that the offshore part of this basin may also contain hydrocarbons. Whether these accumulations will ever be commercially attractive in an area as remote as the Bering Sea remains to be seen. The location of a treaty boundary between the United States and the Soviet Union for subsea development of these lands has not yet been resolved.

The Convention Line of 1867 applies only to the separation of the islands in the Bering Sea (fig. 2).

Lease Schedule

The USGS and the U.S. Minerals Management Service have completed lease sales for the Norton and St. George Basins, and tentative leases were granted in 1983. These sales have since been challenged in court, however, and exploration has been delayed.

Future Exploration

Future exploration in the Bering Sea by the USGS falls into two categories. The first category involves extension of the search for hydrocarbons westward beyond the edge of the shelf. The USGS has already documented the presence of thick sedimentary masses beneath the continental slope and abyssal regions of the Bering Sea (see Cooper and others, 1979). Geophysical surveys have revealed acoustic features in these sedimentary masses that suggest the presence of gas. Additional surveys, including detailed swath mapping of the margin, are planned for deep-water areas of the Bering Sea. Swath mapping is a method of imaging the sea floor in a manner analogous to satellite imaging of the land areas of the Earth. These data should assist the oil industry in the hunt for hydrocarbons as their technology for hydrocarbon extraction allows them to advance into deeper water.

The second category of resource exploration by the USGS involves surveying and sampling of the shallow waters of the inner Bering Sea Shelf adjacent to western Alaska. The search here will center on exploration for strategic and precious metals. Platinum, gold, and silver are currently being mined from the amalgamated geologic terranes of western Alaska. A recent geophysical cruise by the research vessel *S. P. Lee* showed that these terranes extend offshore beneath the inner Bering Sea Shelf. Thus, the metalliferous deposits associated with the on-shore terranes may extend offshore. Discovery of new offshore metalliferous deposits beneath the Bering Shelf would be of great interest to the U.S. mining industry.

References

- Cooper, A. K., Scholl, D. W., Marlow, M. S., Childs, J. R., Redden, G. D., Kvenvolden, K. A., and Stevenson, A. J., 1979, Hydrocarbon potential of Aleutian Basin, Bering Sea: American Association of Petroleum Geologists Bulletin, v. 63, no. 11, pt. 1, p. 2070–2087.
- Fisher, M. A., Patton, W. W., Jr., and Holmes, M. L., 1982, Geology of Norton basin and continental shelf beneath northwestern Bering Sea, Alaska: American Association of Petroleum Geologists Bulletin, v. 66, no. 3, p. 225–285.
- Marlow, M. S., and Cooper, A. K., 1980, Mesozoic and Cenozoic structural trends under southern Bering Sea shelf: American Association of Petroleum Geologists Bulletin, v. 64, no. 12, p. 2139–2155.
- Marlow, M. S., Cooper, A. K., and Childs, J. R., 1983, Tectonic evolution of the Gulf of Anadyr and formation of Anadyr and Navarin basins: American Association of Petroleum Geologists Bulletin, v. 67, no. 4, p. 646–665.



The *S. P. Lee* at Suva, Fiji

Hydrocarbon- and Mineral-Resource Investigations in the Southwest Pacific

By Florence L. Wong, H. Gary Greene, and the
scientific staff of the 1982 CCOP/SOPAC cruise

Introduction

To study the hydrocarbon- and mineral-resource potential of the Southwest Pacific, the USGS research vessel *S. P. Lee* sailed from Honolulu in March 1982, laden not just with an extensive array of geophysical equipment, but also with 10 tons of food and clothing gathered by the Tongan Relief Committee for the victims of Hurricane Isaac (March 2–3, 1982) in Tonga. Three months later, the USGS completed its first field season of geophysical surveys and sampling in the waters off Tonga, Fiji, Vanuatu, the Solomon Islands, and Papua New Guinea (fig. 1). The data gathered during this survey will help address questions of island-arc tectonics; determine the age, evolution, and extent of the as-yet-unexplored marginal sedimentary basins; and assess the hydrocarbon and mineral potential of these areas.

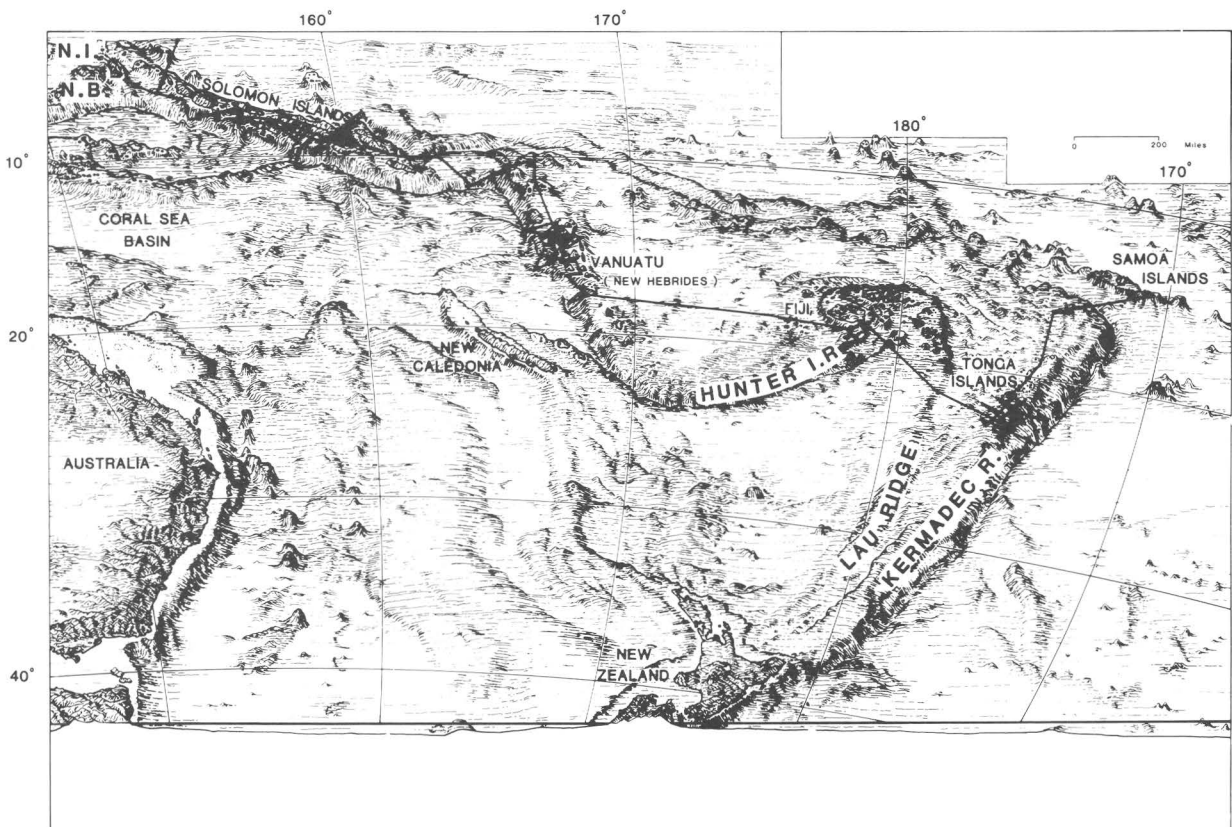


Figure 1. Southwest Pacific, showing sea-floor topography and tracklines covered by U.S. Geological Survey research vessel *S. P. Lee* during 1982 survey. N B, New Britain; N I, New Ireland.

The Southwest Pacific island nations have a great interest in seeing what economic-resource potential lies in their waters. These are nations that have gained their political independence within the past 10 to 15 years and are interested in a measure of economic independence as well, especially with regard to petroleum products, which currently must be imported. Newly adopted 200-mi exclusive economic zones (EEZ) give each nation a larger seabed area within which to work. For the most part, the Melanesian arc has not been so vigorously explored for hydrocarbons as the neighboring Philippines or Indonesia; the traditional belief is that this area is too volcanic and too young to have generated any significant hydrocarbon accumulations. Systematic geologic mapping, however, has gradually chipped away at this belief by defining large areas of marine sediment and providing evidence of source rocks and of a thermal history sufficient for hydrocarbon formation; in addition, the search for hydrocarbon resources has been fueled by the discovery of oil seeps in Tonga and Papua New Guinea (Clark, 1980).

Nonetheless, private concerns are unable to commit large expenditures to exploration without a promise of return, and the dry holes encountered in several recent drilling attempts have dampened industry enthusiasm for a major commitment to this region. The island nations need more information to help them outline developmental priorities. They found that the USGS was willing and able to provide the expertise and equipment to do the work. If such a project were undertaken, the USGS would benefit from the opportunity to work in a new geologic frontier and gain new knowledge about the crustal dynamics, geologic framework, geologic hazards, and mineral- and hydrocarbon-resource potential of this region.

The survey that finally materialized in March 1982 was arranged under the Australia-New Zealand-United States (ANZUS) Tripartite Agreement, in association with the United Nations-sponsored Committee for the Coordination of Joint Prospecting for Mineral Resources in South Pacific Offshore Areas (CCOP/SOPAC) which is based in Fiji. The U.S. Department of State was instrumental in negotiating this agreement and in establishing the framework for cooperative research. The Office of Energy of the U.S. Agency for International Development (AID) funded the implementation and operation of the survey; funding was also provided by the Government of Australia. The CCOP/SOPAC Technical Secretariat in Fiji served as basic coordinator and, along with Australia, New Zealand, and other CCOP/SOPAC member nations, sent scientists to join the USGS staff.

General Geology

The area of the Southwest Pacific in which this mineral- and hydrocarbon-resource-assessment program is being carried out is a tectonically complex segment of the Melanesian arc. The Australia-Indian plate meets the Pacific plate in this area, and their interaction over time has created a series of volcanic island arcs (normal and reversed), expanding marginal basins, transform-fault zones and deep-sea trenches.

The volcanically active outer Melanesian arc, the target area for our studies, is defined, from east to west, by the sinusoidal trace of the Tonga-Kermadec Ridge, the Hunter Island Ridge, Vanuatu, the Solomon Islands, New Britain, and New Ireland (fig. 1). These volcanic island chains are flanked by trenches on either one or both sides; trenches on both sides point to arc reversal during tectonic

evolution. The Solomon Islands and Vanuatu are on the Pacific plate and have inactive trenches on their Pacific side, a relation suggesting that they may once have been part of the Australia-Indian plate (Packham, 1973). The Tonga-Kermadec chain lies within the Australia-Indian plate. Tonga, Vanuatu, and the Solomon Islands became the first targets of this survey because the sea floor adjacent to these areas overlies substantial accumulations of Tertiary sediment.

The islands of Tonga lie astride a north-northeast-trending island arc fronting the Lau Basin to the west (fig. 1), which is apparently a spreading backarc basin. The west boundary of this basin is the Lau Ridge, postulated to have been part of the Tonga Ridge before the opening of the Lau Basin less than 10 m.y. ago. Two island chains comprise Tonga—a western chain of active volcanoes approximately 160 km west of the Tonga Trench axis, and an eastern chain of mostly limestone-covered islands lying 90 to 130 km west of the trench. The Island of Eua is an exception because it occurs in the eastern chain but overlies a lower Tertiary volcanic sequence (fig. 2; Ewart and Bryan, 1973). The sedimentary sequence targeted for study forms a wedge atop the platform underlying the island chains.

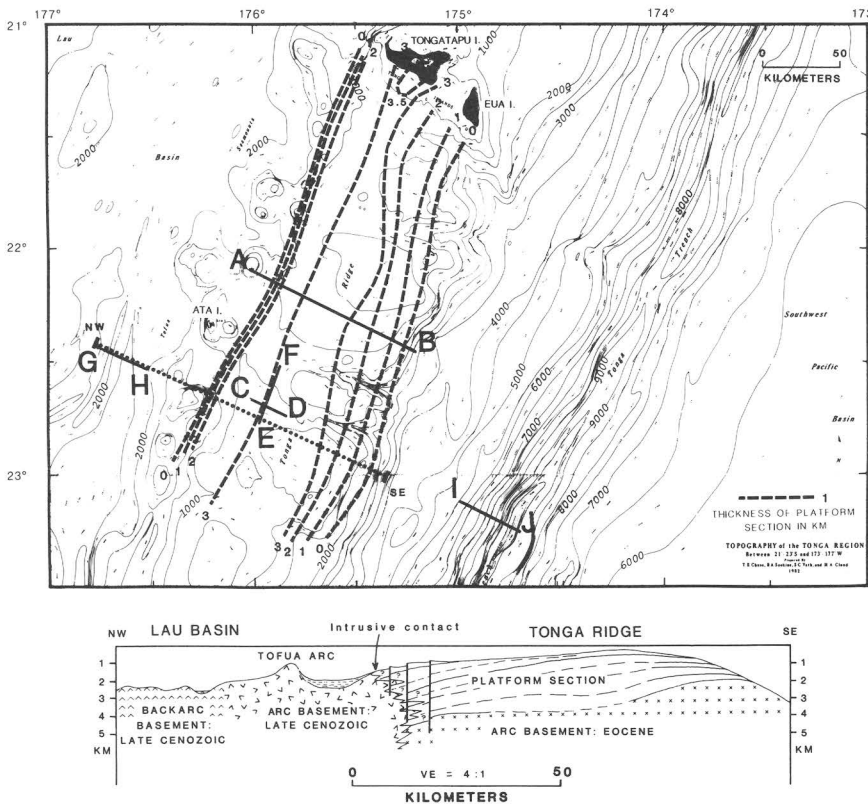


Figure 2. Diagrammatic representation of isopach contours, based on multichannel and sonobuoy refraction velocities and depth calculations, showing thickness of Tonga platform section (in kilometers) and locations of profile segments (A-B through I-J) in figures 5 and 6. Schematic cross section, from the Lau Basin to east edge of the southern Tonga platform, illustrates presumed structural and stratigraphic relations of regional importance (based on sonobuoy refraction data and multichannel reflection profile). Platform section has presumably been truncated by extensional rifting along west side of ridge. Young arc basement is shown intruding truncated edge of section. Missing or western part of section presumably underlies the Lau Ridge, approximately 300 km to the west.

Vanuatu (formerly the New Hebrides) is another recently active volcanic island chain (fig. 3). Three subparallel belts make up this north-northwest-trending island chain. The central belt consists of active volcanoes, flanked on either side by Oligocene to Pliocene volcanic belts (Mallick, 1973). The New Hebrides Trench, which lies 100 to 150 km to the west of this active volcanic chain, is defined by a continuous Benioff zone (Dubois and others, 1973), although the bathymetry suggests a discontinuity where the east-west-trending D'Entrecasteaux fault zone bisects the chain (fig. 3). Tertiary sedimentary basins lie beneath the shelf and the deep-water Central Basin.

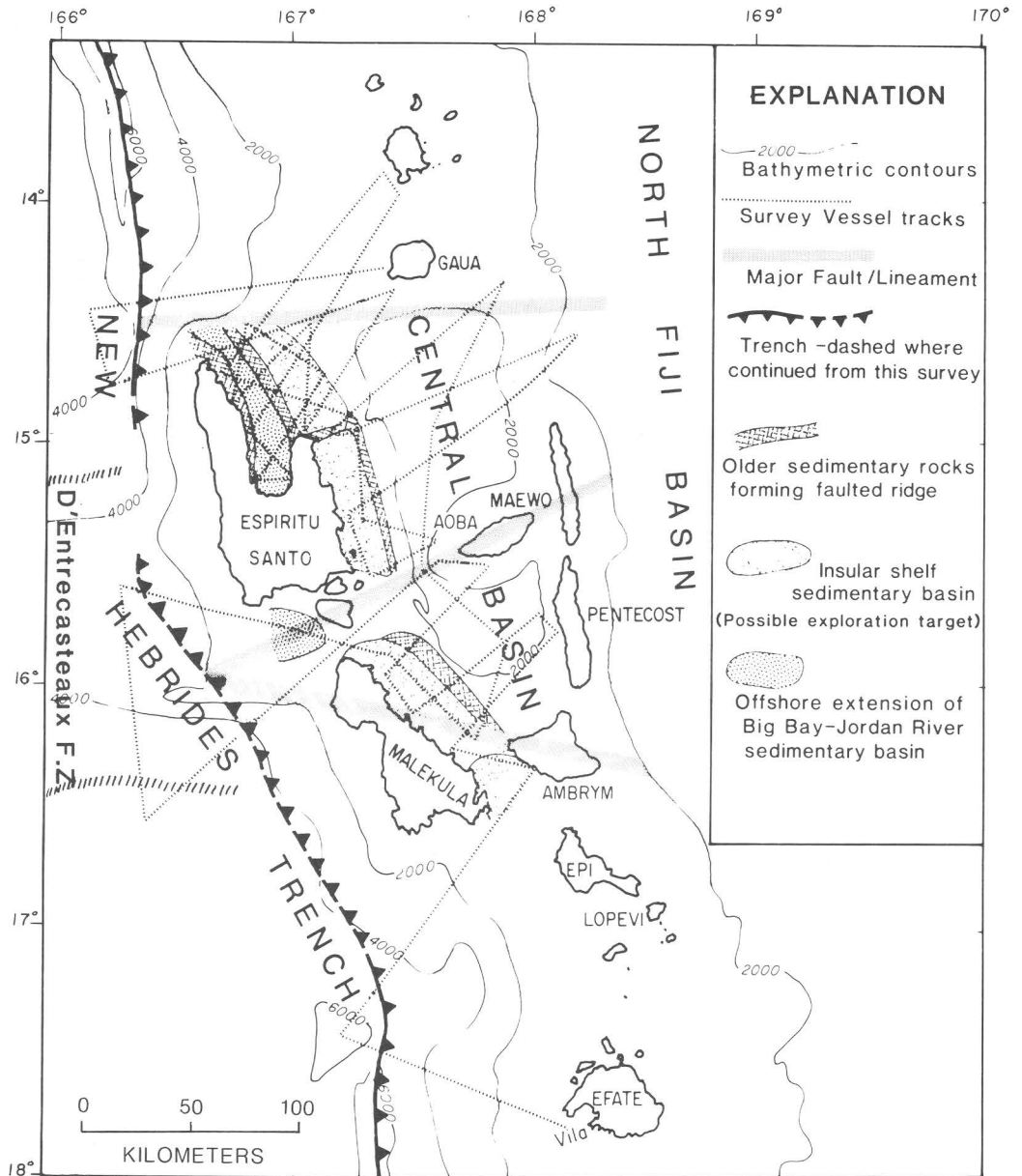


Figure 3. Generalized outline of shelf or shelf-edge sedimentary basins and primary structural features of Vanuatu delineated during leg 2 of S. P. Lee cruise.

The Solomon Islands region encompasses three geologic provinces (Coleman, 1976): The Pacific province, which is underlain by obducted parts of the Ontong-Java Plateau on its northeast flank; the Central province, which is largely underlain by early Tertiary volcanic and volcanoclastic rocks; and the Volcanic province, which includes the late Cenozoic volcanic island arc on its southwest flank. The deep-water (800-1,800 m) intra-arc sedimentary basin targeted for study, which lies between the Volcanic and Central provinces, may contain more than 5 km of sedimentary section in places (fig. 4).

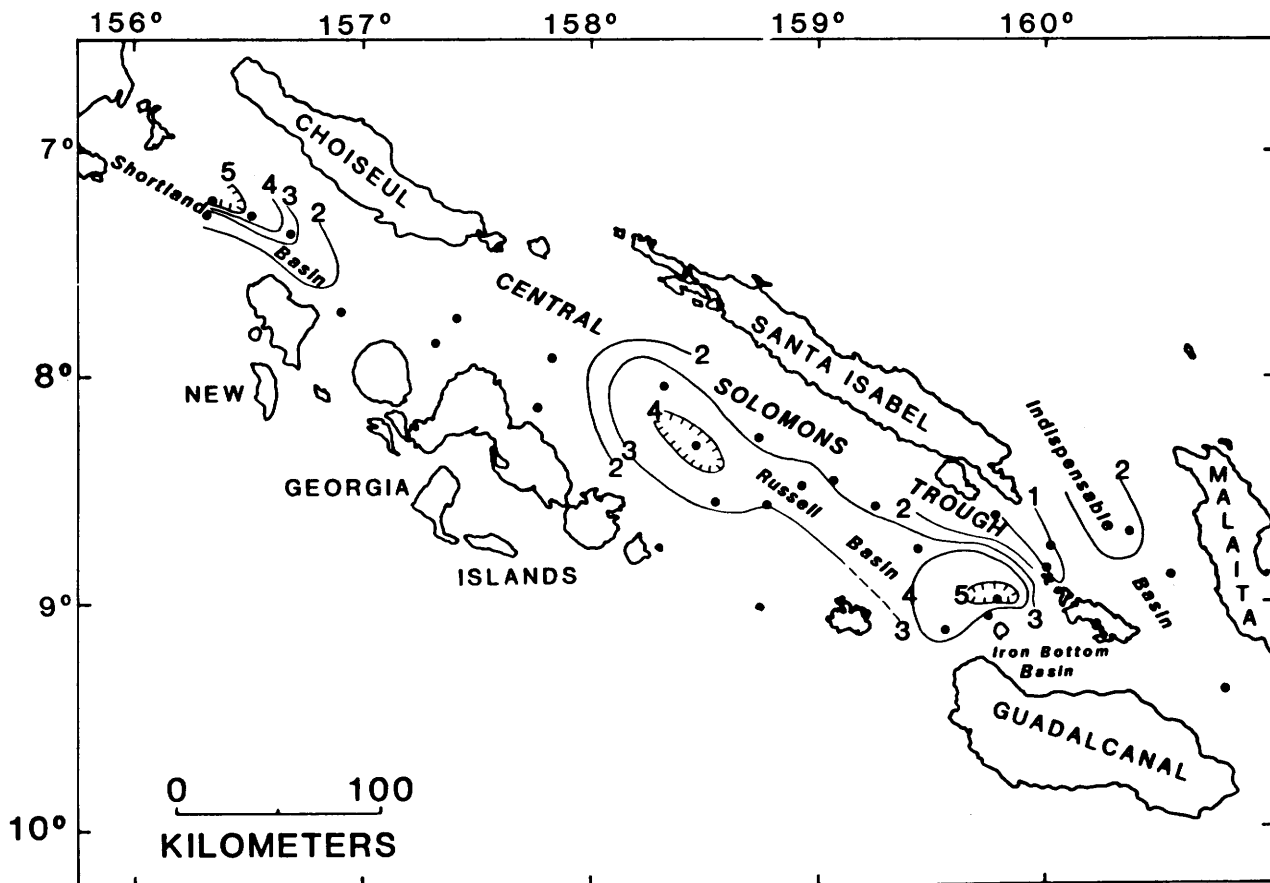


Figure 4. Structural basins and preliminary isopach map of sediment overlying basement rock in the Solomon Islands. Dots, sonobuoy locations at which basement refractors were recorded; contours, sediment thickness (in kilometers).

Results

During the three legs of the cruise, the *S. P. Lee* obtained 7,700 km of Uniboom high-resolution seismic-reflection profiles; 15,700 km of 3.5- and 12-kHz, gravity, and magnetic profiles; 12,300 km of single-channel seismic-reflection profiles; 8,600 km of 24-fold common-depth-point seismic-reflection profiles; and 123 sonobuoy wide-angle reflection-refraction profiles, and occupied 27 sampling stations (Greene and others, 1983).

Tonga

Initial results, reported by Maung and others (1982) and Scholl and others (1984) and summarized here, include: (1) Acoustic resolution of a westward-thickening extensionally deformed platform section (acoustic velocity, less than 4.5 km/s; 2–3 km thick) of chiefly Neogene and younger volcanoclastic and limestone beds overlying a basement of arc-type igneous rocks (acoustic velocity, more than 5 km/s) (figs. 2, 5); (2) identification of a regional unconformity of late Miocene age in the upper part of the platform section that possibly reflects thermal uplift of the ridge just before the opening of the Lau Basin; (3) identification of large moundlike buildups in the lower part of the platform section that may be reefal in origin or may be igneous masses (fig. 5); (4) recognition of evidence that the forearc area, most of which is deeply submerged, may have been a source terrane for some of the volcanoclastic deposits of the platform section; (5) southwestward tracing (for at least 250 km) of an axis of early Tertiary volcanism that is situated along the Pacific side of the platform and passes beneath or close to Eua Island; (6) acoustic tracing of the subducted surface of the Pacific plate 25 to 30 km landward of the inner trench wall (fig. 6) (this slope is not underlain by offscraped low-velocity pelagic oceanic deposits); and (7) probable detection of a magma chamber 3 to 4 km below a spreading axis in the Lau Basin (fig. 6).

Vanuatu

Preliminary onboard data reduction and interpretation (Greene and others, 1984) resulted in: (1) The delineation of three small shelf sedimentary basins east of Malekula and Espiritu Santo; (2) estimation of the minimum sedimentary thickness in the intra-arc Central Basin; and (3) discovery of the northward continuation of the southern New Hebrides Trench (fig. 3).

The three shelf or shelf-edge sedimentary basins that were mapped all lie in water depths of less than 1,000 m and have sediment thicknesses greater than 2 km (fig. 5). Structures capable of trapping oil and gas are present in all three basins. Apparent local connection of the sedimentary rocks identified within these smaller shelf-edge basins with the deeper intra-arc basin (that is, the Central Basin) form potential pathways for petroleum migration from thick sedimentary sections in deep-water marine source beds to shallow-water reservoir beds and traps.

The main part of the Central Basin contains rocks about 5 km thick that have acoustic velocities less than 5 km/s (fig. 7). Preliminary multichannel seismic data indicate that three main seismic-stratigraphic units, all separated by unconformities, compose the basin fill. These units consist, from oldest to youngest, of a poorly bedded sedimentary unit that rests on acoustic basement along the margins of the basin, everywhere overlain by a well-layered sedimentary unit that is, in

turn, overlain by a thin layer of well-bedded unconsolidated sediment. Several large structures deform the youngest units of this fill; these structures do not appear to have igneous rocks at their core.

Multichannel seismic data from the survey indicate that the New Hebrides Trench near the central part of this arc (area of fig. 3) is nearly devoid of sedimentary fill and that the associated accretionary wedge is covered by only a veneer of sediment (Fisher and others, 1982). Rocks within this wedge have high acoustic velocities (4-5 km/s) and are characterized by faint reflections that dip east-northeast toward the arc. Oceanic crust can be traced beneath this wedge for 30 km.

The three shelf-edge basins identified in the survey are considered to be promising sites for further investigations of hydrocarbon potential. They are equivalent in size and sediment thickness to the smaller hydrocarbon producing basins elsewhere in the world. The water depths overlying all these shelf-edge basins are shallow enough for exploitation using current drilling technology.

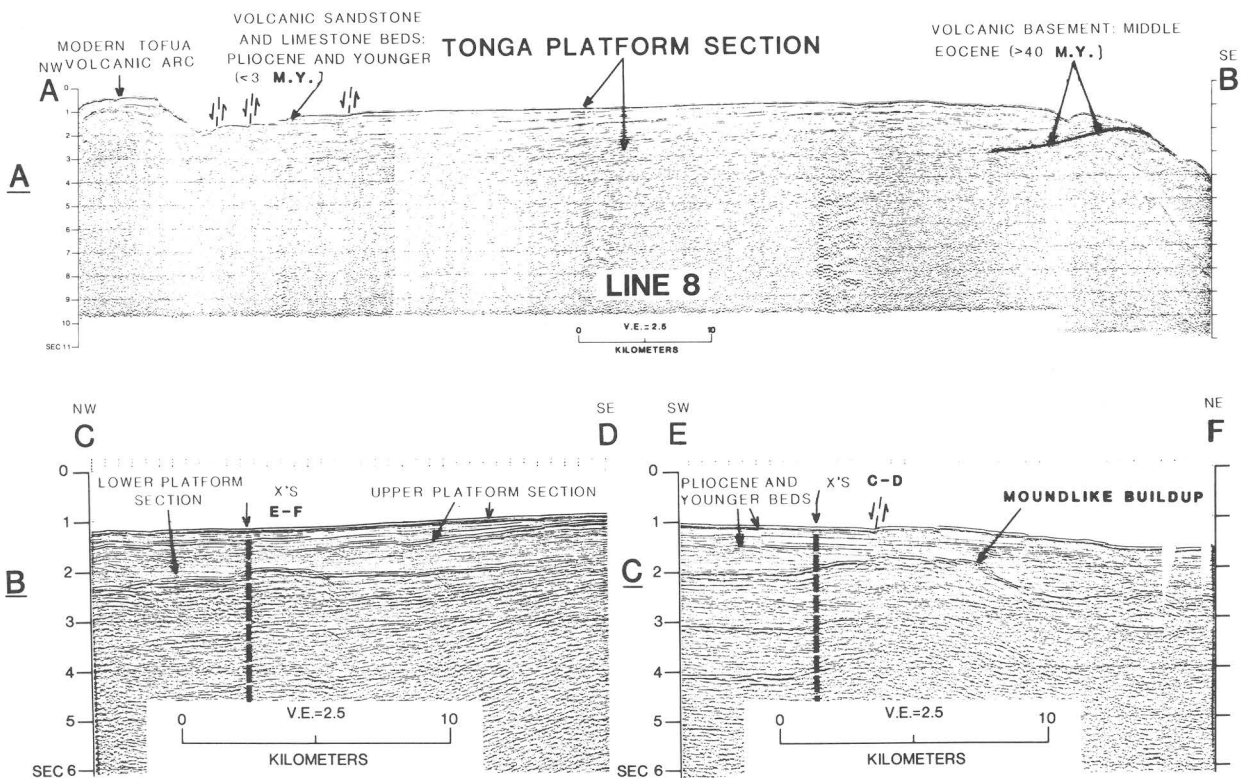


Figure 5. Annotated segment A-B (A) of multichannel line, which traverses crestal platform of the Tonga Ridge, and mutually crossing segments C-D (B) and E-F (C), which reveal a subsurface moundlike structure of possible igneous or reefal origin (see fig. 2 for locations). Platform section noted along segment A-B is constructed of volcanoclastic and limestone beds of post-Eocene age that, generally, are characterized by acoustic velocities of less than about 4.5 km/s. Section underlying acoustic basement is presumably arc-type volcanic and intrusive rocks of Eocene and older age. Upper, more coherently layered strata of platform section are composed of Pliocene and younger beds; underlying moundlike buildup within lower platform section is probably associated with beds of Miocene age.

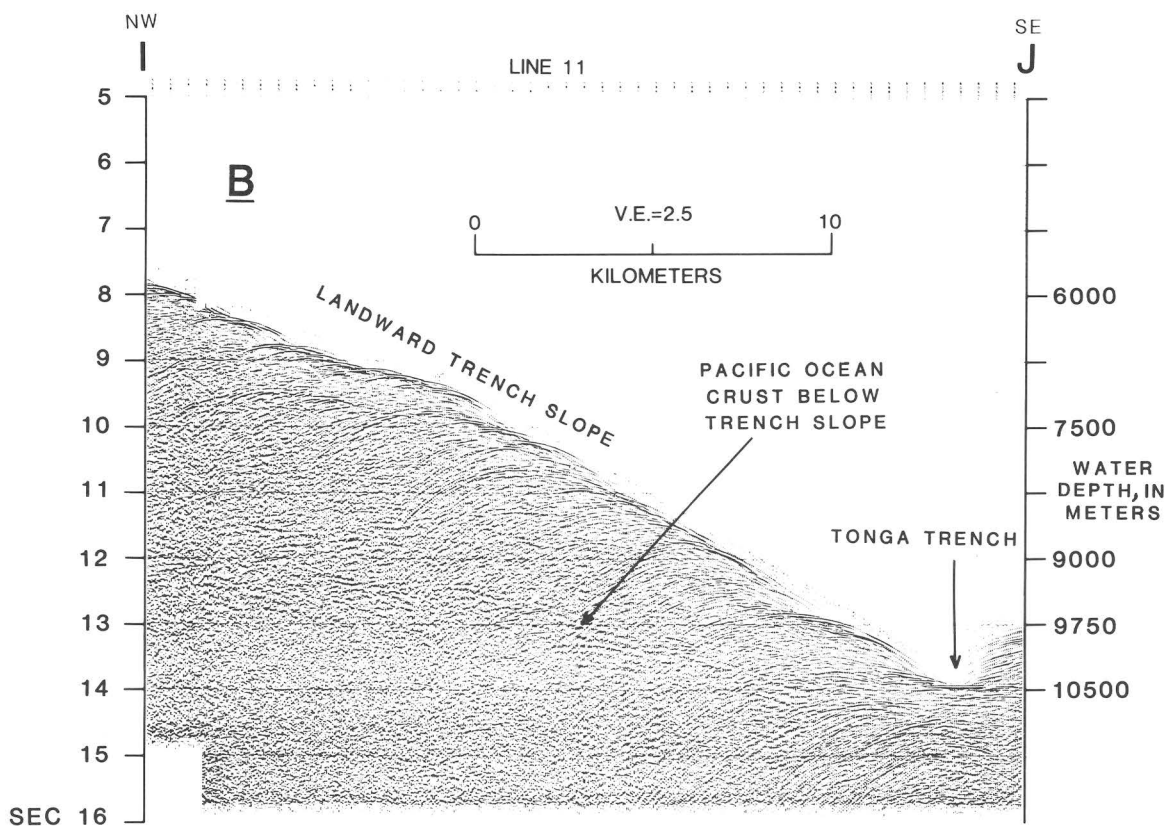
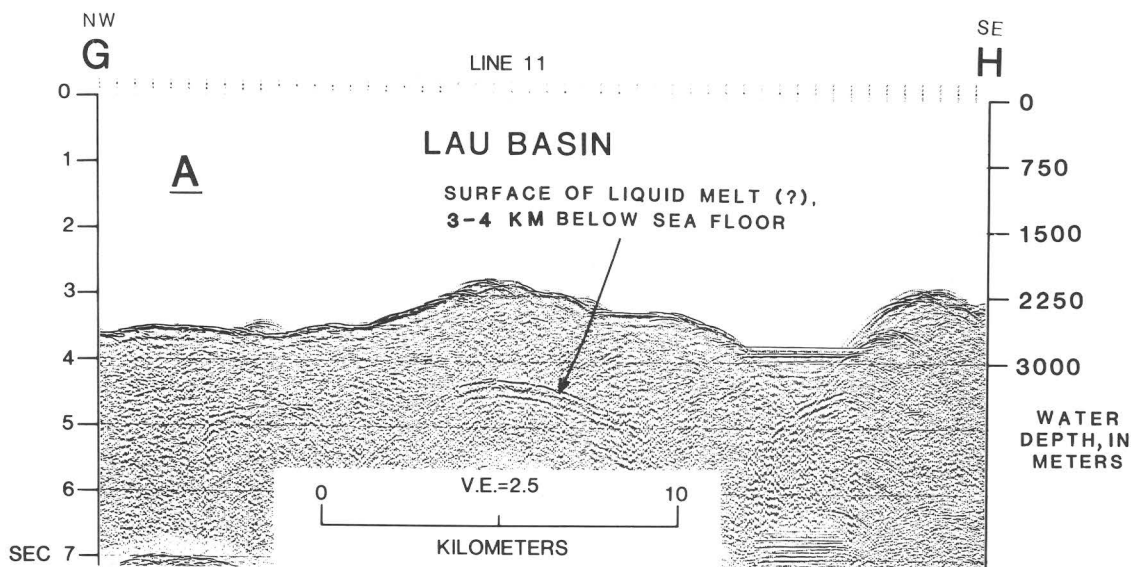


Figure 6. Annotated segments G-H and I-J of multichannel line. *A*, segment G- H, revealing a subsurface upper crustal-reflection horizon near east side of the Lau Basin that may be the top of a magma chamber underlying a spreading center. *B*, Segment I-J, recorded over lower part of landward slope of the Tonga Trench, revealing a deep, subsurface reflection horizon that is presumed to be the top of subducted Pacific oceanic crust. On a true-depth section, the horizon actually dips downward beneath the Tonga Ridge, but a conspicuous velocity pullup effect induced by high-velocity rocks underlying the lower slope causes the horizon to ascend to the west on this reflection-time section.

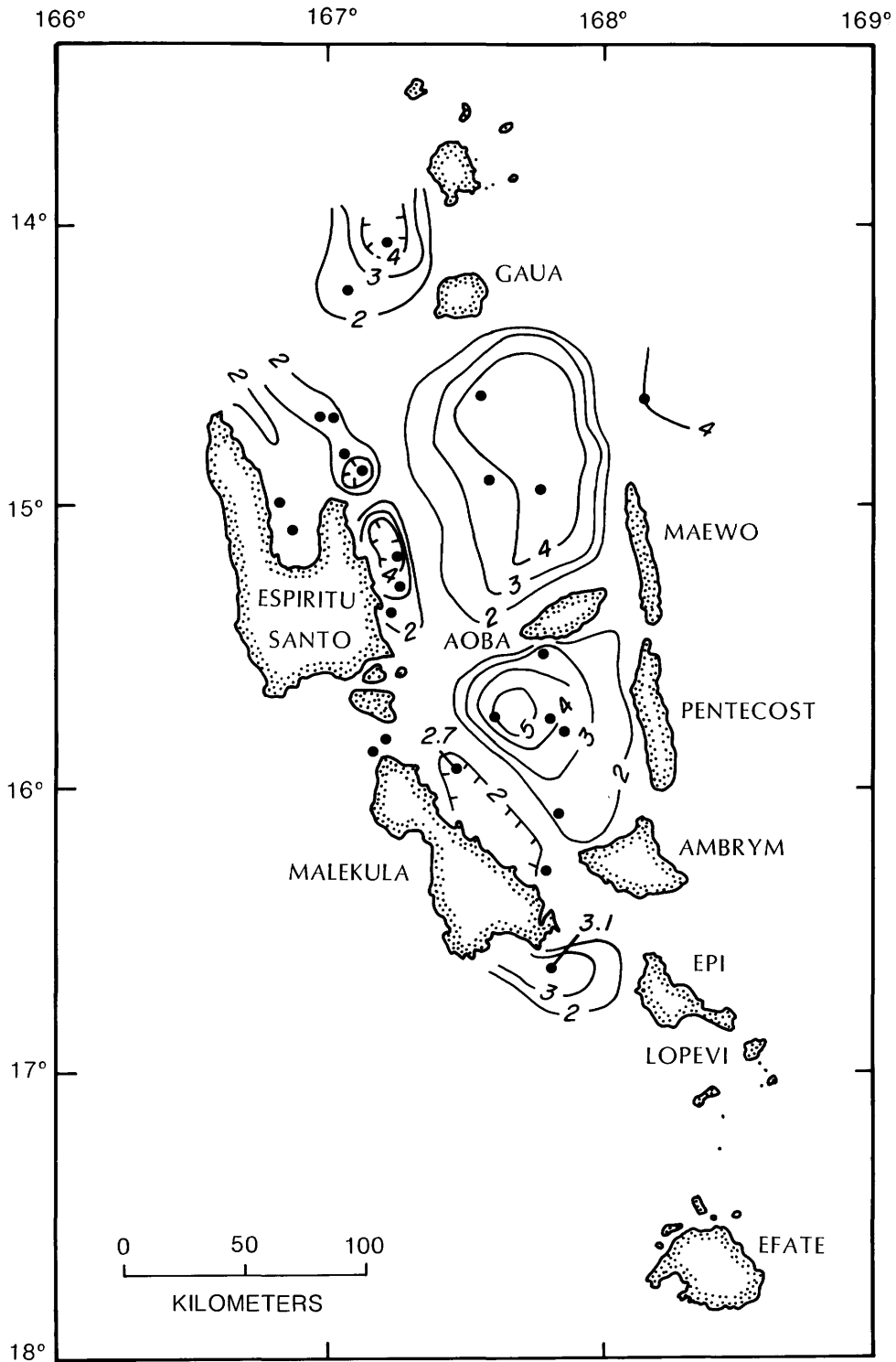


Figure 7. Preliminary isopach map of sediment overlying acoustic-basement rocks of 5-km/s seismic velocity in the Central Basin of Vanuatu. Dots, approximate sonobuoy locations where basement reflectors were recorded; numbered dots denote deepest recorded sediment thicknesses. Contours, sediment thickness (in kilometers).

Solomon Islands

Both wide-angle sonobuoy reflection and refraction data were recorded, and velocity profiles for the sedimentary section and crustal layers were computed from these data. Seismic-refraction arrivals, routinely recorded to a range of 37 to 45 km, provided maximum sedimentary-layer depth estimates of 10 to 12 km beneath the island arc and adjacent ocean basins (Cooper and others, 1982).

Two subsidiary basins separated by a horstlike feature constitute the central Solomons Trough. These newly named structural basins are the Shortland Basin and the Russell Basin (fig. 4). The late Cenozoic Russell Basin is an elongate (60 by 250 km) asymmetric crustal depression containing a 1- to 5-km-thick sedimentary section (fig. 4). Velocities of the crustal rocks beneath this sedimentary section range from 4.8 to 7.5 km/s. The acoustic basement, thought to be composed of volcanic and volcanoclastic rocks that are partly metamorphosed, has velocities of 4.8 to 5.8 km/s; a deeper layer, with a velocity of 6.4 to 7.5 km/s, is 3 to 5 km below the acoustic basement. These higher velocity rocks may include deeper crustal igneous rocks similar to those observed in island outcrops in the Central province.

In addition to the Russell and Shortland Basins, two other sedimentary basins (diagrammed in fig. 6) have been defined: Iron Bottom Basin and Indispensable Basin.

Samples dredged from the perimeter of the Russell and Shortland Basins consist principally of volcanoclastic rocks and reef-detritus limestone (Vedder and others, 1984). In general, the volcanoclastic rocks include poorly sorted foraminiferal sandstone, sandy calcilutite, lapilli tuff, and ashy mudstone that range in texture from indurated to friable. The limestone consists largely of recemented and partly recrystallized coralline and algal reef detritus that suggests downslope transport as well as submergence since deposition. Both the volcanoclastic rocks and the limestone have a low porosity. Calcareous nannofossils in selected samples from each of the dredge stations indicate a Quaternary age, chiefly in the range 0.2–1.6 m.y. (David Bukry, written commun., 1982). Radiocarbon ages on two limestone samples are more than 31,000 years (J. B. Colwell, written commun., 1982).

The two gravity cores from water depths of 1,810 and 1,279 m in the central Russell Basin recovered 192 and 262 cm, respectively, of Holocene laminated to bioturbated foraminifer-rich mud. Thin layers of ashy material occur at intervals in both cores.

Future Work

This first series of investigative cruises to the Southwest Pacific region has provided valuable data that suggest potential sites of important mineral and energy resources. The participating nations look forward to further efforts by the USGS to continue investigations in this region. Multichannel seismic-reflection profiling and sampling have been proposed to address the problems in each of the areas described below.

Investigations in the Tonga area are aimed at determining: (1) The prospects for petroleum occurrence in the far-southern Tonga platform section, (2) the early and middle Tertiary history of the Tonga and Lau Ridges, and (3) whether polymetallic sulfides are forming above the magma chamber(?) identified in the Lau Basin (fig. 6).

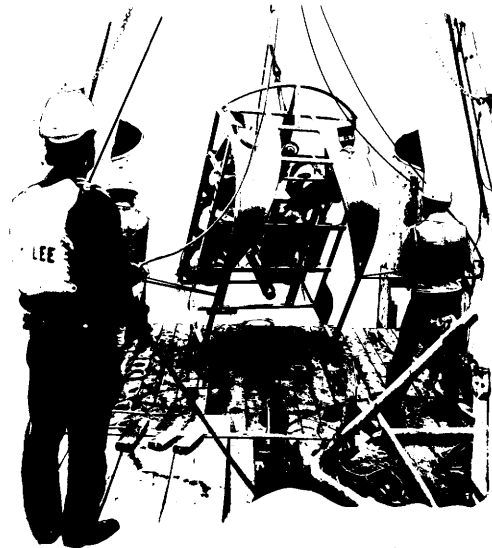
Planned surveys in the Vanuatu area will consider: (1) The possible presence of source rocks, and the past sedimentary history and petroleum-maturation history, of the shelf basins and Central Basin of Vanuatu; (2) the petroleum potential of the sedimentary basins north of the Banks Islands (Vanuatu) and in the Torres-Santa Cruz Islands (eastern Solomon Islands); and (3) the potential for hydrothermal mineral deposits in areas of submarine volcanism, such as east of Epi Island (fig. 3).

The age, composition, and stratigraphic relation of rocks beneath the Solomon Islands arc will be investigated in future surveys of this area. The Central Solomons Trough, Indispensable Strait, and areas east of Bougainville are potential target areas (fig. 4). The possibility that offshore Miocene sequences are largely carbonate and thus have a potential for containing petroleum will be investigated in the area off Papua New Guinea and the adjacent New Ireland Basin.

References

- Clark, W. J., 1980, Forward, *in* Symposium on petroleum potential in island arcs, small ocean basins, submerged margins and related areas: United Nations Economic and Social Commission for Asia and the Pacific, Committee for Co-ordination of Joint Prospecting for Mineral Resources in South Pacific Offshore Areas Technical Bulletin 3, p. 3-4.
- Coleman, P. J., 1976, A re-evaluation of the Solomon Islands as an arc system, *in* Glasby, G. P., and Katz, H. R., eds., Marine geological investigations in the southwest Pacific and adjacent areas: United Nations Economic and Social Commission for Asia and the Pacific, Committee for Co-ordination of Joint Prospecting for Mineral Resources in South Pacific Offshore Areas Technical Bulletin 2, p. 132-140.
- Cooper, A. K., Wood, R. A., Bruns, T. R., and Marlow, M. S., 1982, Crustal structure of the Solomon Islands arc from sonobuoy refraction data [abs.]: *Eos* (American Geophysical Union Transactions), v. 63, no. 45, p.1121.
- Dubois, Jacques, Larue, B. M., Pascal, Georges, and Reichenfeld, C., 1973, Seismology and structure of the New Hebrides, *in* Coleman, P. J., ed., The Western Pacific; island arcs, marginal seas, geochemistry: New York, Crane, Russak & Co., p. 213-222.
- Ewart, A. and Bryan, W. B., 1973, The petrology and geochemistry of the Tongan Islands, *in* Coleman, P. J., ed., The Western Pacific; island arcs, marginal seas, geochemistry: New York, Crane, Russak & Co., p. 503-522.
- Fisher, M. A., Falvey, D. A., and Greene, H. G., 1982, Investigation of the central New Hebrides arc, using multichannel seismic data [abs.]: *Eos* (American Geophysical Union Transactions), v. 63, no. 45, p. 1120.
- Greene, H. G., Falvey, D. A., Macfarlane, Alexander, Cochrane, Guy, Daniel, Jacques, Fisher, M. A., Holmes, M. L., Johnson, David, Katz, H. R., and Smith, G. L., 1984, Preliminary report on the geology, structure, and resource potential of the Central Basin of Vanuatu: Circum-Pacific Energy and Minerals Conference, 3d, Honolulu, 1982, Transactions, p. 631-637.
- Greene, H. G., Wong, F. L. and the scientific staff of the 1982 CCOP/SOPAC cruise, 1983, Hydrocarbon resource studies in the southwest Pacific, 1982: U.S. Geological Survey Open-File Report 83-293, 24 p.
- Mallick, D. I. J., 1973, Some petrological and structural variations in the New Hebrides, *in* Coleman, P. J., ed., The Western Pacific; island arcs, marginal seas, geochemistry: New York, Crane, Russak & Co., p. 193-211.

- Maung, T. U., Exon, N. F., Sandstrom, M. W., Herzer, R. H., Vallier, T. L., Stevenson, A. J., Childs, J. R., and Scholl, D. W., 1982, Tonga Ridge, initial results of new geological and geophysical studies [abs.]: *Eos (American Geophysical Union Transactions)*, v. 63, no. 45, p. 1121.
- Packham, G. H., 1973, A speculative Phanerozoic history of the south-west Pacific, in Coleman, P. J., ed., *The Western Pacific; island arcs, marginal seas, geochemistry*: New York, Crane, Russak & Co., p. 369-388.
- Scholl, D. W., Vallier, T. L., Maung, T. U., Exon, N. F., Herzer, R. H., Sandstrom, M. W., Stevenson, A. J., Mann, D. M., and Childs, J. R., 1984, Initial cruise report, SOPAC Leg 1 (cruise L5-82-SP) southern Tonga platform: *Circum-Pacific Energy and Mineral Resources Conference*, 3d, Honolulu, 1982, *Transactions*, p. 639-644.
- Vedder, J. G., Tiffin, D. L., Kroenke, L. W., Colwell, J. B., Cooper, A. K., Beyer, L. A., Bruns, T. R., Coulson, F. I. E., Marlow, M. S., and Wood, R. A., 1984, Preliminary results of Leg 3 Lee cruise, Solomon Islands: *Circum-Pacific Energy and Minerals Conference*, 3d, Honolulu, 1982, *Transactions*, p. 645-648.



The Juan de Fuca Ridge Metallogensis Program

By William R. Normark, Janet L. Morton, and Randolph A. Koski

Introduction

The need to identify future sources for strategic minerals has led to serious consideration of the potential for hard-mineral resources on the deep-sea floor. The recent establishment of Exclusive Economic Zones extending 200 nautical miles offshore from the U.S. coastline also has intensified commercial interest in deep-sea nonfuel-mineral resources.

Of particular interest to scientists is the evidence of mineral formation along the great 72,000-km-long system of oceanic ridges that encircles the Earth and is the site where new crust is being continuously formed by the upwelling of molten rock from the underlying mantle. As this new crust is formed, it divides and moves away from the spreading axis at half-rates as high as 8 cm per year. Recent investigations have discovered metal-rich submarine hot springs that are a source of potentially valuable minerals along the volcanically active system of spreading ridges. Some areas of the Western United States and Alaska contain remnants of ancient oceanic crust that have been transported by plate-tectonic movement and incorporated into the continental crust. Studying the current mineralization processes on oceanic spreading ridges will thus enhance our ability to identify these onshore areas and target them for mineral exploration.

In 1979, a detailed photographic and geophysical survey of the Pacific sea floor off Mexico discovered several hot springs forming concentrations of zinc, copper, and silver in ore-grade sulfide-mineral deposits on very young glassy volcanic rocks. The initial work, which used unmanned vehicles, was immediately followed by manned-submersible investigation of selected submarine springs; mineral deposits and hot-water samples were recovered. The hydrothermal waters were much hotter (350°C) than in previously observed submarine hot springs. Since the initial discovery, this hydrothermal site at lat 21° N. on the East Pacific Rise has become the focus of investigations into the formation of metallic-mineral deposits on the deep-sea floor. Since 1974, USGS scientists have been involved in studies of the geology, crustal generation, and hydrothermal processes of the sea floor at this site.

Submarine hydrothermal activity on the deep-sea floor is also known from other sites along the oceanic spreading-ridge system. Lower temperature hydrothermal vents have been observed during submersible work along the Galapagos Rift system in the equatorial Pacific. Sulfide minerals have been dredged from the Guaymas Basin in the Gulf of California, and hot-water vents similar to those at lat 21° N. have been photographed on the East Pacific Rise at lat 13° N. off Mexico and at lat 20° S. west of Chile (fig. 1). All these occurrences are on oceanic spreading ridges where the total rate of separation of the plates exceeds 5 cm per year. About half of the global spreading-ridge system has a

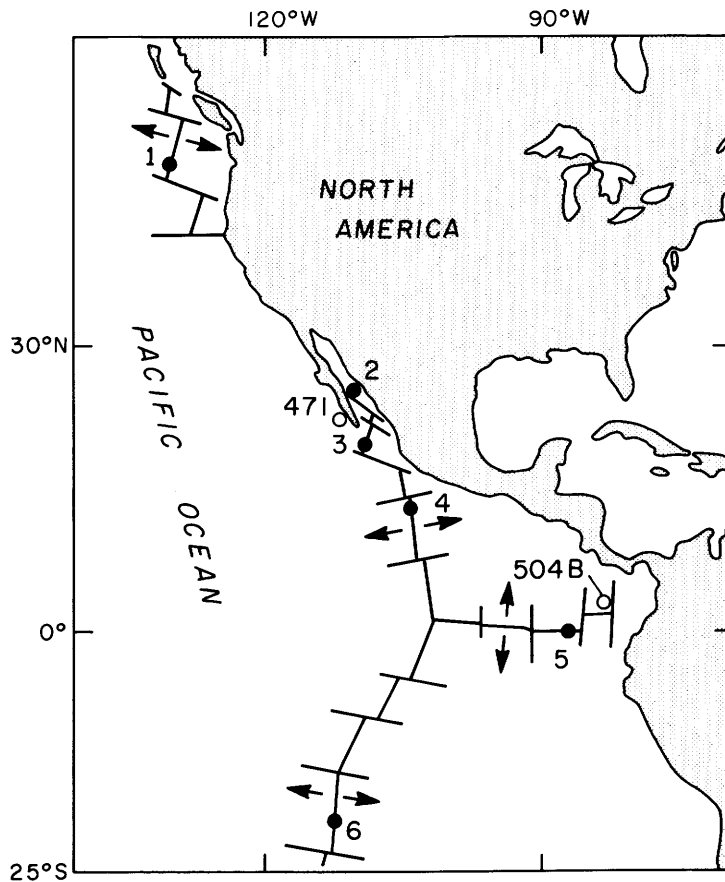


Figure 1. Sketch map of East Pacific region, showing midoceanic-ridge sites (dots) where active hydrothermal circulation and associated massive sulfide deposits have been observed. 1, Juan de Fuca Ridge; 2, Guaymas Basin; 3, East Pacific Rise at lat 21° N.; 4, East Pacific Rise lat 13° N.; 5, Galapagos Rift; 6, East Pacific Rise at lat 20° S. Circles denote Deep Sea Drilling Project sites where similar sulfide deposits have been recovered at depth.

separation rate that exceeds 5 cm per year. All detailed geophysical, photographic, or submersible searches of small segments of ridge crest with separation rates exceeding 5 cm per year have discovered active hydrothermal systems or mineral deposits formed by these submarine springs. Thus, many more areas of actively forming mineral deposits will probably be found on the deep-ocean floor.

Geologic Setting of the Study Area

In September 1981, a research team composed of scientists from the USGS and the University of Washington located hydrothermal vents and dredged samples of sulfide-mineral deposits from a water depth of about 2,200 m at the south end of the Juan de Fuca Ridge, about 500 km off the Oregon coast.

The Juan de Fuca Ridge is a 500-km-long medium-rate spreading center that separates the Juan de Fuca and Pacific tectonic plates off the coast of Oregon and Washington (fig. 2). The south end of this ridge is terminated by the Blanco Fracture Zone, a transform fault that displaces the southward extension of the ridge approximately 350 km to the east, where it is known as the Gorda Ridge.

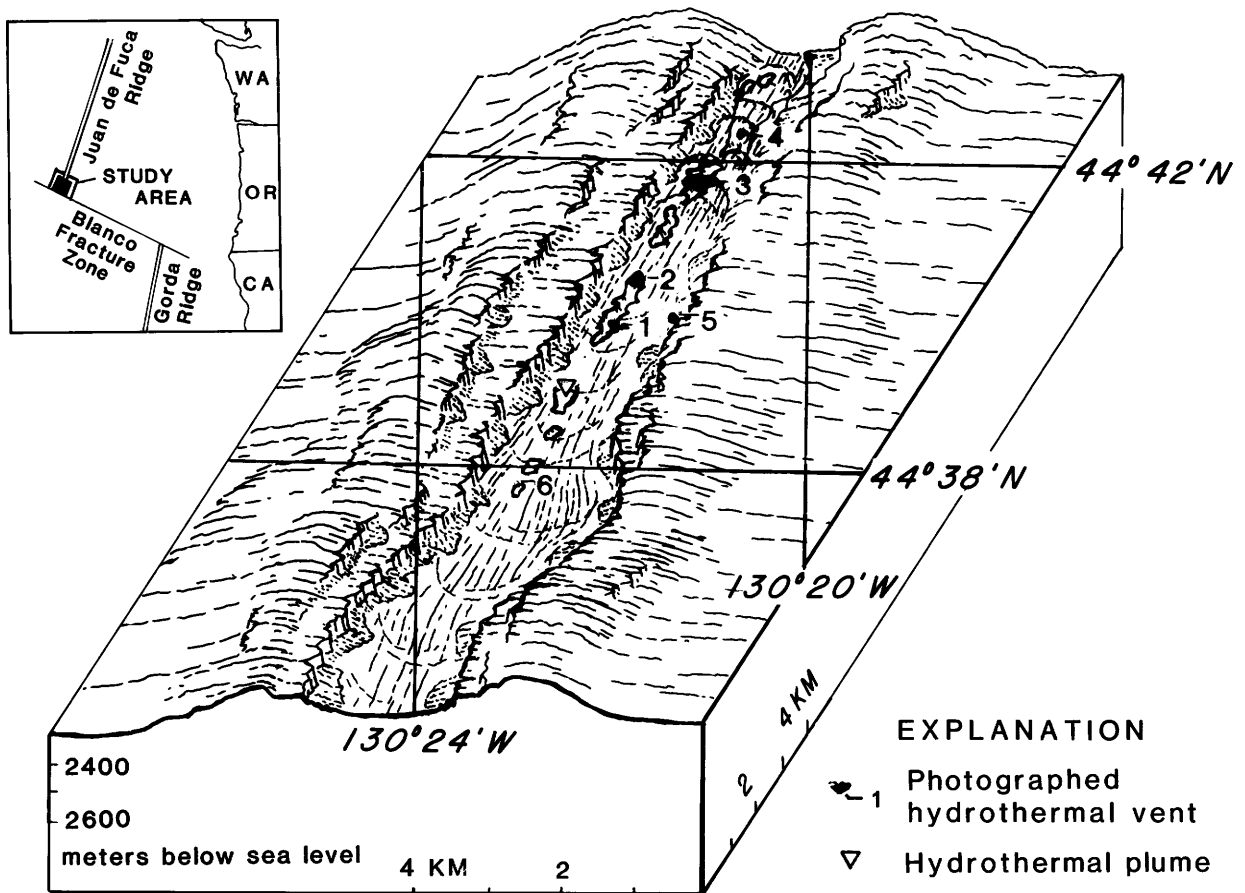


Figure 2. Southern Juan de Fuca Ridge, showing central depression, photographed hydrothermal vents, and hydrothermal plume indicated by water sampling. (Oblique map by T. R. Alpha).

The southern Juan de Fuca Ridge has a simple profile: a smooth, flat 1-km-wide axial valley flanked by steep symmetrical valley walls and ridges. The relief between ridge top and valley floor is 80 to 100 m. The valley walls and a low terrace, about 30 m above the valley floor, are related to steep normal faults formed by continuous separation of the two adjacent plates.

Bottom photographs and pinger records show that the planar valley floor has a narrow and sharply defined medial depression, which is nearly continuous in the northern part of the study area (fig. 2). This topographic feature, which is 50 to 200 m wide and as much as 25 m deep, may have formed by collapse of a submarine lava lake or by faulting.

Bottom photographs also show that the flat axial-valley floor is made up largely of thin flat sheetflows of basaltic lava. Sediment cover is minimal in the current-swept trough. In places, these sheetflows have the ropy surface texture of pahoehoe lava; elsewhere, the flows exhibit a lobate morphology. Undated glassy surfaces on dredged samples of the fresh basalt indicate that these volcanic rocks are less than a few hundred years old. Alteration is limited to coatings of iron and

manganese oxides on exposed surfaces and fractures. Pillow lavas, though sparse on the valley floor, are present on the valley walls. Collapse pits are common along the central third of the axial valley; however, open cracks or fissures are rarely seen on the valley floor. These features contrast with the axial zone of the East Pacific Rise at lat 21° N. and the Galapagos Rift, where complex fault-block terrains and pillow lavas are typical features.

Hydrothermal Vents

Six hydrothermal-vent sites were observed in bottom photographs taken within the axial valley in the north half of the study area (fig. 2); five of these sites are within or along the edges of the axial depression, and the sixth is at the base of the east valley wall. Photographic evidence of the vent sites consists of multicolored crusts, ledges, and mounds of hydrothermal material, as well as concentrations of bottom-dwelling organisms, such as clams, worms, and crabs. A seventh hydrothermal-discharge site is indicated by high concentrations of dissolved manganese in water samples taken at a site near the center of the study area.

The hydrothermal material is easily identifiable in black-and-white photographs (fig. 3). It consists, in part, of a light-colored easily dispersed precipitate that forms a loose cover over volcanic rock and older hydrothermal deposits. Low-lying ledges and small mounds of darker, stony-appearing sulfide minerals make up the bulk of the hydrothermal deposits. Chimney structures constructed of sulfide minerals are sparse, and no black smokers were observed. In a few photographs, however, the bottom water has a cloudy appearance suggesting that the camera was positioned near an active hot spring.

Within the vent sites, small-diameter worm tubes occur in clusters or as solitary individuals that extend upward in the water column from depressions and cracks in the hydrothermal deposits (fig. 3). An abundant but as yet unidentified fauna (fig. 3) is commonly concentrated in low areas around small sulfide mounds. Small mollusks and scattered shell debris are also visible in many photographs.

The ledges and mounds of light and dark hydrothermal precipitates with abundant tall worm tubes are close to the actual vents of hydrothermal discharge as observed in color video obtained during 1983 field operations. Limpets, crabs, and thin coatings of the light-colored precipitate are common features near the periphery of the vent areas.

Composition and Formation of Sulfide Deposits

The sulfide samples recovered from the southern Juan de Fuca Ridge are porous crystalline aggregates of zinc, iron, copper, and lead sulfides. Two types were recovered: angular slabs of somewhat friable granular dark-gray zinc sulfide with an upper crust and interlayers of iron sulfide (fig. 4), and rounded fragments of hard spongy-looking light-gray zinc sulfide. The dark-gray sulfide samples consist largely of the minerals sphalerite, wurtzite, and pyrite, with minor marcasite, galena, and chalcopyrite. Minor nonsulfide minerals include anhydrite, gypsum, barite, and amorphous silica. These minerals generally occur as thin films or clusters of elongate crystals in cavities.



Figure 3. Representative hydrothermal vent field, showing dark ledges of metallic sulfide, light-colored hydrothermal precipitate, and dense communities of mollusks and tubeworms. Scale bar is approximately 1 meter.

Both types of sulfide deposits are rich in zinc, silver, cadmium, and germanium (table 1); on land these deposits would be considered to contain ore-grade concentrations of these metals. The copper concentration in both the dark-gray and light-gray sulfide deposits is lower than in sulfide deposits from the East Pacific Rise and the Galapagos Rift, and the lead concentration in the dark-gray sulfide is higher. The zinc-rich sulfide samples from the Juan de Fuca Ridge may have been recovered from the lower temperature top or edge of a massive sulfide deposit; higher temperature copper-rich sulfide may be present at the base of the massive sulfide deposit, at higher temperature vents, or in fractures within the underlying volcanic rock.

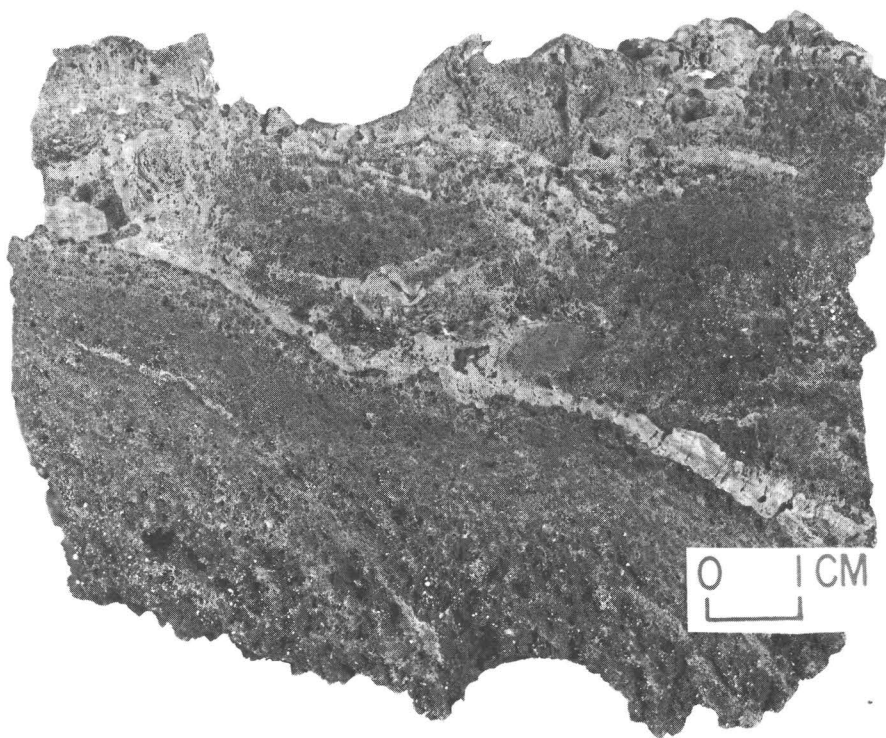


Figure 4. Dark-gray zinc sulfide slab with interlayers and crust of iron sulfide.

Table 1. Composition of massive sulfide samples from the Juan de Fuca Ridge

[Zn, Fe, Cu, and Pb analyses in weight percent; Ag, Cd, and Ge analyses in parts per million]

Sulfide material	Zn	Fe	Cu	Pb	Ag	Cd	Ge
Dark gray----	46.9	15.6	0.35	0.30	290	490	270
Light gray---	61.0	2.19	.08	.20	230	1,060	120

The presence of hydrothermal deposits on the Juan de Fuca Ridge results from large-scale circulation of seawater through the oceanic crust along the tectonically active axis of spreading (fig. 5). The movement of fluid within the circulation cell is related to a nearby heat source, presumably a body of basaltic magma at a shallow level (2–3 km) beneath the ridge. This magma chamber also supplies the lava extruded as sheetflows and pillow flows on the axial valley floor. The fluid enters on the flanks of the ridge, where normally oxidizing seawater penetrates into the cooling basaltic oceanic crust. As the fluid is heated and chemically interacts with the basaltic wallrock, it evolves into a reducing and somewhat acidic solvent capable of extracting and transporting sulfur and iron, manganese, and other metals. Near the ridge axis, the high-temperature metal-rich fluid is quite buoyant and rises along permeable zones, probably normal faults and rock fractures that crosscut the volcanic rocks of the axial valley floor. Metallic sulfides may be precipitated in vein networks beneath the sea floor as the ascending fluid begins to cool. During vigorous flow, however, the still-hot liquid spews out onto the sea floor, mixes with cold seawater, and precipitates metallic sulfides to form massive deposits. Further mixing of the hydrothermal solutions with seawater creates accumulations of iron and manganese oxides on basaltic surfaces surrounding the sulfide deposits.

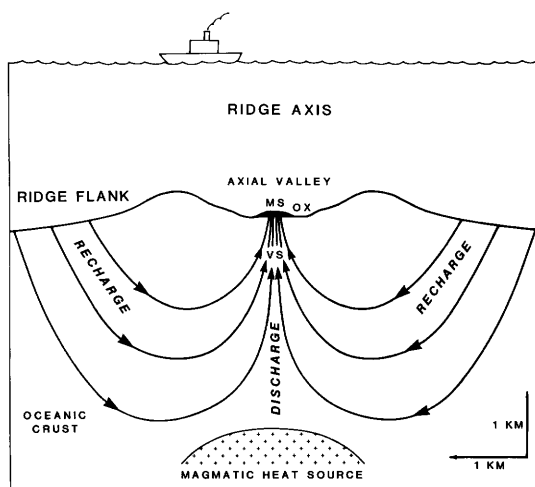


Figure 5. Model illustrating circulation of seawater through oceanic crust at a spreading center, and deposition of vein sulfide (VS) deposit beneath the sea floor and of massive sulfide (MS) and oxide (OX) deposits on the sea floor (size exaggerated). Circulation is driven by a heat source at depth, presumably a body of magma below the axis of spreading. Scale is approximate.

Ongoing Research

The resource potential of the hydrothermal sulfide deposits on the Juan de Fuca Ridge and other spreading axes is uncertain because of short- and long-term economic, political, and technologic questions. Even more fundamental, possibly, is the need for more information regarding the distribution, occurrence, and composition of deposits elsewhere on the oceanic-ridge system.

At least six vent sites were observed in the north half of the 12-km-long USGS study area of the Juan de Fuca Ridge during the 1981 cruise. The sulfide deposits there appear to form shallow ledges, less than 1 m high, with less common mounds of somewhat greater thickness. The width of the deposits traversed is 25 to 50 m, but their dimension parallel to the valley is uncertain. Their presence along all traverses in the northern part of the study area, however, suggests a nearly continuous distribution of deposits along the linear depression. These approximate dimensions and the composition of the samples recovered imply that approximately 100,000 m³, or 250,000 t, of zinc- and silver-rich sulfide minerals may lie within the study area.

Investigations planned for the 1984 field season should yield further information on the size, occurrence, composition, and method of formation of the sulfide deposits on the southern Juan de Fuca Ridge. Detailed mapping and sampling of the hydrothermal deposits and fluids, using the manned submersible Alvin, is planned for the summer of 1984.

The discovery of hot springs presently depositing metallic sulfides on volcanically and tectonically active segments of the sea floor presents a unique opportunity to apply the uniformitarian principle of geology—"the present is the key to the past." Continued research on the midoceanic-ridge system will stimulate and improve our concepts in such diverse fields as volcanology, evolutionary biology, ore genesis, mineral exploration, and deep seabed mining.

Selected References

- Edmond, J. M., and Von Damm, Karen, 1983, Hot springs on the ocean floor: *Scientific American*, v. 248, no. 4, p. 78-93.
- Bischoff, J. L., Rosenbauer, R. J., Aruscavage, P. J., Baedeker, P. A., and Crock, J. G., 1983, Geochemistry and economic potential of massive sulfide deposits from the eastern Pacific Ocean: U.S. Geological Survey Open-File Report 83-324, 24 p.
- Macdonald, K. C., and Luyendyk, B. P., 1981, The crest of the East Pacific Rise: *Scientific American*, v. 244, no. 5, p. 100-116.
- Normark, W. R., Morton, J. L., Koski, R. A., Clague, D. A., and Delaney, J. R., 1983, Active hydrothermal vents and sulfide deposits on the southern Juan de Fuca Ridge: *Geology*, v. 11, no. 3, p. 158-163.
- Spiess, F. N., Macdonald, K. C., Atwater, Tanya, Ballard, R. D., Carranza, Arturo, Cordoba, Diego, Cox, C. S., Diaz-Garcia, V. M., Francheteau, Jean, Guerrero, Jose, Hawkins, J. W., Jr., Haymon, R. M., Hessler, R. R., Juteau, Thierry, Kastner, Miriam, Larson, R. L., Luyendyk, B. P., Macdougall, J. D., Miller, S., Normark, W. R., Orcutt, John, and Rangin, Claude, 1980, East Pacific Rise: Hot springs and geophysical experiments: *Science*, v. 207, no. 4438, p. 1421-1433.

Submerged Sand Resources of Puerto Rico

By Rafael W. Rodriguez

Introduction

The industrialization of Puerto Rico, which began in earnest during the 1950's, has led to increasing demands on domestic sand and aggregate supplies needed for construction. For almost 20 years, the sand resources of Puerto Rico were exploited with little or no consideration of future needs or environmental impacts, and sand was mined from coastal areas (fig. 1). During the late 1960's, Federal and Commonwealth legislation prohibited or strictly regulated sand extraction from some of the preferred sources, such as beaches and dunes. This action, though environmentally wise, has created a drastic reduction in the amount of sand that can be mined.

A citizen's committee reporting to the Governor of Puerto Rico in 1972 (Committee on Puerto Rico and the Sea, 1974, p. 88-89) stated that: "The construction industry will be facing a crisis by the end of this century if an adequate supply of sand is not secured within the next decades." Such predictions have prompted the Government of Puerto Rico to look for alternative sources of sand.

Marine-geologic cooperative studies, conducted jointly by the USGS and the Department of Natural Resources of the Commonwealth of Puerto Rico, have shown that the sand resources of Puerto Rico are not restricted to the narrow fringe of dunes and beaches, but extend offshore on spits and parts of the insular shelf as well (Grove and Trumbull, 1978). So far, three major sand bodies have been located on the shelf. As might be expected in an area of westward-directed winds and water currents, all three sand areas are at the west ends of the islands (fig. 2). The Cabo Rojo West area is near the west end of the south coast of Puerto Rico, the Escollo de Arenas area north of the west end of Vieques Island, and the Isabela area at the west end of the north coast of Puerto Rico. These three areas probably contain the largest sand deposits on the Puerto Rican insular shelf. Estimates indicate about 80 million m³ of sand in the Cabo Rojo West deposit and about 90 million m³ in the Escollo de Arenas deposit. This total volume (170 million m³) could supply Puerto Rico's construction industry needs for about 23 years (on the basis of the current annual consumption rate of approximately 7.3 million m³/yr) and is valued at about \$3.4 billion at the current price of sand (\$15-\$25/m³). Estimates of sand volume are not yet available for the Isabela area.

Before offshore sand extraction can proceed, however, prospective alterations of the offshore bed must be reconciled with prospective damage to the beach because the offshore deposits commonly are linked to beach and inshore sand-transport systems by physical processes. Results of studies (Trumbull and Trias, 1982; Rodriguez, 1979) on the Cabo Rojo West and Escollo de Arenas deposits indicate that both deposits can be mined without detrimental effects to nearby beaches because the sand that enters these systems of shoals is lost to the

beaches. The environmental impact of such removal was assessed by determining the sources, transport paths, and environmental setting of the deposits.

Cabo Rojo

The Cabo Rojo West sand deposit lies in a shallow trough at depths of 10 to 16 m, extending 1 km southwestward and 4 km westward of Cabo Rojo. The greatest observed thickness of the sand is 9 m; it is 3 to 4 m thick over large areas. A hard-rock floor seems to be present nearly everywhere beneath the deposit.

The Cabo Rojo sand deposit is composed almost entirely of calcium carbonate. The major components are mollusk fragments and coralline algae. The deposit has probably formed in place, rather than as a result of transportation of its constituent particles. If so, then this deposit is not linked to the beach/nearshore transport system, and mining of the sand will not cause erosion of the beaches to the east and west of Cabo Rojo.

Escollo de Arenas

The Escollo de Arenas is a linear sand body extending 6 km northwestward of the west end of Isla de Vieques. The shoal relief ranges from about 1 m near-shore to about 7 m along its distal part. Water depths over the shoal generally range from 4 to 8 m except near Vieques, where depths of 2 m are common. The surface of the shoal is broken by prominent sand waves whose crests are oriented mainly parallel to the shoal's axis (fig. 3). These sand waves have wavelengths of about 100 m and amplitudes of 2 to 3 m (figs. 4, 5). The bedforms are highly dynamic and change asymmetrically twice each day in accordance with ebb and flood of the tides, that is, from northeasterly to southwesterly and back again. The current velocities over the shoal commonly exceed 140 cm/s. The high current velocities and shallow water make sampling difficult from a boat. A diver obtained sand samples from the shallowest part of the shoal by dropping from a boat upcurrent of the shoal and scooping up the sand as he was swept across the shoal; the diver was later picked up on the downcurrent side. The balanced net movement of oscillating tidal currents at the shoal's position holds the sand body in place.

The Escollo de Arenas and the nearby north and west coasts of Isla de Vieques contain surface sediment of mixed terrigenous/skeletal sand and gravelly sand. The terrigenous material (grains derived from the rocks of the island) constitutes more than 65 percent of the beach sediment. The proportion of terrigenous material decreases to about 10 to 20 percent on the northern extremity of the escollo, where the sediment composition is dominated by skeletal material (grains formed by the deposition of calcium carbonate by organisms). Both the terrigenous and skeletal grains are subangular to rounded and commonly polished by abrasion.

Terrigenous material reaches the shoal through longshore transport along the north and west coasts of Vieques. The escollo is thus a sink for converging flows of sand, and because no sediment is returned from the shoal to the adjacent beaches, mining the sand body there will in no way affect the sediment budget of the beaches.



Figure 1. North coast of Puerto Rico, showing legal sand extraction of backup dunes (A) and illegal extraction of beach sand (B). Massive sand extraction of north-coast dunes has reduced their natural capability for protection. Where dunes have been completely destroyed, storm waves have eroded the beaches and destroyed ocean-front property, settlements, and mangrove habitats.

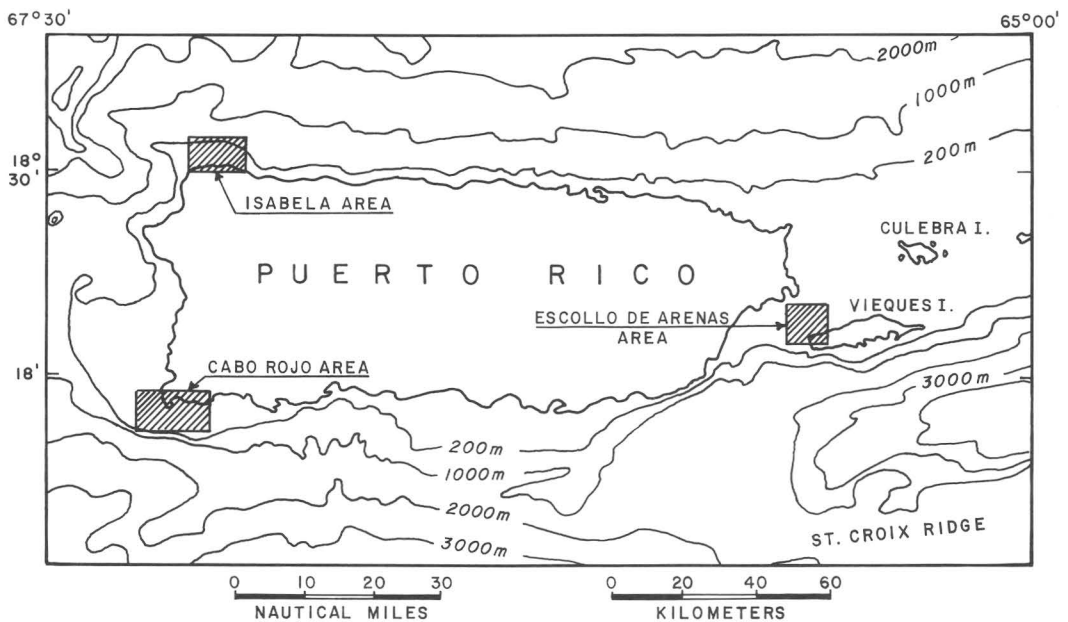


Figure 2. Index map showing locations of three major submerged sand-deposit areas on the insular shelf of Puerto Rico.

Isabela

Fieldwork has just recently started on the Isabela offshore sand deposit. Preliminary results indicate that this deposit lies on offshore terraces in water depths that range from less than 16 to more than 34 m, at distances of 400 to 2,700 m offshore, respectively. The sediment appears to be mostly terrigenous sand, extending as far as 1,800 m offshore. Because the composition of this sand is similar to that of beach, dune, and river sand onshore, the seaward extent of this sand type is interpreted to indicate the seaward extent of beach and near-shore long-term transport.

Farther offshore, the sediment of the shelf is predominantly of skeletal origin. The occurrence there of algal nodules suggests an unstable bottom, where wave action and currents occasionally move these nodules. The skeletal grains are rounded and abrasion-polished, additional evidence of active sediment movement. Wave and current measurements from the Isabela shelf are necessary to assess any impact of dredging on the deposit.

The construction industry in Puerto Rico had been facing a bleak future because of the scarcity of sand onshore. Exploitation of these submerged deposits, however, is an attractive alternative because it will relieve pressure on dunes and beaches that protect inshore areas, and will contribute to Puerto Rico's recreational and environmental resources.

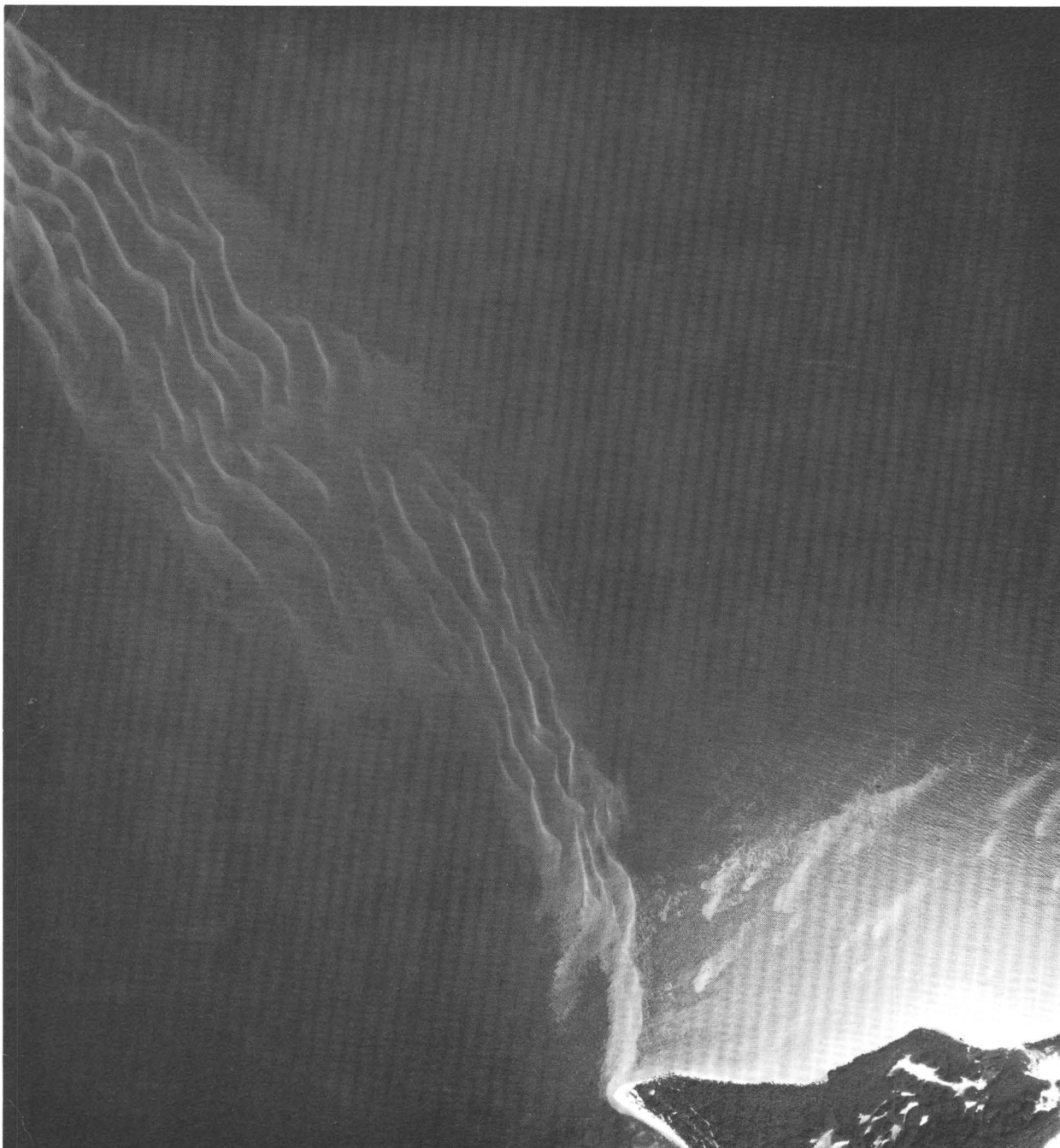


Figure 3. Escollo de Arenas, a subtidal sand body that extends some 6 km north-northwestward of Punta Arenas on the northwest coast of Isla de Vieques, east of Puerto Rico. Sinuous bedforms extending parallel to axis of shoal (and normal to direction of tidal currents) are sand waves with wavelengths of about 100 m and amplitudes of 2 to 3 m. File photo, Puerto Rico Department of Public Works.

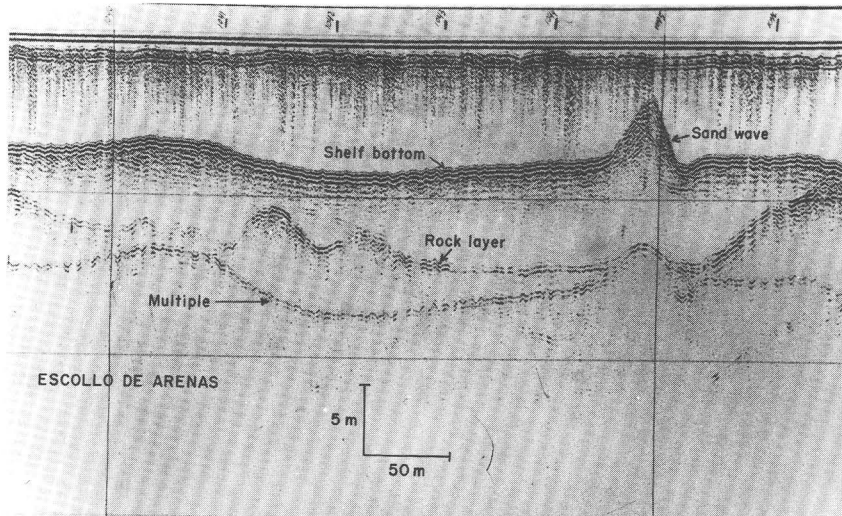


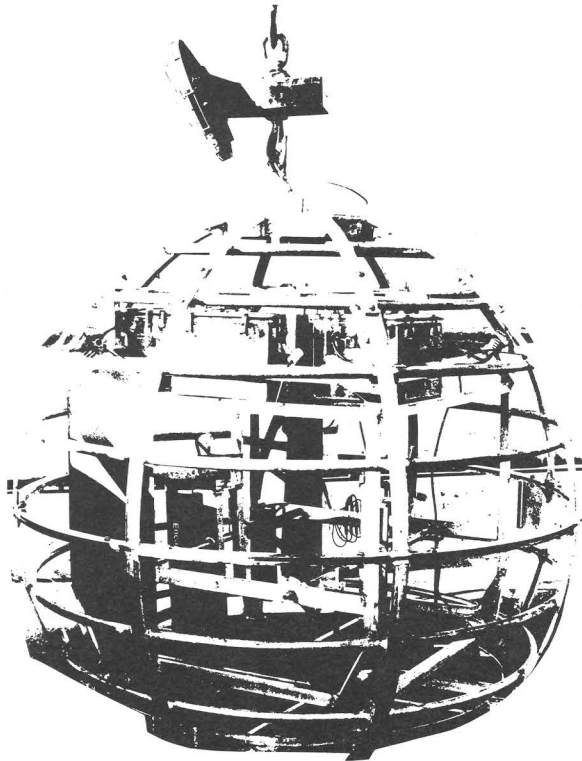
Figure 4. High-resolution seismic-reflection profile of Escollo de Arenas sand deposit, showing the escollo at its distal end. Sand wave shown has a relief of about 4 m, and thickness of the deposit at that point is about 12 m.

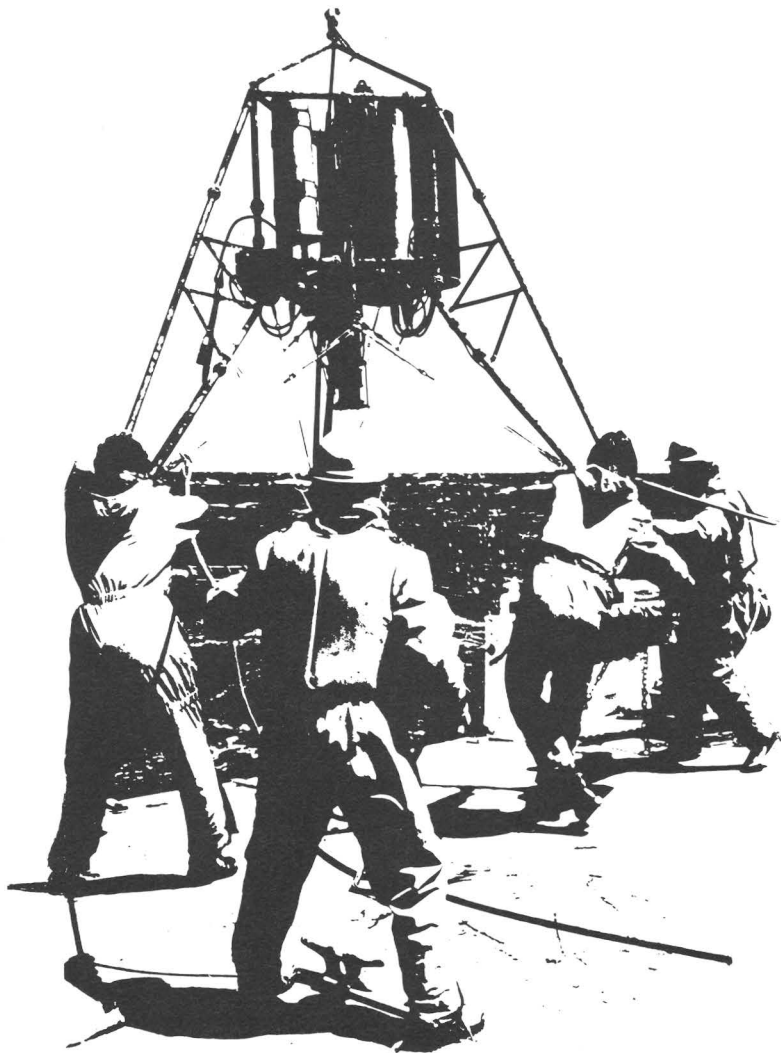


Figure 5. Symmetrical megaripples (wavelength, 1-5 m; amplitude, 0.4 m) during slack water near distal end of Escollo de Arenas. Bedforms are asymmetric in profile during both flood-tidal and ebb-tidal cycles. During flood stage, west-southwestward orientation of slipfaces of megaripples indicates bedform migration in that direction. As current direction changes during ebb-tidal cycle, megaripples reverse their asymmetry and become ebb-oriented.

References

- Committee on Puerto Rico and the Sea, 1974, Puerto Rico and the sea, an action program for marine affairs; a report to the Governor, 1972: San Juan, University of Puerto Rico and Economic Development Administration of Puerto Rico, 129 p.
- Grove, K. A., and Trumbull, J. V. A., 1978, Surficial geologic maps and data on three potential offshore sand sources on the insular shelf of Puerto Rico: U.S. Geological Survey Miscellaneous Field Studies Map MF-1017.
- Rodriguez, R. W., 1979, Origin, evolution, and morphology of the shoal Escollo de Arenas, Vieques, Puerto Rico, and its potential as a sand resource: University of North Carolina at Chapel Hill, M. Sc. thesis, 71 p.
- Trumbull, J. V. A., and Trias, J. L., 1982, Map showing characteristics of the Cabo Rojo West offshore sand deposit, southwestern Puerto Rico: U.S. Geological Survey Miscellaneous Field Studies Map MF-1393, scale 1:20,000.





GEOPROBE launch

The Submarine Landslide of 1980 off Northern California

By Michael E. Field

Introduction

On November 8, 1980, a large ($M = 7.0$) earthquake occurred 40 km off the coast of northern California. Onshore effects from the earthquake were minimal, but offshore of the Klamath River, a large area of the sea floor underwent sediment failure. Initially reported by local fishermen, the failure area was surveyed by the U.S. Geological Survey (USGS) to map its extent and to determine the specific types and causes of failure. What follows here is a synthesis of that work, emphasizing the patterns and processes observed and identifying the implications this study has for development activities on the continental shelf. This report draws heavily on previously published results (Field and others, 1982; Field and Hall, 1982) as well as research that is still in progress.

Submarine Landslides and Their Causes

“Submarine landslide,” as used here, is a general term that includes large-scale movement of sediment and rock due to some external force other than currents. Some submarine landslides are the result of downslope movement of intact blocks of sediment (commonly referred to as slumps or slides), whereas others involve internal reorganization of particles and transport as a flow. Failure in place, without significant transport of particles or blocks, also occurs by liquefaction and collapse of sea-floor sediment.

Submarine landslides are known to occur on virtually every continental margin that has been explored. On the U.S. continental margin, increased exploration related to resource and environmental studies for offshore oil and gas development has resulted in the identification of numerous landslides. Although no clear relation between failures and their causes has emerged, some patterns of failure location and geologic setting have been established. For example, thick deposits of rapidly accumulating sediment are susceptible to failure because of high internal pore pressures and low strength due to gas content, clay mineralogy, and (or) high water content. Initiation of failure generally requires an external triggering force. In tectonically active areas, earthquakes are thought to cause submarine landslides, although only a few such occurrences have been documented. In more stable shallow-water environments, such as the Gulf of Mexico, cyclic loading due to passage of storm waves is believed to be responsible for initiating failure. Static loading due to gravity is also important in causing submarine landslides, but this relation has on occasion led to the erroneous conclusion that relatively steep (greater than 2°) slopes are required for failure to occur or that steep slopes are always more prone than gentle slopes to failure.

Setting of the Northern California Submarine Landslide

The northern California Continental Shelf (fig. 1) exhibits both active tectonism and relatively high rates of sedimentation. Overthrusting of the Gorda plate by the North American plate and right-lateral slip along the Gorda Escarpment generates high levels of seismicity and continuous deformation (Silver, 1971; Couch, 1980). The data of Couch and others (1974) show that since 1920 an average of one earthquake of $M \geq 6.0$ per decade has occurred. Before the 1980 earthquake, two other events of $M > 7.0$ were reported in the area (Real and others, 1978). The shelf off the Klamath River is composed of a complex sequence of folded and faulted Neogene and lower Quaternary strata overlying rocks of the Franciscan complex and overlain, in turn, by undeformed seaward-dipping sediment of late Pleistocene and Holocene age. Upper Quaternary sediment lies on a Pleistocene erosional unconformity and attains a thickness of 20 to 50 m in water depths of 30 to 70 m offshore of the Klamath River (Field and others, 1980). This lobe-shaped sediment body presumably is derived largely from sediment delivered to the coast by the Klamath River, a major contributor of sediment to the northwestern U.S. Continental Shelf. Two main surficial-sediment types occur on the shelf in this area: Muddy sand inshore of the 60-m isobath, and sandy-clayey silt from there seaward (Field and others, 1980; Welday and Williams, 1975).

The Earthquake of November 8, 1980

At 2:27 a.m. P.s.t. on November 8, 1980, a large-magnitude earthquake occurred 60 km west of Trinidad, Calif., on the continental margin. Estimates of the magnitude of this earthquake range from 6.5 (M_L) to 7.2 (M_s). Some damage occurred onshore, but for the most part the effects were relatively minor in comparison with onshore earthquakes of comparable size. Rockfalls and sand boils were reported along the coast, and south of Eureka a bridge on U.S. Highway 101 collapsed (Lajoie and Keefer, 1981). No other immediate reports of damage were received. Several days after the earthquake, however, commercial fisherman in Crescent City reported the presence of one or more northwest-trending scarps offshore of the Klamath River. This area is a smooth, featureless depositional environment that is heavily trawled by fishermen, and the sudden appearance of scarps suggests a causal relation to the earthquake. A survey of the area was conducted in mid-December by the research vessel *S. P. Lee*, using high-resolution seismic-profiling equipment, and at that time several tracklines which had been surveyed before the earthquake were reoccupied. The area was surveyed again in May and October 1981, using high-resolution profiling equipment, side-scan sonar, and bottom cameras.

Surveying the Landslide: Anatomy and Causes

Form and Features

Results from three cruises to the area show that the submarine landslide, or failure zone, is highly complex in shape and origin, and this complexity indicates various processes at work. The part of the shelf that failed appears in cross section as a 1- to 2-km-wide horizontal terrace lying in 60 m of water (fig. 2). The

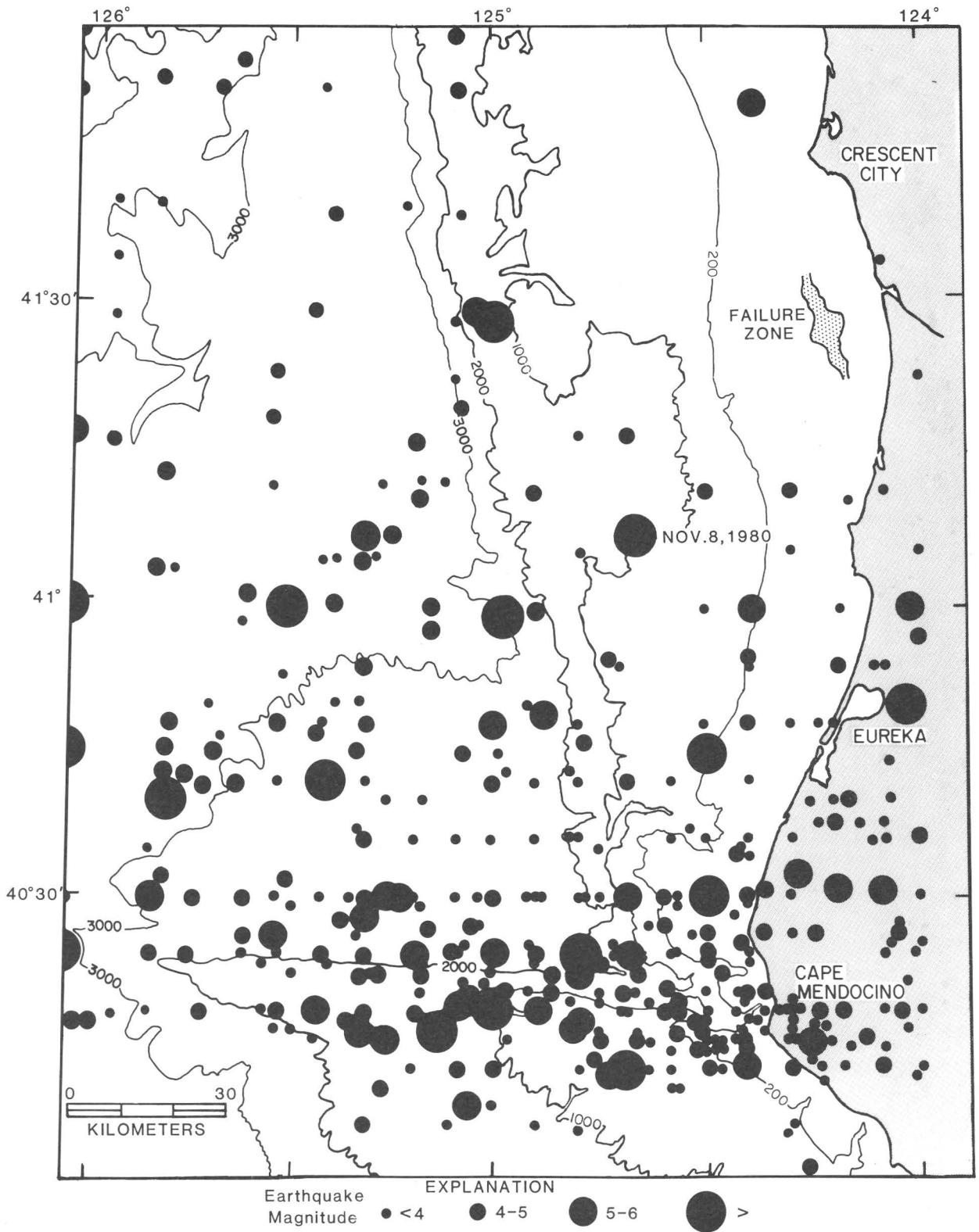


Figure 1. Northern California continental margin, showing epicenters of historical earthquakes (from Couch and others, 1974), and locations of the 1980 earthquake and landslide area off the Klamath River.

seaward edge of this failure terrace is defined by a 1- to 2-m-high toe ridge that is nearly continuous for a distance of 10 to 15 km along slope. Comparison of high-resolution seismic-reflection profiles obtained immediately after the earthquake with profiles collected a year before illustrates the sudden and distinct changes that occurred on the shelf (fig. 2). The slope of the sea floor in the area of failure is approximately 0.25° . Although the subsurface depth of failure is not precisely known, geophysical data indicate that it is at least 5 m and no more than about 15 m.

In map view, the landslide zone is irregular, measures about 2 by 20 km, and extends northwestward along the shelf, parallel to the coast and to shelf contours (figs. 1, 3). The landward side of the zone is marked in some places by a subtle scarp or a change in slope. Various features on and seaward of the failure terrace provide clues as to the mechanisms and processes involved in failure; these features are: the toe ridge, pressure ridges, sand boils, collapse depressions, sediment flows, and gas seeps. A prominent toe ridge and an associated compressional zone of pressure ridges are evident throughout much of the failure zone, particularly in the southern part (fig. 3). Seaward of the toe ridge is a deformed zone, as much as 100 m wide, of sediment consisting of ridges lying parallel or subparallel to the orientation of the toe ridge (figs. 3, 4). Side-scan records collected in May 1981 (6 months after the earthquake) show evidence of the eruption of sand boils onto the failure terrace. Discrete rings, some superimposed on one another, measure from a few meters to as much as 25 m in diameter. Sand boils are commonly observed on land after large earthquakes and show a similar range in size (Herd and others, 1981). In many areas the terrace has a mottled appearance that likely results from wave and current modification of the sand boils.

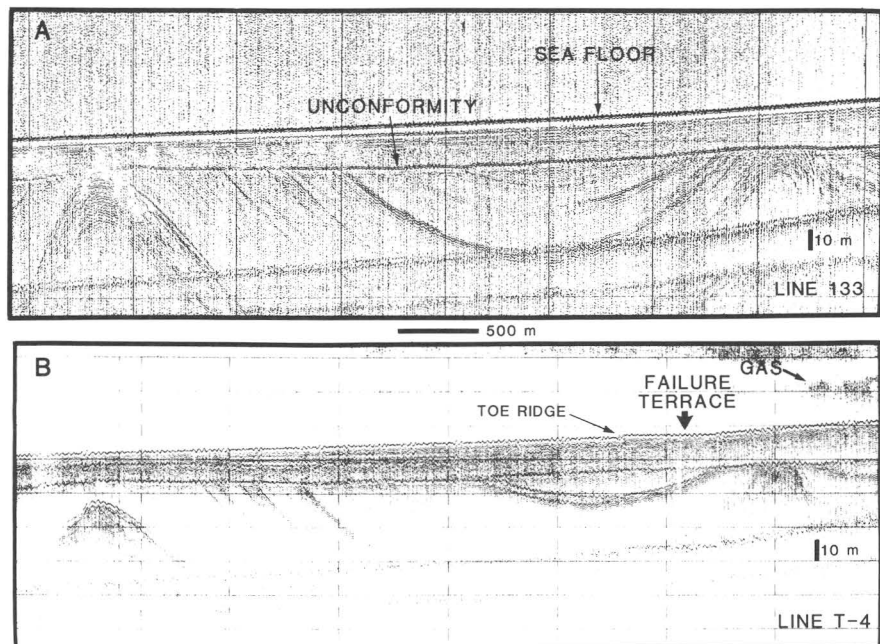


Figure 2. High-resolution seismic profiles obtained before (A) and after (B) the earthquake along the same trackline. Note coincidence of submarine structure. In figure 2B, note the presence of a toe ridge (scarp) and a nearly flat failure terrace.

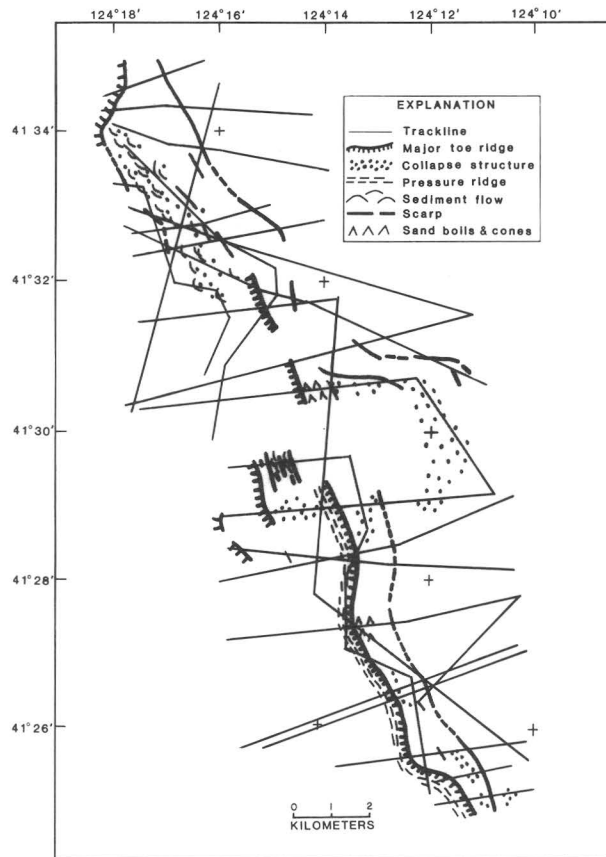


Figure 3. Map showing shape and individual features of the submarine landslide on the Klamath River prodelta, based on high-resolution geophysical data, side-scan sonar, and bottom photography.

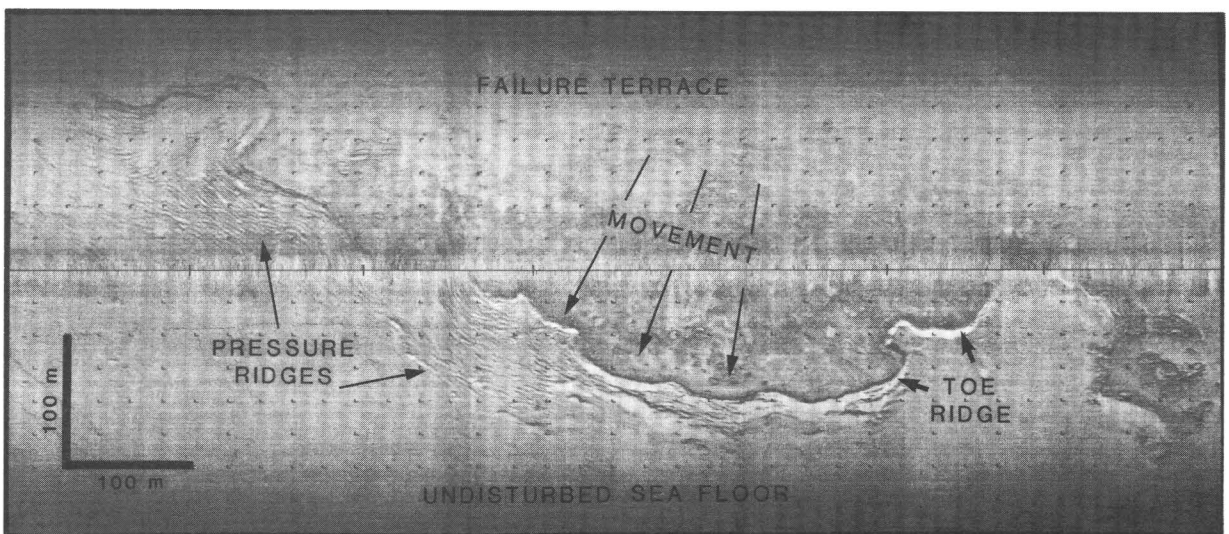


Figure 4. Side-scan sonar record from the landslide zone, showing surface pattern of toe ridge, failure terrace, and pressure ridges.

Collapse of sediment on the failure terrace occurred throughout the area and at a broad range of scales. Individual areas of collapsed sediment coalesced to form minor scarps generally less than 0.5 m high. Some collapse structures measure less than several meters across; others are approximately 25 m across and form shallow irregular depressions that are roughly circular to elliptical. Sonographs and bottom photographs from the north half of the failure zone show evidence of sediment-flow deposits. These deposits are shaped into overlapping lobes measuring as much as several hundred meters across; they result from the flow of fluidized sediment for short lateral distances. Individual deposits are generally of low relief (less than 0.5 m) and show subtle variations in sediment texture. As many as five successive overlapping lobes were identified in one locality. Most deposits that were interpreted to result from surface flowage do not show evidence of having moved significant horizontal distances (that is, more than 100 m).

There is also evidence, in the general vicinity of the landslide zone, of seepage of hydrocarbon gases. This evidence appears on both high-resolution seismic-reflection records and on sonographs obtained at intervals of 1, 6, and 11 months after the earthquake; the seeps are thought to derive from a thermogenic source. Gas, which appears on sonographs as black smears, is evident from the presence of bubbles dispersed in the water column, small vents, and several large active seeps (Field and Hall, 1982).

Styles of Failure

The complex and varied features in the failure zone all provide information about the processes that occurred shortly after the earthquake. Apparently the progression of failure was complex, and, in fact, several styles of failure are indicated by the anatomy of the landslide deposit. The styles of failure, as reported by Field and others (1982), are lateral spreading, liquefaction, and sediment collapse and flowage. Lateral spreading is inferred from the presence of a nearly continuous toe ridge that bounds the flat-lying failure terrace, the gentle slope, and flat surface, and the presence of a zone of compression (pressure ridges) lying seaward of the failure zone. The occurrence of lateral spreading in itself suggests shallow-seated liquefaction, as does the presence of sand boils and collapse features. Overlapping sediment lobes suggest that fluidization of sediment occurred as part of the failure process. Figure 5 shows a block diagram of these processes. Subsurface liquefaction is inferred at shallow depths as a result of excess pore pressures in sand generated by the earthquake and, possibly, enhanced by the presence of gas. The primary mode of failure, liquefaction, resulted in lateral spreading of approximately 800×10^6 m³ of sediment and ejection of sand onto the sea floor. Following liquefaction, or as a part of the process, reorganization of the subsurface sand into a denser packing arrangement and expulsion of pore fluids and gases occurred and led to collapse and flow of surface sediment.

Implications for Offshore Planning

This study documents the occurrence of large-scale failure of continental-shelf sediment in response to a major earthquake. The landslide zone covers an area of 20 to 40 km² and is 5 to 15 m thick. Although the thickness of disruption was relatively small, it certainly was sufficiently large to cause damage to pipelines, anchoring systems, and, possibly, to supports of offshore platforms.

Several important aspects of the landslide are significant to understanding and planning for the likelihood of similar events occurring:

1. Failure occurred off the Klamath River on a nearly flat (0.25°) area of the sea floor. Much of the continental margin has greater declivities ($1.0^\circ - 4.0^\circ$) and thus is even more susceptible to failure by earthquake shocks (assuming that sediment thickness and composition are similar).
2. The earthquake had a magnitude of about 7.0 and occurred 60 km distant from the landslide. Earthquakes of 10 times that force and much closer to the California shelf have occurred in the past and are probable in the future; thus, the probability of similar or greater landslide occurrences in the future is high.
3. Late Quaternary sediment is only 20 to 30 m thick at the landslide site; thus, thick accumulations of modern sediment are not requisite for failure. This thickness of late Quaternary sediment is equaled or exceeded in many areas of the California Shelf and Slope.

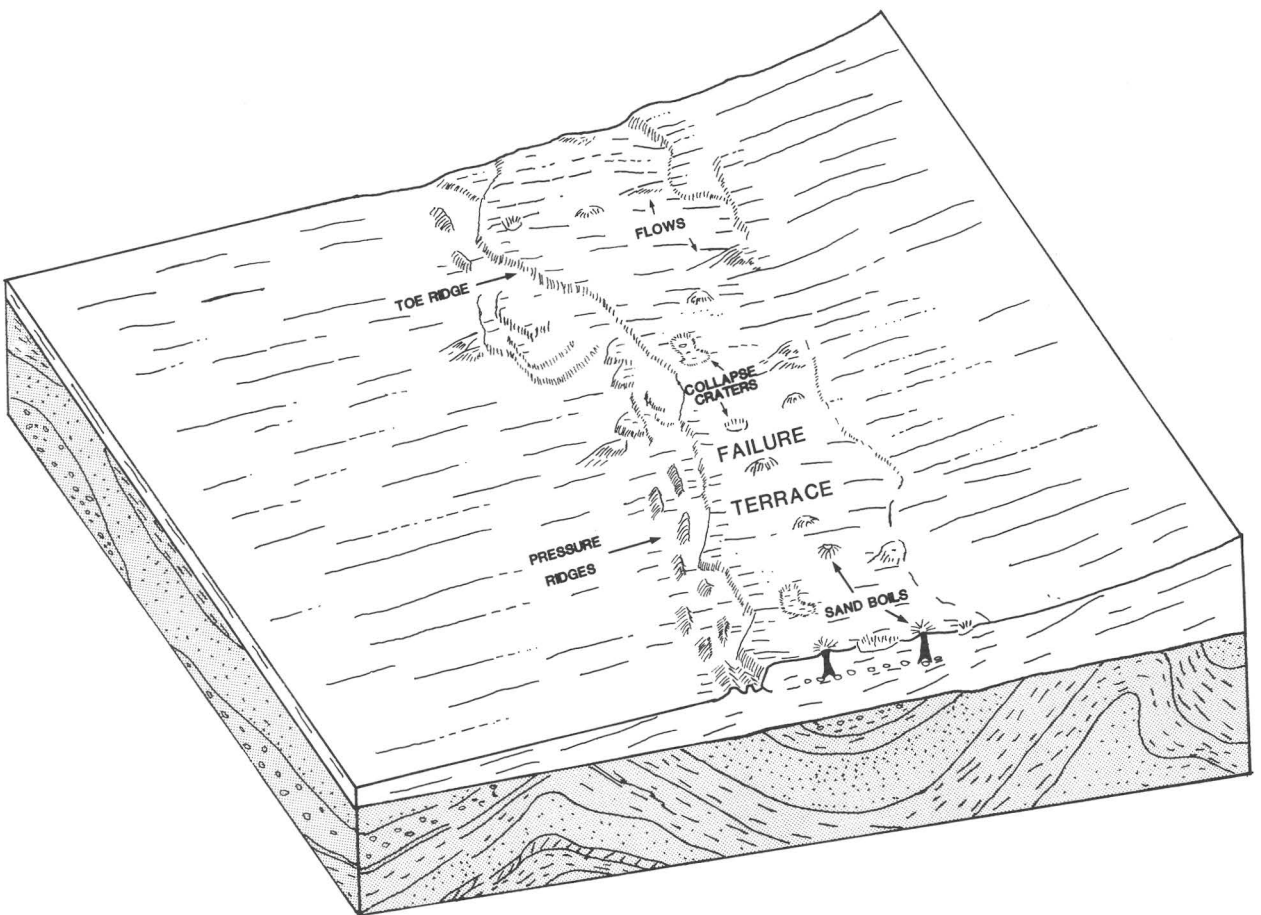


Figure 5. Conceptual block diagram showing variety and types of features observed in the failure zone.

4. Failure occurred in Holocene terrigenous sediment on the prodelta of a medium-size river. Many other such prodeltas exist in seismically active areas of the U.S. Pacific coast, and these are also probable sites of submarine landslides.
5. The surface manifestations of the landslide were small (maximum relief, 2 m) and may go undetected by conventional geophysical surveys. Furthermore, the failure occurred in relatively shallow water (60 m) and is subject to smoothing and obliteration of diagnostic features by waves and currents and by subsequent deposition. Therefore, absence of evidence of submarine landslides in other shallow-shelf environments does not necessarily indicate that failure has not taken place; it merely indicates that failure has not occurred within the past several years or decade.

References

- Couch, R. W., 1980, Seismicity and crustal structures near the north end of San Andreas fault system, *in* Streitz, Robert, and Sherburne, R. W., eds., Studies of the San Andreas fault zone in northern California: California Division of Mines and Geology Special Report 140, p. 139–151.
- Couch, R. W., Victor, Linda, and Keeling, Kenneth, 1974, Coastal and offshore earthquakes of the Pacific Northwest between 39° and 49°10' N latitude and 123° and 131° W longitude: Corvallis, Oregon State University, School of Oceanography, 67 p.
- Field, M. E., Clarke, S. H., Jr., and White, M. E., 1980, Geology and geologic hazards of offshore Eel River Basin, northern California continental margin: U.S. Geological Survey Open-File Report 80-1080, 80 p.
- Field, M. E., Gardner, J. V., Jennings, A. E., and Edwards, B. D., 1982, Earthquake-induced sediment failures on a 0.25° slope, Klamath River delta, California: *Geology*, v. 10, no. 10, p. 542–546.
- Field, M. E., and Hall, R. K., 1982, Sonographs of submarine sediment failure caused by the 1980 earthquake off northern California: *Geo-Marine Letters*: v. 2, no. 3–4, p. 135–142.
- Herd, D. G., Youd, T. L., Meyer, Hanjürgen, Arango, J. L., Person, W. J., and Mendoza, Carlos, 1981, The great Tumaco, Colombia, earthquake of 12 December 1979: *Science*, v. 211, no. 4481, p. 441–445.
- Lajoie, K. R., and Keefer, D. K., 1981, Investigations of the November 1980 earthquake in Humboldt County, California: U.S. Geological Survey Open-File Report 81-397, 30 p.
- Real, C. R., Topozada, T. R., and Parke, D. L., 1978, Preliminary earthquake epicenter map of California, showing events from 1900–1974 equal to or greater than magnitude 4.0 or intensity V: Sacramento, California Department of Conservation, California Resources Agency Open-File Report 78-4 SAC, scale 1:1,000,000.
- Silver, E. A., 1971, Tectonics of the Mendocino triple junction: *Geological Society of America Bulletin*, v. 82, no. 11, p. 2965–2977.
- Welday, E. E., and Williams, J. W., compilers, 1975, Offshore surficial geology of California: California Division of Mines and Geology Map Sheet 2, scale 1:500,000.

Undercurrents and Nearshore Erosion During Storms

By Asbury H. Sallenger, Jr.

Introduction

During storms, offshore transport of sand exposes dunes and cliffs to erosion by storm waves. This process undermines the foundations of coastal structures and exposes structures directly to forces of breaking waves. The importance of this offshore sediment transport was demonstrated on both the east and west coasts of the United States during the severe storms of the fall and winter of 1982-83. For example, during two storms in October 1982 on the coast of North Carolina, 12 houses were undermined by erosion and either severely damaged or destroyed (fig. 1). As a result of many winter storms in California, 27 homes and 12 businesses were totally destroyed, and 3000 homes and 900 businesses were damaged (California Coastal Commission, unpub. data, 1983). Damage to coastal structures in California during the winter of 1983 was greater than \$100 million.

The processes which cause sand to be transported offshore during storms are not well understood. Without this understanding, it is difficult to predict the amount of nearshore erosion that will occur during a given storm. The USGS is conducting research with the ultimate objective of developing this predictive capability. The purpose of this chapter is to present some recent findings of this research. I will focus on the nature of surf-zone circulation during storms and will suggest that this circulation may be important in forcing offshore sediment transport.

In the 1920's, the journal *Science* served as a forum for discussions on how water circulates in the surf zone. A popular hypothesis of the period was that water flowed seaward as a steady "undertow." Surf-zone circulation was thought to be in the vertical plane, with landward flow high in the water column and seaward flow, or "undertow," at depth. However, in the *Science* articles, observations were presented that were inconsistent with steady seaward flows at depth in the surf zone. Rather, circulation was observed to be in the horizontal plane, with water flowing seaward in narrow, rapidly flowing "streams" spaced on the order of 100 m along the shoreline. In areas between streams, net flow was slowly landward. These streams later became known as rip currents.

The consensus which emerged from the discussions in *Science* prevails today: Surf-zone circulation is in the horizontal plane, and water returns seaward in rip currents. Though the term is still commonly used by the public, undertow is generally considered by the scientific community to be a myth. In recent years, however, a few sets of measurements have been obtained which suggest the possible importance of circulation in the vertical plane.



Figure 1. Nags Head, N.C., showing 2 of 12 houses destroyed during the October 1982 storms.

In this chapter, I present data obtained during a storm, showing the existence of strong offshore-directed undertow-like flows, which I call undercurrents. These undercurrents may contribute, along with other processes, to the seaward transport of sediment during storms.

Experiment Description

During October 1982, a comprehensive field experiment was conducted to determine the processes which cause nearshore morphology to change during storms. The experiment was conducted at the Field Research Facility (FRF) of the U.S. Army Corps of Engineers' Coastal Engineering Research Center in Duck, N.C. Participating in the experiment were investigators from the USGS, U.S. Army Corps of Engineers, Oregon State University, and the University of Washington. The USGS and Corps of Engineers jointly funded the USGS involvement in the experiment.

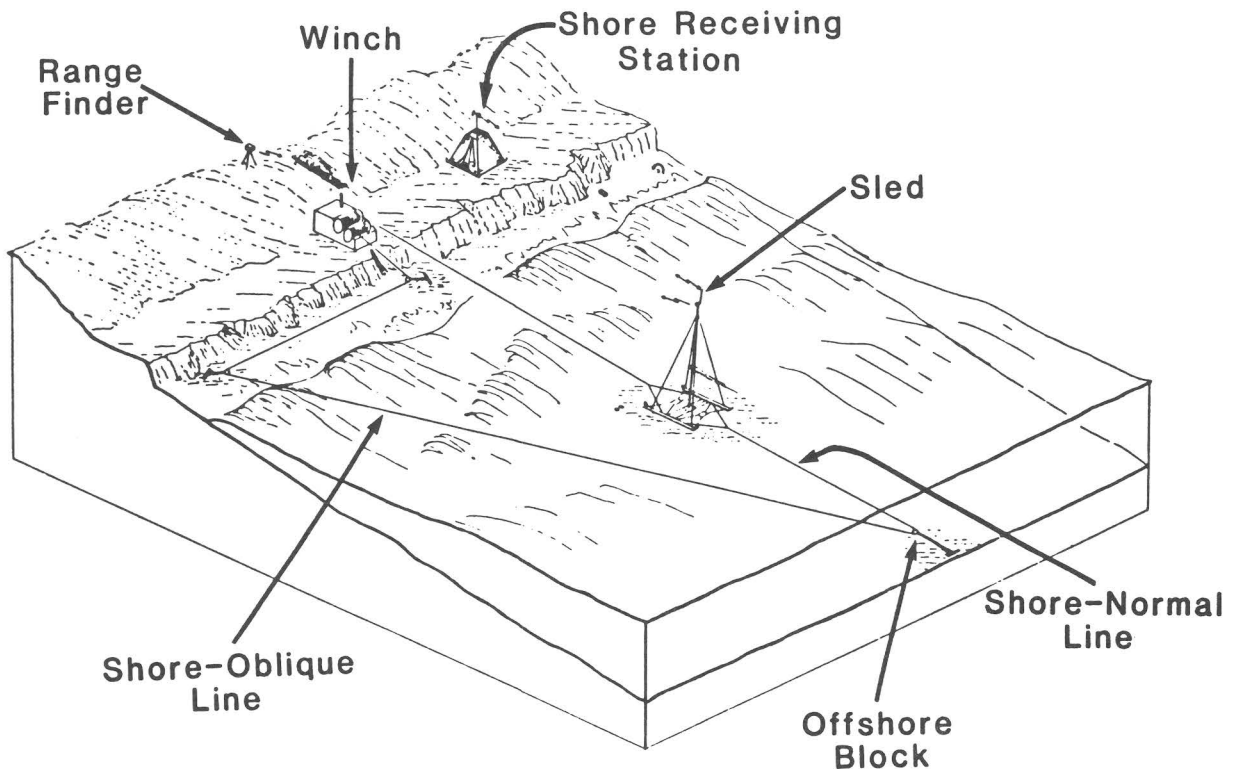


Figure 2. Sketch showing how the USGS sled system works. The sled is connected to the shore-normal side of the triangular line arrangement and is pulled offshore by one drum of the winch and onshore by the other drum.

One goal of the USGS part of the experiment was to measure the vertical profile of cross-shore flow at different locations across the surf zone during a storm. These measurements were obtained with the USGS sled system, which consists of an instrumented sled that was towed along the bottom, both offshore and onshore, with a double-drum winch and triangular line arrangement (figs. 2, 3). On the sled, electromagnetic currentmeters were mounted in a vertical array at 0.5, 1.0, and 1.75 m above the bottom. The data were telemetered to a shore receiving station where they were recorded. As the sled moved along the shore-normal transect, the nearshore profile was measured, using an infrared range-finder on the beach and optical prisms mounted on top of the sled's mast. The USGS sled system has successfully obtained surf-zone data in plunging breakers with heights greater than 5 m. The sled system was set up 500 m north of the FRF's pier to avoid effects that the pier has on local flows and sediment transport.

In addition to the flowmeters on the sled, two additional flowmeters were located on fixed mounts spaced along the beach, located 13 and 43 m north of the sled line and about 30 m offshore. These analog signals were hardwired to an onshore station, where they were digitized and recorded.



Figure 3. The USGS sled is 5.5-m long, 4.0-m wide, and weighs about 800 kg in air. A 10-m mast is mounted vertically on the sled and is held in place by guy wires.

Results

The flow data discussed here were obtained during a storm in October 1982. Northeasterly winds with a maximum speed of 13 m/s generated offshore significant wave heights of about 2.5 m (fig. 4). Wind decreased in speed over a 3-day period, but offshore significant wave heights remained high, ranging from 2.0 to 2.5 m. Waves changed from short-period high-energy sea waves on day 1 of the storm to long-period, high-energy swell waves by day 3 (fig. 4).

Prior to the storm, a small-scale longshore bar was present (fig. 5). Profiles measured to either side of the sled line showed the bar to be reasonably linear and shore parallel. During the 3-day period when wave heights were large (days 1-3 on fig. 4), the bar became much better developed and migrated offshore about 57 m. Owing to the large waves, we were unable to determine the three-dimensional configuration of the bar during the storm. There is some evidence in the literature, however, for the dominance of linear bars during periods of high energy, with crescentic bars forming during periods of decreasing energy. In fact, after the storm (after day 3), the bar became progressively crescentic, a configuration consistent with an initially linear bar during the storm. In any case, assuming a linear shore-parallel bar during the storm, the observed offshore migration of the bar represented a net offshore sediment transport.

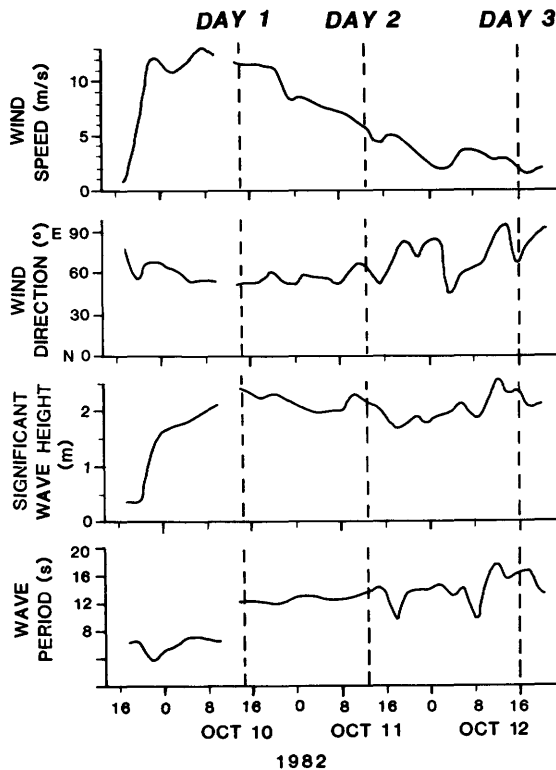


Figure 4. Wind and wave characteristics for the storm. Dashed vertical lines denote times at which flow measurements were made each day.

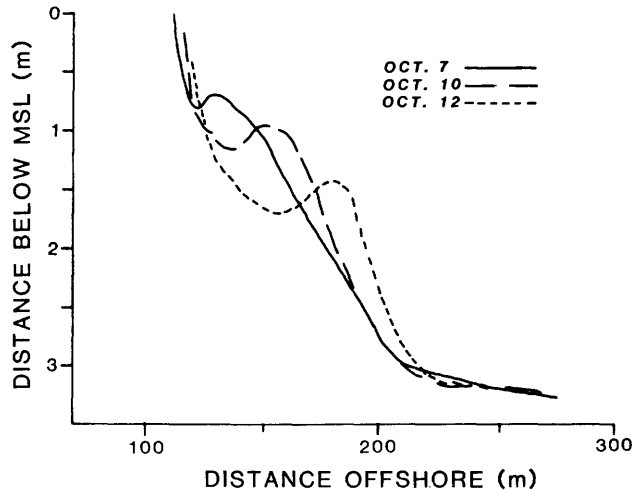


Figure 5. Nearshore profiles measured with USGS sled system before and during the October storm of figure 4. Vertical datum is mean sea level (MSL).

Vertical profiles of time-averaged flow measured at the bar crest (fig. 6A) and bar trough (fig. 6B) show, for all three days, well-developed offshore mean flows, or undercurrents. Over the bar crest, the flow profiles were nearly identical for all three days; maxima in offshore flow of about 35 cm/s occurred in about 75 percent of the total water depth (fig. 6A). In the bar trough, offshore mean flow on day 1 reached a maximum velocity of nearly 50 cm/s; trough flow on the other two days decreased to maximum velocity of about 30 cm/s.

Note that undercurrents occurred in the lower 80 percent (or more) of the stillwater depth (figs. 6A, B). Of course, there must have been landward mass transport which balanced seaward mass transport associated with these undercurrents. This landward transport evidently occurred high in the water column above the level of wave troughs in crests of breaking waves. However, I do not consider here flow data obtained above the trough level, because the reliability of Eulerian flow measurements from wave crests, where the flowmeter becomes subaerial during part of the wave phase, is uncertain.

During the storm, there was no evidence for significant circulation in the horizontal plane. For the 3-day period, the flowmeters located on fixed mounts along the shoreline measured mean offshore flows. It seems unlikely that these flows, together with the mean offshore flows measured on the sled line, were the result of nearshore circulation cells with rip currents equally spaced along the beach. In any case, such circulation cells were not apparent visually. Such mean offshore flows were, however, consistent with the presence along the beach of undercurrents.

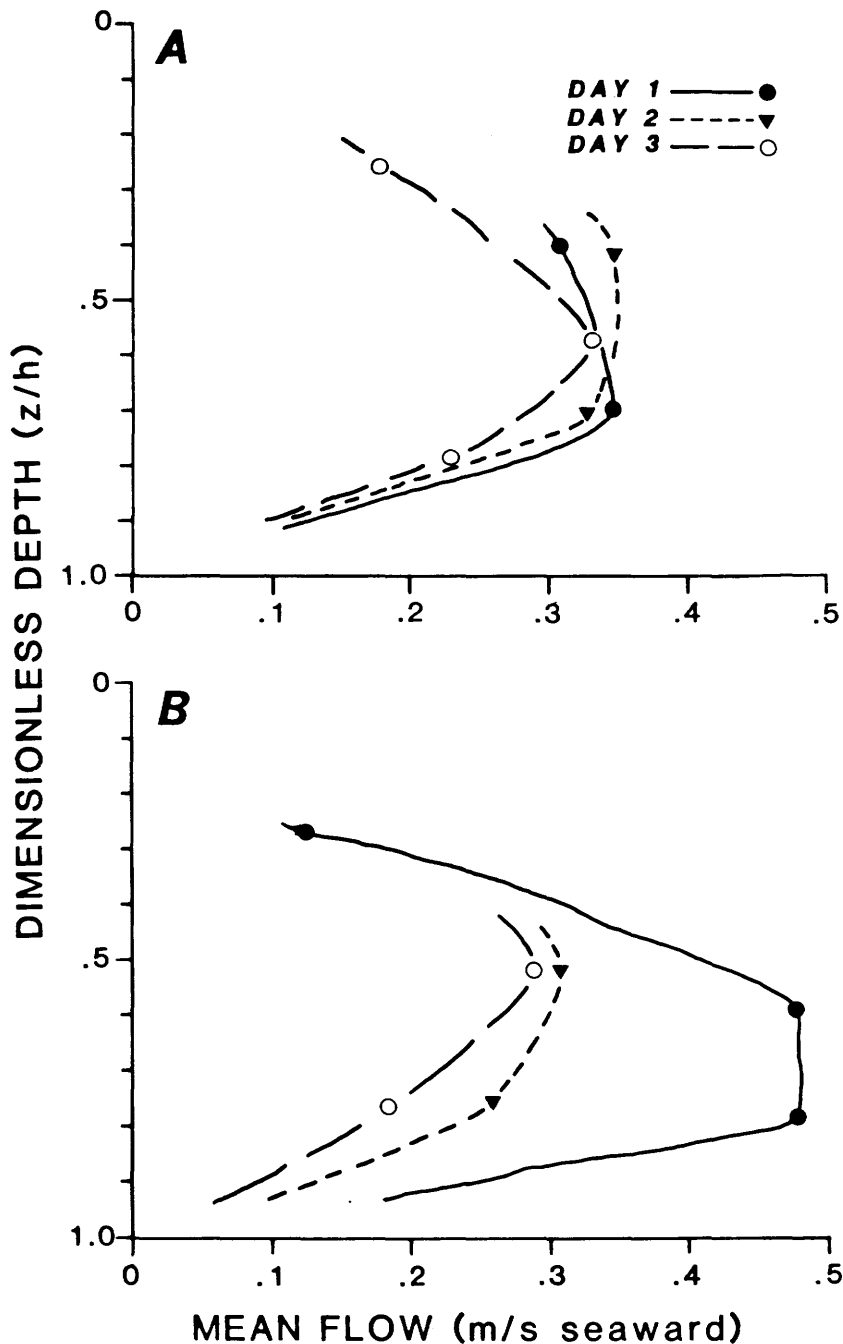


Figure 6. Vertical profiles of mean flow over bar crest (A) and in bar trough (B) for the three days indicated in Figure 4. Dimensionless depth is the depth of measurement, measured positively downwards from still-water level (z), divided by the total depth (h). Record lengths over which the means were calculated were 34.1 minutes. Note that because the bar moved seaward during the storm the measurement locations also moved seaward. All flow records were obtained in the surf zone; the largest waves were breaking several hundred meters farther offshore than the bar crests plotted in figure 5. All data used in plotting the flow profiles of figure 6 were obtained from flow meters that were continuously submerged; that is, data were not used if a flow meter became subaerial in any part of the wave phase.

Because the flow data were gathered under onshore wind conditions that ranged in intensity from strong to weak, the role of wind in possibly driving circulation in the vertical plane can be assessed. Strong onshore winds can drive water onshore at the surface and a return flow, or undercurrent, at depth. The strong onshore winds on day 1 (fig. 5) may have contributed to the particularly strong undercurrent observed in the trough on that day (fig. 6). Undercurrents persisted, however, in the absence of strong winds on days 2 and 3. Undercurrents are likely driven by wave related processes where net landward mass transport in the crest of breaking waves balances the seaward mass transport associated with undercurrents.

Preliminary analyses of additional data under lower energy conditions indicate that undercurrents are best developed in the surf zone when offshore waves are large. This observation may explain the paucity of previous measurements of undercurrents because, until recently, no adequate means were available to obtain flow measurements in the surf zone under high-energy conditions. Under lower energy conditions, rip currents were apparent, and nearshore circulation appeared to be in the horizontal plane.

As previously noted, during the period when we were measuring significant undercurrents, the bar migrated offshore (fig. 4). Undercurrents may be very important in migrating the bar offshore and thus in driving net offshore sediment transport. However, the mechanisms whereby these mean flows, superimposed upon wave oscillations, drive offshore sediment transport are presently unclear.

Conclusions

Under-high energy conditions, surf-zone circulation can be in the vertical plane, with strong mean offshore flows, or undercurrents, at depth. Under nonstorm conditions, surf-zone circulation in the horizontal plane seems to prevail. Undercurrents should prove to be significant in transporting sediment offshore under high-energy conditions and thus may be effective in eroding nearshore areas during storms.

Environmental Monitoring on Georges Bank: Trace-Metal Analysis of Bottom Sediment

By Michael H. Bothner

Introduction

Petroleum exploration in the rich fishing grounds of Georges Bank has always been controversial. Exploratory drilling was delayed in the courts until July 1981 because questions about the potential impact of drilling on the proven-renewable biologic resources could not be answered. Included in the settlement of the dispute between the U.S. Department of the Interior and protesting State and environmental groups was the creation of a Biological Task Force (BTF), comprising representatives from five Government agencies (the U.S. Geological Survey, the U.S. Bureau of Land Management, the Fish and Wildlife Service, the U.S. National Oceanic and Atmospheric Administration, and the Environmental Protection Agency). The BTF was to recommend studies which would evaluate the environmental impact of exploratory drilling and provide early warning of adverse effects.

A program for monitoring Georges Bank was designed by a subcommittee of the BTF (assisted by scientists from Federal agencies, research institutions, universities, and industry) and was recommended by the BTF in April 1981. The major objective of this program was to determine whether or not exploratory drilling would cause adverse effects on the benthic (bottom dwelling) animals. Emphasis was placed on the animals that live in and on the sea floor because a large fraction of discharged drilling mud quickly sinks to the bottom, where, because of their low mobility, benthic animals are most likely to be exposed to the mud. In addition, benthic organisms are an important food source for the commercial species of fish and shellfish on Georges Bank.

Study Program

In support of this major objective, the Georges Bank Monitoring Program was designed to address the following specific questions: (1) What are the nature, chemical composition, and amount of material discharged during drilling operations? (2) where do drilling discharges accumulate, and in what concentrations? (3) what are the predrilling concentrations of chemical contaminants (both organic and inorganic) in sediment and benthic organisms, and how do contaminant concentrations change as drilling proceeds? and (4) what changes, if any, in the populations or species of benthic organisms are attributable to offshore drilling?

An extensive field program has been conducted to address these questions. Sampling cruises were made during each season of the year, beginning in July 1981 just before the drilling began on Georges Bank, and are to continue until May 1984. The sampling locations were chosen on both a regional and a site-specific scale.

Regional stations (fig. 1) were selected to assess changes in environmental parameters over a broad area during the entire period of exploratory drilling and any subsequent production drilling. Some stations were located in such areas as the "Mud Patch" south of Martha's Vineyard (Bothner and others, 1981), the deep part of the Gulf of Maine, and the heads of Lydonia and Oceanographer Canyons, in which sediment transported away from Georges Bank is expected to accumulate. Most of these regional stations were oriented in three transects across the south flank of the bank. The mean current flow on this part of the continental shelf is to the southwest (Butman and others, 1982); thus, transect 1 is an up-stream control transect which is not likely to be affected by drilling discharges. Transect 2 cuts through the blocks leased in Sale 42, and transect 3 is downstream from the drilling activity.

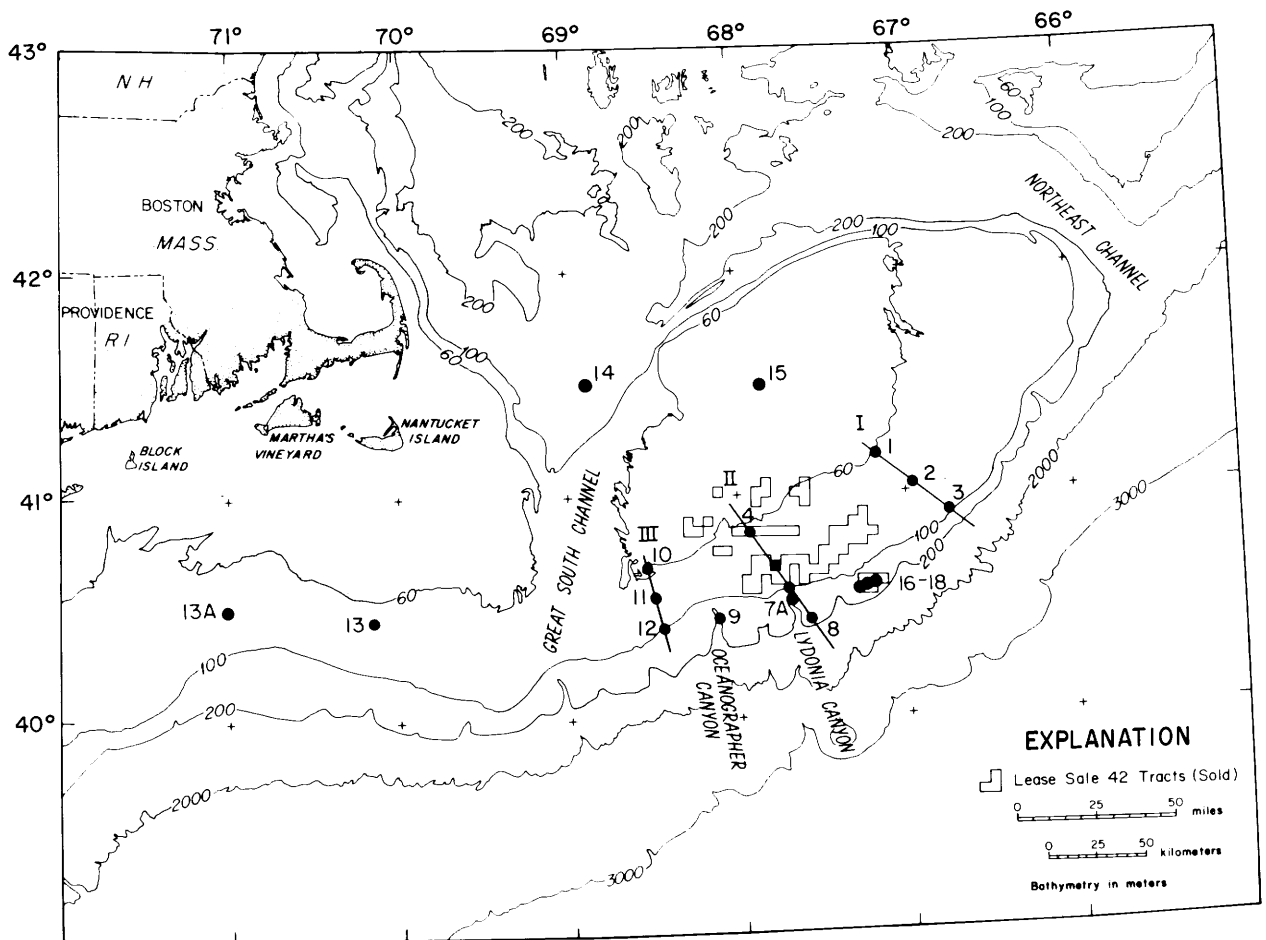


Figure 1. Georges Bank region, showing locations of sampling stations. Site-specific array in Block 312 is centered at station 5.

In addition to the regional stations, more detailed sampling was conducted around two drillsites. A total of 29 stations were selected around the drill rig in Lease Block 312 (fig. 2), and 3 stations were chosen at the drill rig in Block 410 (stations 16–18, fig. 1). Data from this detailed sampling defines the local changes in environmental parameters adjacent to the drilling activity.

At each sampling site, replicate grab samples of the bottom sediment (fig. 3) are routinely taken for analysis of trace metals, organic geochemistry, and benthic biology. The upper 2 cm of bottom sediment is chemically analyzed so that only the most recently deposited material is assayed for any drilling-related contaminants. Samples of large benthic organisms (such as clams, crabs, and flatfish) are collected with an otter trawl (fig. 4) or clam dredge. Photographs are taken of the bottom to monitor populations of large animals, and the salinity and dissolved-oxygen content are measured at each station.

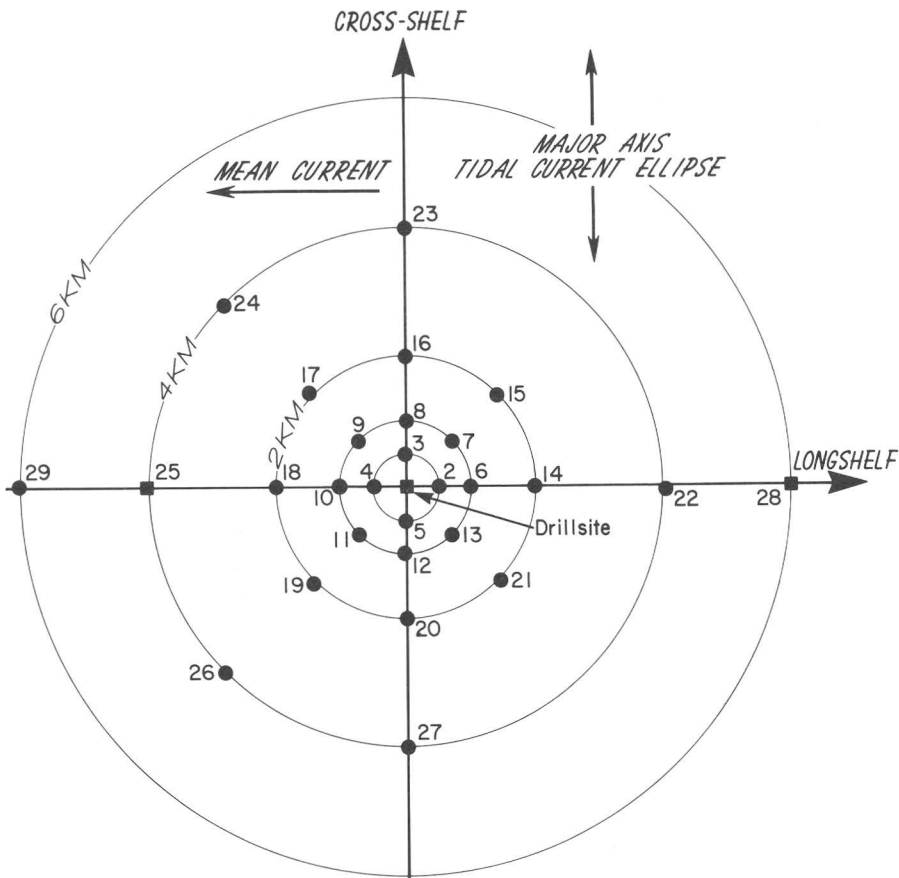


Figure 2. Site-specific sampling array around regional station 5.

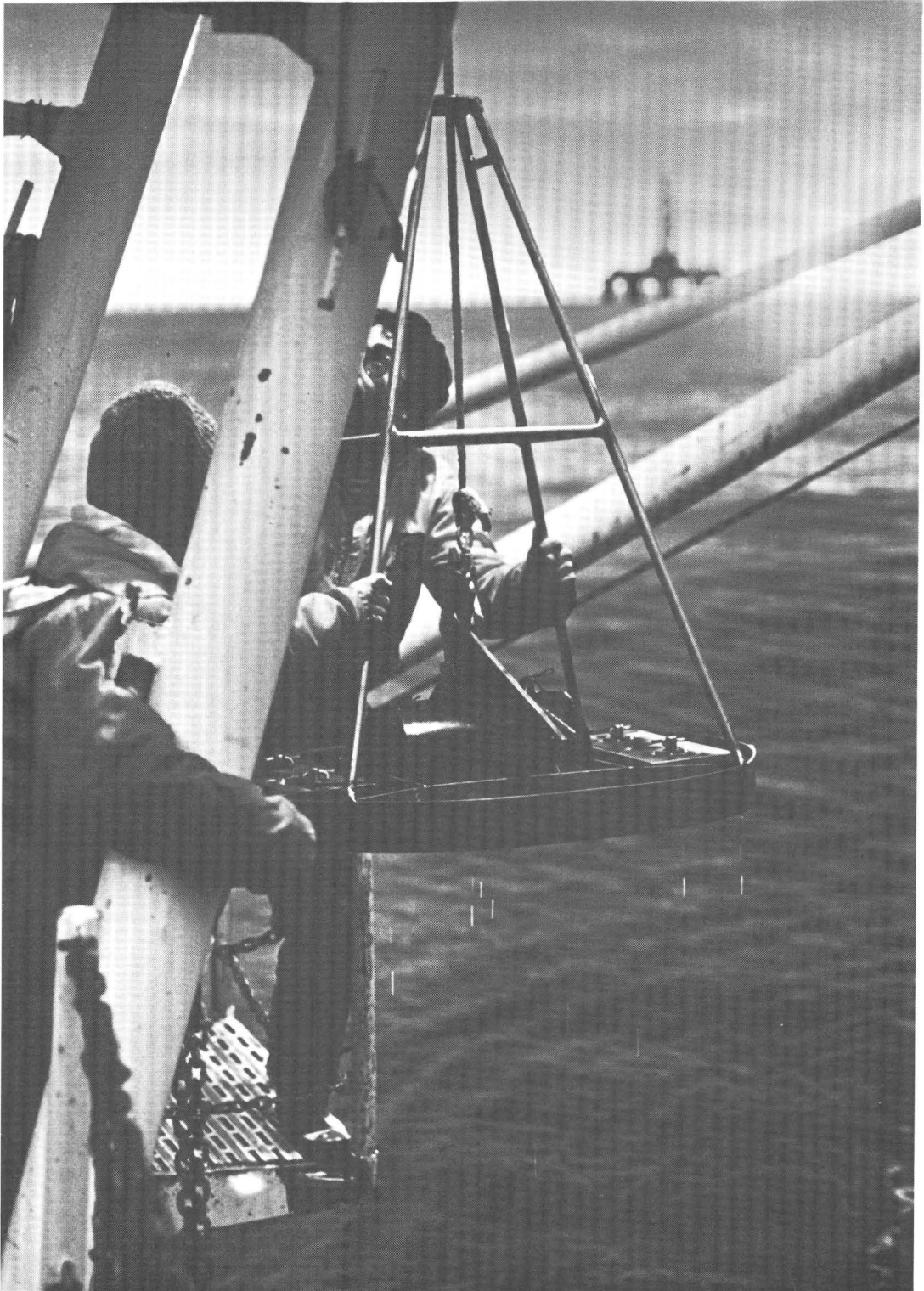


Figure 3. Deployment of a Van Veen grab sampler to collect bottom sediment near an active drill rig on Georges Bank.



Figure 4. Recovery of an otter trawl used to collect near-bottom fish and shellfish.

The Georges Bank Monitoring Program is a cooperative interdisciplinary effort. The USGS is responsible for the collection and analysis of sediment trace metals. The organic geochemical analysis of sediment and the chemical analysis of organisms are being conducted by Science Applications, Inc., of San Diego, Calif. The analyses of benthic biology are the joint responsibility of scientists from Battelle New England Laboratories, Duxbury, Mass., and the Biology Department of the Woods Hole Oceanographic Institution, Woods Hole, Mass. Funding and administration for the \$1.8 million-per-year program is provided by the Outer Continental Shelf Environmental Studies Program of the U.S. Minerals Management Service.

Results

Analyses of samples obtained during the first year of the monitoring program, which were collected just before and during the first phase of exploratory drilling on Georges Bank, have been completed. Even at stations adjacent to the drill rigs, the concentrations of petroleum hydrocarbons in organisms and sediment did not increase as a result of drilling (Payne and others, 1982), possibly because petroleum hydrocarbons were not discovered and because diesel fuel was added to the drilling fluid on Georges Bank on only two occasions to free stuck drill pipe (Danenberger, 1983). Trace-metal concentrations in benthic organisms (Payne and others, 1982) also did not increase. Although the populations of benthic organisms changed somewhat during the four seasons sampled, no changes were attributable to drilling (Blake and others, 1983). Surveys of organic and inorganic contaminants in fish and shellfish, conducted by the U.S. National Marine Fisheries Service, revealed no increases in contaminants as a result of drilling (Cooper, 1982).

The only environmental parameter in sediment which showed a clear increase as a result of drilling was the concentration of barium (Ba). Ba is present in the heavy mineral barite (barium sulfate [BaSO_4]) that is added to drilling mud to increase its density; the dense mud floats rock cuttings away from the drill bit and helps to prevent blowouts. The greatest increase between predrilling and postdrilling levels of Ba in bottom sediment was observed at station 16, located within 200 m of the drill rig in Block 410 (fig. 5; Bothner and others, 1982). At this station, Ba concentrations increased from 30 to 107 ppm. In Block 312, at stations within 500 m of the drill rig, Ba concentrations in bulk sediment have increased by a factor of 1.8 (from 37 to 66 ppm) since drilling began. Smaller increases were measured in the detailed sampling within a 6-km radius around Block 312. No increases in Ba concentration were measured at the more distant regional stations, and no changes in the concentrations of other metals commonly present in drilling mud (Al, Cd, Cr, Cu, Fe, Hg, Mn, Ni, Pb, V, or Zn) were observed in bulk sediment during the first year of the monitoring program.

To put the magnitude of the observed increases in Ba concentration into perspective, note that the maximum Ba concentrations measured adjacent to the drill rigs were less than those measured in predrilling samples collected in many places on the bank. In addition, barium sulfate, the main constituent of barite, is considered to be nontoxic from its applications in medicine. Suspensions containing about 500,000 ppm Ba (as BaSO_4) are ingested by patients undergoing X-ray diagnosis of abdominal ailments.

Most of the material in drill mud is finer than 60 μm . When these fine particles fall to the sea floor, they mix with natural sediment, primarily sand, and their concentrations are thus heavily diluted. To enhance our ability to observe very small increases in the proportion of drilling components within the sediment, the samples were separated into fractions finer than 60 μm (which should contain any drilling-related material) and coarser than 60 μm (which should contain primarily natural sediment). This separation was done with a nylon screen. This technique of separating and analysing the fine fraction of sediment improves our ability to understand the transport of drilling fluids in this dynamic continental-shelf environment.

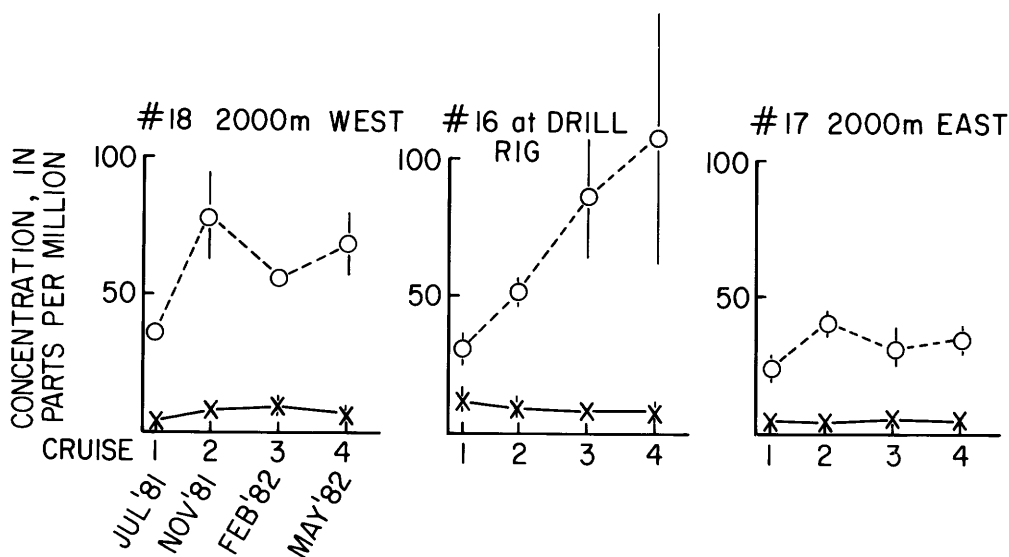


Figure 5. Concentrations of Ba (circles) and Cr (X's) in bulk sediment on different sampling occasions near drillsite at Block 410. Drilling began after the first cruise. Error bars are one standard deviation among three individual samples.

In the fraction of bottom sediment finer than 60 μm , Ba concentrations in the samples collected at Block 410 after drilling was completed were 36 times higher than in the predrilling samples (fig. 6). The concentrations of Al, Cr, Cu, and Hg in the sediment fraction finer than 60 μm increased by a factor of 2 to 3 as a result of drilling, but the highest concentrations observed, though higher than those previously measured in the sediment of Georges Bank, were near or below those of average crustal material. The average concentration of metals in the Earth's crust is commonly used as a reference level for natural unpolluted sediment. Measurable increases in Cr, Cu, and Hg concentrations were not found in the fine sediment fraction at any other stations. Analysis of metals in the fine-sediment fraction at the drillsite in Block 312 showed an increase in Ba concentration by a factor of 22 as a result of drilling, but no changes in the other trace-metal concentrations were observed (Bothner and others, 1982).

Discussion

The Georges Bank Monitoring Program provides possibly the most comprehensive environmental data ever obtained in a frontier offshore area before, during, and after petroleum exploration. This program not only defines the environmental impact of the drilling that took place during 1982 but also provides an extensive data base with which to assess the impact of other events, such as oilspills from tankers or future wells, or even of natural events, such as exceptionally violent storms. In addition, a major contribution has been made to the description and understanding of the biologic and chemical parameters that characterize the benthic environment in this rich commercial-fishing area.

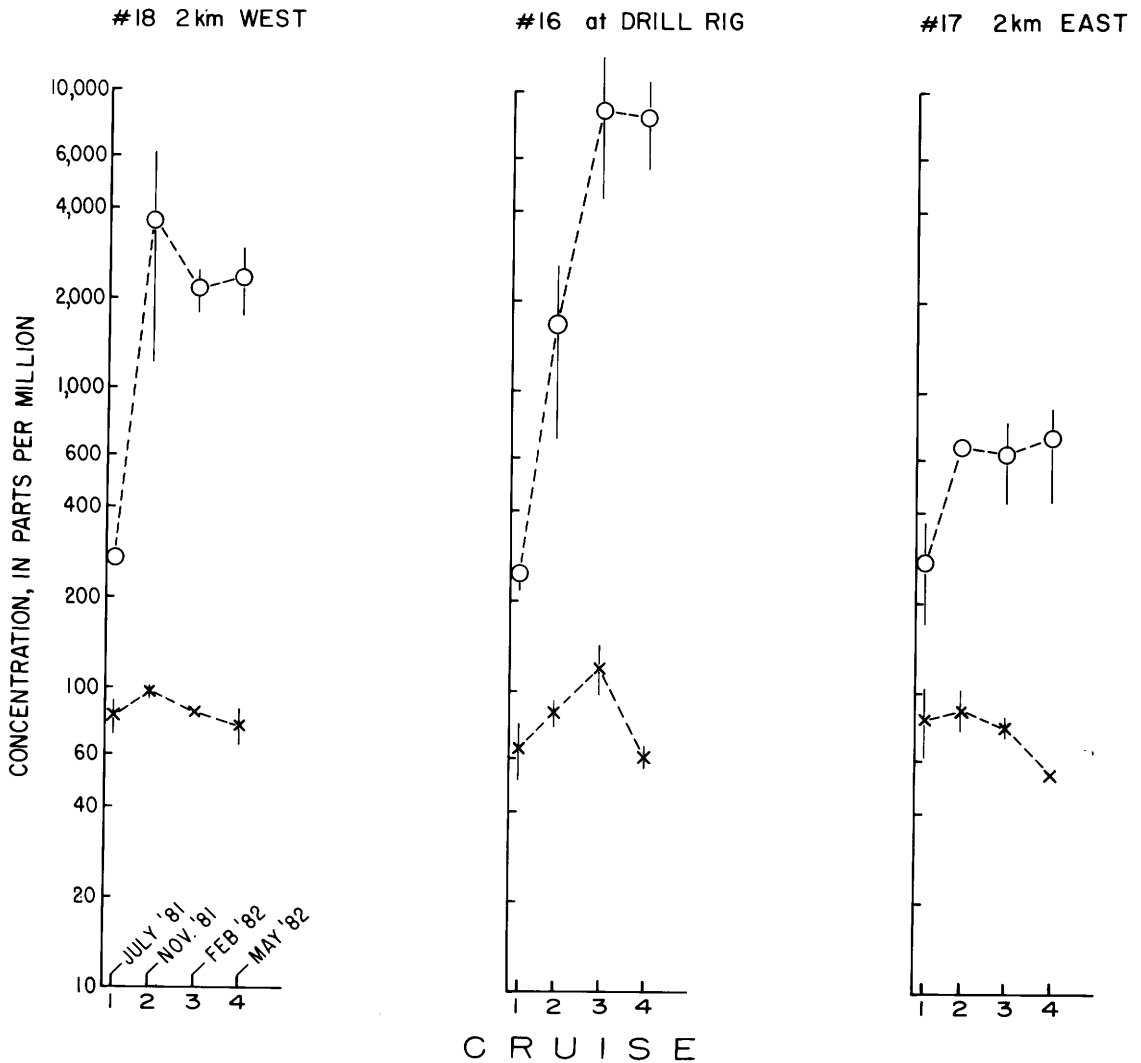


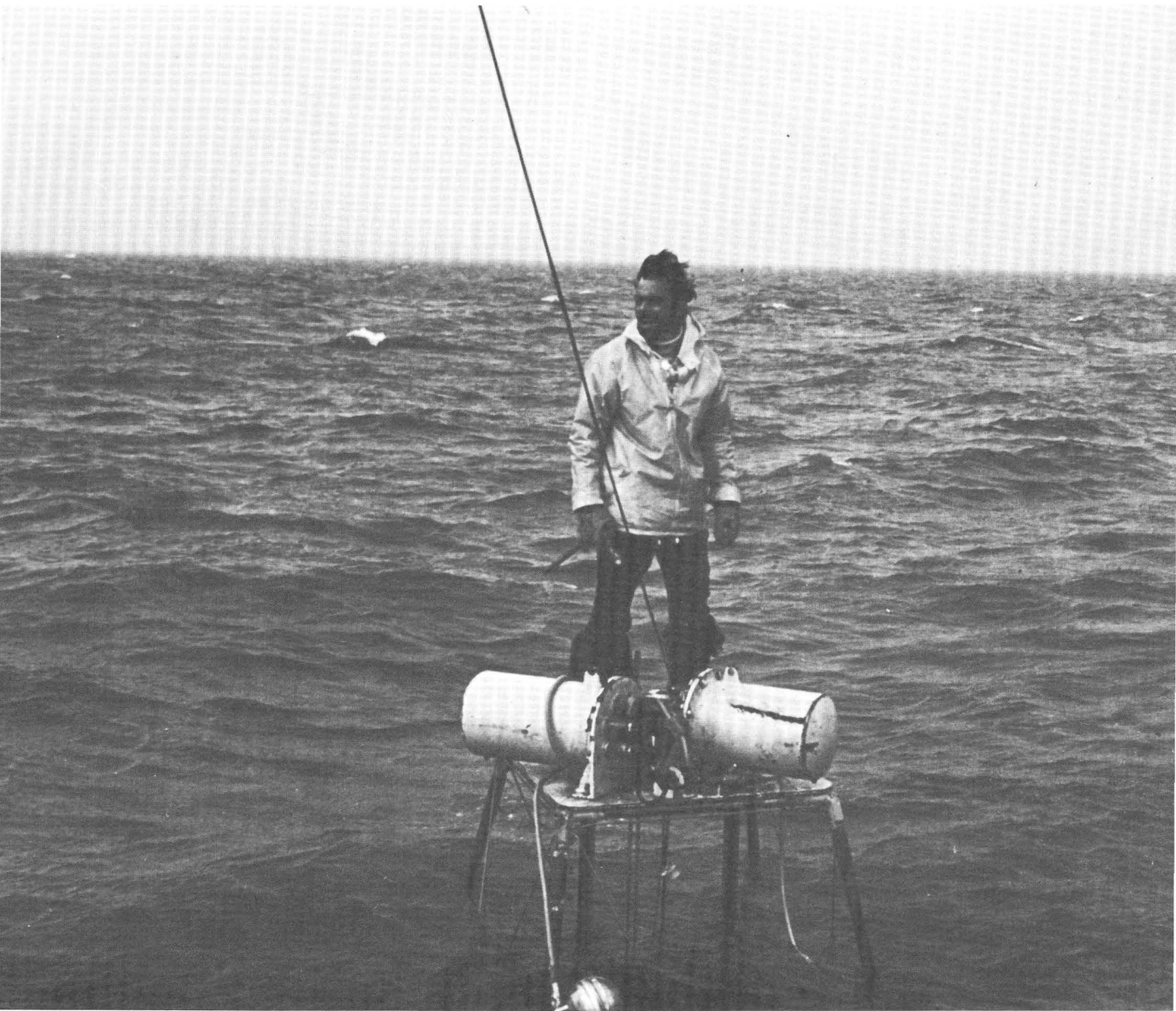
Figure 6. Concentrations of Ba (circles) and Cr (X's) in fine fraction of sediment. Drilling began after the first cruise. Error bars are one standard deviation among three individual samples.

To date, the analyses of heavy metals, petroleum products, and benthic populations in the bottom sediment of Georges Bank have revealed no adverse effects due to the present phase of exploratory drilling, even in samples obtained at stations adjacent to the drill rigs.

Analyses of samples collected during the second and third years of the program are presently underway. The rate of decrease in Ba concentration within the bottom sediment in Blocks 312 and 410 is of particular interest, now that exploration drilling has been completed at these sites. This information will provide baseline data with which to assess the fate of drilling-mud contaminants if commercial discoveries of petroleum are made and several production wells are drilled in the area.

References

- Blake, J. A., Grassle, J. F., Maciolek-Blake, Nancy, Neff, J. M., and Sanders, H. L., 1983, The Georges Bank Benthic Infauna Monitoring Program: final report to U.S. Department of the Interior, Minerals Management Service, Atlantic OCS Region, under Contract 14-12-0001-29192, 153 p.
- Bothner, M. H., Rendings, R. R., Campbell, E., Doughten, M. W., Aruscavage, P. J., Dorrzopf, A. F., Jr., Johnson, R. G., Parmenter, C. M., Pickering, M. J., Brewster, D. C., and Brown, F. W., 1982, The Georges Bank Monitoring Program: Analysis of trace metals in bottom sediments: final report to U.S. Department of the Interior, Minerals Management Service, Atlantic OCS Region, under Contract AA851-IA2-18, 62 p.
- Bothner, M. H., Spiker, E. C., Johnson, P. P., Rendigs, R. R., and Aruscavage, P. J., 1981, Geochemical evidence for modern sediment accumulation on the continental shelf off southern New England: *Journal of Sedimentary Petrology*, v. 51, no. 1, p. 281-292.
- Butman, Bradford, Beardsly, R. C., Magnell, Bruce, Frye, Daniel, Vermersch, J. A., Schlitz, Ronald, Limeburner, Richard, Wright, W. R., and Noble, M. A., 1982, Recent observations of the mean circulation on Georges Bank: *Journal of Physical Oceanography*, v. 12, no. 6, p. 569-591.
- Cooper, R. A., 1982, Pre-oil drilling benchmarks of ocean floor fauna, habitats, and contaminant loads on Georges Bank and its submarine canyons: Woods Hole, Mass., U.S. National Marine Fisheries Service, Northeast Fisheries Center newsletter, 11 p.
- Danenberger, E. P., 1983, Georges Bank exploratory drilling (1981-1982): Hyannis, Mass., U.S. Department of the Interior, Minerals Management Service, North Atlantic District, 20 p.
- Payne, J. R., Lambach, J. L., Jordan, R. E., McNabb, G. D., Jr., Sims, R. R., Abasumara, Adel, Sutton, J. G., Generro, Don, Gagner, Susan, and Shokes, R. F., 1982, Georges Bank Monitoring Program: Analysis of hydrocarbons in bottom sediments and analysis of hydrocarbons and trace metals in benthic fauna: final report to U.S. Department of the Interior, Minerals Management Service, Atlantic OCS Region, under Contract AA851-CT2-33, 189 p.



Vibracoring in the Arctic Ocean

Significance of Long-Term Variations in Estuarine Benthos

By Frederic H. Nichols

Introduction

The benthos, the assemblage of such invertebrate animals as clams, worms, and crustaceans that live on or in the bottom substrate of aquatic environments, is important for the following reasons. (1) These animals consume living and non-living material gathered from the sediment or water and become, in turn, a source of protein for fish, birds, and mammals (including humans). (2) They contribute to the flux of dissolved and particulate material between the bottom sediment and the overlying water. For example, the activities of benthic animals contribute markedly to the stabilization or destabilization of surface sediment. Further, by removing living microscopic plants from the overlying water in shallow areas, they may contribute importantly to the prevention of eutrophication (the unusual enhancement of plant growth through nutrient addition). (3) The types of benthic animals and the changes in their abundance are commonly used as indicators of water quality.

Benthic organisms are generally sessile; they live most of their lives (several months to several years) in the same place. Thus, the benthic community provides a continuing record, through changes in species composition or abundance, of the effects of both short- and long-term changes in the environment. This feature has led, understandably, to the use of benthic-community structure in analyses of human impact, assuming that the benthic-community composition is stable (or varies regularly) over time. If such an assumption is valid, a measured deviation in community composition from the previous norm could be interpreted as a possible result of environmental degradation.

As long-term data are gathered on estuarine and coastal communities, however, the hypothesis of stability becomes increasingly unsupportable. Long-term investigations reveal that major changes in species composition and abundance are routine in all the habitats studied. The interpretation of existing data and the possible prediction of future changes require a much greater understanding of the amplitude and periodicity of change in these communities and of the factors that contribute to such change.

Sources of Natural Variation in Benthic Communities

Animal populations respond, predictably, to cyclic changes in their environment. For example, seasonally changing water temperature and salinity (figs. 1A, 1B) trigger physiologic responses in aquatic invertebrates, such as the initiation of reproduction with the annual rise in water temperature. The common result in temperate estuaries is that invertebrate abundance peaks during the spring and summer months, and declines owing to natural mortality in autumn and winter.

Because the timing and relative magnitude of seasonal changes in environmental variables vary from year to year, and each species is affected differently, the relative year-to-year abundance of each species at a particular locality is directly affected.

Animal populations also respond to intermittent, unpredictable physical and chemical changes in their habitat, many of which derive from unusual climatic events. Storms, for example, generate wind waves and currents that can, to an unusual degree, scour and transport bottom sediment and fauna. Storm-related freshwater runoff can change the characteristics of the water mass above the bottom. When the destructive force abates, the disturbed sediment is immediately colonized by the first species to arrive, typically "opportunistic" species adapted to rapidly exploit disturbed environments.

Human impacts can have a similar effect on a benthic community. Although a single disturbance, such as dredging, can eliminate the community occupying the site, this disturbance is followed by a gradual return of the same community once the dredging ceases. A chronic disturbance, however, such as the discharge of waste from an aquatic outfall, commonly results in a change in the local community that is as permanent as the outfall.

Often, a change in an animal community cannot be explained on the basis of an observed change in the environment. For example, the interplay among the species themselves (for example, predator-prey interactions, competition for food or space) commonly results in intermittent changes in the relative ranking of numeric or ecologic importance among the species.

The result of the combination of internal and external forces acting to change the abundance of individual species is a highly dynamic community that, at any given moment, is probably undergoing a process of transition from some previous "disturbance" event.

San Francisco Bay

The San Francisco Bay is a large (1,240 km²) estuary that is connected to the ocean at the Golden Gate and receives freshwater from the Sacramento and San Joaquin Rivers at the northeast end of the bay. The inner parts of the bay are generally very shallow, with characteristically wide intertidal and shallow subtidal mudflats incised by narrow midbay channels (fig. 2).

An interdisciplinary investigation of the physical, chemical, geologic, and biologic processes that characterize the San Francisco Bay estuary has focused on understanding the interactions among the separate components (see Conomos, 1979) and evaluating the human influence (for example, through manipulation of freshwater inflow and disposal of wastes) on the estuary's natural processes (see Kockelman and others, 1982). As part of that investigation, an ongoing long-term study of the benthos at an intertidal site in the southern San Francisco Bay (Nichols and Thompson, 1984) has provided insight into the importance of interplay among species, and between species and an inconstant environment, in determining long-term patterns in estuarine benthic communities. This study has demonstrated the need for understanding natural long-term variations within natural communities before attempting to assess human impacts.

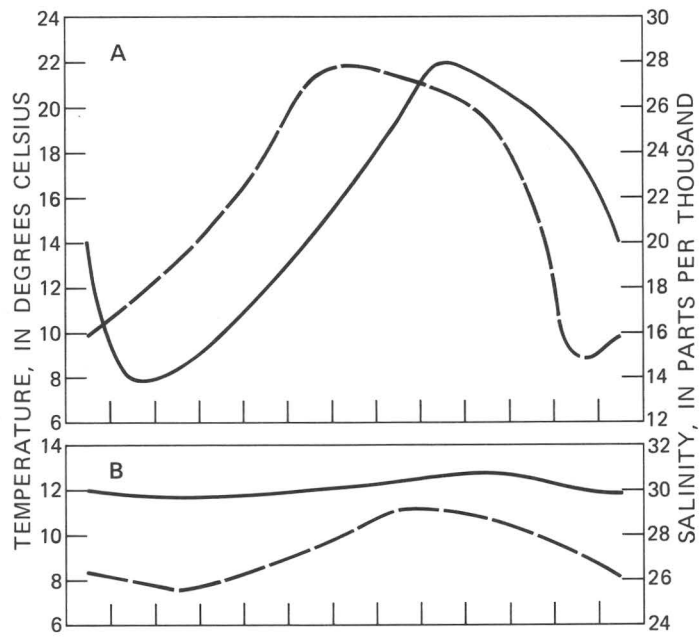


Figure 1. Typical seasonal patterns of temperature (dashed curves) and salinity (solid curves) in the bottom water of two Pacific Coast estuaries: A, San Francisco Bay and B, Puget Sound.

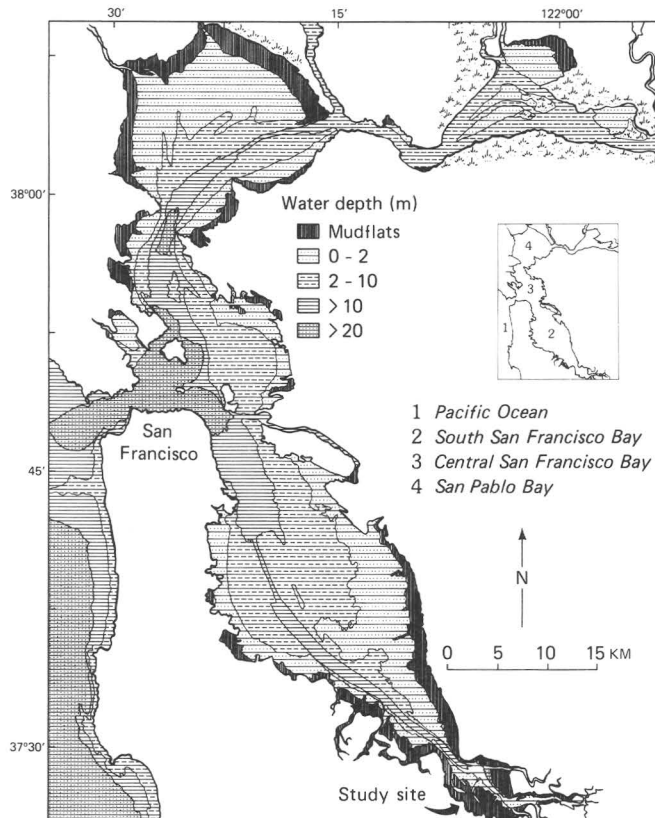


Figure 2. San Francisco Bay, showing depth zones.

The intertidal mudflats of the San Francisco Bay are inhabited by relatively few (less than 40) species, most of which were introduced accidentally during the past century when live oysters were imported from the east coast and grown in the bay (Carlton, 1979). Analogous to introduced weedy plant species, these accidentally introduced invertebrates rapidly exploited the vast inner reaches of the San Francisco Bay and are today the numerical dominants throughout much of the bay. Their success may reflect the fact that the native invertebrate community was species poor, owing to the estuary's geologic youth and geographic isolation from other west-coast estuaries; that is, there were unused space and food resources. Additionally, major disturbances of the estuarine habitat just before these species introductions—the great flood of 1862, when the San Francisco Bay was for a few weeks a freshwater lake (Hedgpeth, 1979), and, over the next two decades, the inundation of the bay with massive amounts of hydraulic-mining debris (Gilbert, 1917)—may have provided appropriate exploitable substrate.

Species composition and relative abundance among the species on southern San Francisco Bay mudflats have, over the 9-year period of observation, remained reasonably constant. However, a large short-term variation in community structure reflects large-amplitude seasonal and annual fluctuations in the abundance of the commoner species. The commonest of the introduced invertebrates (the clam *Gemma gemma*, the polychaete *Streblospio benedicti*, and the am-

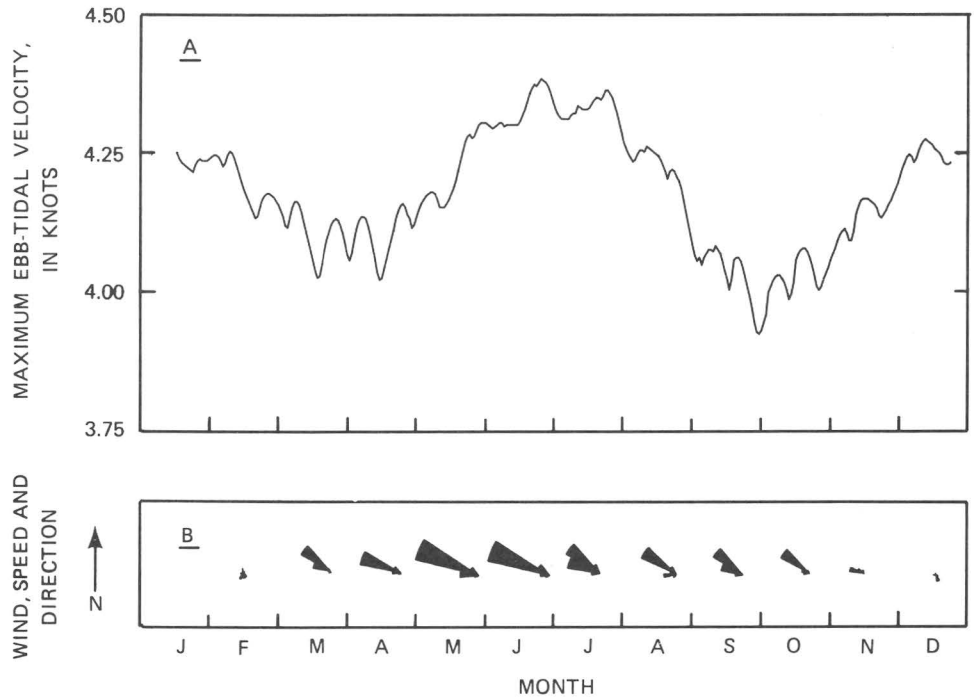


Figure 3. Factors affecting resuspension of surficial sediments in San Francisco Bay. A, Daily maximum ebb-tidal velocities (running 29-day averages) at the Golden Gate. B, Wind-speed and wind-direction vectors (3-hour averages) at San Francisco International Airport; vectors point in direction from which wind was blowing. All data from 1980.

phipod crustacean *Ampelisca abdita*) occur in very large numbers, in some places exceeding 150,000 adults per square meter. A disturbance of the habitat can lead to rapid shifts in the numeric balance among the species.

The recovery process that follows a single disturbance may take days, months, or years, depending on the timing, intensity, and duration of the disturbance. Although “opportunists,” through rapid maturity, high reproductive capacity, and ease of dispersal over wide areas, can rapidly exploit a recently disturbed sediment surface, the most successful species is generally one that is available at the time of the disturbance. However, because physical disturbance of the estuarine environment of the San Francisco Bay is recurrent, the biotic community is routinely in a recovery process, and so the same opportunists continue to prevail.

The major changes in the mudflat community we have studied are, in some instances, directly traceable to an observed change in the mudflat or the water mass above it, and indirectly to interactions among the different species as they respond to their inconstant environment. For example, seasonal resuspension of shallow sediment, caused by increasing wind velocities and the resulting wind waves that coincide in summer with increasing tidal velocities (fig. 3), is a typical feature of the San Francisco Bay. A major incidence of surface-sediment erosion in 1974 resulted, during 1 month, in the removal of about 8 cm of sediment from the mudflat surface (event B, fig. 4). However, recolonization by the resident species occurred within 2 months.

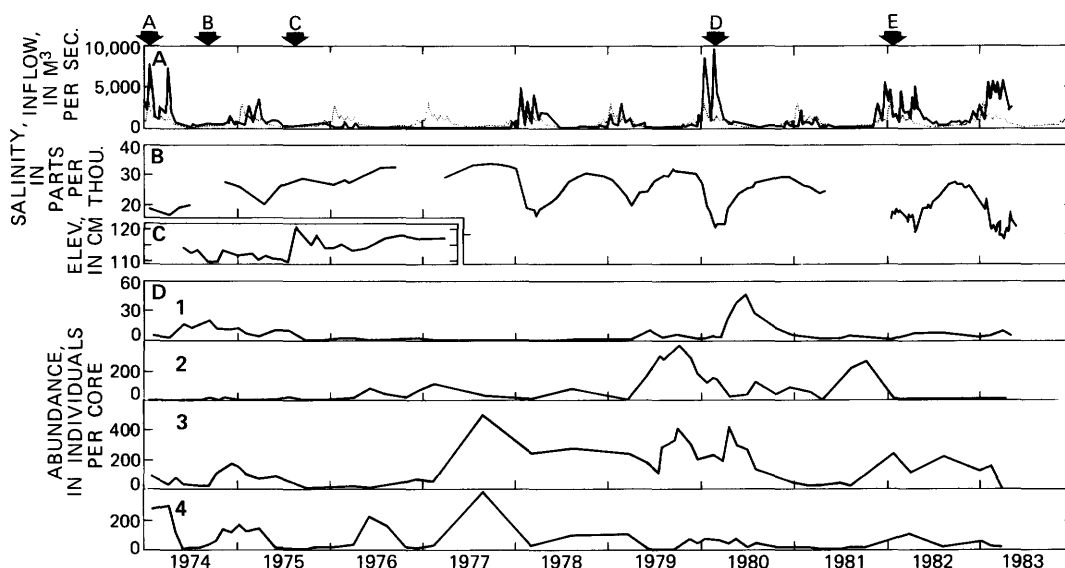


Figure 4. Changes in a San Francisco Bay intertidal mudflat community and related environmental factors. A, Average daily inflow of freshwater into the bay from the Sacramento/San Joaquin River system (yearly data superimposed on 10-year average for 1970–79. B, Near-surface salinity measured at a mid-channel site in South San Francisco Bay. C, Elevation of mudflat surface above mean lower low water. D, Mean abundance of four species collected in core samples at a South San Francisco Bay mudflat: 1, *Macoma balthica*; 2, *Ampelisca abdita*; 3, *Gemma gemma*; 4, *Streblospio benedicti*. Arrows, labeled A through E, indicate specific events described in text.

Nonetheless, the occurrence of unpredictable events may have a much greater and longer lasting effect on the benthos. An unusual deposition and subsequent decay of a 20- to 30-cm-thick macroalgal mat during summer 1975, seen as a marked increase in the mudflat elevation (event C, fig. 4), created anoxic conditions at the mudflat surface and smothered the benthic community. Because the decaying organic matter remained on the mudflat surface for several months, full recovery was delayed for many more months. Such algal blooms, involving several different species, have occurred intermittently around the bay in recent years. The combination of increasing nutrient levels (largely from domestic sewage) and reduced bay-water turbidity because of decreasing river flow (a response to increased diversion of freshwater for agriculture) evidently contributes to this situation and provides the potential for more widespread, frequently occurring nuisance blooms.

Hydrodynamic processes are also important to habitat disturbance and the competitive interplay among species. For example, heavy freshwater inflow in January of both 1974 and 1980 (events A and D, fig. 4) coincided with both the reduced abundance of the amphipod *Ampelisca abdita* and the unusually successful establishment of the clam *Macoma balthica*. Normally, this amphipod is abundant on the mudflat and may effectively prevent the clam larvae from settling. Unusually high freshwater inflow (and with it increased turbidity and sedimentation) is generally followed by an immediate and precipitous decline in the abundance of this amphipod. Subsequently, the clam and other species occupy the mudflat sediment in greater than normal abundance. Particularly high freshwater inflow in the late winter and spring of 1982 and 1983 further reduced the abundance of many species on the mudflat and virtually eliminated *Ampelisca abdita* from the mudflat community (postevent E, fig. 4). *Macoma balthica* has, possibly as a consequence, thrived during these wet years.

These typically large abundance fluctuations over short time scales (months) effectively mask all but extreme disturbances. Only very long term data sets may provide evidence of any permanent trends in the benthos associated with human activities.

A similar but longer term study of the benthic community on the physically stable bottom of Puget Sound at 200-m depth (Nichols, 1984) has shown that changes in the relative abundances of species occur there at a much lower frequency than in the San Francisco Bay. However, the amplitude of these infrequent changes can be as large as those in the shallow, much less stable San Francisco Bay environment. These more gradual changes may reflect interactions among longer lived species (characteristic of deeper, more stable benthic communities) as they compete for space and food resources and, possibly, as they respond to longer term climatic cycles.

Summary

Long-term studies of estuarine and coastal benthos suggest that very large changes in community composition occurring over varying time scales (from months to years) are normal and that studies of the benthos for evaluating human influence must be of sufficient duration to separate short-, medium-, and long-term cycles from unidirectional trends.

A major component of the variation in benthic communities is that associated with the normal life-history responses of invertebrates (the annual cycle of reproduction, growth, and mortality) to seasonal changes in the environment. However, other equally important components of observed variations are much less predictable. Commonly, community changes reflect varying climatic patterns. Climate affects riverflow into estuaries and, thus, water chemistry, circulation, and productivity; these changes in the water, in turn, affect aquatic organisms, including benthic invertebrates. With or without external stresses, however, benthic communities can change in response to interactions between species as they compete for space and (or) food. The result of these complex interrelations is a temporal mosaic that, in combination with the spatial mosaic resulting from the heterogeneity of the estuarine environment (that is, large differences in sediment composition, water depth, and food supply over short distances), generally masks all but extreme natural and human impacts on these communities.

Simultaneous analyses of long-term records of climate, water properties and circulation, and biotic communities, and the development of an understanding of the amplitude and periodicity of the natural variations associated with them, are leading to a much better understanding of the important factors that bear on these communities. Such understanding may lead to an enhanced capability, through modeling, for predicting the response of biotic communities to future natural or human-induced changes in the environment.

References

- Carlton, J. T., 1979, Introduced invertebrates of San Francisco Bay, *in* Conomos, T. J., ed., *San Francisco Bay: The urbanized estuary*: San Francisco, American Association for the Advancement of Science, Pacific Division, p. 427–444.
- Conomos, T. J., ed., 1979, *San Francisco Bay: The urbanized estuary*: San Francisco, American Association for the Advancement of Science, Pacific Division, 493 p.
- Gilbert, G. K., 1917, Hydraulic mining debris in the Sierra Nevada: U.S. Geological Survey Professional Paper 105, 154 p.
- Hedgpeth, J. W., 1979, San Francisco Bay—the unsuspected estuary; a history of researches, *in* Conomos, T. J., ed., *San Francisco Bay: The urbanized estuary*: San Francisco, American Association for the Advancement of Science, Pacific Division, p. 9–29.
- Kockelman, W. J., Conomos, T. J., and Leviton, A. E., 1982, *San Francisco Bay: Use and protection*: San Francisco, American Association for the Advancement of Science, Pacific Division, 310 p.
- Nichols, F. H., 1984, Abundance fluctuations among benthic invertebrates in two Pacific estuaries: *Estuaries* (in press).
- Nichols, F. H., and Thompson, J. K., 1984, Persistence of an introduced mudflat community in South San Francisco Bay, California: *Marine Ecology Progress Series* (in press).



Gray Whales, Tillers of the Sea Floor

By C. Hans Nelson and Kirk R. Johnson¹

Introduction

California gray whales, twice hunted nearly to extinction, have rebounded to pre-exploitation population levels of about 16,000. Each year, nearly all the gray whales migrate 6,000 km from their winter breeding and calving lagoons in Baja California, Mexico, to their summer feeding grounds in the Bering, Chukchi, and Beaufort Seas between Alaska and Siberia. This study is concerned with the shallow (less than 50 m deep) Chirikov Basin in the northeastern Bering Sea, an important area of the summer feeding grounds that sustain the whales for the entire year (fig. 1).

Studies of the stomach contents of gray whales taken in these waters show that they feed primarily on bottom-living crustaceans, mainly the ampeliscid amphipod *Ampelisca macrocephala*. These amphipods create characteristic mucus-lined burrows that extend as much as 10 cm deep into the sediment. When the population of amphipods becomes large, the densely packed tubes form a mat that binds the surface sediment and is the main food source for gray whales.

The precise mechanism by which gray whales feed on the amphipods is not well understood; apparently they roll on one side, mouth parallel to the sea floor, and create suction by the retraction of the large muscular tongue in the mouth cavity and thus excavate patches of amphipod-rich sediment. The sediment is then expelled through the baleen on the opposite side of the head, while the amphipods are retained. This feeding mechanism results in the formation of shallow (10 cm deep) oval pits on the bottom of the Bering Sea.

The pits created during feeding have been studied by underwater television, scuba-diver observations, and side-scan sonar. The side scan is a planographic mapping device using sound waves to generate sea-floor pictures that are analogous to aerial photographs of land areas (fig. 2). During a 5-year survey for geohazards, the USGS collected more than 4,500 km trackline of side-scan profiles with a 105-kHz system. Several hundred kilometers more of 500-kHz high-resolution data were taken for the National Oceanic and Atmospheric Administration's Outer Continental Shelf Environmental Assessment Program (NOAA-OCSEAP) studies on marine mammals. Features on profiles from the two side-scan systems were calibrated with one another and with measurements made by scuba divers.

Through use of side-scan sonar, the geometry, distribution, and history of feeding traces can be interpreted. These data are then used to estimate the total areal extent of feeding pits and the intensity of whale feeding in the Chirikov

¹ Present address: Department of Geology/D4, University of Pennsylvania, Philadelphia, PA 19104.

Basin. We correlate these patterns of feeding features with sediment distribution, amphipod abundance, and whale sightings from aerial surveys. These correlations allow us to outline the area of the gray-whale-feeding ground and estimate the amount of the food resource utilized by whales in the northeastern Bering Sea. Such knowledge aids in making sound ecologic decisions concerning resource development on the Alaskan Continental Shelf.

Definition of Whale-Feeding Traces and Areas

Maps of amphipod distribution and sediment grain size show that zones of dense amphipod concentrations can be correlated with the distribution of a thin (less than 2 m thick) fine-sand layer (fig. 1). This sand layer was deposited over the Chirikov Basin as the sea level rose, and an ancient shoreline transgressed over this region 10,000–12,000 years ago after the end of the latest ice age. Toward the margin of the basin, transgressive fine sand is replaced by coarser and more heterogeneous ancient beach sand, amphipod density decreases abruptly, and gray-whale feeding diminishes.

During summer feeding periods, aerial surveys by research biologists show that most gray whales are in the central part of the basin. Because of the whales' feeding on the bottom sediment, plumes of mud from whale mouths are commonly noted in the water column; and these plumes identify areas of active gray-whale feeding.

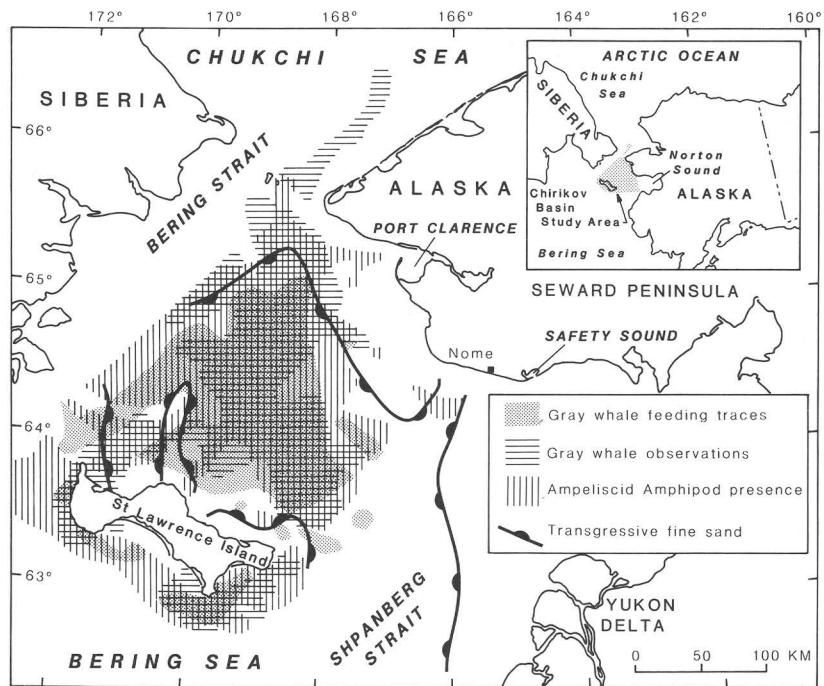
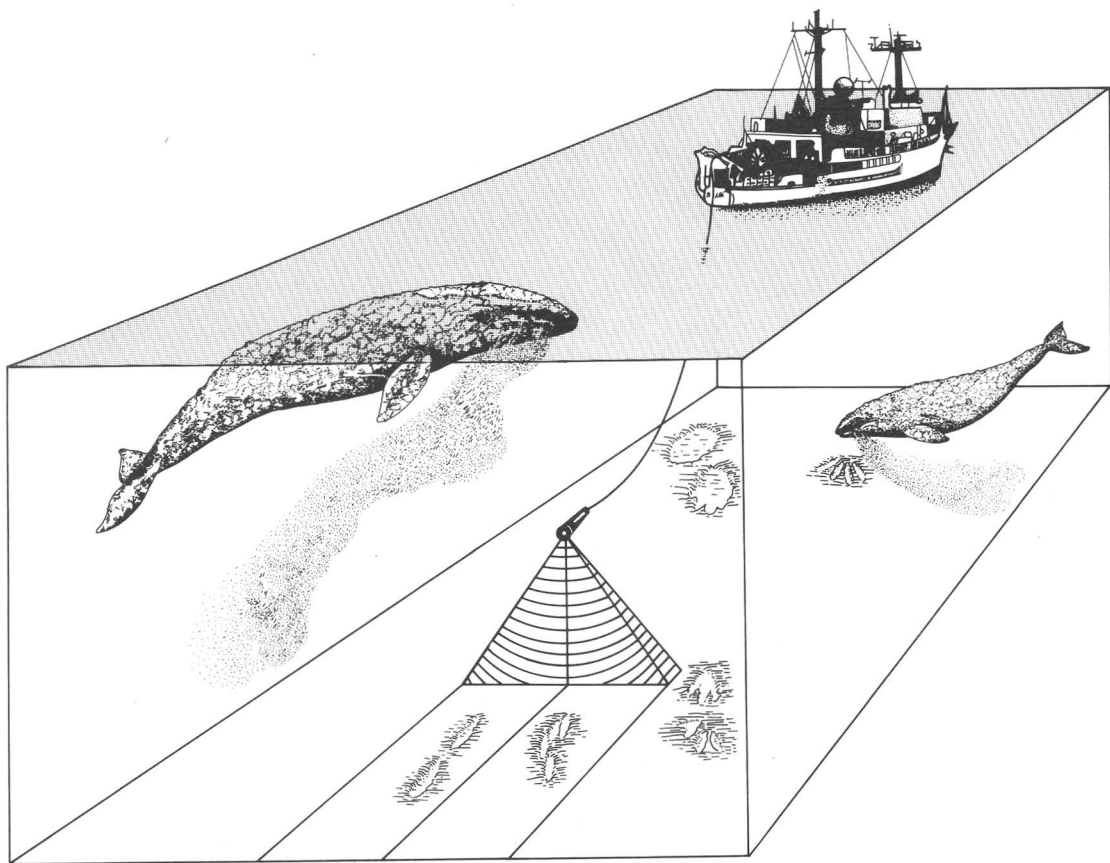
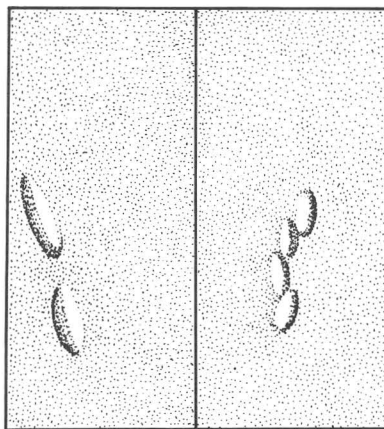


Figure 1. Chirikov Basin on northeastern Bering Shelf, showing area covered by the transgressive fine-sand sheet, area with ampeliscid amphipods living in the sea floor, zone where gray whales have been sighted feeding by National Oceanic and Atmospheric Administration (NOAA) aerial observers in 1979, and areas where we have recognized gray-whale-feeding pits in sea-floor sonographs.



Port Channel Stbd. Channel



Resulting Side-Scan Sonograph

Figure 2. Sketch illustrating gray-whale-feeding methods as observed by side-scan-sonar techniques. The side-scan sonar sends out multiple echo soundings that bounce off low-relief sea-floor features to create a relief map of the ocean bottom. Pictured in the water column are gray whales engulfing the sediment-surface mat of amphipods and expelling sediment while straining these bottom dwellers out. Pictured on the sea floor are single and multiple whale-feeding pits, as well as a sequence of pits that subsequently are enlarged by bottom-current scour.

Three types of pits have been defined from side-scan records collected in whale feeding areas of the Chirikov Basin (figs. 3, 4; table 1). These pits are interpreted as gray-whale-feeding traces because of their size, arrangement in ordered groups, and position in areas of heavy whale-feeding pressure and abundance of prey. These feeding traces and their patterns also do not resemble any known physical sedimentary features.

The pits are classified into three types because of differences in the size, shape, and grouping of features in three different areas (figs. 3, 4; table 1). Type I are elliptical pits in the east-central part of the Chirikov Basin, type II are elongate pits in the main northeastern feeding area, and type III are oval pits on the south and west margins of the basin.

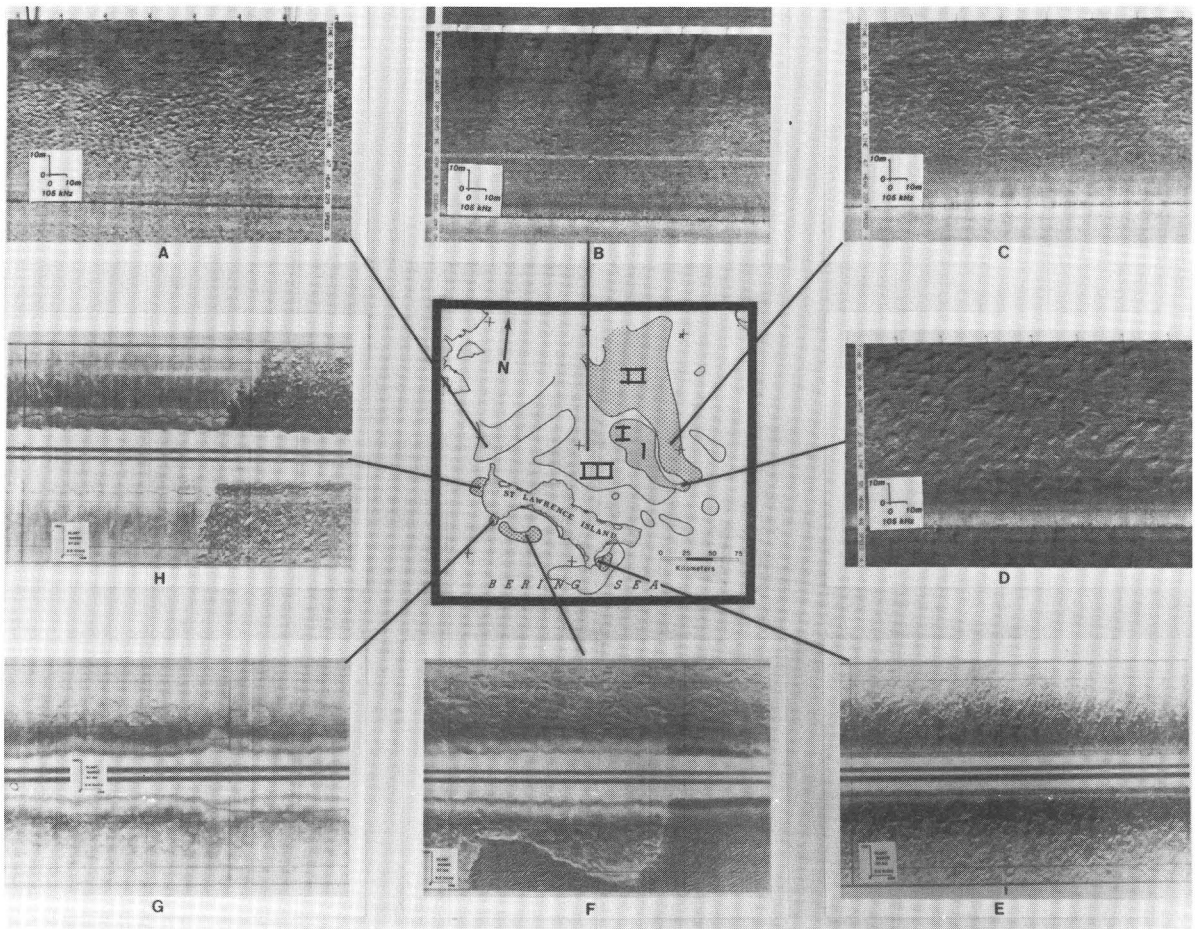


Figure 3. Locations of sonographs in Bering Sea area, showing three bottom-pit types attributed to gray-whale feeding and subsequent current scour. A, 105-kHz sonograph, showing type III dense wide elliptical pits. B, 105-kHz sonograph, showing type III sparse wide elliptical pits. C, 105-kHz sonograph, showing type II dense elongate (narrow elliptical) pits. D, 105-kHz sonograph, showing type I current-enlarged pits with regional lineation. E, 500-kHz sonograph, showing type I current-enlarged pits with regional lineation. F, 500-kHz sonograph, showing type II elongate (narrow elliptical) pits in inner-shelf, transgressive fine sand adjacent to and overlying coarse basal transgressive sand which has been worked into sand waves. Note sinuous distortion of sand waves and elongate pits due to wave swell effect on the side-scan-sonar tow fish. G, 500-kHz sonograph showing type I current-enlarged pits. H, 500-kHz sonograph, showing type II elongate (narrow elliptical) pits (left), fuzzy pit margin, and absence of relief shadows indicating infilling by finer sediment. Rock outcrop is to right.

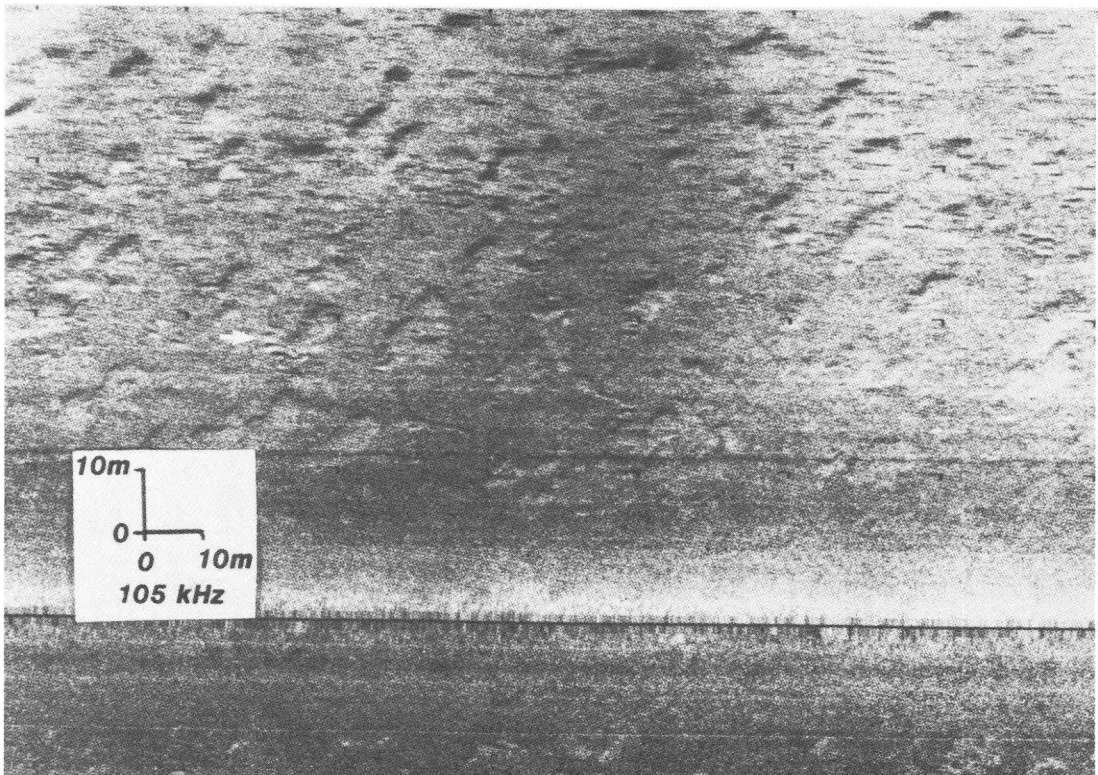
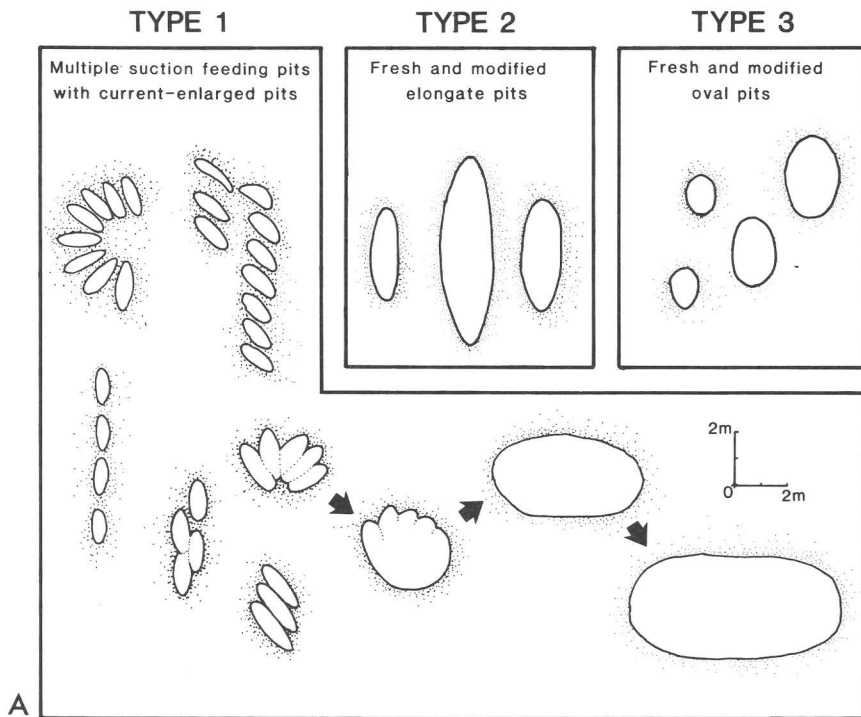


Figure 4. Whale-feeding pits. A, Sketch illustrating different types of whale-feeding pits. B, Enlarged view of a 105-kHz sonograph, showing fresh (arrow) and current-enlarged (to right of arrow) whale-feeding pits at station 1. (See fig. 1 for location).

The type I area is characterized by fresh feeding pits found in groups that apparently result from multiple-suction feeding events (fig. 4A). These fresh feeding pits are commonly associated with older pits that have been modified by subsequent current scour (figs. 3D, 3E, 3G, 4B). The postulated mechanism of formation of the current-enlarged type I pit is as follows. Whale-feeding activity removes the amphipod mat which binds the sediment surface. Then, during periods of strong bottom currents from fall storms, the sand exposed by removal of the mat undergoes additional erosion. The remaining mat around the margins of the pits is undercut and slumps into the pits. This continues until the pits are quite large. When a pit floor covers a sufficiently large area or sufficient time has elapsed, colonizing amphipods are able to reestablish a mat community in the center of the pit and redevelop the cohesive mat of tubes.

Elongate pits, which characterize the type II area, represent a combination of fresh feeding and current-scour modification parallel to the long axes of the feeding pits. Types I and II features in the central part of the basin correlate closely with areas of high amphipod concentration (figs. 1, 3); they are clearly formed by intensive whale feeding. In contrast, the isolated oval pits (figs. 3A, 3B, 4A) in the type III area at the basin margin may result from increasing grain size of the substrate toward the basin edge and a coincident decrease in amphipod abundance. This coarsening of sediment may physically control type III pit morphology because the coarser sediment is less cohesive and thus more subject to slumping around the pit margins, and so the pits widen and assume an oval shape. The sparsity of amphipods in the coarser substrate, in turn, may cause sporadic whale feeding behavior and development of isolated pits.

The central part of the Chirikov Basin and nearshore areas of St. Lawrence Island in the northeastern Bering Sea encompass approximately 22,000 km² of sea floor that exhibits gray-whale-feeding pits (fig. 1). The extent of sea floor disturbance by fresh feeding pits and by current-scour-enlarged pits averages 12 percent in type I areas, 10 percent in type II areas, and 5 to 7 percent in type III areas (table 1). Whale-feeding pressure can be more accurately estimated by classifying the pits according to size. Fresh whale feeding pits can be distinguished from current-scour-enlarged pits because the fresh pits form a separate statistical group, the smallest and original size class of feeding pits (fig. 5). Using 5.3 m² as an upper limit for the area of a fresh pit, the average extent of sea-floor disturbance is estimated at 5.6 percent during a whale-feeding season in the Chirikov Basin (table 1).

Biologic Significance

Quantifying the annual feeding area on the Bering Shelf by mapping bottom disturbance from whale-feeding pits makes it possible for the first time to calculate the proportion of food resources utilized during one season. Data on the area of feeding pits, amphipod biomass in sediment, and whale food-consumption rates can be combined to estimate the amount of feeding on the northeastern Bering Shelf and the percentage of food resource that this shelf provides for the total gray-whale population.

The area of fresh pits can be taken as a measure of the minimum yearly feeding pressure, assuming that fresh pitting is not cumulative for different years.

Table 1. Definition of the three types of whale-feeding pits observed on side-scan sonographs (n=1,027) and plotted on size-frequency histograms

Type	Description and origin	Average length (m)	Average width (m)	Average length/width ratio	Shape class	Average percentage of sea floor disturbed	
						Fresh and modified features	Fresh features observed
I	Multiple suction feeding pits with current-enlarged pits.	4.6	1.9	2.5	Elliptical-----	12	4.2
II	Fresh and partially modified elongate pits.	4.1	1.3	3.2	Narrow elliptical---	10	6.8
III	Oval pits-----	2.4	1.3	1.9	Wide elliptical-----	5.7	3.5

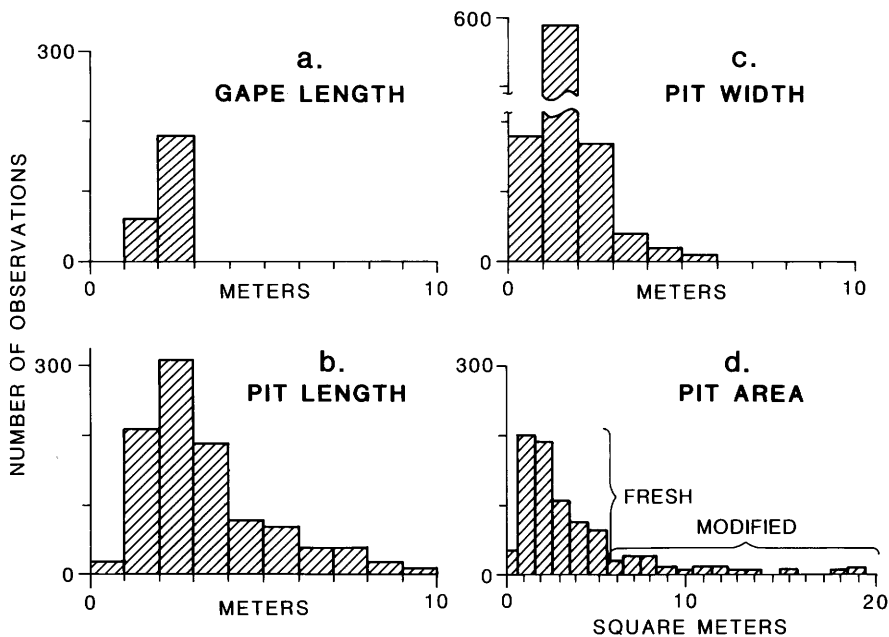


Figure 5. (a) Histogram of gray-whale gape length measured on 240 whales. Histograms of (b) feeding-pit length, (c) width, and (d) area, based on measurements of 64 pits at each of 16 side-scan-quantification stations in the Chirikov Basin.

This assumption appears to be valid because of the seasonality of summer feeding followed by late autumn storm-induced currents that modify fresh pits.

The amount of biomass consumed by feeding whales can be estimated because the amphipod concentration in the central part of the Chirikov Basin has been measured by several biologists (Nerini, Stoker and Thompson) and averages 171 g/m². Using values for the total area disturbed (1,217 km²) and the biomass per unit area, the whale consumption of amphipod biomass in the northeastern Bering Sea is estimated as 208.1 million kg for the entire 1980 season.

The amount of food that a mature gray whale consumes each day has been estimated to average 1,100 kg (Rice and Wolman, 1971). Using these whale-feeding rates and the calculations of amphipod biomass consumed in the northeastern Bering Sea, we estimate the number of whale-feeding days (WFD) in these areas at up to 191,500 for the entire 1980 feeding season.

The relative importance of the northeastern Bering Sea as a gray-whale-feeding area can be determined by totaling the number of WFD's per season for the entire gray-whale population in the Bering Sea. Assuming a 1980 population of 16,000 whales (Moore and Ljungblad, 1984) that spend at least 180 WFD per year in the Bering and Chukchi Seas, this population accrues a total of 2,880,000 WFD per season. Thus, 22,000 km² of the northeastern Bering Sea or 2 percent of the total summer feeding range of gray whales (estimated at 1,000,000 km² by biologists Frost and Lowry, 1981) accounted for 6.5 percent of the entire gray-whale-feeding pressure in Arctic areas during the 1980 season.

These estimates can be treated as minimums because side-scan sonar underrepresents the small (fresh) features that do not parallel the trackline, and whales may graze along the margins of the large scour-enlarged pits.

The extensive disturbance of the sea floor by gray-whale feeding and then subsequent current scour has important implications for predator-prey relations. The baleen of gray whales apparently has a wide enough spacing to allow juvenile amphipods smaller than 4 mm to be expelled with the sediment plume; subsequently, they settle back on the disturbed sea floor. If juveniles are expelled by the gray whales, then there exists an interesting symbiotic relation between the whales and their amphipod prey. These amphipods are known to be tube-building, colonizing species that thrive in areas of substrate disturbance. The whales may be redistributing or "seeding" the young small amphipods expelled in feeding plumes into areas of fresh whale-caused disturbance; at the same time, they are consuming or "harvesting" the mature amphipods. In short, whales may be "farming" the sea floor. The current-scour modification, triggered by foraging whales, may enhance this process.

The biogenic and physical reworking of the sediment also is an effective process for rapid recycling of nutrients in the ecosystem. Thus, the whales contribute to the primary productivity of the area and "farming of the sea floor" in two ways: (1) By addition of their feces as biological nutrients to the water column, and (2) by mixing of the nutrient-rich sediment into the water column and epifaunal environment of the amphipods.

Geologic Significance and Hazards Susceptibility

Whale feeding and subsequent current scour over a period of a few years result in a complete reworking and homogenization of the surface sediment on the northeastern Bering shelf. This process may lead to winnowing and removal of the finer particles; it also destroys sedimentary structures formed when the sand was originally deposited. The whales are a major factor in initiating conditions for current scour and sediment loss because they remove the amphipod mat that binds sediment and provides a protective cover against erosive bottom currents. They also resuspend and inject large amounts of sediment in the water column when whales suck up the amphipod mat and expel it through the baleen.

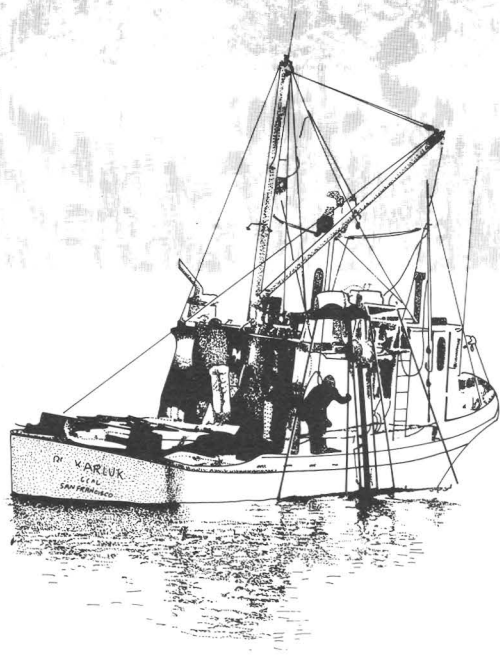
Assuming that 5.6 percent of the total feeding area is excavated to a 10-cm depth, a minimum 120×10^6 m³ of sediment (equivalent to nearly three times the yearly sediment load of the Yukon River) is excavated and injected into the water column by the gray whales feeding there each season. As a result of (1) this sediment resuspension by whales, (2) average current speeds of 10.7 cm/s northward during the feeding season, and (3) enhanced postfeeding current scour because of bottom roughening, 2.5×10^6 m³ of clays are advected from the Chukchi Sea each year, sand gradually is transported northward and fills old feeding pits, and modern mud does not accumulate in this region.

The feeding grounds are sensitive to various environmental changes. For example, the amphipod food resource is known to be highly susceptible to damage by oil spills or toxic wastes. The thin substrate of fine sand that supports the amphipods is also sensitive to impacts from human activities. One such impact is mining of the sand in some areas to construct artificial islands for oil drilling. The sandy substrate, which is less than a meter thick in most of the Chirikov Basin, is a relict sediment that will not be replaced by modern processes. The loss of this substrate would permanently affect feeding grounds for a significant proportion of the whale population.

The loss of feeding grounds for even part of a summer season could severely affect approximately 5.6 percent or more of the gray-whale population supported by amphipods in the northeastern Bering Sea. This effect is particularly important because the whales must migrate great distances to these specific feeding grounds, and they have a limited feeding season that must sustain them for the entire year.

Selected References

- Frost, K. J. and Lowry, L. F., 1981, Foods and trophic relationships of cetaceans in the Bering Sea, *in* Hood, D. W., and Calder, J. A., eds., *The eastern Bering Sea shelf: Oceanography and resources*: Seattle, University of Washington Press, v. 2, p. 825–836.
- Moore, Sue, and Ljungblad, Don, 1984, The gray whale (*Eschrichtius robustus*) in the Bering, Beaufort and Chukchi Seas: Distribution and sound production, *in* Jones, M. L., Swartz, S., and Leatherwood, S., eds., *The gray whale: Eschrichtius robustus*: New York, Academic Press (in press).
- Nelson, C. H., Rowland, R. W., Stoker, S. W. and Larsen, B. R., 1981, Interplay of physical and biological sedimentary structures of the Bering Sea epicontinental shelf, *in* Hood, D. W. and Calder, J.A., eds., *The eastern Bering Sea shelf: Oceanography and resources*: Seattle, University of Washington Press, v. 2, p. 1265–1296.
- Nerini, Mary, 1984, The feeding ecology of the gray whale: A review, *in* Jones, M. L., Swartz, S., and Leatherwoods, S., eds., *The gray whale: Eschrichtius robustus*: New York, Academic Press (in press).
- Oliver, J. S., Slattey, P. N., Silberstein, M. A., and O'Connor, E. F., 1984, A comparison of gray whale feeding in the Bering Sea and Baja California: *Fishery Bulletin*, v. 81 (in press).
- Ray, G. C. and Schevill, W. E., 1974, Feeding of a captive gray whale: *Marine Fisheries Review*, v. 36, no. 1, p. 31–37.
- Rice, D. W. and Wolman, A. A., 1971, The life history and ecology of the gray whale (*Eschrichtius robustus*): *American Society of Mammalogy Special Publication* 3, 142 p.



The Georges Bank Border Dispute

By John S. Schlee

Introduction

Dispute over the U.S.-Canadian border on Georges Bank goes back many years, and, in the refined language of diplomats, the two countries have debated the intricacies of mineral exploration, fishing rights, and territorial jurisdiction for two decades. Elliot Richardson, as U.S. Acting Secretary of State, rejected the Canadian claim to the eastern third of Georges Bank. The Canadian Government, which had leased this area for exploration in an effort to develop its continental-margin areas, claimed the east half of Georges Bank because this area is geographically closer to Nova Scotia than to Cape Cod. Meanwhile, the U.S. Government claimed the entire bank, including Northeast Channel, because of the topographic continuity of the shelf eastward of the margin south of New England (fig. 1) and because of a long history of scientific study and fishing exploitation by the United States. When their first "midpoint" line dividing Georges Bank was not accepted by the U.S. Government, the Canadian Government came up with a second line that was even closer to New England and would eliminate Cape Cod, Martha's Vineyard, and Nantucket Island as valid parts of U.S. coastline from which the midpoint line was to be measured; Cape Cod and the islands were only sandy excrescences from the solid bedrock coastline of New England!

Geologic Investigation

Direct involvement of the USGS in the dispute began in 1980, when David Folger and Sally Needell wrote a report for the Intelligence and Research Bureau of the U.S. Department of State that offered geologic evidence in support of the U.S. claim that Canada could not consider this area as their public land. The main points of Folger and Needell's report were as follows.

1. Georges Bank forms a major barrier to the Gulf of Maine, and Northeast Channel is the main connection between the gulf and the open sea. Great South Channel is but a minor channel that separates the bank from the Nantucket Shoals.
2. The presence of a seasonal clockwise gyre in the surface waters over Georges Bank affects the unique ecosystem of the bank. Strong tidal currents also oscillate over the northern part of the bank.
3. The Georges Bank water mass is separated from Browns Bank by divergent flows at all levels. Some residual currents flow southwestward across Great South Channel and carry fine sediment (and, possibly, pollutants) to the shelf south of Martha's Vineyard and Nantucket for deposition there.

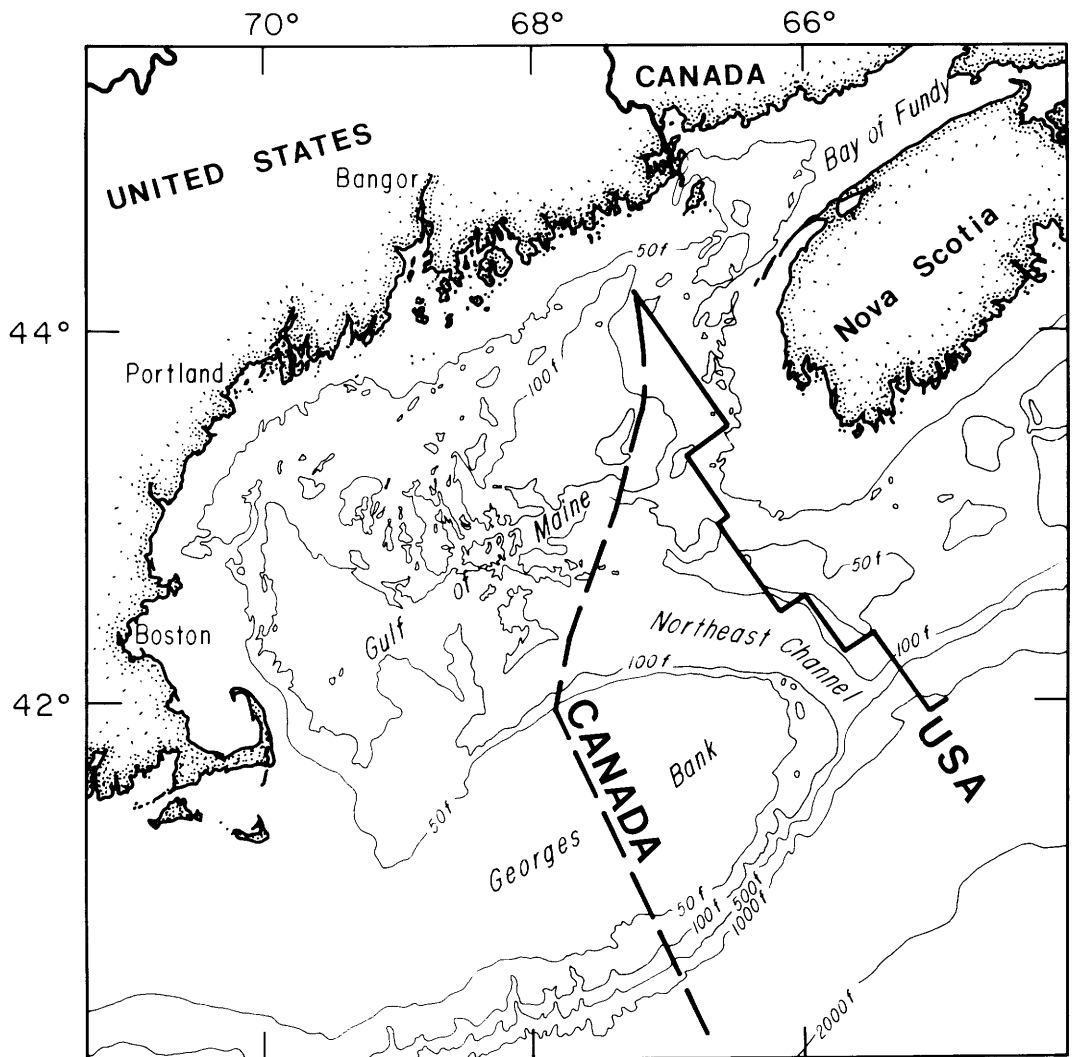


Figure 1. Bathymetric map off the Northeastern United States, showing projected offshore boundaries of the United States and Canada.

4. In the past 17,000 to 18,000 years since the latest major glaciation, sea level has risen 80 m, and so Georges Bank has been covered to a maximum during this interglacial interval.
5. Georges Bank would have been contiguous with the continental United States during times of glacially lowered sea level and could have been populated by humans and large mammals from this country (known as the “Red, White, and Blue Woolly Mammoth argument”).
6. In the surficial sediment between Georges Bank and Browns Bank, gravel composition ranges from granite and felsite in the Browns Bank area to mainly vein quartz, quartzite, and chert on Georges Bank.

Discussion

The present USGS effort to aid the U.S. Department of State began in 1981 as the United States began to prepare for a hearing of the case before the International Court of Justice (ICJ) by filing Memorials and Counter Memorials² in 1982-83. State Department personnel visited Woods Hole, Mass., several times in 1982 and began to develop a strategy. To help give them a basic understanding of the area, Kim Klitgord, Elazar Uchupi of the Woods Hole Oceanographic Institution, and I put together a five-chapter description of the area which included basic geologic terms, the evolution of the North American continental margin, the evolution of Georges Bank, and the physiography of the region. This effort, however, was too technical for the lawyers at the State Department, and so Lt. Comdr. Peter Comfort, on loan from the U.S. Department of Defense, was assigned to translate our information into terms understandable to the legal profession. Scientists at Woods Hole guided Comfort in this endeavor: Elazar Uchupi took responsibility for the bathymetry-physiography of the area, and Kim and I for the tectonic framework of Georges Bank.

The U.S. Department of State retained two geologic experts as possible witnesses, namely, K. O. Emery and Manik Talwani. In the meanwhile, we all read the Memorial and Counter Memorials filed in the Tunisia-Libya case, a similar jurisdictions case, and tried to understand the legal nuances.

In February 1982, Kim and I made a trip to the U.S. Minerals Management Service in Washington to look at their proprietary seismic data over Northeast Channel. I visited Ottawa to view recently released geophysical data in the Browns Bank area. By late September 1982, the Memorials were filed, and there was major agreement by the two Governments on most points. The Canadian Government, however, tried to portray Georges Bank as an "island" province whose jurisdiction could be split with United States, whereas we insisted that the area is a prolongation of the U.S. Continental Shelf eastward to Northeast Channel. The subsurface geology is essentially continuous from area to area and thus not much of an issue.

In June 1983, the U.S. Department of State filed a Counter Memorial to refute the remaining differences. Concerning one of these differences, the Canadian estimates of hydrocarbon resources in the disputed area, we enlisted the aid of Charles Masters of the USGS's World Energy Resources Program to evaluate their figures. I went to Washington to brief Davis Robinson, the agent for the State Department in the case, and tried to help him visualize what Georges Bank would look like if the water disappeared and one could hike from the Nantucket Shoals to Northeast Channel. I emphasized the overall flatness of the area, the low angle of the slopes involved, and the low dunelike physiography of the ubiquitous sand waves over the north half of Georges Bank. I used some new U.S. National Ocean Survey 1:250,000-scale charts to show the complexity of the sand-wave bathymetry of Georges Bank. We also called the State Department's attention to a Canadian Chart (fig. 2) that seemed to depict Georges Bank as we were envisioning it.

²Memorials and Counter Memorials are the legal documents filed by contestants in support of their respective claims.

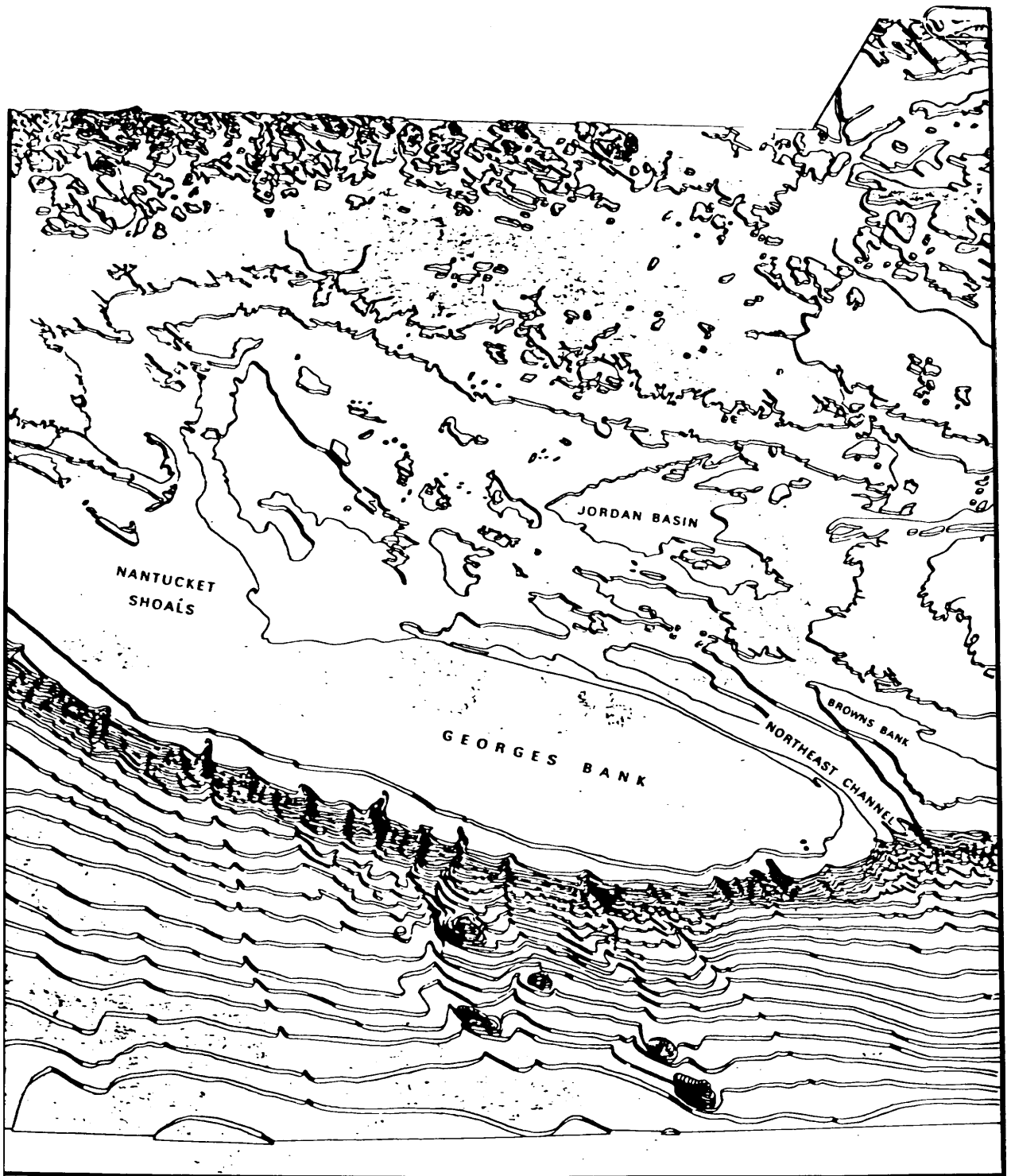
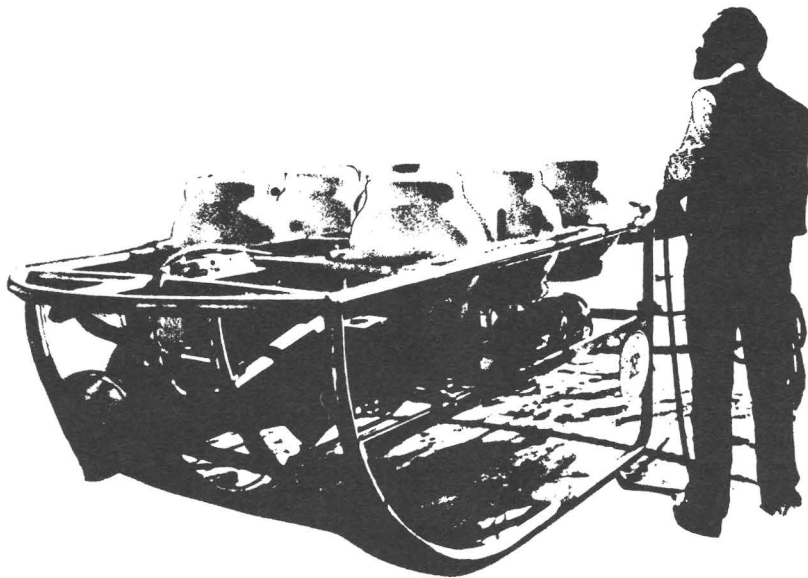


Figure 2. Part of Canadian Hydrographic Service Chart 810 "Continental Margin of Eastern North America."

The actual presentation of the case before the ICJ was scheduled for 1984 at The Hague, Netherlands. There will be great interest not only in what the Court decides but also in which arguments will be most telling with the Court. For those of us involved, it has been a lively balancing act of developing a useful strategy and at the same time keeping the science from being misquoted in defense of a legal point. Only three more borders with Canada are left to be adjudicated.

Acknowledgments

I thank my colleagues for their support and comments, among them W. P. Dillon, K. D. Klitgord, D. W. Folger, Elazar Uchupi, K. O. Emery, C. D. Masters, and Harley J. Knebel. At the U.S. State Department, Peter W. Comfort and Bruce C. Rashkow read my material and “translated” it for use in their Memorial and Counter Memorial.





Diver measuring small-scale bedforms

Principles and Applications of Marine Gravity Surveys

By Jonathan R. Childs

Introduction

Local variations in the density of the Earth's lithosphere and mantle cause small but measurable changes in the gravitational field measured at the surface of the Earth. This phenomenon is of particular importance to Earth scientists because measurement of these small gravitational differences, commonly called anomalies, provides indirect evidence of the density of the underlying rocks and, therefore, an important clue to the subsurface geology. Gravitational measurements can be used to detect salt domes, igneous dikes, sedimentary basins, high-angle faults, or any geologic structure in which rocks of different densities are juxtaposed. Of great use to the geophysicist, gravity measurements are also of concern to missile and space engineers because gravitational variations affect both inertial guidance systems and flight trajectories.

Background

The principles underlying the gravitational effects of the Earth are probably among the most widely understood of all physical concepts. Objects near the surface of the Earth tend to fall toward the Earth with ever-increasing velocity. The rate of this increase, or the acceleration due to gravity, was shown by Galileo Galilei in the early 17th century to be constant for all objects, regardless of shape or mass. Later in the same century, Isaac Newton generalized this observation when he postulated the universal law of gravitation:

$$F = G \frac{M_1 M_2}{r^2},$$

where F is the attractive force between two bodies of mass M_1 and M_2 , separated by the distance between their centers, r ; the constant of proportionality, G , is the universal gravitational constant. This equation applies to any two objects, for example, a pair of billiard balls. Whereas billiard balls and most other objects within our realm of experience have masses so small that the force between them is inconsequential, the Earth represents a very substantial mass, and so we have no trouble observing the gravitational effect between the Earth and nearby objects. To a first-order approximation, we can calculate the gravitational effect of the Earth on an object of mass M by replacing M_1 by M_E , the mass of the Earth, and r by R_E , the radius of the Earth. The gravitational equation then becomes:

$$F = \frac{M_E m}{R^2}.$$

Force is the product of mass and acceleration,

$$f = ma,$$

and so we can rearrange the gravitational equation to define gravitational acceleration, g :

$$g = \frac{F}{M} = G \frac{M_E}{R_E^2}.$$

This value, as Galileo observed, is constant for all objects, as long as M_E and R_E remain unchanged.

Extensive effort was made in the 18th and 19th centuries to determine the gravitational constant, G , and the gravitational acceleration, g ; or, conversely, the mean density of the Earth. The first attempt to measure G was made by Henry Cavendish, who took advantage of the fact that the attraction between spheres is equivalent to that between massive point objects located at the centers of the spheres. The force of attraction was then determined from the torque exerted on a suspended beam. This apparatus was improved over the next two centuries, and the presently accepted value for the universal gravitational constant G is 6.672×10^{-8} cgs units (centimeters squared per gram per second squared).

Progressively better measurements of g were made over the years, generally using pendulum instruments, as described below. Though dependent on the geographic location of the measurement, gravitational acceleration is approximately 980 cm/s^2 (32 ft/s^2). To simplify reference, a centimeter per second squared is called a gal, after Galileo. The milligal (mGal), one-thousandth of a gal, is more commonly used in geologic applications because of the very small differences in gravity that result from density differences in the Earth's upper crust.

Geodesy and Normal Gravity

If the Earth were a spherically symmetrical, nonrotating solid whose density was a function only of depth, this would be the end of the story. Gravity would change only if one moved away from the center of the Earth and would be a very dull subject indeed, although it would make the business of aiming missiles much more predictable.

Clearly, several factors perturb the gravitational field. Gravity over the Earth ranges from about 978 to 983 Gal, increasing toward the poles. The two primary factors causing this variation are the shape of the Earth, which is an oblate spheroid, and its revolution about an axis. A point at the pole is closer to the center of the Earth than a point at the equator, a factor accounting for an increase in gravity of about 6.3 Gal at the poles. Because the Earth is spinning about an axis, there is also a small diminution of the gravitational vector due to centripetal acceleration. This acceleration, which is greatest at the Equator and disappears at the poles, accounts for an additional increase of 3.6 Gal. The total gravitational difference between the poles and the Equator is, however, only 5.2 Gal, significantly less than the combined total of the two aforementioned factors. The decrease in the expected difference is due to the attraction of the added mass that constitutes the equatorial bulge.

All the above effects account for what is called normal gravity. One significant factor that causes the measured gravitational field to differ from normal is local density variation in the near-surface (upper 80 km) of the Earth's crust. The following table lists the range of densities for various minerals within the crust.

<i>Material</i>	<i>Density (g/cm³)</i>
Seawater-----	1.03
Salt-----	2.20
Serpentine-----	2.20
Calcite-----	2.57
Orthoclase feldspar---	2.57
Quartz-----	2.65
Average crustal rock--	2.67
Plagioclase feldspar--	2.70
Biotite-----	3.00
Hornblende-----	3.20
Olivine-----	3.30
Chromite-----	4.50
Pyrite-----	5.00
Magnetite-----	5.00
Galena-----	7.50

The average density of the lithosphere is generally considered to be about 2.67 g/cm³. Localized gravity anomalies are small, ranging from many hundreds of milligals over mountain ranges (caused by the low-density roots that underly mountain masses), down to the limits of measurability (tenths or hundredths of a milligal).

Local anomalies are easier to distinguish when the larger geodetic effect, or normal gravity, is removed. Because the Earth is axially symmetrical, normal gravity (in milligals) is a function of latitude (θ) as expressed in the formula adopted in 1967 by the International Geodesic Association:

$$g(\text{normal}) = 978,031.85 (1 + 0.0053024 \sin^2 \theta - 0.0000059 \sin^2 2\theta),$$

which accounts for all the effects due to the eccentricity and rotation of the Earth. The difference between the measured gravity at a geographic point on the Earth and the normal gravity calculated for that same point is called the anomalous gravity. In terrestrial surveys, a correction must be made to account for the elevation differences between measurement stations. This correction, -0.3086 mGal per meter of elevation, accounts for differences in the distance of the observation from the Earth's center. Measurements are each reduced to a reference datum, generally sea level, as though all the intervening material were removed; thus, this correction is called the free-air correction. Marine surveys are generally assumed to be at constant sea level, where the correction is always zero. Hence, marine gravity anomalies are generally referred to as free-air anomalies.

The objective in gravity studies is to remove the effects of all the mass differences that can be calculated, leaving only those that arise from unknown density variations. Several additional corrections are commonly applied to gravity data. The most significant of these corrections is the Bouguer correction, which accounts for the excess or missing mass caused by the Earth's topography. For

marine data, the Bouguer correction removes bathymetric differences by artificially replacing the seawater column by a rock column with the density of average crustal material. This correction removes, for example, the negative gravity anomaly over submarine canyons that derives from the increased amount of low-density seawater. In practice, Bouguer corrections are only infrequently applied to marine data.

Instrumentation

The study of gravitational effects has always depended on advances in instrumentation to catch up with theory. Gravitational changes are so small that very high precision is required to detect them at all. Measurements of geologic interest require a precision of 1 mGal or less, or better than one part per million. Because most instruments are based on mechanical principles, the problem is one of isolating the instrument from other effects of the environment, such as friction and vibration.

Gravity instruments fall into one of two general categories: those that measure the absolute gravity at a point on the Earth, and those that measure the relative gravity differences between two points. The most direct and obvious way to measure absolute gravity is to measure the free-fall rate of an object near the Earth's surface. Early attempts to use this method failed, however, because of the difficulty in measuring small time intervals. A free-falling object travels about 5 meters in the first second, which must be measured to one part in a million for an accuracy of 1 mGal. Until recently, such precision was unattainable.

The earliest successful measurements of gravity employed the pendulum principle. The period of the arc of a pendulum, F , is proportional to the square root of the length of the pendulum arm, l , divided by the gravitational acceleration, g :

$$F = \left(\frac{l}{g} \right)^{1/2},$$

and is independent of all other factors. In fact, the earliest evidence that gravity actually changes over the surface of the Earth was the observation made in the 17th century that pendulum clocks require an adjustment of their pendulum length when moved from one place to another.

Double pendulums, which consist of two pendulums swinging in opposite directions on the same axis, were used in the early 19th century to obtain the first accurate measurements of absolute g . Instrumentation advanced until 1906, when measurements reported by Kühnen and Furtwängler led to an internationally accepted value at Potsdam, Germany, of 981.274 Gal. This value remained the basis for the world gravity net until very recently, when results of new free-fall instruments indicated that it was approximately 14 mGal too high. The presently accepted value at Potsdam is now 981.260 Gal.

Accurate measurements of relative gravity are much easier, and instruments use a wide variety of physical principles. Most such instruments measure the displacement of a mass at the end of a string or a beam. Probably the most widely used field gravimeter in the United States is the LaCoste and Romberg meter, illustrated schematically in figure 1. The sensing mass is located at the end

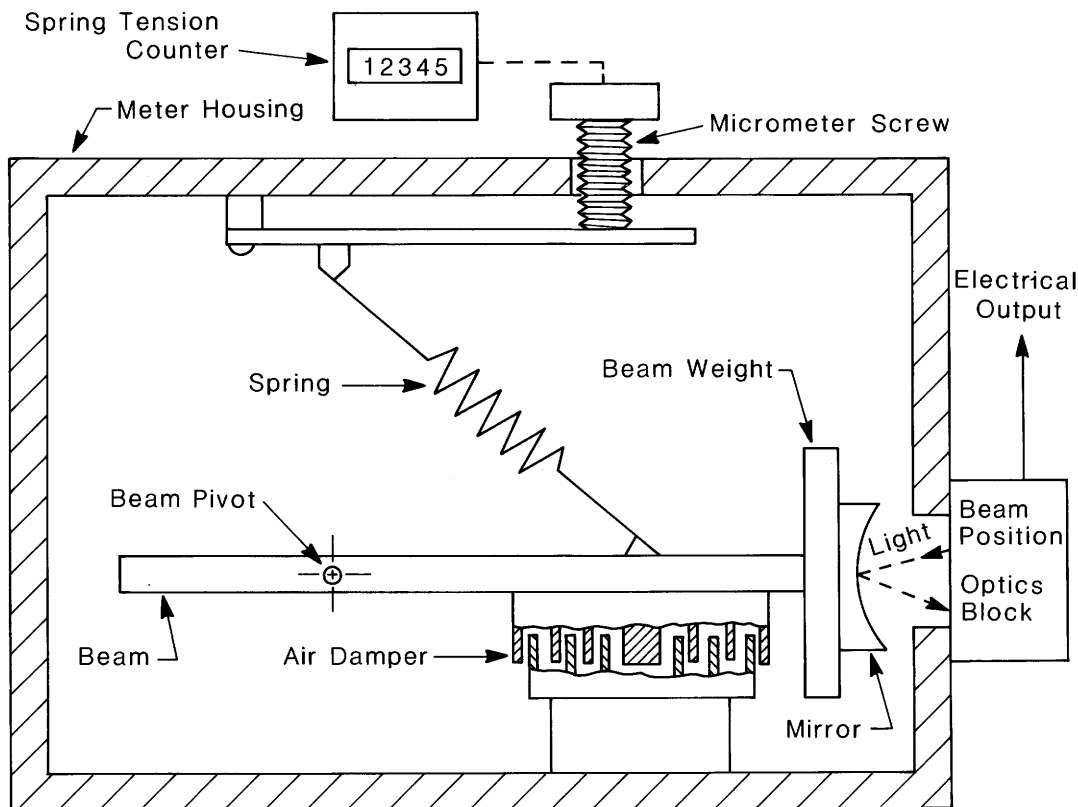


Figure 1. Schematic diagram of LaCoste and Romberg sea gravimeter. The sensors of LaCoste and Romberg sea and land gravimeters are essentially identical, except that the beam in the sea gravimeter is allowed to continuously move about a null position.

of a mechanical beam, which is hinged and supported by a spring. As the gravity varies, displacement of the mass causes the beam to depart from the null position, and the tension on the spring is manually adjusted to return the beam to equilibrium. The observed “spring tension” is highly proportional to the relative gravity. With this instrument, the gravity differences between two points on the Earth can be measured as accurately as 0.01 mGal.

Measuring gravity from a moving platform, such as a ship or an airplane, introduces an entirely different set of instrumentation problems because any acceleration of the platform will generate a force that is indistinguishable from gravity. For example, a gravimeter aboard a ship is subject to various motions (roll, pitch, heave, course and speed changes), all of which cause accelerations that are large in comparison with the gravitational differences being measured. Fortunately, most of these motions have periods that are small (less than 2 minutes) relative to true gravitational changes that would be detected at normal ship speeds. The smallest gravitational anomalies of interest to geologists are about 2 km wide; at ship speeds of 10 knots (18.5 km/h) this distance represents a period of about 6.5 minutes. Therefore, by filtering the gravity data to exclude periods of less than 3 to 4 minutes, the effects of ship motion can be effectively differentiated from the geologic sources of interest.

The gravimeters used by the USGS are LaCoste and Romberg sea gravimeters, nearly identical to the one described above. They have been modified by allowing the beam to oscillate, while a feedback mechanism continually changes the spring tension so as to keep the average position of the beam null. The movement of the beam is heavily damped to limit the velocity of its motion, and the feedback mechanism is filtered to remove the effects of ship motion. These sea gravimeters, which represent a triumph in instrumentation, achieve an accuracy of between 2 and 5 mGal even under moderate sea conditions.

Measuring gravity on a moving platform is also complicated by the fact that any platform motion in an east-west direction contributes to the centripetal acceleration detected by the gravity sensor. The Earth travels with an easterly rotation, and so travel along an easterly heading increases the centripetal acceleration, while travel along a westerly heading decreases the centripetal acceleration. This Eötvös effect is a maximum at the Equator, and disappears at the poles.

The Eötvös effect is a function of ship speed, ship heading, and latitude, according to the relation:

$$E = 7.5v \cos(\text{latitude}) \sin(\text{heading}),$$

where the Eötvös effect, E , is in mGal and the velocity, v is in nautical miles per hour (knots). At the Equator, along a heading of 90° and a ship speed of 10 knots, the Eötvös correction would be 75 mGal, which is comparable in amplitude to the anomalies being measured. Therefore, navigational precision is as important to a gravity survey as the gravity measurement itself. In fact, navigation is generally the limiting factor in gravity surveys because determination of ship heading and speed to a precision equivalent to that of the gravimeter measurements is possible only with the most sophisticated of navigation aids. The Eötvös effect disappears if tracklines are run in a north-south direction, with no east-west component. However, since the derivative of the sine function is a maximum at zero, small deviations from a true north or south heading result in large relative changes in the Eötvös effect. Therefore, gravity surveys are generally run along east-west lines, where the Eötvös effect is maximum but most accurately measurable.

Networks

Because most gravimeters measure only a relative value, any gravity survey must contain a fixed, known point, commonly called a tie. Therefore, gravity surveys are always networked, and each new measurement is an extension of a previously measured point. It is critical that the net remain internally consistent. Although several nets are currently in use, the most widespread is the International Gravity Net, based on the value at Potsdam given above. This net contains primary nodes in most countries of the world. The primary network node in North America is located in the Commerce Building in Washington, D.C. This value is an extension of the value at Potsdam, by way of Bad Harzburg, F.R.G., and Teddington, England. Figure 2 shows the world network of Woollard and Rose (1963).

Marine Gravity Surveys

Gravity measurements have proved to be a valuable research and exploration tool in the earth sciences. Marine surveying was pioneered in the 1930's by

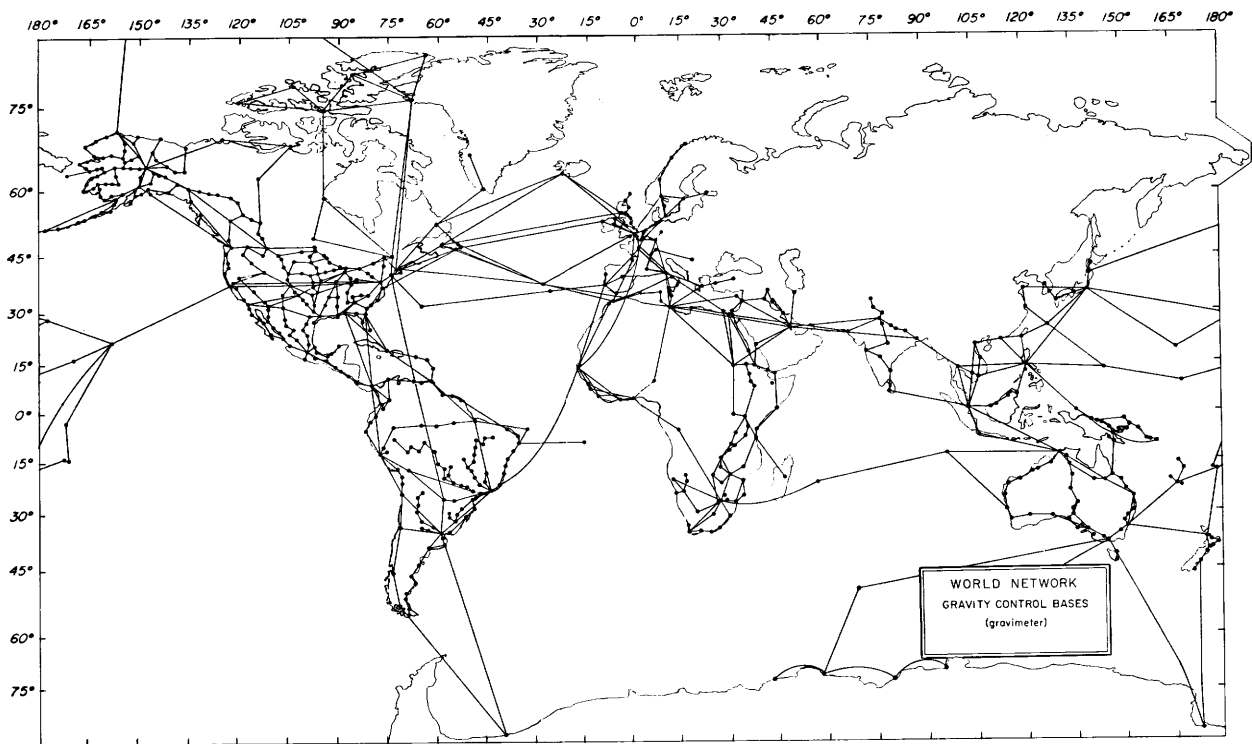


Figure 2. World gravity network (by permission of publisher from Woollard and Rose, 1963, fig. 1.5).

Vening Meinesz, who made numerous pendulum measurements aboard submarines. These surveys, which exposed very large negative anomalies at continental margins throughout the world, provided the first evidence of deep ocean trenches. Though caused in part by the increased column of low density seawater in the trenches, these large negative anomalies were later shown by Manik Talwani to be caused primarily by low-density sediment within the trenches and (or) low-density oceanic crust subsiding beneath the trenches. Figure 3 shows a represen-

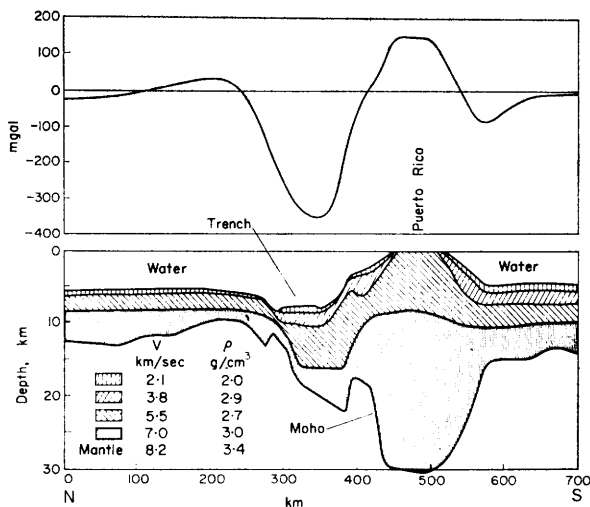


Figure 3. Crustal section through the Puerto Rico Trench, determined from seismic refraction and gravity profile (by permission of publisher from Garland, 1965, fig. 7.4).

tative section through the Puerto Rico Trench. The normal gravity has been removed from the profiles in these illustrations, leaving only the anomalous profile. Gravity data are commonly interpreted in conjunction with seismic refraction or reflection data, which help to delineate the rock layers within the crust and upper mantle of the Earth. The bounds placed by one type of data on the structural geometry or material densities allow a unique model to be developed. Without these bounds, an infinite number of possible configurations exist that could cause a particular gravity expression.

Gravity measurements were instrumental in early oil exploration, particularly for locating salt domes in the Gulf of Mexico. Salt is a relatively low density material that is impermeable to fluids. Because of its low density, buried salt tends to rise through overlying sediment, in the form of mushroom-shaped domes. Where the salt truncates hydrocarbon-reservoir beds, structural traps are formed. This fact was well known to early oil geologists, who drilled along the flanks of salt domes with regular success. Finding oil became a problem of locating salt domes, and before the development of seismic surveys, the search was made with gravimeters. The low-density salt creates a distinctive negative profile, as illustrated in figure 4.

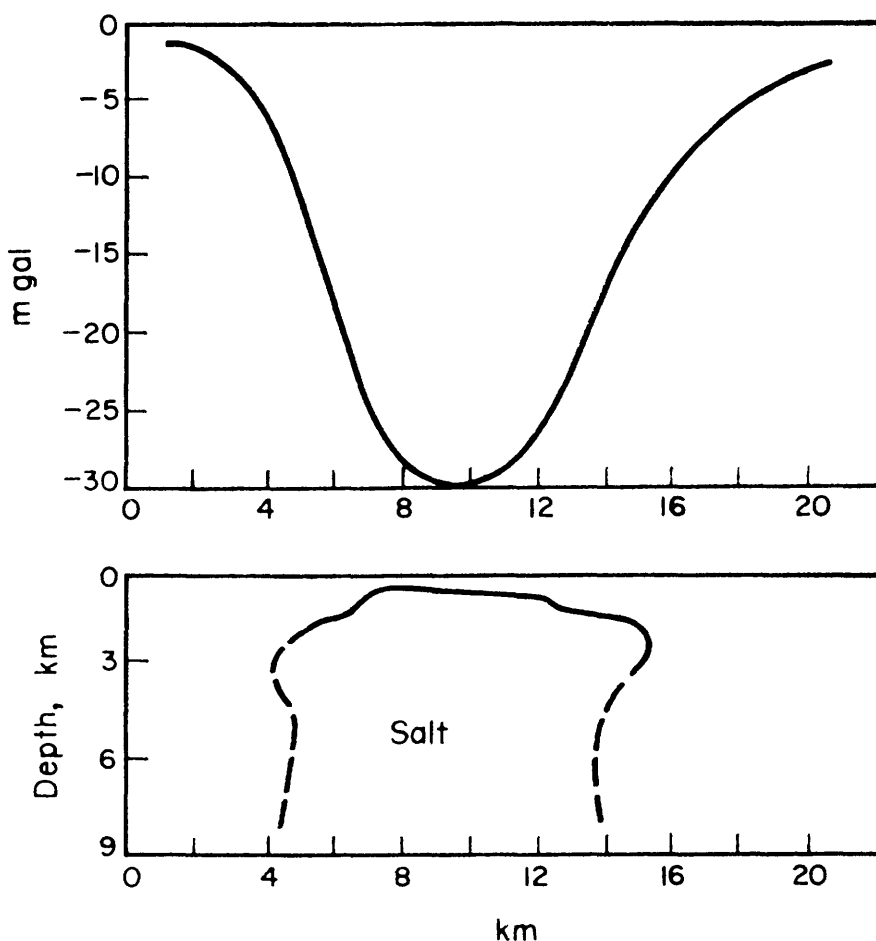


Figure 4. Gravity anomaly across a salt dome (by permission of publisher from Garland, 1965, fig. 8.3).

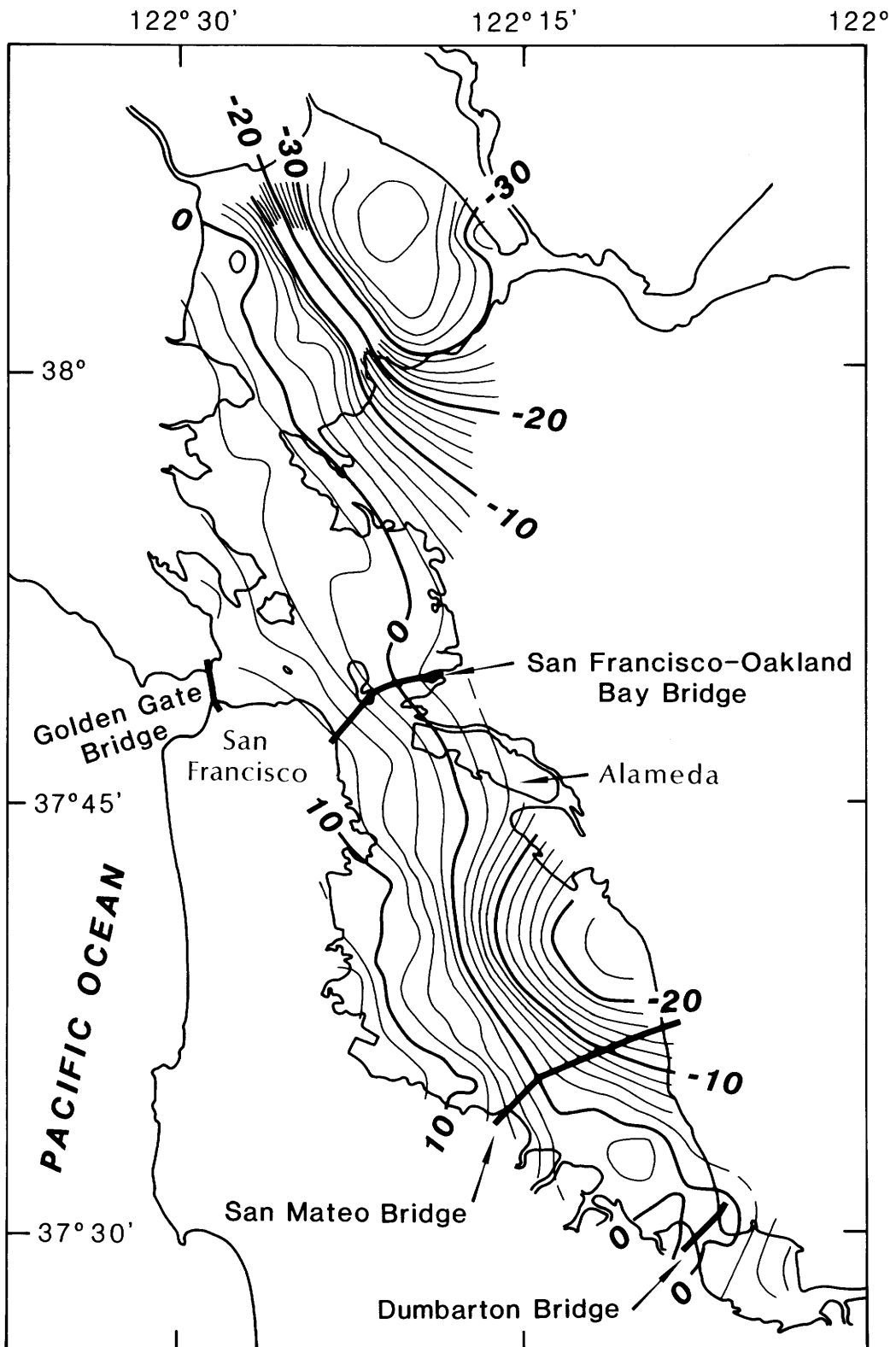


Figure 5. Gravity-anomaly map of the San Francisco and San Pablo Bays. Contour interval, 2 mGal.

On a regional scale, gravity measurements have been used to determine the location, extent, and depth of sedimentary basins that are candidates for hydrocarbon exploration. Because marine gravity surveys are probably an order of magnitude less expensive than seismic surveys, they are highly useful in regional exploration. Areas of high potential can be located with gravity measurements, and then intensively explored with seismic methods. With the advent of airborne gravimetry, this approach may be highly useful in remote areas where access is limited. Even after an area has been explored seismically, gravity data provide important ancillary information about rock density and seismic velocity, which is a function of density.

USGS Marine Gravity Programs

Sea gravity data are routinely collected during all geophysical surveys conducted by USGS research vessels. Many hundreds of thousands of line miles of gravity data that have been collected have resulted in recent publication of new gravity maps of the Bering and Arctic Seas, the Gulf of Alaska, central and southern offshore California, the Atlantic coast, the Gulf of Mexico, and, most recently, areas of the South Pacific in the vicinity of the Tonga, Vanuatu, and Solomon Islands groups.

The USGS also is currently collecting high-precision gravity data from shallow-water marine areas in cooperation with the Defense Mapping Agency of the U.S. Department of Defense. The first survey completed under this program was a bottom-meter survey of the San Francisco Bay. Previously, gravity measurements had been made only about the perimeter of the bay and along the few bridges that cross it. A total of 281 new stations were collected, and interpretation of the new data is presently underway. This study will shed light on the fault pattern that underlies the bay, and improve our understanding of the structure and evolutionary history of the bay region. Figure 5 shows a preliminary gravity-anomaly map of the San Francisco Bay region.

A second survey area includes the east and west coasts of Florida, from Atchafalaya in the northeastern Gulf of Mexico to the Florida Keys, and then up the southern Atlantic seaboard. This survey, which covers more than 8,000 nautical-trackline miles, will provide a critical continuum between existing land data and marine data collected farther offshore. These data will be used primarily by the U.S. Defense Mapping Agency in their program to develop detailed maps of the Earth's gravitational field, but will also be available for geologic interpretation of areas that have been only sparsely explored and that may have significant resource potential.

References

- Dehlinger, Peter, 1978, *Marine gravity*: Elsevier, Amsterdam, 322 p.
Garland, G. D., 1965, *The earth's shape and gravity*: Pergamon, Oxford, U.K., 183 p.
Woollard, G. P. and Rose, J. C., 1963, *International gravity measurements*: Tulsa, Okla., Society of Exploration Geophysicists, 518 p.

Program EEZ-SCAN: A Reconnaissance View of the Western U.S. Exclusive Economic Zone

By James V. Gardner

Introduction

Marine geology has progressed in the past century from a primitive science in which buckets and lead weights dangling from hemp ropes were dragged along the sea floor in the hope of collecting sediment to one that utilizes sophisticated electronic and mechanical devices to obtain views and samples of the sea floor or of various layers beneath it. However, equipment that allows a reconnaissance view of the sea floor has been slow in development. This has created a difficult situation for marine explorers, who have had to produce regional-scale maps from a synthesis of detailed but widely spaced geophysical information. In contrast, geologists working on land typically approach an unknown area by first obtaining Landsat satellite images of the region and studying them for large-scale trends and patterns. The Landsat photos typically cover a swath about 185 km wide, providing an areal reconnaissance. Next, the geologist might gather all the large-scale aerial photographs available; these typically have a swath width of about 5 km. By studying these photographs, trends and patterns found in the Landsat data can be confirmed, and the mesoscale trends as seen on the aerial photographs can be noted. The final step would be to visit the area and take outcrop photographs and samples from areas of interest, determined, in part, from the Landsat data and aerial photographs. The land geologist has thus progressively focused his attention from a large-scale reconnaissance survey to the details of an outcrop.

The marine geologist traditionally has had to reverse this sequence to study the sea floor and the rock layers beneath it, by first conducting a seismic survey of the unknown area, a survey that typically produces swaths of data less than 0.1 km wide that are separated from each other by tens or even hundreds of kilometers. This provides widely spaced, rather detailed information in the form of vertical slices through the sea floor and subbottom. Commonly, dredges, cores, and photographs of the sea floor are then taken, again with widely spaced samples. Thus, initially no large-scale reconnaissance view of the sea floor is available from which to further refine the data; instead, the reconnaissance view is derived from his interpretation of widely separated lines or locations of detailed data.

Side-scan sonar is a tool that can provide a plan view of relatively wide expanses of the sea floor. Initially, it was developed for military applications, but it has since found ready use in marine surveys. The principle of side-scan sonar is relatively simple. An instrument called a fish sends out a beam of sound that images, or insonifies, the sea floor (fig. 1), and the reflected acoustic energy is recorded by the fish. The data are transmitted from the fish to a ship-borne recorder that analyzes and displays them in a graphic form as a sonograph of the sea floor (fig. 2). This process is somewhat analogous to side-looking radar imag-

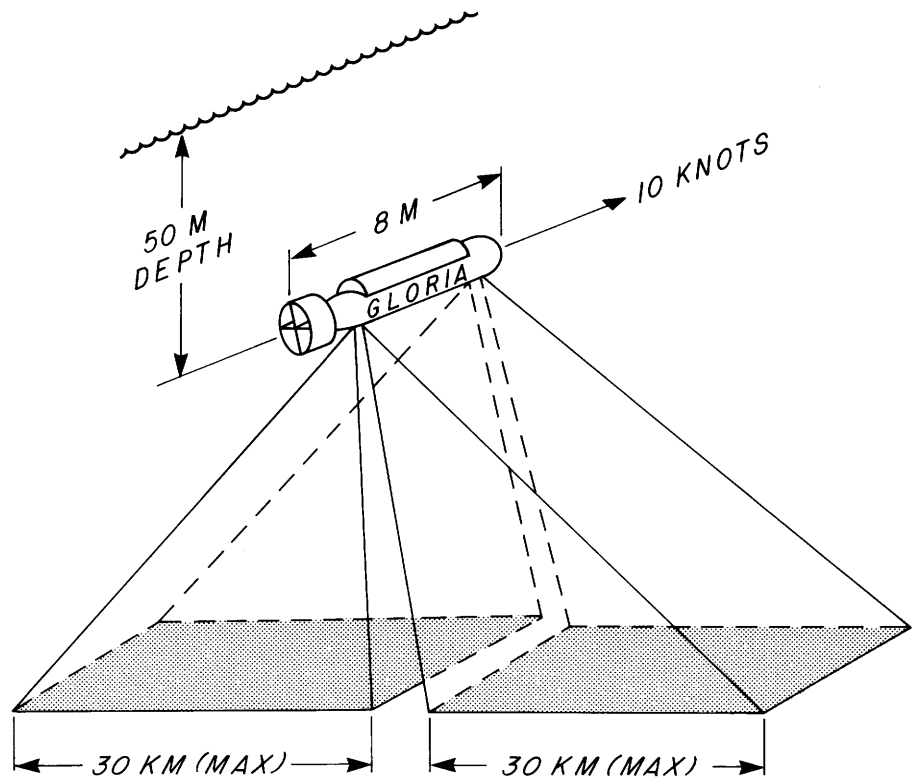


Figure 1. Cartoon depicting the two sonar beams transmitted to either side of the GLORIA side-scan-sonar fish. A 2-second pulse is transmitted out, and the system listens for 20, 30, or 40 seconds, whichever is chosen for the survey.

ing, and the resulting sonographs are similar in appearance to radar images of the Earth's surface.

Although side-scan sonar has been available to the marine geologist for many years, the capabilities of the equipment until recently have been limited. Conventional side-scan sonar can insonify swaths typically less than 1 km wide. These instruments must be towed close to the sea floor; consequently, they are generally restricted to water depths of a few hundred meters because of the long electrically conductive tow cables required, and to ship speeds of less than about 3 knots. However, two systems, SeaMARC and SeaBeam, recently developed by International Submarine Technology, Ltd., in the United States, are able to obtain mesoscale coverage of the sea floor with swath widths of about 10 and 3 km, respectively; and a third system, GLORIA (Geological Long-Range Inclined Asdic), developed by the Institute of Oceanographic Sciences-I.O.S.- (United Kingdom), can obtain true large-scale reconnaissance views of the sea floor. GLORIA is a side-scan-sonar system that, because of its unique design, can insonify a maximum 60-km-wide swath (30 km to either side of the ship's track). Because it is towed only 50 m below the sea surface, GLORIA can survey at relatively fast speeds (10 knots), allowing it to cover an area of as much as 27,700 km² per day. It can operate in water as shallow as 150 m and has no maximum-water-depth limit.

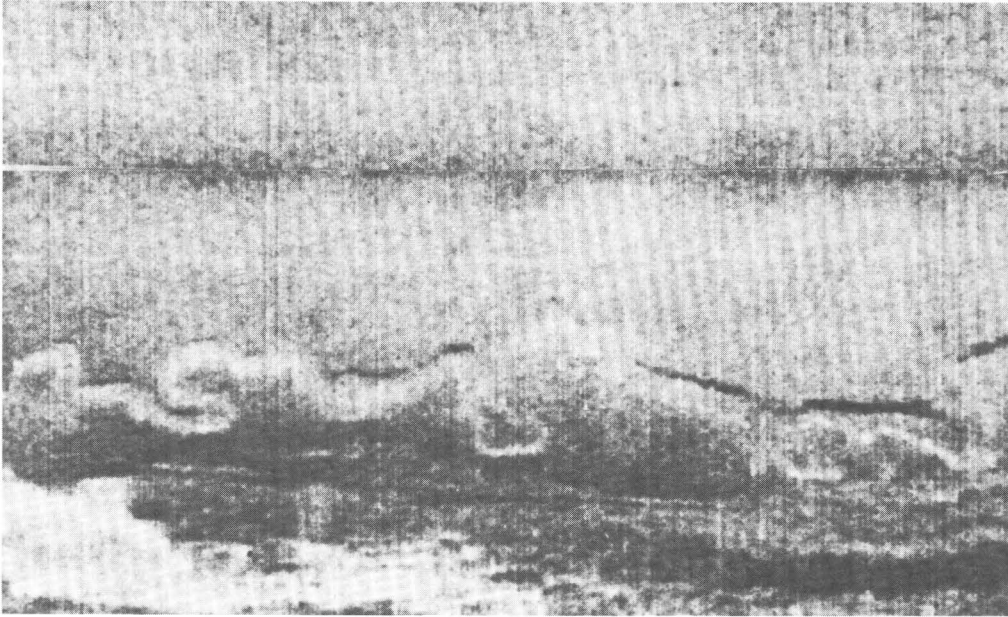


Figure 2A. Digital sonograph of a meandering channel and fault 70 km west of Cape Mendocino, northern California. Channel shows classic oxbow meanders similar to those found on land. Linear feature just south of this channel is a fault associated with the Mendocino Fracture Zone; this feature has been traced on sonographs for more than 180 km. Area shown is about 9 by 26 km and lies at an average water depth of 2,500 m.

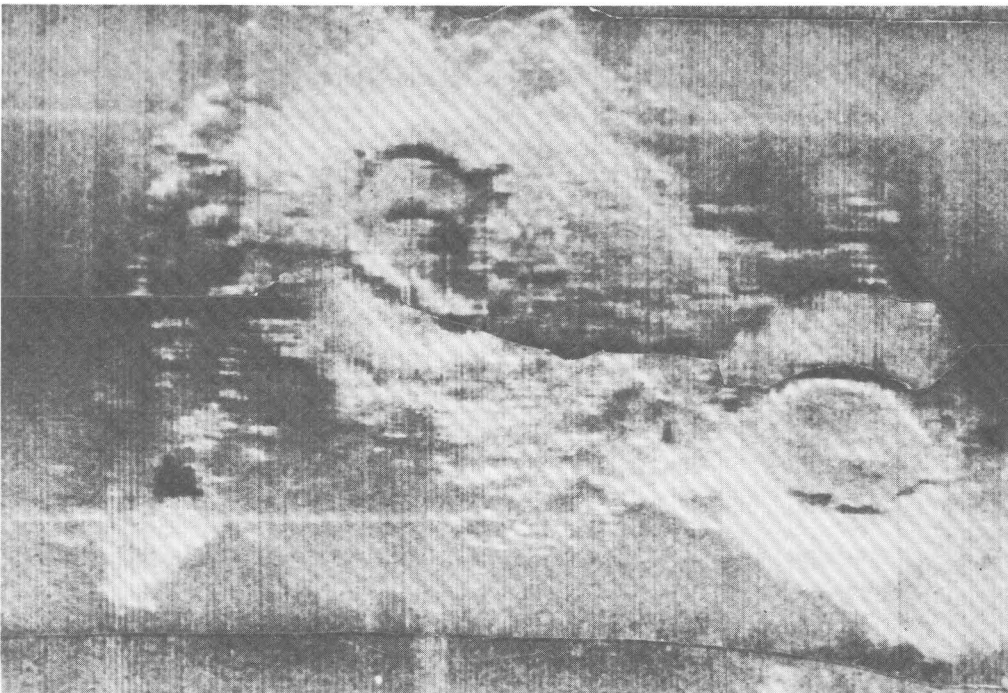


Figure 2B. Taney Seamounts, as viewed with GLORIA. Summit of largest seamount is 8.3 km in diameter. Note that the morphology of the seamounts appears to be more typical of submarine calderas than of submarine extrusive-type seamounts. Water depth above sea floor is about 4,200 m, and above seamount summits about 2,000 m. The Taney Seamounts are situated about 280 km southwest of San Francisco, Calif.

The GLORIA System

The GLORIA system is composed of a side-scan-sonar fish that is 8 m long (fig. 3) and weighs 2 tons in air. The GLORIA gantry automatically lowers the fish over the fantail of the ship, and the fish is towed beneath the sea surface by a single cable connected to its nose. The sonar array is composed of two rows of 30 transducers each, on either side of the fish. The transducers send out a burst of energy with a frequency of 6.5 kHz and a 100-Hz bandwidth. The incoming “reflections” from the port and starboard sides are recorded separately, and the data are corrected for distortions due to slant-ranging and changes in the ship’s speed. The system has the capability to identify features only 20 cm high, features separated by only 45 m in the direction perpendicular to the ship’s track, and features about 100 m long in the direction parallel to the ship’s track. The initial data, slant-ranged and anamorphically corrected in real time aboard the ship, are presented as a reconnaissance plan view of the sea floor that resembles an aerial photograph taken from high altitude. Because the data are in a digital format, they are amenable to a multitude of computer-aided image processing and enhancement techniques.

GLORIA has been successfully used in surveys of the Atlantic margins of the United Kingdom and the United States, the Gulf of Mexico, the Amazon Fan, the



Figure 3. The GLORIA fish mounted aboard the British research vessel *Farnella*.

Laurentian Fan, the Iberian margin, the Gulf of Cadiz, the Mid-Atlantic Ridge and East Pacific Rise, the Nares Abyssal Plain, the Blake-Bahama Ridge and Rockall Bank, the Mediterranean Sea, and the Bay of Biscaye (see the bibliography for a partial list of studies that deal with GLORIA surveys of various regions). These surveys have discovered major new morphologic features on the sea floor, such as large meandering channels on submarine fans and previously unrecognized major sediment drifts formed by deep boundary currents. GLORIA data also have been used to significantly advance our understanding of fault geometries and processes at fracture zones and midoceanic ridges. Program EEZ-SCAN will be the first extensive use of GLORIA in the Pacific.

The Program

When the United States declared a 200-mile Exclusive Economic Zone (EEZ) in 1983, it claimed sovereign rights and jurisdiction over an area that extends 365 km (200 nautical miles) seaward from its shores, in effect increasing the national boundary of the United States by an area equivalent to about two-thirds of the combined areas of the U.S. and Alaska. This vast region is mostly unknown geologically, but what is known indicates that the region has significant economic potential. The small percentage of the region that has been studied has reserves of oil and gas, as well as hard-mineral deposits, including polymetallic sulfides, cobalt-rich manganese crusts, sand and gravel, phosphates, gold, and others.

The first program to systematically map the EEZ along our Pacific margin, termed EEZ-SCAN, will result in a broad, regional reconnaissance survey (fig. 4) to provide a foundation for subsequent, more detailed studies focused on areas identified as being of special interest. The program, established in cooperation with the Institute of Oceanographic Sciences (U.K.), began in April 1984 with a survey extending from the edge of the continental shelf seaward to the 200-mile limit, and from the U.S.-Mexican border to the U.S.-Canadian border. Ship tracks were aligned so that virtually the entire area is insonified. The first cruise sailed from San Diego and surveyed the area between the U.S.-Mexican border and the latitude of Point Conception. The second cruise sailed from Los Angeles and surveyed the region between Point Conception and Point Arena. The third cruise covered the area between Point Arena and latitude 44° N., and the fourth cruise completed the survey northward to the U.S.-Canadian border. From the data obtained during EEZ-SCAN, we will attempt to identify, classify, and map major geomorphic and sedimentologic features, including major slumps on the continental margin, large-scale and mesoscale features such as submarine canyons, channels, valleys, and bedforms, and various types of surface sediment.

Data from GLORIA will be processed at the USGS, using sophisticated computer-enhancement techniques developed by the USGS for space and planetary science programs. These data will be interpreted by scientists from the USGS and the Institute of Oceanographic Sciences, among others. Interpretations of GLORIA data and compilations of the sonographs will be published as a preliminary atlas of sonographs. This atlas, to be composed of thirty-three 2° sheets at a scale of 1:500,000, will be available generally and will, for the first time, provide an overall view of the vast region that lies hidden beneath the sea adjacent to the Pacific coast of the United States.

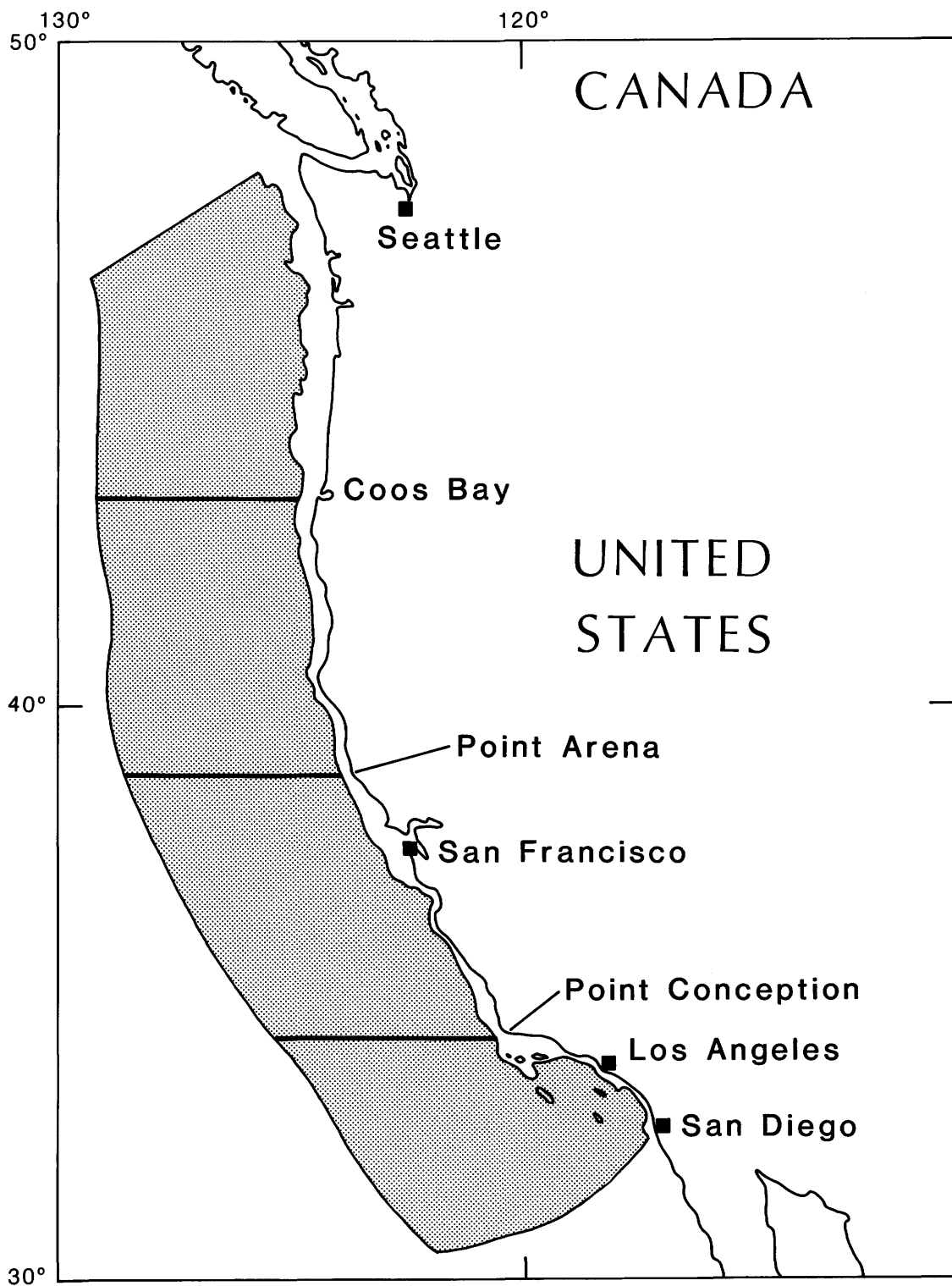
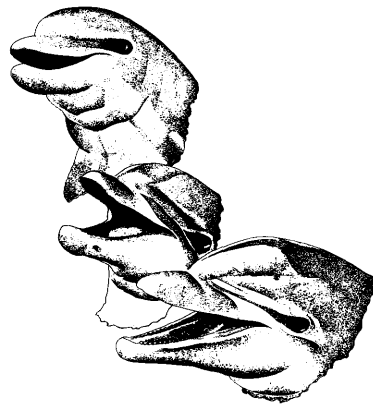


Figure 4. Conterminous U.S. Pacific EEZ area covered in program EEZ-SCAN.

Selected References

- Belderson, R. H., and Kenyon, N. H., 1976, Long-range sonar views of submarine canyons: *Marine Geology*, v. 22, p. M69–M74.
- Belderson, R. H., and Kenyon, N. H., 1977, Outer ridges of orogenic arc systems, *in* Angel, M. (ed.), *A voyage of discovery: George Deacon 70th anniversary volume*, Pergamon Press Ltd., Oxford, p. 627–635.
- Belderson, R. H., Kenyon, N. H., and Stride, A. H., 1972, Sonographs of the sea floor: Elsevier, Amsterdam, 185 p. Belderson, R. H., Kenyon, N. H., and Stride, A. H., 1974, Features of submarine volcanoes shown on long range sonographs: *Geological Society of London Journal*, v. 130, p. 403–410.
- Garner, J. V., and Kidd, R. B., 1983, Sedimentary processes on the Iberian continental margin viewed by long-range side-scan sonar Part 1: Gulf of Cadiz: *Oceanologica Acta*, v. 6, p. 245–254.
- Kenyon, N. H., and Belderson, R. H., 1973, Bed forms of the Mediterranean Undercurrent observed with side-scan sonar: *Sedimentary Geology*, v. 9, p. 77–99.
- Kenyon, N. H., and Belderson, R. H., 1977, Young compressional structures of the Calabrian, Hellenic and Cyprus Outer Ridges, *in* Biju-Duval, B. and Montadert, L. (eds.), *International symposium on the structural history of the Mediterranean Basin*, p. 233–240.
- Kenyon, N. H., Belderson, R. H., and Stride, A. H., 1978, Channels, canyons and slump folds on the continental slope between south-west Ireland and Spain: *Oceanologica Acta*, v. 1, no. 3, p. 369–380.
- Kidd, R. B., 1982, Long-range sidescan sonar studies of sediment slides and the effects of slope mass sediment movement on abyssal plain sedimentation, *in* Saxov, S. and Nieuwenhuis, J. K. (eds.), *Marine slides and other mass movements*, NATO Conference Series IV: Marine Sciences, Plenum Press, New York, p. 289–303.
- Laughton, A. S., 1981, The first decade of GLORIA: *Journal of Geophysical Research*, v. 86, p. 11511–11534.
- Laughton, A. S., and Searle, R. C., 1979, Tectonic processes on slow spreading ridges, *in* Talwani, M., Harrison, C. G., and Hayes, D. E. (eds.), *Deep drilling results in the Atlantic Ocean crust: Maurice Ewing Series*, American Geophysical Union, v. 2, p. 15–32.
- Roberts, D. G., and Kidd, R. B., 1979, Abyssal sediment wave fields on Feni Ridge, Rockall Trough: Long-range sonar studies: *Marine Geology*, v. 33, p. 175–191.
- Roberts, D. G., and Kidd, R. B., 1984, Sedimentary and structural patterns on the Iberian continental margin: an alternative view of continental margin sedimentation: *Marine and Petroleum Geology*, v. 1, p. 37–48.
- Rusby, S. J., 1970, A long range side-scan sonar for use in the deep sea: *International Hydrographic Review*, v. 47, p. 25–39.
- Rusby, J. S. M., and Revie, J. A., 1975, Long-range sonar mapping of the continental shelf: *Marine Geology*, v. 19, p. M41–M52.
- Rusby, J. S. M., and Somers, M. L., 1977, The development of the 'Gloria' sonar system from 1970 to 1975, *in* Angel, M. (ed.), *A voyage of discovery: George Deacon 70th anniversary volume*, Pergamon Press Ltd, Oxford, p. 611–625.
- Searle, R. C., 1979, Side-scan sonar studies of North Atlantic fracture zones: *Geological Society of London Journal*, v. 136, p. 283–292.
- Searle, R. C., 1980, Tectonic pattern of the Azores spreading centre and triple junction: *Earth and Planetary Science Letters*, v. 51, p. 415–434.
- Searle, R. C., 1981, The active part of Charlie-Gibbs Fracture Zone: A study using

- sonar and other geophysical techniques: *Journal of Geophysical Research*, v. 86, p. 243–262.
- Searle, R. C., 1983, Multiple, closely spaced transform faults in fast-slipping fracture zones: *Geology*, v. 11, p. 607–610.
- Searle, R. C., Francis, T. J. G., Hilde, T. W. C., Somers, M. L., Revie, J. A., Jacobs, C. L., Saunders, M. R., Barrow, B. J., and Bicknell, S. V., 1981, 'Gloria' side-scan sonar in the east Pacific: *Eos*, v. 62, p. 121–122.
- Searle, R. C., and Laughton, A. S., 1981, Fine-scale sonar study of tectonic and volcanism on the Reykjanes Ridge: *Oceanologica Acta*, Proceedings of the 26th International Geological Congress, Geology of oceans symposium, Paris, p. 5–13.
- Somers, M. L., Carson, R. M., Revie, J. A., Edge, R. H., Barrow, B. J., and Andrews, A. G., 1978, Gloria II - an improved long range side-scan sonar: *Oceanology International* 78, p. 16–24.
- Stride, A. H., 1970, Mapping the ocean floor: *Science Journal* [London], v. 6, no. 12, p. 56–58.
- Stride, A. H., Belderson, R. H., and Kenyon, N. H., 1977, Evolving miogeanticlines of the East Mediterranean (Hellenic, Calabrian and Cyprus Outer Ridges): *Philosophical Transactions, Royal Society of London, Series A*, v. 284, no. 1322, p. 255–285.
- Whitmarsh, R. B., 1971, Interpretation of long range sonar records obtained near the Azores: *Deep-Sea Research*, v. 18, p. 433–440.
- Whitmarsh, R. B., and Laughton, A. S., 1975, The fault pattern of a slow-spreading ridge near a fracture zone: *Nature*, v. 258, p. 509–510.
- Whitmarsh, R. B., and Laughton, A. S., 1976, A long-range sonar study of the Mid-Atlantic Ridge crest near 37° N (FAMOUS area) and its tectonic implications: *Deep-Sea Research*, v. 23, p. 1005–1023.



**Abstracts of Selected Papers Submitted For Publication
from January 1, 1980, to December 31, 1983**

REGIONAL GEOLOGIC FRAMEWORK

Early evolution of the Bering Sea by collision of oceanic rises and North Pacific subduction zones

Ben-Avraham, Zvi, and Cooper, A. K., 1981, Geological Society of America Bulletin, pt. 1, v. 92, p. 485-495.

Three major bathymetric features exist in the Bering Sea: Shirshov Ridge, Bowers Ridge, and Umnak Plateau. New refraction data over Umnak Plateau and previous geophysical data across Bowers Ridge indicate that a thickened welt of crustal material is present beneath both features. The crustal structure is transitional between oceanic and continental types.

Various models for the origin of these features have been investigated. One that has not been proposed previously assumes that the protostructures of Bowers Ridge and Umnak Plateau could have formed outside of the present Bering Sea. According to this model, before formation of the Aleu-

tian Ridge in late Mesozoic or earliest Tertiary time, these protostructures moved into their present Bering Sea positions.

Prior to the arrival of these two structures in the Bering Sea, oceanic crust was subducted along the Bering continental margin connecting Alaska and Siberia. The collision of the Umnak Plateau protostructure with the southeastern edge of the margin may have caused subduction to terminate here and move southward. The new southerly position of subduction beneath the Aleutian Ridge was therefore controlled by late Mesozoic or early Tertiary locations of Umnak Plateau, Bowers Ridge, and possibly, the north-trending Shirshov Ridge farther to the west.

Cenozoic coccoliths from the Deep Sea Drilling Project

Bukry, David, 1981, Society of Economic Paleontologists and Mineralogists Special Publication 32, p. 335-353.

Coccoliths, as the dominant constituent of many Deep Sea Drilling Project cores, have provided the means of rapid and detailed biostratigraphic zonation to help guide ocean-sediment coring operations aboard D. V. Glomar Challenger. The Cenozoic has been divided into 50 to 60 zones and sub-zones which are most effective for middle- and low-latitude sites. Because key stratigraphic coccoliths have proved more resistant to diagenetic change than planktic foraminifers, they contributed to dating of sedimentary beds within and just above basalt, directly demonstrating the correctness of the sea-floor spreading hypothesis. An unexpected discovery of Braarudosphaera beds in the South Atlantic produced valuable speculation on the response of coccolithophorids to paleoceanographic changes.

Samples from the diversity of oceanic terrains explored by early cruises of Glomar Challenger helped in the recognition of the effects of differential preservation—etching and overgrowth from species to species—and in the determination of biogeographic ranges which would affect the taxonomic, paleoecologic and biostratigraphic assignments of coccoliths. DSDP sites have provided the matrix needed to outline depth sequences based on dissolution rank, and paleotemperature sequences based on abundance along latitudinal traverses. New Hydraulic Piston Corer capabilities will make possible application of magnetic reversal stratigraphy to undisturbed cores where coccolith evolutionary transitions and datum-interval stratigraphy can be established.

Cretaceous Arctic silicoflagellates

Bukry, David, 1981, Geo-Marine Letters, v. 1, p. 57-63.

Cretaceous silicoflagellate assemblages from Arctic Ocean USGS Core 437 show Vallacerta siderea the most abundant species; most species of Lyrumulula disappear halfway up the core; only L. burchardae, n. sp., persists into the upper sections. These occurrences are untypical of the few documented Cretaceous assemblages from other areas. A Campanian or Maestrichtian age is suggested by correlation,

but the uniquely high abundance of V. siderea and lack of Corbisema suggests that a difference in both age and general environment could be involved. If Core 437 is latest Maestrichtian, then the evidence from this core would constrain the timing of the ocean-freshening model for the Cretaceous-Tertiary boundary extinctions.

Upper Cenozoic silicoflagellates from offshore Ecuador, Deep Sea Drilling Project Site 504

Bukry, David, 1983, Deep Sea Drilling Project Initial Reports, v. 69, p. 321-342.

Diverse and abundant late Miocene to Pleistocene silicoflagellates at DSDP Site 504 can be correlated by tropical biostratigraphic zones and relative paleotemperature values to eastern tropical Pacific reference site DSDP 503A farther to the west. Early Pliocene assemblages, which were poorly known until now, are present and can be correlated locally between DSDP Hole 504, 503A, and 495, using species events associated with the new Dictyochoa pulchella Subzone and Dictyochoa angulata Subzone. Silicoflagellate relative paleotemperature values show major warming at 4.7 to 5.0 Ma (Cores 45-48), 3.4 to 3.8 Ma (Cores 32-33), 1.5 to 1.7 Ma

(Cores 12-16), and 0.5 to 0.8 Ma (Cores 3-6). Major coolings occurred at 5.0 to 5.1 Ma (Core 51), 3.9 to 4.4 Ma (Cores 38-44), and 1.0 to 1.3 Ma (Cores 8-10). The appearance of Dictyochoa longa is proposed to replace the asperoid/fibuloid ratio reversal as the bottom of the Dictyochoa fibula Zone, because the non-evolutionary ratio reverses several times in the upper Miocene of Hole 503A, and at least once in Hole 504. Three new Pliocene silicoflagellates are defined: Dictyochoa concinna Bukry, n. sp., D. helix Bukry, n. sp., and D. tamarae Bukry, n. sp.

Geologic hazards in Navarin Basin province, northern Bering Sea

Carlson, P. R., Karl, H. A., Fischer, J. M., and Edwards, B. D., 1982, 14th Offshore Technology Conference Proceedings, v. 1, p. 73-87.

Navarin Basin, scheduled for leasing in 1984 (OCS sale 83), may contain vast accumulations of oil and gas. Several geologic and oceanographic processes that may be active in and around Navarin Basin province could be hazardous to commercial development. These potential hazards include

submarine slides; sea-floor instability resulting from disturbance of gas-charged sediment; sediment transport and erosion caused by storm waves, tsunamis, internal waves, or bottom currents; pack ice; and active faults and ground motion.

Linear island and seamount chains, aseismic ridges and intraplate volcanism: results from DSDP

Clague, D. A., 1981, in Warme, J. E., Douglas, R. G., and Winterer, E. L., eds., The Deep Sea Drilling Project: a decade of progress: Society of Economic Paleontologists and Mineralogists Special Publication No. 32, p. 7-22.

The Deep Sea Drilling Project drilled a substantial number of sites that bear on the origin of linear island and seamount chains, aseismic ridges and other more regional expressions of intraplate volcanism. Drilling in the Emperor Seamounts during Leg 55 was particularly successful. Results from this leg include: 1) the volcanoes of the Hawaiian-Emperor chain continue to increase in age away from Kilauea as predicted. 2) Suiko Seamount formed at a paleolatitude of $26.9 \pm 3.5^\circ\text{N}$, 7° north of present-day Hawaii, but far south of its present latitude of 44.8°N . 3) the volcanic rock types recovered include hawaiite, mugearite, alkalic basalt and tholeiitic basalt in the sequence and relative volume expected for Hawaiian volcanoes. 4) the tholeiitic and alkalic basalts recovered are geochemically similar to those in the Hawaiian Islands, only the ratio of $^{87}\text{Sr}/^{86}\text{Sr}$ appears to change through time. All the lavas appear to be derived from a source that has small-scale heterogeneities, but is homogeneous on a large scale. 4) The Emperor Seamounts were once volcanic islands that underwent subaerial and shallow marine erosion,

and deposition of shallow-water biogenic carbonate sediments that capped all or most of each volcano.

Drilling in other regions has yielded less conclusive results. For example, it is uncertain if the Line Islands are an age progressive chain (hot-spot trace) or result from some other type of intraplate volcanism. The mid-Pacific Mountains also show evidence of originating from a regional episode of volcanism in the mid-Cretaceous. Drilling in the Nauru Basin encountered a voluminous mid-Cretaceous volcanic flow-sill complex that overlies Jurassic magnetic anomalies, yet is composed of depleted tholeiite. In the Indian Ocean, drilling on the Ninety-East Ridge established that it 1) is volcanic in origin; 2) is older to the north; 3) formed in shallow water; and 4) formed further south and has moved northward. It appears that the Ninety-East Ridge, like the Hawaiian-Emperor chain, is a hot spot trace. In the Atlantic Ocean, drilling on the Iceland-Faeroe Ridge and the Rio Grande Rise-Walvis Ridge suggests that all these aseismic ridges are hot spot traces generated by the Iceland and Trista de Cunha hot-spots.

Petrology and trace element geochemistry of the Honolulu Volcanics, Oahu: implications for the oceanic mantle below Hawaii

Clague, D. A., and Frey, F. A., 1982, Journal of Petrology, v. 23, part 3, p. 447-504.

The Honolulu Volcanics comprises small volume, late-stage (post-erosional) vents along rifts cutting the older massive Koolau tholeiitic shield on Oahu, Hawaii. Most of these lavas and tuffs of the Honolulu Volcanics have geochemical features expected of near-primary magmas derived from a peridotite source containing Fo₈₇₋₈₉ olivine; e.g. 100 Mg/(Mg + Fe²⁺) 65, 250 p.p.m. Ni, and presence of ultramafic mantle xenoliths at 18 of the 37 vents. Consequently, the geochemistry of the alkali olivine basalt, basanite, nephelinite and nepheline melilitite lavas and tuff of the Honolulu Volcanics have been used to deduce the composition of their mantle source and the conditions under which they were generated by partial melting in the mantle.

Compositional trends in 3 samples establish that the magmas were derived by partial melting of garnet (10 percent) lherzolite source, which we infer to have been carbon-bearing, from analogy with experimental results. This source was isotopically homogeneous (Sr, Lanphere & Dalrymple, 1980; Pb, Sun, 1980; Nd, Roden et al., 1981), and we infer that the source was compositionally uniform in all major-element oxides except TiO₂, in compatible trace elements (Sc, V, Cr, Mn, Co and Ni), and in highly incompatible trace elements (P, Th, La, Ce). However, the source appears to have been heterogeneous in TiO₂, Zr, Hf, Nb, and Ta, elements that were not strongly incompatible during partial melting. Some nepheline melilitite samples may be derived from a source with distinct Sc and heavy-rare-earth-element

(REE) abundances, or which had a phase or phases controlling the distribution of these elements.

The relatively limited abundance range for several elements, such as Ti, Zr, Nb, is partly a consequence of the low degrees of melting inferred for the series (2 per cent for nepheline melilitite, 11 per cent for alkali olivine basalt), which failed to exhaust the source in minor residual phases. We infer that these residual phases probably included phlogopite, amphibole, and another Ti-rich phase (an oxide?), but not apatite.

In comparison with estimates of a primordial mantle composition and the mantle source of mid-oceanic-ridge basalt the garnet peridotite source of the Honolulu Volcanics was increasingly enriched in the sequence heavy REEs, Y, Tb, Ti, Sm, Zr, and Hf all P Nd Sr Ce La Nb Ta. A multi-stage history for the source of the Honolulu Volcanics is required because this enrichment was superimposed on a mantle that had been previously depleted in incompatible elements, as indicated by the relatively low $^{87}\text{Sr}/^{86}\text{Sr}$ ratio, high $^{143}\text{Nd}/^{142}\text{Nd}$ ratio and low contents of K, Rb, Ba, and Th. The composition of the source of the Honolulu Volcanics differs from the source of the previously erupted tholeiitic shield. The modal mineralogy of the source of the Honolulu Volcanics is not represented in the upper-mantle xenoliths, e.g. the garnet pyroxenite and olivine-poor garnet lherzolite included within the lavas and tuff of the unit.

Minor and trace element geochemistry of volcanic rocks dredged from the Galapagos spreading center: role of crystal fractionation and mantle heterogeneity

Clague, D. A., Frey, F. A., Thompson, Geoff, and Rindge, Susan, 1981, *Journal of Geophysical Research*, v. 86, no. B10, p. 9469-9482.

A wide range of rock types (abyssal tholeiite, Fe-Ti-rich basalt, andesite, and rhyodacite) were dredged from near 95°W and 85°W on the Galapagos spreading center. Computer modeling of major element compositions has shown that these rocks could be derived from common parental magmas by successive degrees of fractional crystallization. However, the P_2O_5/K_2O ratio averages 0.83 at 95°W and 1.66 at 85°W and implies distinct mantle source compositions for the two areas. These source regions also have different rare earth element (REE) abundance patterns, with $La/Sm_{EF} = 0.67$ at 95°W and 0.46 at 85°W. The sequence of fractionated lavas differs for the two areas and indicates earlier fractionation of apatite and titanomagnetite in the lavas from 95°W. The mantle source regions for these two areas are interpreted to be depleted in incompatible (and volatile?) elements, although the source region beneath 95°W is less severely depleted in La and K. Incompatible trace element abundances in 26 samples are used to infer that the range of Fe-Ti-rich basalt from 85°W represents 19 to 35% residual liquid following crystal fractionation of a mineral assemblage of plagioclase,

clinopyroxene, and lesser olivine. The most highly differentiated samples have also had less than 1% titanomagnetite removed. Most samples from 85°W can be related to a common parental magma that contained approximately 9 wt % FeO^* , 1 wt % TiO_2 , and had an Mg number ($Mg\# = 100 Mg/(Mg + Fe^{2+})$) of about 65. Although the samples from 95°W cannot all be derived from a common parental magma, the inferred parental magmas may have been derived by varying degrees of partial melting of a common source. The fractionation sequence consists of two parts: an initial iron enrichment trend followed by a silica enrichment trend. We interpret the trace element data to indicate that the most iron rich lavas represent about 32% residual liquid derived by crystal fractionation of plagioclase, clinopyroxene, and lesser olivine from a parental magma with an Mg number of about 66. The silica enrichment trend results from crystallization of titanomagnetite and some apatite. Fractionation of pigeonite, which is a minor phase in the major element models, cannot be distinguished from clinopyroxene fractionation by using trace elements.

Progradational sequences in Miocene shoreline deposits, southeastern Caliente Range, California

Clifton, H. E., 1981, *Journal of Sedimentary Petrology*, v. 51, no. 1, p. 165-184.

An exceptionally well exposed marine-nonmarine transition in middle Miocene strata exists in the southeastern Caliente Range, California. About 50 individual progradational sequences form a succession that ranges in thickness from approximately 1000 m (where predominantly nonmarine) to more than 2500 m (where predominantly marine). Paleogeographic evidence in basalt flows near the top of the succession and in overlying fluvial deposits indicates that these middle Miocene strata were deposited across a north-northwest trending shoreline.

A complete progradational sequence typically is several meters to a few tens of meters thick and includes strata that represent three intertonguing stratigraphic units. Individual sequences generally rest on a thin gravel deposit interpreted as a transgressive lag on an erosional surface. The gravel is overlain by structureless siltstone or fine-grained sandstone deposited at water depths where the rate of faunal mixing exceeded that of production of structures by physical processes. These rocks grade upward into bedded fine sandstone deposited closer to shore where physical processes exceeded bioturbation. Crossbedded lenses of coarse sand or fine gravel in the upper part of this facies suggest the presence of fairly long-period surface waves. The bedded fine sandstone is sharply overlain by a cross bedded coarse sandstone facies that is interpreted as a combined

offshore bar-rip channel-surf zone assemblage. Cross-strata dip dominantly offshore, suggesting substantial deposition from rip currents. A secondary, shore-parallel mode of cross-strata direction suggests longshore currents produced by surface waves from the northwest. The crossbedded coarse-grained sandstone grades upward into planar-bedded medium-grained sandstone that is interpreted as a beach foreshore. This facies grades upward through structureless medium-grained sandstone into nonmarine or lagoonal red and green mudstone of the Caliente Formation.

The middle Miocene succession was deposited in a subsiding basin that was otherwise remarkably stable tectonically; the position of the strand line differed no more than a few kilometers through a period of 1 to 3 m.y. The average duration of the transgressive-regressive cycles, a few tens of thousands of years, together with their distribution in groups of three or four in the lower two-thirds of the succession, is consistent with the pattern of long-term climatic cycles produced by periodicity of the earth's solar orbit and may be related to eustatic sea level changes attendant to the development of the Antarctic ice cap. Changes in the pattern of progradation in the upper part of the succession and nearby basaltic eruptions may have been precursors to the onset of movement along the San Andreas fault in this area 12-14 m.y. ago.

Multichannel seismic evidence bearing on the origin of Bowers Ridge, Bering Sea

Cooper, A. K., Marlow, M. S., and Ben-Avraham, Zvi, 1981, *Geological Society of America Bulletin*, pt. 1, v. 92, p. 474-484.

Bowers Ridge is a large, arcuate submarine ridge that extends north and west from the Aleutian Ridge and separates the abyssal Aleutian and Bowers Basins in the Bering Sea. Two multichannel seismic-reflection lines recorded in 1976 over Bowers Ridge and the adjacent basins confirm the existence of 8- to 10-km-thick sediment wedges on the north side of Bowers Ridge and at the base of the Bering continental margin. Deformed sediment within the Bowers wedge indicates that subduction of the adjacent ocean crust beneath

the ridge probably occurred prior to middle Cenozoic time. Flat-lying reflectors near the bottom of the trench suggest that a bathymetric trough and large ridge existed in Mesozoic time. The major period of underthrusting, subsidence, and infilling of the trench probably occurred from Mesozoic to early Tertiary time. Small amounts of underthrusting may have continued after the early Tertiary development of the Aleutian Ridge; however, by middle Miocene time, the formerly subaerial Bowers Ridge had subsided below sea level.

The multichannel seismic data do not show evidence for a buried spreading center within the eastern Aleutian Basin. Consequently, the sediment wedges (trenches) at both Bowers Ridge and the Bering continental margin are believed to be the consequence of subduction that occurred during the convergence of the ridge and the margin. The large size of

Bowers Ridge suggests that a large amount of convergence has occurred since Mesozoic time. If Bowers Ridge was a large feature in Mesozoic time, as suggested by the apparent bathymetric trough, then the ridge may be as old or older than the Aleutian Ridge to which it connects.

Origin and geochemistry of redox cycles of Jurassic to Eocene age, Cape Verde Basin (DSDP Site 367), continental margin of northwest Africa

Dean, W. E., and Gardner, J. V., 1982, in Schlanger, S. O., and Cita, M. B., eds., *Nature and origin of Cretaceous carbon-rich facies*: Academic Press, p. 55-78.

The entire stratigraphic section cored at Deep Sea Drilling Project Site 367 in the Cape Verde Basin is characterized by variations in color and/or concentration of organic matter in rocks and sediment that range in age from Late Jurassic to Eocene. Late Jurassic (Oxfordian-Kimmeridgian) redox cycles consist of red and green nodular limestones. The Late Jurassic to Early Cretaceous organic carbon-rich facies consists of alternating light-gray limestone and organic carbon-rich olivine marlstone in which concentrations of organic carbon are commonly several percent but reach 33%. The Middle to Upper Cretaceous section consists of alternating green and black or green and red shales or claystones, grading into Cretaceous-Tertiary green and red clays, and finally Eocene green and black clays. The youngest sediment (Miocene to Pleistocene) is a carbonate facies that also shows evidence of cyclic interbedding of marl and ooze, but the nature of interbedding has been obscured by drilling disturbance. Most green clays and claystones of all ages have concentrations of organic carbon of less than 0.5% whereas the black clays and shales commonly contain more than 2% organic carbon and have a maximum of 37%.

Many trace elements tend to be enriched in the more reduced lithology in the cyclic redox couplets, i.e. they are more abundant in black or dark-olive colored lithologies than in adjacent light-colored green or red lithologies. Elements that have the greatest variability are V, Cr, and Ni.

The cyclic interbeds are chemically more-reduced and less-reduced, or reduced and oxidized lithologies are interpreted as being mainly the result of cyclic variations in diagenetic redox conditions within the sediments in response to variable rates of supply of organic detritus transported by turbidity currents from shallower water. The accumulation of organic carbon-rich strata is not dependent on having low-oxidation conditions in the bottom waters, but would be aided by restricted bottom-water circulation and low oxygen concentrations. The accumulation of organic carbon-rich strata in the Cape Verde Basin began in the Late Jurassic or the Early Cretaceous and continued intermittently at least into the Eocene. However, the main period of accumulation of organic matter was during the Middle Cretaceous, a period of high organic productivity and decreased oceanic circulation in the world ocean. High concentrations of organic matter of marine, terrestrial or mixed origin accumulated along the shallow continental margins of the North and South Atlantic and was periodically transported to deeper-water environments of sediment accumulation by turbidity currents. In the absence of a high rate of supply of oxygen-consuming organic debris, the bottom waters of the Atlantic Ocean generally contained enough dissolved oxygen to permit the accumulation of oxidized sediments.

Tertiary carbonate-dissolution cycles on the Sierra Leone Rise, eastern equatorial Atlantic Ocean

Dean, W. E., Gardner, J. V., and Cepek, Pavel, 1981, *Marine Geology*, v. 39, p. 81-101.

Most of the Tertiary section on Sierra Leone Rise off northwest Africa consists of chalk, marl, and limestone that show cyclic alterations of clay-rich and clay-poor beds about 20-60 cm thick. On the basis of biostratigraphic accumulation rates, the cycles in Oligocene and Miocene chalk have periods which average about 44,000 years, and those in Eocene siliceous limestone have periods of 4000-27,000 years. Several sections were sampled in detail to further define the cycles in terms of content of CaCO_3 , clay minerals, and relative abundances of calcareous nannofossils. Extending information gained by analyses of Pleistocene cores from the continental margin of northwest Africa to the Tertiary cycles on Sierra Leone Rise, both dilution by noncar-

bonate material and dissolution of CaCO_3 could have contributed to the observed relative variations in clay and CaCO_3 . However, dissolution of CaCO_3 as the main cause of the carbonate-clay cycles on the Sierra Leone Rise, rather than dilution by clay, is suggested by the large amount of change (several thousand percent) in terrigenous influx required to produce the observed variations in amount of clay and by the marked increase in abundance of dissolution-resistant discoasters relative to more easily dissolved coccoliths in low-carbonate parts of cycles. The main cause of dissolution of CaCO_3 was shoaling of the carbonate compensation depth (CCD) during the early Neogene and climatically induced fluctuations in the thickness of Antarctic Bottom Water.

Mesozoic development and structure of the continental margin off South Carolina

Dillon, W. P., Klitgord, K. D., and Paull, C. K., 1983, in Gohn, G. S., ed., *Studies related to the Charleston, South Carolina, earthquake of 1886—Tectonics and Seismicity*: U.S. Geological Survey Professional Paper 1313-N, N1-N16.

A nearly undeformed wedge of Mesozoic and Cenozoic strata forms the Continental Shelf and Blake Plateau off South Carolina. The wedge is built on an unconformity, known as the postrift unconformity, at the top of beveled Triassic and Lower Jurassic sedimentary deposits, Paleozoic crystalline basement rocks, Paleozoic sedimentary rocks of various stages of metamorphism, and Mesozoic volcanic and

plutonic mafic igneous rocks. The postrift unconformity generally forms both seismic basement and magnetic basement. This unconformity is marked by two zones of major subsidence off South Carolina, separated by the apparent landward continuation of the deep-sea Blake Spur fracture zone. South of that fracture zone, beneath the Blake Plateau, is the broad Blake Plateau basin, reaching depths of 14

km. North of the fracture zone and parallel to the continental margin is the narrow Carolina trough, which is as much as 11 km deep. The postrift unconformity is formed by a strongly reflecting layer beneath the Continental Shelf off South Carolina that probably represents a seaward extension of the lower Mesozoic volcanic flows penetrated by drilling near

Charleston. During Jurassic time, the Blake Plateau basin and Carolina trough subsided rapidly and were filled with sediment to a depth of more than 7 km. In contrast, Cretaceous subsidence of the continental margin was widespread and relatively uniform and resulted in the accumulation of a blanket of sediment 1 to 4 km thick.

Growth faulting and salt diapirism: Their relationship and control in the Carolina Trough, eastern North America

Dillon, W. P., Popenoe, Peter, Grow, J. A., Klitgord, K. D., Swift, B. A., Paull, C. K., and Cashman, K. V., 1982, in Watkins, J. S., and Drake, C. L., eds., *Studies in continental margin geology: American Association of Petroleum Geologists Memoir No. 34*, p. 21-46.

The Carolina Trough is a long, linear, continental margin basin off eastern North America. Salt domes along the trough's seaward side show evidence of active diapirism and a normal growth fault along its landward side has been continually active at least since the end of the Jurassic. This steep fault extends to a strong reflection event at about 11 km depth that may represent the top of a salt layer. We infer that faulting is caused by seaward flow of salt from the deep part of the trough into domes, thereby removing support for

the overlying block of sedimentary rock. Diapirs off eastern North America seem to be concentrated in the Carolina Trough and Scotian Basin, where basement seems to be thinner than in other basins off eastern North America, south of Newfoundland. Thinner basement, probably due to greater stretching during rifting, may have resulted in earlier subsidence below sea level, a longer life for the salt evaporating pans in these basins, and thus a thicker salt layer, which would be more conducive to diapirism.

High-resolution carbonate and organic-carbon stratigraphies for the late Neogene and Quaternary from the western Caribbean and eastern equatorial Pacific

Gardner, J. V., 1982, *Deep Sea Drilling Project Initial Reports*, v. 68, p. 347-364.

Concentrations of calcium carbonate and organic carbon were determined in closely spaced samples from two nearly continuous sections of the late Neogene and Quaternary, one from Site 502 in the western Caribbean and the other from Site 503 in the eastern equatorial Pacific. Each section records the past 7.5 m.y. with a sampling interval of approximately every 5 k.y. Both sections show cyclic carbonate concentrations with three classes of dominant periodicities. The longest-period carbonate cycles have periods of 500 to 600 k.y. and appear to be broad-scale oceanic responses. These cycles appear throughout the entire Pacific record but only occur in the 4.0 to 7.5 m.y. interval in the Caribbean record. This difference is probably related to the more active tectonic setting of Site 502 and the oceanic character of Site 503. Intermediate-scale carbonates, S-cycles, occur throughout both records, but the only interval that can be correlated between the two is the 0 to 1.4 m.y. interval. These cycles can also be correlated with records of changes in other Pleistocene sections. The range of periodicities of

the S-cycles suggests they are responses to global climatic changes that are in phase with the eccentricity of the Earth's orbit.

The smaller-scale carbonate cycles, C-cycles, also occur throughout both records but are difficult to correlate because of the different settings of the two sites. C-cycles are apparently out-of-phase between the two sites from 7.5 to 4.0 Ma, but then, inexplicably, they become much more similar in trend from 4.0 Ma to present. C-cycles have periodicities that fall in the range typical of these of the obliquity of the Earth's orbit, again suggesting a control by global climatic changes.

Organic-carbon concentrations show no correlation with carbonate in the western Caribbean section but they show a strong negative correlation with carbonate in the eastern equatorial Pacific record. The relationship in the Pacific section is opposite to that found by others, and the relationships at both sites are opposite to what one would intuitively expect.

Faulting in outer continental shelf of southern Bering Sea

Gardner, J. V., and Vallier, T. L., 1981, *American Association of Petroleum Geologists Bulletin*, v. 65, no. 9, p. 1568-1573.

Synthesis of more than 10,000 line-km of high-resolution seismic data indicates the distribution, types, and trends of faults present on the outer continental shelf of the southern Bering Sea. Faults are classified into three types as to whether they (1) offset the sea floor (surface fault), (2) show less than 5 m of displacement (minor fault), or (3) show more than 5 m of displacement (major fault). The distribution of surface faults follows the outline of St. George basin

and suggests that the basin is presently subsiding. Minor faults are concentrated throughout St. George and Amak basins but are not common elsewhere in the region. Major faults appear to be associated with the boundary faults of St. George and, to a lesser extent, Amak basins. The faulting is probably a result of earthquake-induced energies that reactivate zones of weakness inherited from the collapse of the margin during the late Mesozoic-early Tertiary.

Constraints of geologic processes on petroleum development in the western Beaufort Sea

Grantz, Arthur, and Dinter, D. A., 1981, in *Petromar 80—Petroleum and the marine environment—a conference sponsored by Eurocean (Association Europeenne Oceanique)*: London, Graham and Trotman, Ltd., p. 285-298.

Active progradation, Holocene tectonism, and frigid temperatures have created geologic conditions that uniquely complicate petroleum development in the Beaufort Sea. Although most of the western Beaufort shelf is ice free and accessible to drill ships for up to two months during favorable years, drilling will still be hampered by troublesome subsea conditions in large areas. Natural gas hydrate with a zone of free gas at its base 300 to 700 m beneath the seafloor is widespread where water is deeper than 400 to 600 m. Shale diapirs, presumably overpressured, disrupt the continental slope east of 147°W long. Shallow, low-angle bedding-plane slides as wide as 38 km underlie most of the outer shelf. The slides are sufficiently young to preserve open crevasses as deep as 17 m (exceptionally 37 m). Subsea permafrost, com-

monly containing gas pockets, extends from near the seabottom to depths of several hundred meters in sediments near the coast and may present thawing and compaction hazards to drillholes on the inner shelf.

The westward-drifting polar ice pack, which lies seaward of a zone of shorefast and bottom-fast ice inside the 10- to 20-m isobath, will be a major obstacle to production activities. In addition, the seabed between the coastline and at least the 60-m isobath is gouged by keels of drifting ice. Subbottom completions in this zone, and pipelines crossing it, will have to be buried below the gouges, which locally exceed 5 m in depth. East of 146°W long production facilities may be subject to earthquakes as large as magnitude 6 and in places to active faulting, uplift, and subsidence.

Rifting history and structural development of the continental margin north of Alaska

Grantz, Arthur, and May, S. D., 1983, in *Watkins, J. S., and Drake, C. L., eds., Studies in continental margin geology*: American Association of Petroleum Geologists Memoir 34, p. 77-100.

Seismic-reflection profiles in the Alaskan Beaufort Sea and onshore geology indicate that the continental margin north of Alaska is of Atlantic type. Rifting appears to have begun in earliest Jurassic time, about 190 to 185 m.y. ago, when crustal extension created a rift-valley system beneath the Beaufort shelf and part of the adjacent coastal plain. Subsequent crustal warming caused rift-margin uplift and

erosion, created a breakup unconformity, and initiated breakup and seafloor spreading in the Canada Basin about 125 m.y. ago. Subsequent cooling caused rapid subsidence of the margin, which was followed by vigorous progradation of the present continental terrace of the Beaufort Sea beginning in Albian time.

Deep structure and evolution of the continental margin off the eastern United States

Grow, J. A., and Sheridan, R. E., 1981, *Oceanologica Acta*, no. SP 387, p. 11-19.

Continental rifting and crustal thinning took place between North America and Africa during the Triassic and Early Jurassic, and sea floor spreading began in the Early to Middle Jurassic. Very rapid and variable subsidence along the continental margin off the eastern United States during the Jurassic was controlled by transverse fracture zones, which segmented the margin into four major sedimentary basins—the Georges Bank Basin, the Baltimore Canyon Trough, the Carolina Trough, and the Blake Plateau Basin.

Upper Triassic to Lower Jurassic evaporite deposits (including salt) have been drilled in Georges Bank Basin, and linear chains of salt(?) diapirs have been found along the East Coast Magnetic Anomaly in the Carolina and Baltimore Canyon Troughs. The maximum thicknesses of undeformed postrift sedimentary units in these basins are 7, 13, 11, and 12

km respectively. The thickness of deformed synrift sedimentary units (sediments deposited during active rifting) within faulted Triassic grabens beneath these basins probably exceeds 5 km in some places. Gravity models across the three northern basins indicate that 8 to 15 km of transitional crust underlie the basins. The transitional crust probably was formed by extension and thinning of the pre-existing continental crust. Thicker transitional crust (15 to 25 km) that underlies the 350-km-wide Blake Plateau Basin may include mixed continental fragments and extensive volcanics. An eastward jump of the spreading center from beneath the western Blake Plateau to the Blake Escarpment 10 to 15 m.y. after initial continental separation appears to have caused this anomalously wide basin.

Geology of the Kodiak Shelf, Alaska: environmental considerations for resource development

Hampton, M. A., 1983, *Continental Shelf Research*, v. 1, no. 3, p. 253-281.

Geologic features and processes pose several environmental concerns to resource development on the Kodiak Shelf in the Gulf of Alaska. Tectonism causes fault movement, strong seismic ground shaking, and changes in sea-floor elevation. Earthquake epicenters and structural deformation are areally concentrated, which implies areal variation in the severity of tectonic hazards. Exposures of bedrock appear to provide competent foundational material over broad areas of the sea floor, although locally rough topographic expression of inclined bedrock strata might influence the siting of engineering structures. Stable deposits of gravely unconsolidated

sediment, derived from Pleistocene glaciers, are also widespread. Deposits of fine-grained sediment in areas of negative relief might possess less desirable foundational properties than bedrock or coarse unconsolidated sediment, but their thickness is only a few tens of meters in most places. Evidence of sediment slides is rare on the shelf, which implies general slope stability, but large slides, whose activity is related to tectonism, are abundant just seaward of the shelf break. Local occurrences of gas-charged sediment show limited indication of overpressuring and no evidence of instability, but low sediment strength is possible. Fields of

large sand waves might be sites of high-energy bed-load transport with the potential for erosion and abrasion problems. As inferred from sediment dispersal patterns, pollut-

ants that become incorporated into bottom sediment could be concentrated and stored long-term in troughs that trend transversely across the shelf.

Chert petrology and geochemistry, mid-Pacific Mountains and Hess Rise, Deep Sea Drilling Project Leg 62

Hein, J. R., Vallier, T. L., and Allan, M. A., 1981, Deep Sea Drilling Project Initial Reports, v. 62, p. 711-__.

Sixty-five chert, porcellanite, and siliceous-chalk samples from Deep Sea Drilling Project Leg 62 were analyzed by petrography, scanning electron microscopy, analysis by energy-dispersive X-rays, X-ray diffraction, X-ray spectroscopy, and semiquantitative emission spectroscopy. Siliceous rocks occur mainly in chinks, but also in pelagic clay and marlstone at Site 464. Overall, chert probably constitutes less than 5% of the sections and occurs in deposits of Eocene to Barremian ages at sub-bottom depths of 10 to 820 meters. Chert nodules and beds are commonly rimmed by quartz porcellanite; opal-CT-rich rocks are minor in Leg 62 sediments 65 to 108 m.y. old and at sub-bottom depths of 65 to 520 meters. Chert ranges from white to black, shales of gray and brown being most common; yellow-brown and red-brown jaspers occur at Site 464.

Seventy-eight percent of the studied cherts contain easily recognizable burrow structures. The youngest chert at Site 463 is a quartz cast of a burrow. Burrow silica maturation is always one step ahead of host-rock silicification. Burrows are commonly loci for initial silicification of the host carbonate. Silicification takes place by volume-for-volume replacement of carbonate sediment, and more-clay-rich sediment at Site 464. Nannofossils are commonly pseudomorphically replaced by quartz near the edges of chert beds and nodules. Other microfossils, mostly radiolarians and foraminifers, whether in chalk or chert, can be either filled with or replaced by calcite, opal-CT, and (or) quartz.

Chemical micro-environments ultimately control the removal, transport, and precipitation of calcite and silica. Two cherts from Site 465 contain sulfate minerals replaced by quartz. Site 465 was never subaerially exposed after sedimentation began, and the formation of the sulfate minerals and their subsequent replacement probably occurred in the

marine environment. Several other cherts with odd textures are described in this paper, including (1) a chert breccia cemented by colloform opal-CT and chalcedony, (2) a transition zone between white porcellanite containing opal-CT and quartz and a burrowed brown chert, consisting of radial aggregates of opal-CT with hollow centers, and (3) a chert that consists of silica-replaced calcite pseudospherules interspersed with streaks and circular masses of dense quartz.

X-ray diffraction analyses show that when data from all sites are considered there are poorly defined trends indicating that older cherts have better quartz crystallinity than younger ones, and that opal-CT crystallite size increases and opal-CT d -spacings decrease with depth of occurrence in the sections. In a general way, depth of burial and the presence of calcite promote the ordering in the opal-CT crystal structure which allows its eventual conversion to quartz. Opal-CT in porcellanites converts to quartz after reaching a minimum d -spacing of 4.07 Å. Quartz/opal-CT ratios and quartz crystallinity vary randomly on a fine scale across four chert beds, but quartz crystallinity increases from the edge to the center of a fifth chert bed; this may indicate maturation of the silica.

Twenty-four rocks were analyzed for their major- and minor-element compositions. Many elements in cherts are closely related to major mineral components. The carbonate component is distinguished by high values of CaO, MgO, Mn, Ba, Sr, and (for unknown reasons) Zr. Tuffaceous cherts have high values of K and Al, and commonly Zn, Mo, and Cr. Pure cherts are characterized by high SiO₂ and B. High B may be a good indicator of formation of chert in an open marine environment, isolated from volcanic and terrigenous materials.

Paleomagnetism and Mesozoic tectonics of the Seven Devils volcanic arc in northeastern Oregon

Hillhouse, J. W., Gromme, C. S., and Vallier, T. L., 1982, Journal of Geophysical Research, v. 87, no. B5, p. 3777-3794.

Upper Triassic volcanogenic rocks of the Seven Devils Group and Huntington Formation of Brooks (1979b) in northeastern Oregon record two episodes of magnetization. The older magnetization, which predates Late Jurassic deformation of the volcanic arc terrane comprising the Seven Devils Group, was probably acquired in Late Triassic time. The inclinations of both normal and reversed polarity magnetizations indicate that the Triassic rocks originated approximately 18° from the paleoequator. The results are consistent with paleomagnetic data from similar Triassic rock assemblages on Vancouver Island and in south central Alaska. We interpret these assemblages as displaced fragments of Wrangellia, a once coherent late Paleozoic volcanic arc and early Mesozoic volcanic plateau that was torn apart and carried

north by plate motion along the continental margin. We interpret the younger magnetization, which fails the fold test, as a widespread thermochemical overprint caused by Late Jurassic and Early Cretaceous plutonism. This magnetization yields a paleomagnetic pole at 60°N, 295°E ($\alpha_{95} = 7^\circ$), and is similar to the pole obtained from plutons that intrude the Seven Devils Group. The angular difference between the pole from the plutons and the Late Jurassic-Early Cretaceous reference pole for stable North America suggests that the Seven Devils volcanic arc has undergone a large clockwise rotation (66° ± 21°). The rotation may reflect the last stages of the arc's accretion to the continental margin or later large-scale block movements in the Pacific Northwest.

Structural implications of stratigraphic discontinuities across the southern California borderland

Howell, D. G., and Vedder, J. G., 1981, in Ernst, W. G., The geotectonic development of California: Englewood Cliffs, N. J., Prentice-Hall, p. 535-558.

Throughout mainland California, geologic events recorded in Jurassic and younger rocks indicate a nearly continuously active continental margin. By analogy, rocks on

the California Continental Borderland suggest episodes of subduction and transform faulting similar to those on the mainland. Two types of basement rocks are juxtaposed:

Upper Jurassic(?) through Lower Tertiary(?) melange and blueschist of a subduction or accretionary complex that are overthrust by Upper Jurassic ophiolite, arc-volcanogenic and forearc sedimentary rocks. The distribution of basement within the overriding plate, when compared with correlative rocks elsewhere in California, implies east-west foreshortening. The spatial relations of both the upper and lower plate rocks suggest northwest-directed dislocation of basement blocks in the borderland.

Cretaceous and Lower Tertiary strata are discontinuously exposed along the mainland coast and underlie much of the central part of the borderland. These thick clastic wedges are composed largely of turbidites that accumulated

in forearc basins. Local middle Cretaceous and late Paleocene hiatuses in sedimentation and concurrent regional lapses in magmatism may represent times of transform faulting that interrupted subduction.

The modern topography of the borderland began to take shape in Oligocene and Miocene time, and ridges and basins grew in a wrench-tectonic setting within the evolving pliant margin between the Pacific and North American plates. Tholeiitic and calc-alkaline volcanism accompanied the early stages of development of typical borderland features. Miocene volcanogenic rocks commonly are present on ridges and knolls throughout the borderland, but it is improbable that these rocks are coextensive with basin floors.

Crustal structure beneath the southern Appalachians: nonuniqueness of gravity modeling

Hutchinson, D. R., Grow, J. A., and Klitgord, K. D., 1983, *Geology*, v. 11, p. 611-615.

Gravity models computed for a profile across the long-wavelength paired negative-positive Bouguer anomalies of the southern Appalachian Mountains show that the large negative anomaly can be explained by a crustal root zone, whereas the steep gradient and positive anomaly east of the root may be explained equally well by three different geometries: a suture zone, a mantle upwarp, or a shallow body. Seismic data support the existence of a mountain root but are inadequate

to resolve differences among the three possible geometries for the positive anomaly. The presence of outcropping mafic and ultramafic rocks in the southern Appalachians and the inferred tectonic history of the Appalachian orogen are most consistent with the suture-zone model. Crust similar to continental crust probably exists beneath the Coastal Plain and inner continental shelf where the gravity anomalies return to near-zero values.

Deep structure and evolution of the Carolina Trough

Hutchinson, D. R., Grow, J. A., Klitgord, K. D., and Swift, B. A., 1983, in Watkins, J. S., and Drake, C. L., eds., *Studies in continental margin geology: American Association of Petroleum Geologists Memoir 34*, p. 129-152.

Multichannel seismic-reflection data together with two-dimensional gravity and magnetic models suggest that the crustal structure off North Carolina consists of normal continental crust landward of the Brunswick magnetic anomaly

(BMA), rift-stage crust in the 80-km-wide zone between the BMA and the East Coast magnetic anomaly (ECMA), and the normal oceanic crust seaward of the ECMA.

Multiple microtektite horizons in upper Eocene marine sediments: no evidence for mass extinctions

Keller, G., D'Hondt, Steven, and Vallier, T. L., 1983, *Science*, v. 221, p. 150-152.

Microtektites have been recovered from three horizons in eight middle Eocene to middle Oligocene marine sediment sequences. Five of these occurrences are coeval and of latest Eocene age (37.5 to 38.0 million years ago); three are coeval and of early late Eocene age (38.5 to 39.5 million years ago); and three are of middle Oligocene age (31 to 32 million years ago). In addition, rare probable microtektites have been found in sediments with ages of about 36.0 to 36.5 million years. The microtektite horizon at 37.5 to 38.0 million years can be correlated with the North American tektite-strewn field, which has a fission track age (minimum) of 34 to 35 million years and a paleomagnetic age of 37.5 to 38.0 million years. There is no evidence for mass faunal extinctions at

any of the microtektite horizons. Many of the distinct faunal changes that occurred in the middle Eocene to middle Oligocene can be related to the formation of the Antarctic ice sheet and the associated cooling phenomena and intensification of bottom currents that led to large-scale dissolution of calcium carbonate and erosion, which created areally extensive hiatuses in the deep-sea sediment records. The occurrence of microtektite horizons of several ages and the lack of evidence for faunal extinctions suggest that the effects of extraterrestrial bolide impacts may be unimportant in the biological realm during middle Eocene to middle Oligocene time.

Mesozoic tectonics of the southeastern United States coastal plain and continental margin

Klitgord, K. D., Dillon, W. P., and Popenoe, Peter, 1983, in Gohn, G. S., ed., *Studies related to the Charleston, South Carolina, earthquake of 1886—Tectonics and seismicity: U.S. Geological Survey Professional Paper 1313-P*, p. P1-P15.

Many of the major structures associated with Paleozoic and Mesozoic tectonic events along the Southeastern U.S. Coastal Plain and continental margin have distinctive geophysical and geological properties, which are described in this integrated study of magnetic, gravity, seismic-reflection, and drill-hole data. These data are used to identify three

major tectonic boundaries that separate terranes of Paleozoic, Triassic, and Jurassic tectonic activity and to map sedimentary basins that were formed by Triassic and Jurassic rifting events. The major tectonic boundaries are: (1) An offshore hinge zone in basement that separates an area of crustal subsidence associated with the Jurassic-age marginal

basins from an area of significantly less subsidence associated with Triassic and older basement structures to the west; (2) a line of narrow grabens, associated with the magnetic low in the Brunswick magnetic anomaly, that separates a Paleozoic basin underlying northeastern Florida, which was not greatly affected by late Paleozoic or Triassic tectonic activity, from a broad zone of considerable Triassic tectonic activity and sediment accumulation in the Charleston, S. C., region; and (3) a narrow east-west zone near 33° N. that separates the geophysically distinctive northeast-trending Piedmont to the north from the Charleston region. The Triassic sedimentary basins are of two types: (1) narrow basins or grabens within

the Piedmont and along the major tectonic boundaries and (2) broad zones of sediment accumulation over a block-faulted Paleozoic basin in northwestern Florida and in areas delineated by low-gradient magnetic and gravity fields in parts of the Charleston region. Deep continental margin basins, containing sedimentary rock as much as 14 km thick, formed at sites of Jurassic rifting and subsequent ocean opening seaward of the basement hinge zone. Reconstruction of the positions of the North American, South American, and African continents during the Early Jurassic provides a framework for relating the Mesozoic tectonic events and structures to major Paleozoic orogenic events and lithotectonic units.

North East Pacific Rise: magnetic anomaly and bathymetric framework

Klitgord, K. D., and Mammerickx, Jacqueline, 1982, *Journal of Geophysical Research*, v. 87, No. B8, p. 6725-6750.

The oceanic crust in the eastern Pacific between 7°N and 30°N and east of 127°W contains a fairly complete history of the spreading centers associated with the East Pacific Rise since 25 m.y.B.P. (late Oligocene). In this paper, we have summarized the seafloor spreading magnetic-anomaly data and the bathymetric data that reflect the record of this tectonic history. The well-defined magnetic lineations north of the Clarion fracture zone, in the mouth of the Gulf of California, and on the east flank of the East Pacific Rise (EPR) are carefully examined and used to provide a guide for interpreting the spreading pattern between the Clarion and Clipperton fracture zones, southward of the Rivera fracture zone over the Mathematician Ridge, and over the entire EPR east of the Mathematician Ridge between the Rivera and Siqueiros fracture zones. The bathymetric data provide a trace of the fracture zone pattern in each of the above

mentioned areas. The fracture zone bathymetry and the seafloor spreading magnetic lineations on the EPR south of the Rivera fracture zone have a distinctive fanning pattern caused by close poles of rotation and plate boundary reorganizations. All these data provide a good record of the plate reorganizations in the middle Miocene at magnetic anomaly 5A time (12.5 to 11 m.y.B.P.), in the late Miocene at magnetic anomaly 3'-4 time (6.5 m.y.B.P.), and in the Pliocene at magnetic anomaly 2'-3 time (3.5 m.y.B.P.). Several abandoned spreading centers, including the Mathematician Ridge, were left behind as a result of these reorganizations. The Mathematician Ridge is shown to be a set of ridges and trough whose origin is related to the tectonic activity associated with each of the above mentioned reorganizations since anomaly 5A.

Basement structure, sedimentation, and tectonic history of the Georges Bank basin

Klitgord, K. D., Schlee, J. S., and Hinz, Karl, 1982, in Scholle, P. A., and Wenkam, C. R., eds., *Geological studies of the COST Nos. G-1 and G-2 wells, United States North Atlantic outer continental shelf: U.S. Geological Survey Circular 861*, p. 160-186.

The sediment-filled basins beneath Georges Bank formed as the continental margin subsided during and following the rifting of Africa from North America. We shall develop a tectonic history for this region by examining the crustal foundation beneath these basins and by outlining the stages in sedimentary buildup. The analysis of magnetic and gravity data integrated with seismic reflection profiles provides clues as to the nature of basement rocks, their depth of burial, composition, and tectonic setting. The interpretation of seismic reflection profiles and the correlation of seismic stratigraphic units with lithostratigraphic units at the COST Nos. G-1 and G-2 wells gives a history of basin filling over the past 200 m.y., including major trends in rock types and their thicknesses, relative ages of interregional unconformities, and the relationship of the basin sedimentation to the construction of the adjacent continental slope and rise.

Before the G-1 and G-2 wells were drilled, most of the information concerning the subsurface of Georges Bank was derived from a combination of geophysical data and the extrapolation of stratigraphy from the Shell Mohawk well on the Scotian shelf. (See, for instance, Ballard and Uchupi, 1972; Mattick and others, 1974; Schlee and others, 1976, 1979; Klitgord and Behrendt, 1979; Austin and others, 1980.) In this report, magnetic and gravity data are used in conjunction with multichannel seismic reflection data (fig. 71) to outline the basement structures, to interpolate seismic basement features between seismic lines, and to provide

depth estimates for basement in regions of limited acoustic penetration.

The seismic stratigraphy for the Georges Bank shelf, slope, and rise was determined from correlation with the lithostratigraphy at the Shell Mohawk well (Schlee and others, 1976), at the COST Nos. G-1 and G-2 wells (Amato and Bebout, 1980; Amato and Simonis, 1980; Poag, this volume), at the Nantucket well (Folger and others, 1978), and at Deep Sea Drilling Project (DSDP) sites (Klitgord and Grow, 1980). Additional information concerning the shallow stratigraphy was provided by the 1976 Atlantic Margin Coring Project (AMCOR) (Hathaway and others, 1976, 1979) and other multichannel seismic data (Austin and others, 1980). The correlation of deep-sea and shelf seismic stratigraphy is tenuous, because a buried shelf edge of Lower Cretaceous and older carbonate rocks (Schlee and others, 1979) obscures the acoustic record of the transition across the shelf and slope.

Interval velocities determined from the USGS multichannel seismic data have been used to correlate the stratigraphy on the seismic lines with the lithostratigraphy in the various drill holes (Schlee and others, 1976; Ditty, 1980; Waetjan, 1980; Poag, this volume). This same velocity information has also been used to produce depth sections (fig. 72), isopach maps, and structure contour maps (fig. 3 in Schlee and Klitgord, this volume). The interval velocities were determined from the multichannel profile velocity scans using the method of Taner and Koehler (1969).

Wandering terranes in southern Alaska: the Aleutia microplate and implications for the Bering Sea

Marlow, M. S., and Cooper, A. K., 1983, *Journal of Geophysical Research*, v. 88, no. B4, p. 3439-3446.

Paleomagnetic and geological data suggest that much of southern Alaska is a collage of tectonostratigraphic terranes which originated in Mesozoic time at paleolatitudes far south of their present position. The time of 'docking' of the terranes against cratonic Alaska is critical to defining their amalgamated size and extent during their northward motion as well as their role in the evolution of the Bering Sea. One of the largest of the tectonostratigraphic terranes, the Peninsular terrane of south central and southwestern Alaska, extends offshore along the outer Bering Sea continental margin (Beringia). Paleomagnetic data suggest that this terrane has moved northward through all of Cenozoic time, but geologic data imply that the terrane had accreted to Alaska by the end of the Mesozoic. In early Cenozoic time the eastern part of the Aleutian arc appears to have been superimposed on the Peninsular terrane, and postulated northward Cenozoic motion of the terrane would therefore have required northward motion of the arc. Two accretion models, based on docking times for terranes in Alaska, are proposed, and they illustrate that large areas of the abyssal Bering Sea, the Alaska Peninsula, the Aleutian arc, and the Beringian continental margin may be part of a superterrane or microplate called Aleutia (microplate as defined by Beck

et al. (1980), i.e., a microplate is a displaced segment of lithosphere that has crustal roots, whereas a superterrane is an amalgamation of terranes which may or may not be rootless). Model A implies that the Aleutian arc developed in situ on the southern edge of Aleutia after the microplate had docked. In model B, the final docking time of the Peninsular terrane is late Cenozoic, which implies that the Aleutia microplate encompasses a mammoth area that includes parts of southern Alaska, the Alaska Peninsula, the southern Beringian margin, the abyssal Bering Sea (Kula plate), and the Aleutian arc. If model A is correct, the docking time of the Peninsular terrane is late Mesozoic or earliest Tertiary. The Aleutia microplate in this model is made up solely of the abyssal Bering Sea (Kula plate), which presumably docked at the same time or slightly after the Peninsular terrane accreted against Alaska. If model B is correct, that is, if the Aleutia collided with nuclear Alaska during the Cenozoic, then a late Cenozoic suture zone, the vestige of a large open sea that must have closed between Aleutia and Alaska, must exist in south central and southwest Alaska. Either evidence for Cenozoic closure and suturing has been obliterated in Alaska or the inferences of Cenozoic terrane motion derived from paleomagnetic data are suspect.

Tectonic evolution of Gulf of Anadyr and formation of Anadyr and Navarin basins

Marlow, M. S., Cooper, A. K., and Childs, J. R., 1983, *American Association of Petroleum Geologists Bulletin*, v. 67, no. 4, p. 646-665.

The Gulf of Anadyr is underlain by two major sedimentary basins, Kresta basin and East Anadyr trough, that trend east to southeast and contain, in places, more than 9 km (29,500 ft) of fill. The basins are flanked on the east and north by the Okhotsk-Chukotsk volcanic belt, a broad bedrock high composed of plutonic and volcanic rocks that extends from eastern Siberia along the inner Bering Sea shelf at least to St. Matthew Island. The East Anadyr trough extends onshore and connects with the larger Anadyr basin, which underlies the lowlands between the Koryak Range and Okhotsk-Chukotsk volcanic belt of eastern Siberia.

New seismic reflection and refraction data reveal that Anadyr basin is separated from Navarin basin by Anadyr ridge, a southeast-northwest-trending bedrock high that is characterized by high-amplitude, short-wavelength magnetic anomalies. Anadyr ridge may be an offshore extension of the melange belt underlying the Koryak Range. Sonobuoy refraction data indicate that the velocity profile of strata in East Anadyr trough is similar to that in Navarin basin. Structurally, the basins are different: Navarin basin is complex and contains both compressional and extensional elements, whereas Anadyr basin is a simple, broad crustal sag semicircular in outline. Correlation of our reflection data from the

offshore part of the Anadyr basin (including the East Anadyr trough and Kresta basin) with drilling data onshore allows us to differentiate three distinct sequences in the offshore portion of the basin. These sequences are separated by two strong reflectors, and are tentatively identified with increasing depth as boundaries separating the Neogene and Paleogene, and Paleogene and Mesozoic, respectively.

In the northeastern corner of the Gulf of Anadyr, across the Anaut uplift, shallow beds are folded and broken by faults that commonly offset the sea floor. Furthermore, earthquake epicenters recorded landward of Anadyr basin from Cape Navarin to the southwest and around the Chukotsk Peninsula to the northeast suggest recent tectonic movement in the Gulf of Anadyr near Cape Navarin and near Kresta Bay. We believe that Anadyr basin originally formed as a fore-arc basin during the Cretaceous as a result of underthrusting of the Kula plate beneath Siberia. The collision of the Kula plate with Siberia resulted in the formation of the Okhotsk-Chukotsk volcanic arc north of Anadyr basin and the Koryak melange belt south of the basin. Anadyr basin continued to subside during the Cenozoic and major uplift in the Koryak Range occurred in the late Miocene to Pliocene.

Ancient plate boundaries in the Bering Sea region

Marlow, M. S., Cooper, A. K., Scholl, D.W., and McLean, Hugh, 1982, in Leggett, J. K., ed. *Trench-forearc geology*: Geological Society of London, Special Publication 10, London, Blackwell Scientific Publications, p. 201-212

Plate tectonic models of the Bering Sea suggest that the abyssal Bering Sea Basin is underlain by oceanic crust, a supposition supported by refraction and magnetic data. The oceanic crust is thought to be a remnant of the Kula(?) plate that was isolated within what is now the Bering Sea when the proto-Aleutian arc began to form between the Alaska Peninsula and Kamchatka in late Mesozoic or earliest Tertiary time. Prior to the formation of the Aleutian arc,

the Kula(?) plate moved northwest, directly underthrusting eastern Siberia; the plate's eastern edge either obliquely underthrust or slid past the Bering Sea margin along a transform boundary.

The Koryak Range in eastern Siberia is composed in part of melange units that include Palaeozoic and Mesozoic allochthonous blocks juxtaposed within a matrix of Cretaceous sedimentary rocks. Structural trends suggest that

these blocks were accreted into the Koryak area from the south along an ancient subduction zone formed by underthrusting of the Kula(?) plate.

The base of the Bering Sea continental margin that extends from eastern Siberia to the Alaska Peninsula — the so-called Beringian margin — is underlain by a thick (7 to 10 km) sedimentary section along the base of the slope. Rocks dredged from basement exposed farther up the slope (1,500 to 2,000 m deep) include shallow-water Upper Jurassic sandstone that is unconformably overlain by shallow-water Eocene to Miocene diatomaceous mudstone. Fauna in the dredge samples indicate that the shelf edge has subsided several kilometers since late Palaeogene time, perhaps in response to the cessation of motion relative to the adjacent oceanic plate and subsequent sediment loading of the oceanic plate.

Origin of the Canada Basin as inferred from the seismic geology of offshore northern Alaska

May, Steven D., and Grantz, Arthur, 1982, *Alaska Geological Society Journal*, v. 2, p. 9-16.

An extensive multichannel seismic-reflection survey of the continental margin north of Alaska was conducted by the U.S. Geological Survey in 1977. Grantz, Eittrheim, and Dinter (1979) used this seismic-reflection data set and other data to interpret the geologic history of the continental margin and its implications for the origin of the Canada Basin of the Arctic Ocean. Further processing of the data, using refined velocity picks, has made possible a more detailed interpretation. This paper summarizes the major aspects of the development of the continental margin north of Alaska in light of this more detailed information. Grantz and May (1982) treat the subject in more detail.

Recent seismic-refraction studies (Mair and Lyons, 1981; Grantz, Eittrheim, and Whitney, 1981) and earlier work on the dispersion of Lg-phase seismic waves (Oliver, Ewing, and Press, 1955) indicate that the Canada Basin, with depths of nearly 4,000 m, is floored by oceanic crust and therefore was formed by sea-floor spreading. The southern boundary of the Canada Basin is the continental margin off northern Alaska (i.e., the Beaufort slope and upper rise). This continental margin must be in contact with the oceanic Canadian Basin in one of three ways: a convergent or once-convergent boundary (a subduction zone); a transform (strike-slip) boundary; or a passive boundary created by continental rifting. No evidence for either a convergent boundary (compressional structures, accretionary prism, or subduction zone) or for a transform boundary (through-going vertical or near-vertical faults and fault blocks that parallel the continental slope) is present on any of our several seismic-reflection profiles that traverse from the shelf to the slope and rise in the Beaufort Sea. The structural and stratigraphic features of the margin (figs. 1 through 6) do, however, closely resemble the general model of a passive (Atlantic type)

Uplift of the former plate boundary exposed in the Koryak Range occurred principally in late Cenozoic time, and collapse of the adjacent plate boundary, the Beringian margin, began in earliest Tertiary time and has continued to the present. Both tectonic events occurred after the site of active plate collision shifted south to near the present Aleutian Trench. We are uncertain as to why these two ancient, yet adjacent former plate boundaries should behave so differently, i.e., why one area was folded and uplifted while the other was extensionally deformed and subsided, both apparently in response to the cessation of convergent or strike-slip plate action.

continental margin as described by Falvey (1974) and Falvey and Mutter (1981). The model has four lithotectonic elements and a breakup unconformity, and all or most of these features are observed on the seismic-reflection profiles presented in this paper (figs. 3-6). The four elements of Falvey's model and the correlative features of the continental margin north of Alaska are compared in table 1.

The juncture of the oceanic Canada Basin and continental northern Alaska appears to be a passive (Atlantic type) continental margin. Nearly all the structural and stratigraphic elements predicted in a general model of a passive continental margin (Falvey, 1974; Falvey and Mutter, 1981) have been recognized, while none of the structural features found at convergent-or transform-type margins have been identified on our multichannel seismic-reflection profiles.

Spreading of Arctic Alaska away from the Canadian Arctic islands about a pole in Alaska or the Mackenzie delta region has been proposed by several authors (including Carey, 1958; Tailleux, 1969 and 1973; Rickwood, 1970; Grantz, Eittrheim, and Dinter, 1979; and Newman, Mull, and Watkins, 1979). If this spreading geometry is accepted and a fairly typical spreading rate of 3 cm/yr is assumed across the center of the Canada Basin from Point Barrow to Prince Patrick Island, approximately 20 m.y. would be required for the Canada Basin to achieve its present width. Prince Patrick Island, which lies adjacent to the Canada Basin in the western part of the Canadian Arctic islands, is about 1,100 km northeast of Point Barrow. If, as we propose in table 1, breakup and the initiation of spreading in the Canada Basin began about 120 m.y.B.P., the basin may have reached its full width and become a stable ocean basin about 100 m.y.B.P.

Mechanisms of subduction accretion along the central Aleutian Trench

McCarthy, Jill, and Scholl, D. W., in press, *Geological Society of America Bulletin*.

We have used migrated 24-fold seismic records to study mechanisms of subduction accretion along the central Aleutian Trench. Two major structural units underlie the landward trench slope, they are separated by an acoustically defined decollement surface that can be traced at least 20 km landward of the trench axis. The upper unit consists of three or four types of structural blocks of deformed trench fill. Each block possesses its own internal structure and is bound by major landward dipping thrust faults. These blocks include: monoclinical sequences, antiforms, synforms, and faulted folds. Beneath the decollement nearly undeformed trench fill approximately 1 km thick is being subducted along with the underlying oceanic lithosphere. This basal section is an intervening unit between the offscraped sediment and the rough igneous oceanic basement, and may possibly prevent

the oceanic crust from being incorporated into the subduction complex at the front of the subduction zone.

Owing to bending stresses, the oceanic crust faults normally beneath, and at least 16 km landward of, the trench axis and produces offsets within both the subducting and the offscraped sediment. Subduction of irregular basement highs results in the temporary displacement of the overlying fault-bound sediment packets and promotes the development of the structures found within the accretionary prism. Tectonic rifting of the accreted sediment by the passage of the basement relief may also provide a mechanism by which underthrusting sediment are decoupled from the subducting lithosphere and underplated to the base of the Aleutian accretionary complex.

Plate-tectonic map of the circum-Pacific region explanatory notes

Moore, G. W., 1982, Tulsa, Okla., American Association of Petroleum Geologists, 14 p.

Publication of the six sheets of the "Plate-Tectonic Map of the Circum-Pacific Region" was completed in 1982. This map series, the work of 42 specialists from 15 countries is one of eight series being prepared by the Circum-Pacific Map Project, a cooperative international effort to produce new maps showing the geology, geophysics, and energy and mineral resources of the Pacific Ocean and surrounding continental areas.

The theory of plate tectonics constitutes one of the great revolutions in scientific understanding. It touches almost all aspects of the earth sciences: the origin of mountains, earthquakes, and volcanoes, the distribution of fossils, the formation of metalliferous ores, and the generation of petroleum. It is the starting point for scientists and engineers striving to predict and minimize the consequences of natural disasters such as volcanic eruptions and earthquakes. Although the theory was only linked together in complete and coherent form in 1965, it has filled such a basic need in the science of geology that a majority of

the world's geologists now understand the tenets of plate tectonics and are applying them.

Volcanoes and earthquakes around the circum-Pacific "ring of fire" were important factors in developing the theory of plate tectonics. They are represented on the map sheets in several categories, along with major faults, plate boundaries, directions and rates of motion of the plates, and records of past plate motion that are registered on the sea floor by magnetic anomalies, parallel lines where the Earth's magnetic field differs from the expected field. These explanatory notes interpret the data shown on the map sheets and discuss the principles of the theory of plate tectonics on the basis of its historical development.

The "Plate-Tectonic Map of the Circum-Pacific Region" provides a framework for understanding the geologic information on which the theory of plate tectonics is based, and it serves as a starting point for research to apply and further develop the theory. It is a practical tool for solving geologic problems and directing the search for energy and mineral resources.

Offshore geology, circum-Pacific region

Moore, George W., 1983, in Explanatory notes for the geologic map of the circum-Pacific region: Tulsa, Okla., American Association of Petroleum Geologists.

Thick Quaternary deposits ring the Pacific Basin and cover adjacent abyssal plains as a result of sediment plumes from streams, deep-sea fans, and slide-generated turbidity currents. Along the Equator, a belt of Quaternary carbonate ooze, 1000 km wide and as much as 20 m thick, occurs where nutrient-rich water wells up along the Equatorial divergence and enhances biologic productivity. In other parts of the deep basin, however, productivity is insufficient to balance seafloor dissolution. Many such places are at a steady state of no net accumulation, and at others, erosion of underlying older deposits occurs by means of both dissolution and bottom currents, such as those caused by the sinking and lateral flow of cold dense water from near Antarctica. Accumulation is sufficiently slow in the central Pacific Basin to cause lower Tertiary strata to crop out or to lie within 1 m below the seafloor over broad areas.

Many volcanic plateaus have a geologic age that matches that of the oceanic crust which underlies them. These prominences formed where eruption rates were anomalously high along spreading axes, usually at leaky transform faults. Other seamounts of the midplate-hotspot type are younger than the underlying oceanic crust. Along fault scarps, dredges commonly recover coarse-grained basalt and gabbro, slowly cooled at depth below the seafloor. Along major transform faults, the crust is disrupted to sufficient depth to expose metamorphic rocks such as greenschist, and in some places, serpentinite from the Earth's mantle. Serpentinite also crops out along some trench slopes. Uplift and disruption of subcrustal material in the upper plate of a subduction zone is believed to cause most of these trench-slope exposures of serpentinite.

Structural dynamics of the shelf-slope boundary at active subduction zones

Moore, George W., 1983, in Stanley, D. J., and Moore, G. T., eds., The shelfbreak: critical interface on continental margins: Society of Economic Paleontologists and Mineralogists Special Publication 33, p. 97-105.

About 40 subduction-zone segments have been identified worldwide on the basis of intermediate-focus earthquakes, calc-alkalic volcanic arcs, and lines of rapid tectonic uplift. The total length of these actively convergent plate boundaries is 57,000 km. Of this length 42% is of the Japan type, in which the upper plate is relatively stable with respect to the subduction zone; 37% is of the Andes type, in which the upper plate actively overrides the trench; and 21% is of the Himalaya type, in which continental plates or microplates collide with other continental bodies.

Subduction zones of both the Japan and Andes types are marked by basement highs at the trench-slope break. Uplift of the crust and upper mantle at the edge of the upper plate causes these basement highs where a relatively low-density prism of accreted oceanic material is emplaced below. The accretionary prism for each cycle of subduction forms within 5 m.y. after a new subduction zone is established, while the megathrust is evolving from an initial dip of about 30° near the zone's seafloor outcrop to a steady-

state dip of about 10°. Except during this relatively brief period of accretion, most oceanic sediment at subduction zones is believed to be carried deeply into the lithosphere.

Elongate sedimentary basins form on both sides of the uplift at the trench-slope break: forearc basins toward the arc, and trench-slope basins toward the trench. Depending on the balance between sedimentation and tectonic displacement, the topographic shelf-slope boundary may be located anywhere in the forearc basins, approximately to the upper edge of the trench-slope basins. At the lower trench slope, compression usually removes the seawater involved in primary oil migration before thermal maturation of oil precursors can occur. Elsewhere at the active margin, although a low geothermal gradient caused by the subduction of cool oceanic crust delays hydrocarbon maturation, such thermal maturation can nevertheless resume when a normal geothermal gradient is reestablished after continental collision or after the subduction-zone alignment moves to a new position.

The Yakutat block: an actively accreting tectonostratigraphic terrane in southern Alaska

Plafker, George, 1983, Geological Society of America Abstracts with Programs, v. 15, no. 5, p. 406.

The Yakutat block is a composite tectonostratigraphic terrane 600 km long by 200 km wide in the process of accreting to southern Alaska in the northern Gulf of Alaska region.

Basement consists of upper Mesozoic flysch and melange in the eastern part of the block and probable upper Paleocene to lower Eocene oceanic crust in the western 2/3 of the block. Basement rocks are overlain by a lower Eocene through Quaternary bedded sequence of variable thickness. Structural, seismic, and paleoseismic data indicate that the Yakutat block has been moving with the Pacific plate at almost the full average relative plate velocity of 5.8 cm/yr for at least the last 100,000 years. Thick locally-derived clastic shelf basin fills of middle Miocene to Holocene age reflect uplift and erosion of the Saint Elias and Chugach Mountains along the northern margin of the block due to

collision with, and underthrusting of, the North American plate.

The most probable source of the Yakutat block is the continental margin of southeasternmost Alaska and British Columbia based on 1) occurrence of a displaced upper Mesozoic flysch and melange sequence in the eastern part of the Yakutat block; 2) the metamorphic-plutonic provenance of pre-Miocene Tertiary sedimentary rocks; and 3) northward displacement of floras and faunas in Paleogene bedded rocks. Available data suggest that the Yakutat block was sliced off the continental margin southeast of Chatham Strait about 25 Ma ago after which it was displaced some 550 km northwestward along the Queen Charlotte-Fairweather transform fault system. Concurrently, an additional 900 km of dextral displacement was accommodated along the Transition fault system between the Yakutat block and Pacific plate.

Late Cenozoic subduction—rather than accretion—at the eastern end of the Aleutian arc

Plafker, George, and Bruns, T. R., 1982, Geological Society of America Abstracts with Programs, v. 14, no. 7, p. 589.

The eastern Aleutian arc is part of a classic underthrust plate margin defined by an oceanic deep, an andesitic volcanic chain, and a Benioff zone that extends northward beneath the arc. Data from the great 1964 Alaska earthquake indicate that the megathrust system between the North American and Pacific plates dips northward at an average angle of less than 10° for about 200 km from the vicinity of the Aleutian Trench. Convergence is orthogonal to the arc at an average rate of 5 to 7 cm/yr, and at least 600 km of the Pacific plate has been consumed since initiation of the present pulse of subduction during the Miocene. Uplift of the coastal mountains and arc volcanism resulted in late Cenozoic sedimentation rates as high as 1.5+0.3 km/m.y. in the trench and adjacent ocean floor. The combined thickness of post-Oligocene pelagic, hemipelagic, and turbidite sediment overlying oceanic crust is up to 3-1/4 km at the present trench.

The present inner wall of the Aleutian Trench is an ideal site for accumulation of an accretionary sedimentary prism owing to the combination of long-continued low-angle underthrusting, a high convergence rate, and a thick sedimentary sequence in the trench. However, deep dredging along the base of the trench inner wall has recovered terrestrially-derived Paleogene sedimentary strata that correlate with the Middleton Island well on the adjacent continental shelf. Multichannel seismic reflection profiles clearly show that the Paleogene sequence along the trench inner wall has been underthrust by undeformed ocean sediment for at least 14 km from the base of the inner wall. These data require that the Pacific plate, with its thick sedimentary section, has been subducted beneath the North American plate without any appreciable offscrapings of Neogene age.

Stratigraphic reference section for Georges Bank basin—depositional model for New England passive margin

Poag, C. W., 1982, American Association of Petroleum Geologists Bulletin, v. 66, no. 8, p. 1021-1041.

A multichannel seismic reflection profile (U.S. Geological Survey line 19) calibrated with the COST G-1, COST G-2, and Shell Mohican I-100 wells, and seismic-sequence analysis shows that the chronostratigraphic and lithostratigraphic units and depositional history of the Georges Bank basin are similar to those of the Scotian basin. Carbonate rocks of the Iroquois and Abenaki Formations, as much as 16,000 ft (4,800 m) thick, dominated the eastern half of the Georges Bank basin during the Jurassic. As much as 7,500 ft (2,300 m) of the coeval terrigenous clastic deposits of the Mohican, Mohawk, and MicMac Formations accumulated updip (westward)

in sublittoral, paralic, and nonmarine environments. Siliciclastic deposition, as much as 6,000 ft (1,800 m), dominated the entire basin throughout the Cretaceous and Cenozoic, and it was punctuated briefly by carbonate deposition during the Hauterivian and Paleogene. Tentative correlation between the Georges Bank basin sequences and those of the adjacent, deep North American basin suggests that the deep-sea facies were strongly influenced by depositional events on the shelf. Deposition in both areas has been sensitive to changes in sea level and to paleoclimatic cycles.

Seismic stratigraphy of Baltimore Canyon Trough

Schlee, J. S., 1981, American Association of Petroleum Geologists Bulletin, v. 65, no. 1, p. 26-53.

Examination of approximately 3,000 km of multichannel seismic-reflection profiles collected over the U.S. Middle Atlantic Shelf (Cape Hatteras to Long Island) shows that the margin was rifted prior to the separation of

Africa and North America and that it broadly subsided after the separation. Major accumulation of sediment is centered in the Baltimore Canyon Trough, where more than 15 km of Triassic(?) and younger sedimentary rocks has been

deposited. The trough is asymmetric in that the thickest sedimentary section is beneath the outer part of the shelf seaward of a hinge zone; further, the trough is wider on the north off New Jersey than it is seaward of Virginia. Flanking the trough are two block-fault platforms (Long Island and Carolina) where thickness of the sedimentary cover is 1 to 4 km.

Eight depositional sequences have been delineated in analysis of the profiles by use of the techniques Vail and others have presented in AAPG *Memoir 26*. Marked changes in reflection characteristics and unconformities are used to bound the sequences. The oldest sequence (Late Triassic-Early Jurassic) is thought to be nonmarine and restricted-marine sediments associated with a complexly faulted crust. The changing seismic facies of younger sequences chronicle the transition to more open marine shelf and slope paleoenvironments during the Cretaceous and Tertiary. The

thickest units accumulated during a phase of rapid basin subsidence in the Jurassic; sediment accumulation decreased substantially during the Late Cretaceous and Cenozoic so that the sequences are thinner and unconformities are more evident. The most conspicuous unconformities seismically are correlated with the Albian, Turonian-Coniacian, Late Cretaceous-Paleocene, Oligocene, and late Miocene-early Pliocene, by correlation with COST (Continental Offshore Stratigraphic Test) and coastline wells. Several of these breaks coincide with pronounced fluctuations in the Vail curve of relative sea level, particularly during the Tertiary, when indicators of falling sea level were widespread. Lastly, the records confirm the presence of a carbonate platform along the seaward edge of the trough during the Jurassic and Early Cretaceous. The stages of formation of the continental margin here are similar to those of the margin off the Canadian Maritime Provinces.

Seismic stratigraphy of the Georges Bank Basin complex, offshore New England

Schlee, J. S., and Fritsch, J., 1982, in Watkins, J. S., and Drake, C. L., eds., *Studies in continental margin geology*: American Association of Petroleum Geologists *Memoir 34*, p. 223-251.

A regional synthesis of 3,350 km of multichannel seismic-reflection profiles over the Georges Bank area reveals that subsidence concentrated in several areally restricted rift basins of Early Jurassic age and older. Beneath the northwestern half of Georges Bank area, these small sub-basins form narrow grabens within a structurally shallow platform (4 km deep). Beneath the southern half of Georges Bank and Nantucket shoal area are three deep sub-

basins containing more than 10 km of sediments. The sedimentary fill is divided into six seismic units that reveal a change from an older, thick sequence of rift-filling (synrift) continental and evaporitic deposits (0 to 8 km thick) of Late Triassic to Early Jurassic age, to younger, more widespread open-marine shelf sequences of carbonate and clastic sedimentary rocks of Jurassic and younger ages.

The paleoenvironment and development of the eastern North American continental margin

Schlee, J. S., and Jansa, L. F., 1981, *Oceanologica Acta*, Proceedings 26th International Geological Congress, Geology of continental margins symposium, Paris, July 7-17, 1980, p. 71-80.

Geophysical studies (multichannel seismic reflection profiles, gravity and magnetic surveys) have been combined with drill hole data so that the major structural elements of the eastern North America continental margin and the seismic stratigraphy of the offshore sedimentary prism can be outlined. The sedimentary basins, trough and platforms are built over a zone of rifted and thinned crust of variable width (20-300 km). Upper Paleozoic and Triassic-Lower Jurassic red beds were deposited in northeast trending grabens that formed prior to or synchronous with rifting (pre- and synrift). During the late synrift phase, Upper Triassic and Lower Jurassic evaporitic sequences were precipitated in a southward encroaching Tethyan seaway. Studies of drill cores on the present shelf indicate that major marine incursions occurred during the Early and Late Middle Jurassic and culminated in the buildup of a series of carbonate platforms and banks that continued to flourish into the Albian on the

Eastern Blake Plateau. Off the eastern United States, these banks appear to have formed in the vicinity of the ocean-continent boundary, and may have been associated with secondary volcanic dikes and sills which were emplaced 20-30 m.y. after continental separation. Influxes of terrigenous detritus during the Early to middle Cretaceous broadly prograded the margin as deltaic and mixed inner shelf and nonmarine deposits. A series of marine transgressions in the Late Cretaceous and early Tertiary changed the shelf to a deep-water setting and resulted in the deposition of chalks and marly shale. Major marine regressions in the Oligocene, Miocene and Quaternary contributed to periodic cutback of shelf and slope, exposure of Cretaceous and lower Tertiary strata in submarine canyons, accentuation of the shelf-slope-rise profile, and construction of a broad sedimentary prism beneath the continental rise.

Subduction and the rock record of the Pacific margins

Scholl, D. W., and Vallier, T. L., 1983, in Carey, S. W., ed., *The expanding earth, a symposium*, Sydney, 1981: Brunswick, Impart Printing (Vic.) Pty. Ltd., p. 235-245.

Strong arguments against continental drift initially took note of the fact that many Pacific-bordering mountain belts of eugeosynclinal or ensimatic deposits included only small quantities of oceanic pelagic sediment, and that other coastal ranges are underlain by miogeoclinal deposits and cratonic or ensialic basement. It was reasoned that if drifting continental fragments had advanced toward the Pacific from Pangaea, that this fact would be manifested by the accretion of a wide mass of ensimatic deposits rich in

oceanic sediment to their Pacific-facing edges. Notwithstanding this argument, marine geologic and geophysical data confirmed continental drift.

On an earth of constant radius this conclusion required that during the past 200 my from 5,000 to 15,000 km of oceanic crust have underthrust or been subducted beneath sectors of the Pacific rim. But the concept of crustal underthrusting or subduction did not obviate the problem of accounting for the missing oceanic deposits and the presence

of the trench-bordering terranes of orotonic and miogeoclinal rocks in lieu of ensimatic or eugeosynclinal assemblages. These puzzling circumstances (for a nonexpanding Earth) vanish, however if subduction processes not only involve the accretion of oceanic sediment and crustal fragments to ocean margins, but also the subduction of sediment and the underlying igneous crust to mantle depths and the tectonic erosion of the margin's bedrock framework. Drilling and geophysical investigations at ocean margins have demonstrated that relative to the accumulative process of subduction accretion, the regional or local efficacy of the consumptive processes of sediment subduction and subduction erosion determines the lithologic and structural character of

the rock sequence formed at many modern and ancient Pacific margins.

The first order structural, lithologic, and volumetric parameters of Pacific margin ensimatic masses, which provide direct evidence for crustal subduction, attest to only a few hundred or perhaps a thousand kilometers of subduction. Ironically, evidence for thousands of kilometers of subduction—a requirement on an Earth of constant girth—is best preserved in volumetrically small bits and pieces of allochthonous rock debris and somewhat larger crustal terranes that retain a palaeomagnetic or palaeogeographic memory of distant origin and long transport.

Sedimentation and deformation in the Amlia fracture zone sector of the Aleutian Trench

Scholl, D. W., Vallier, T. L., and Stevenson, A. J., 1982, *Marine Geology*, v. 48, p. 105-134.

A wedge-shaped, landward thickening mass of sedimentary deposits composed chiefly of terrigenous turbidite beds underlies the west-southwest-trending Amlia sector (172°20'–173°30'W) of the Aleutian Trench. Pacific oceanic crust dips northward beneath the sector's sedimentary wedge and obliquely underthrusts (30° off normal) the adjacent Aleutian Ridge. The trench floor and subsurface strata dip gently northward toward the base of the inner trench slope. The dip of the trench deposits increases downsection from about 0.2° at the trench floor to as much as 6–7° just above basement. The wedge is typically 2–2.5 km thick, but it is thickest (3.7–4.0 km) near the base of the inner slope overlying the north-trending Amlia Fracture Zone and also east of this structure. Slight undulations and relatively abrupt offsets of the trench floor reflect subsurface and generally west-trending structure within the wedge that are superimposed above ridges and swales in the underlying oceanic basement. The southern or seaward side of some of these structures are bordered by high angle faults or abrupt flexures. Across these offsets the northern side of the trench floor and underlying wedge is typically upthrown.

West-flowing turbidity currents originating along the Alaskan segments of the trench (1200 km to the east) probably formed the greater part of the Amlia wedge during the past 0.5 m.y. The gentle northward or cross-trench

inclination of the trench floor and underlying wedge probably reflects regional downbending of the oceanic lithosphere and trench-floor basement faulting and rotation. Much of the undulatory flexuring of the trench wedge can be attributed to differential compaction over buried basement relief. However, abrupt structural offsets attest to basement faulting. Faulting is associated with extensional earthquakes in the upper crust. The west-trending basement offsets are probably normal faults that dip steeply south or antithetic to the north dip of the subducting oceanic crust. Up-to-arc extensional faulting can be attributed to the down-bending of the Pacific plate into the Aleutian subduction zone. The rupturing direction and dip is controlled by zones of crustal weakness that parallel north Pacific magnetic anomalies, which were formed south of a late Cretaceous–early Tertiary spreading center (Kula–Pacific Ridge). The strike of these anomalies is fortuitously nearly parallel to the Amlia sector. The up-to-arc fracturing style may locally assist in elevating blocks of trench deposits to form the top of the trench's landward slope, which is in part underlain by a compressionaly thickened accretionary mass of older trench deposits. Compressional structures that can be related to underthrusting are only indistinctly recorded in the turbidite wedge that underlies the trench floor.

Geologic evolution of the Aleutian Ridge—implications for petroleum resources

Scholl, D. W., Vallier, T. L., and Stevenson, A. J., 1983, *Journal of the Alaska Geological Society*, v. 3, p. 33-46.

The Aleutian Ridge consists geomorphically of two provinces: a west-trending, flat-topped (guyot-like) submarine cordillera, the Aleutian island arc, that rises 4,000 meters above its Pacific and Bering Sea bases; and a 30–90-kilometer-wide forearc province that includes a broad forearc basin, the Aleutian Terrace, and the landward slope of the Aleutian Trench. The ridge's upper crustal rocks can be grouped into a three-tiered chronostratigraphic sequence: a lower series of mostly Eocene volcanic rocks; a middle series of mostly Oligocene through lower middle Miocene strata that includes large volumes of sedimentary beds; and an upper series of middle Miocene to Holocene deposits that are dominantly sedimentary beds but include the upper Cenozoic eruptive masses of the arc's modern volcanic centers.

Except for the landward trench slope, the ridge's upper crustal framework is a massive antiformal consisting of a sediment-draped igneous massif of chiefly lower series rocks produced rapidly by voluminous submarine volcanism prior to about 35 million years ago. The massif is at least 200 kilometers wide and extends from the landward trench slope northward beneath the forearc basin and adjacent cordillera of the island arc to the abyssal floor of the Bering Sea. In post-Eocene time, igneous activity effectively ceased over

the flanks of the ridge and, except for a pulse in early middle Miocene time, greatly diminished along the arc's summit region. In Oligocene through early Neogene time, debris eroded from the regionally elevated and volcanically dying crest of the arc accumulated on the submerged (or submerging) flanks and basal regions of the ridge as middle series deposits.

The post-middle Miocene history of the ridge crest records the dominance of extensional collapse and erosion over continuing but localized volcanic buildup of the arc's igneous massif. Wave-base erosion carved a summit platform across the top of the arc. The truncation was accompanied by the deposition of basinal sequences of upper series beds in summit grabens and perhaps by extensive subsidence of the arc's sloping flanks. In the more deeply submerged forearc area, relative uplift of the seaward part of the ridge's igneous basement framed the structural basin of the Aleutian Terrace, which was collaterally filled with 3–5 kilometers of upper series deposits. Also in conjunction with the formation of this basin, a mass of trench deposits, predominantly of Alaskan origin, was compressionaly accreted to the lower part of the adjacent landward trench slope.

The rock fabric of the Aleutian Ridge (arc + forearc) records a two-part history of early Tertiary growth and subsequent erosion and structural modification. This formative sequence can be roughly linked to major changes in the plate tectonic setting along the northern rim of the Pacific Basin. Because of the relative dominance of processes of erosion, sedimentation, and deformation during the ridge's second-stage evolution, its igneous framework is blanketed by Oligocene and younger sedimentary masses that

are potential habitats for petroleum accumulations. Petroleum is most likely to occur in the 3-5 kilometer-thick, slightly deformed basinal sections of upper series and perhaps middle series deposits that underlie the Aleutian Terrace and fill summit grabens. Middle and upper Cenozoic sandstone and siltstone beds associated with these sections are little altered and have favorable organic contents and porosity and permeability properties.

Geochemistry and petrology of igneous rocks, Deep Sea Drilling Project Leg 62

Seifert, K. E., Vallier, T. L., Windom, K. E., and Morgan, S. R., 1981, Deep Sea Drilling Project Initial Reports, v. 62, p. 945

Igneous rocks were recovered from three sites on Hess Rise during Deep Sea Drilling Project Leg 62: altered basalt at Site 464, at the northern end of Hess Rise; and altered trachyte from site 465, and rounded basalt pebbles in upper Albian to middle Miocene sediments from Site 466, both at the southern end of Hess Rise. Major-, minor-, and trace-element data for basalt from Hole 464 are consistent with these rocks being transitional tholeiites that have undergone low-temperature alteration by reaction with sea water. Trachyte from Hole 465A exhibits as many as three generations of plagioclase along with potash feldspar that are flow aligned in groundmasses altered to smectites and random mixed-layer clays. Textural evidence indicates that these rocks were erupted subaerially. Chemical data show a range of values when plotted on two- and three-component variation diagrams. The observed variations may result in part from differentiation, but they also reflect the high degree of alteration. Several oxides and elements show

strong correlation with H_2O^+ : K_2O , SiO_2 , Rb and Lu decrease and MgO increases with increasing H_2O^+ . These trends, except for that of Lu, are consistent with experimentally determined changes in chemistry that accompany alteration. The trend for Lu has not been previously reported; it may result from a more-intense alteration of the HREE-rich mafic minerals than of the LREE-rich feldspars. Despite their alteration, the trachytes compare favorably with alkalic differentiates from oceanic islands.

We interpret Hess Rise as a volcanic platform formed by eruption of off-ridge volcanic rocks onto MORB oceanic crust during the Aptian and Albian stages after the basement had migrated away from the spreading center. By analogy with present oceanic islands, we propose that early tholeiitic basalts were followed by alkalic basalts and their differentiation products (trachytes), producing a volcanic archipelago of islands and seamounts. Subsequent tectonism and subsidence led to the present state of Hess Rise.

Land-sea geologic cross section of the southern Oregon continental margin

Snively, P. D., Jr., Wagner, H. C., and Lander, D. L., 1984, U.S. Geological Survey Miscellaneous Investigations Series, Map I-1463.

In order to understand more fully the stratigraphic and tectonic framework of the Oregon and Washington continental margin, a series of land-sea geologic cross sections are being prepared. These sections are based upon onshore geologic mapping, the interpretation of 24-channel seismic-reflection profiles and magnetic data, and the correlation of acoustical units with the subsurface stratigraphy encountered in deep exploratory test wells drilled offshore by industry in the mid-1960's (Braislin and others, 1971; Snively and others, 1977, 1981a). The first published cross section in the series for the Oregon continental margin using this kind of information (see fig. 1, line MC-28J) was prepared for the U. S. Geodynamics Committee and published by the Geological Society of America (Snively and others, 1980).

The geologic cross section A-A" described in this report extends generally westward from the west flank of the Oregon Coast Range to the edge of the Continental Shelf at latitude $44^{\circ}12'N$ (fig. 1). The geology used to construct the onshore portion of this cross section is based upon geologic mapping by Baldwin (1956), on unpublished mapping by Snively in the Heceta Head and Mapleton quadrangles, on subsurface data in the Sinclair Oil and Gas Company Federal-Mapleton No. 1 well (fig. 1), and on magnetic data from a U.S. Geological Survey open-file report (1970). The interpretation of the offshore geology is based mainly upon a 24-channel seismic-reflection profile and magnetic data (figs. 2, 3) collected aboard the U. S. Geological Survey's Research Vessel S. P. Lee (Snively, 1981), and upon subsurface stratigraphic data in the Shell Oil Company P-087 offshore well (figs. 1, 7). Also collected were deep-penetration single-channel and high-resolution seismic-reflection profiles and gravity data. The geologic interpretation, where extrapolated

westward from the shoreline to the eastern end of seismic profile A-A', is based in part on a shallow-penetration single-channel seismic-reflection profile collected by Oregon State University (Kulm and Powler, 1970). Because our unmigrated 24-channel seismic profile is not of uniform quality, the interpretation of the profile should be considered no more than a working model. As new information becomes available, seismic-refraction data in particular, this model will doubtless be revised. Moreover, the stratigraphic and tectonic history of this segment of the Oregon continental margin as presented in this report is influenced by our understanding of the regional Tertiary geology of western Oregon and Washington and the adjacent continental margin as formulated from field studies onshore and interpretation of seismic-reflection profiles offshore.

A preliminary geologic interpretation of the 24-channel profile A-A" (fig. 4) and extension onto the western flank of the Oregon Coast Range was published previously by Snively and others (1981b). Three other cross sections for the southern Oregon continental margin immediately south of section A-A" have already been published (Braislin and others, 1971; Seely and others, 1974; Couch and Braman, 1980). These sections are based upon geophysical data and in part on subsurface information in the Union Oil Company Fulmar P-0130 well and in the Sinclair Federal-Mapleton No.1 well (fig. 1). Braislin and others (1971) constructed a diagrammatic regional cross section that showed the generalized Tertiary structure and stratigraphy from Heceta Bank eastward to the Cascade Range. Seely and others (1974) presented an interpretation of a 12-channel seismic-reflection profile that extended from the abyssal plain to a point on the Continental Shelf about midway between the Union P-0130 well and the coastline. In their report, they propose that imbricate

thrusting accounts for the structural thickening and uplift of sediments of the Continental Slope of this and other convergent continental margins. The tectonic framework of the Oregon and Washington outer continental margin and slope, as interpreted from 24-channel seismic profiles by Snively and others (1980, 1981b), agrees in most respects with the compressional thrusting and folding model proposed by Seely and others (1974). Couch and Braman (1980) presented a regional crustal section from the abyssal plain eastward across Heceta Bank to the Willamette Valley. Their cross section gives a geologic interpretation based chiefly on analysis of their gravity data. Snively and others (1981a) show the lithology and time-stratigraphic correlations between Tertiary rocks penetrated in five exploratory wells drilled on the southern Oregon shelf and in the Sinclair Oil and Gas Co. Federal-Mapleton and General Petroleum Corporation Long Bell wells onshore (fig. 1).

Sections showing biostratigraphy and correlation of Tertiary rocks penetrated in wells drilled on the southern Oregon Continental Margin

Snively, P. D., Jr., Wagner, H. C., and Rau, W. W., 1982, U.S. Geological Survey Miscellaneous Field Studies Map MF-1482.

Geologic interpretation of seismic reflection profiles on the Continental Shelves of Oregon and Washington is measurably enhanced through the knowledge of the Tertiary subsurface stratigraphy penetrated in 10 deep exploration wells drilled in the mid-1960's (Braislin and others, 1971; Snively and others, 1977). These subsurface data make it possible to relate the acoustic units differentiated on seismic-reflection profiles to time-stratigraphic units as determined from micropaleontological studies of samples collected from these wells. These biostratigraphic data also permit correlations between time-stratigraphic units in the offshore test wells and between those units and formations penetrated in onshore test wells, as well as strata that crop out in coastal Oregon and Washington.

The purpose of this report is to present information on the stratigraphy and micropaleontology of the Tertiary sequence penetrated in five offshore test wells drilled on the southern part of the Oregon Continental Shelf (fig. 1) and to show time-stratigraphic correlations between these offshore wells and two deep test wells drilled on the west flank of the Oregon Coast Range (fig. 2). These data were first made available to the public in preliminary form by Snively and others (1981a).

The biostratigraphic and petrographic data that form the framework for correlations between the offshore wells is based upon the studies of sidewall cores and ditch samples generously made available to the U. S. Geological Survey by the oil companies who were operators for the exploratory wells. The operators and wells include: Pan American Petroleum Corporation P-0112 (now AMOCO Production Corporation); Shell Oil Company P-087; Standard Oil Company of California P-0103; and Union Oil Company of California P-093 and P-0130. We also gratefully acknowledge permission by these operators to publish the results of our studies of the subsurface samples.

The writers wish particularly to acknowledge David Burkry's biostratigraphic ages based upon his identification of phytoplankton from wells P-087, P-0112, and P-0130. We are also grateful for his helpful discussions concerning Tertiary

Biostratigraphic age assignments used in this report are based upon identifications of phytoplankton by David Bukry (table 1; written commun., 1980-81). The interval velocities assigned to acoustical units in constructing cross section A-A' at true scale (fig. 5) were derived from sonic logs of the Shell P-087 well on the line of section, the Union P-093 and P-0130 wells (fig. 1), and from velocity analyses based on "gatherers" from the S. P. Lee 24-channel data. The sonic logs for the test wells drilled on the southern Oregon shelf indicate that interval velocities of acoustical units of the same age vary depending in part on their depths of burial and (or) structural complexities. As sonobouy measurements are lacking along the line of section, the thickness of time-stratigraphic units shown on the geologic section are doubtless subject to change.

biostratigraphic ages as determined by coccoliths and benthic foraminifers in the Pacific Northwest.

Braislin and others (1971) made the first attempt to tie the geology of the Coast Ranges with that on the Continental Shelf using subsurface data in the Standard-Union Nautilus No. 1 (P-0103) test well (fig. 1) and seismic reflection profiles collected by the petroleum industry in the early 1960's. Snively and others (1977) published general stratigraphic information on the 10 test wells drilled on the Oregon-Washington Continental Shelf; included was a west-trending 160 kJ single-channel profile through the Nautilus (P-0103) well. Seely and others (1974) published a geologic interpretation of a 12-channel seismic profile across the Oregon continental margin near latitude 44°N., but did not tie this profile to the onland geology. Couch and Pitts (1980) prepared generalized crustal geologic cross sections near latitudes 43°15'N. and 44°N. These sections were based upon a geologic interpretation of gravity, magnetic, and subsurface stratigraphic data in the Union Oil Company of California Fulmar No.1 (P-0130) and Sinclair Oil and Gas Company Federal-Mapleton No. 1 wells for the northern cross section and the Pan American Petroleum Corporation Coos Bay No. 1 (P-0112) and E. M. Warren Coos County 1-7 wells for the southern cross section (fig. 1). Biostratigraphic age determinations based upon a study of foraminifers found in strata penetrated in these wells were made by McKeel (1980) and by Rau (1973a) for the Warren 1-7 well. The first attempt to prepare a geologic cross section from the Oregon Coast Range westward to the abyssal plain, utilizing onshore detailed geologic mapping, 24-channel and single-channel seismic-reflection profiles, and subsurface stratigraphic information in the Standard Union Nautilus (P-0103) well, was published by Snively and others (1980b). A geologic interpretation of a 24-channel seismic-reflection profile on the Continental Shelf through the Shell P-087 well was extended onto the west flank of the Oregon Coast Range and tied to the Sinclair Federal-Mapleton well (Snively and others, 1981b).

The geologic history of the mid-Pacific mountains in the central north Pacific Ocean—A synthesis of Deep-Sea Drilling studies.

Thiede, Jrn, Dean, W. E., Rea, D. K., Vallier, T. L., and Adelseck, C. G., 1981, Deep Sea Drilling Project Initial Reports, v. 62, p. 1073-1120.

The Mid-Pacific Mountains constitute of the largest aseismic rises in the central North Pacific Ocean. They have been generated by mid-plate volcanic events prior to

Barremian time, but their volcanic activity continued through the remainder of the Cretaceous. Evidence of the latest stages of this volcanism are the trachytic ashes included in

mid- and Late Cretaceous sediments and the presence of guyots atop the main volcanic pedestal.

The thermal and volcanic history of the oldest part of the Pacific Plate and its plate tectonic movements since Cretaceous time have led to considerable horizontal and vertical movements of the Mid-Pacific Mountains. Reconstruction of their subsidence and evidence from the sediments from Site 463 suggest that they once, in Cretaceous time, constituted large, tropical volcanic islands which were covered by vegetation and which shed their erosional debris over the adjacent island slopes. Neritic fossils in Maastrichtian sediments document the presence of shoal areas until the end of the Mesozoic. Since then they have subsided to their present water depth. The horizontal movements of the Pacific Plate have carried the Mid-Pacific Mountains from a position well south of the Cretaceous equator to their present position under the unproductive surface waters of the subtropical central North Pacific Ocean. Site 463, on the western Mid-Pacific Mountains, probably crossed the equator in Maastrichtian time.

Shallow-water-derived calcareous fossils are incorporated into the pelagic sediments covering the Mid-Pacific Mountains. They have been displaced from their source areas along the flanks of seamounts over the adjacent

regions during times of low sea-level stands. Debris of land plants in Aptian sediments documents the presence of emergent volcanoes during that time.

The pelagic sediments penetrated at Site 463 consist largely of a sequence of Cretaceous chalks, limestones, and cherts which accumulated fast and which document the presence of highly productive surface water masses around the former volcanic islands and above the shoals. The development of oxygen-deficient depositional environments and the lack of evidence for intensive reworking suggest at the same time very sluggish water movements in the meso- and bathypelagic environment during Early and mid-Cretaceous times.

The Cenozoic calcareous oozes, on the other hand, are very condensed. They are interrupted in several places by hiatuses, and despite their position well above the CCD they show effects of dissolution and poor preservation of the calcareous faunas and floras. The frequency of reworked pelagic material together with the hiatuses indicate episodes of intensive renewal of the meso- and bathypelagic water masses which generated intensive sea-floor erosion and which were probably triggered by the climatic deterioration in the polar regions.

Earthquakes in the Orozco Transform Zone: seismicity, source mechanisms, and tectonics

Trehu, A. M., and Solomon, S. C., 1983, *Journal of Geophysical Research*, v. 88, No. B10, p. 8203-8225.

As part of the Rivera Ocean Seismic Experiment, a network of ocean bottom seismometers and hydrophones was deployed in order to determine the seismic characteristics of the Orozco transform fault in the central eastern Pacific. We present hypocentral locations and source mechanisms for 70 earthquakes recorded by this network. All epicenters are within the transform region of the Orozco Fracture Zone and clearly delineate the active plate boundary. About half of the epicenters define a narrow line of activity parallel to the spreading direction and situated along a deep topographic trough that forms the northern boundary of the transform zone (region 1). Most focal depths for these events are very shallow, within 4 km of the seafloor; several well-determined focal depths, however, are as great as 7 km. No shallowing of seismic activity is observed as the rise-transform intersection is approached; to the contrary, the deepest events are within 10 km of the intersection. First motion polarities for most of the earthquakes in region 1 are compatible with right-lateral strike slip faulting along a nearly vertical plane, striking parallel to the spreading direction. Another zone of activity is observed in the central part of the transform (region 2).

The apparent horizontal and vertical distribution of activity in this region is more scattered than in the first, and the first motion radiation patterns of these events do not appear to be compatible with any known fault mechanism. Pronounced lateral variations in crustal velocity structure are indicated for the transform region from refraction data and measurements of wave propagation directions. The effect of this lateral heterogeneity on hypocenters and fault plane solutions is evaluated by tracing rays through a three-dimensional velocity grid. While findings for events in region 1 are not significantly affected, in region 2, epicentral mislocations of up to 10 km and azimuthal deflections of up to 45° may result from assuming a laterally homogeneous velocity structure. When corrected for the effects of lateral heterogeneity, the epicenters and fault plane solutions for earthquakes in region 2 are compatible with predominantly normal faulting along a topographic trough trending NW-SE; the focal depths, however, are poorly constrained. These results suggest an echelon spreading center or leaky transform regime in the central transform region.

Upper Cretaceous subsurface stratigraphy and structure of coastal Georgia and South Carolina

Valentine, P. C., 1982, U.S. Geological Survey Professional Paper 1222, 22 p.

Upper Cretaceous subsurface stratigraphy and structure of coastal Georgia and South Carolina is based on the study of 24 wells along two transects, one extending across the seaward-dipping sedimentary basin termed the "Southeast Georgia Embayment" northeastward to the crest of the Cape Fear Arch, and the other aligned east-west, parallel to the basin axis and including the COST GE-1 well on the Outer Continental Shelf. A new biostratigraphic analysis, using calcareous nannofossils, of the Fripp Island, S. C., well and reinterpretations of the Clubhouse Crossroads corehole 1, South Carolina, and other wells in South Carolina, Georgia, and northernmost Florida have made possible the comparison and reevaluation of stratigraphic interpretations of the region made by G. S. Gohn and others in 1978 and 1980 and by P. M. Brown and others in 1979. The present study indicates that within the upper Cretaceous section the stratigraphic units formerly assigned a Cenomanian (Eaglefordian

and Woodbinian) age are Coniacian (Austinian) and Turonian (Eaglefordian) in age. A previously described hiatus encompassing Coniacian and Turonian time is not present. More likely, a hiatus is probably present in the upper Turonian, and major gaps in the record are present within the Cenomanian and between the Upper Cretaceous and the pre-Cretaceous basement.

After an erosional episode in Cenomanian time that affected the section beneath eastern Georgia and South Carolina, Upper Cretaceous marine clastic and carbonate rocks were deposited on a regionally subsiding margin that extended to the present Blake Escarpment. In contrast, during Cenozoic time, especially in the Eocene, subsidence and sedimentation rates were uneven across the margin. A thick progradational sequence of carbonate rocks accumulated in the Southeast Georgia Embayment and also built the present Continental Shelf, whereas farther offshore

a much thinner layer of sediments was deposited on the Blake Plateau.

There is no general agreement on the exact placement of the Cenomanian-Turonian boundary in Europe or the United States Western Interior, and the widespread *Sciponoceras gracile* ammonite zone represents an interval of equivocal age between accepted Cenomanian and Turonian strata. The extinction of the foraminifer genus *Rotalipora* took place within the *Sciponoceras gracile* zone; it is used here to identify to Cenomanian-Turonian boundary.

Geologic evolution of Hess Rise, central north Pacific Ocean

Vallier, T. L., Dean, W. E., Rea, D. K., Thiede, Jörn, 1983, Geological Society of America Bulletin, v. 94, p. 1289-1307.

Cores from four Deep Sea Drilling Project (DSDP) sites (310, 464, 465, and 466) and seismic-reflection profiles provide data that are used to interpret the geological evolution and paleoenvironments of Hess Rise, a prominent oceanic plateau in the central North Pacific Ocean. Hess Rise apparently formed in the Southern Hemisphere along the western flank of the Pacific-Farallon Ridge 110 to 100 m.y.B.P. Core stratigraphies and lithologies show the response of sedimentation to subsidence and northward movement of Hess Rise on the Pacific Plate. Oceanic islands, which crowned Hess Rise during its early evolution, were eroded and subsequently subsided below sea level.

Major structural trends include three northwest-trending (327°) arms, or ridges, and an east-northeast-trending southern Hess Rise that parallels the Mendocino Fracture Zone (060°). Normal faults offset basement as much as 3,000 m along the southern edge and 1,500 m on the western flank of Hess Rise. Many faults were active during sedimentation.

Tholeiitic basalt from the base of Hole 464, trachyte from the base of Hole 465A, and alkalic basalt clasts within

Pollen zone IV (*Complexiopollis-Atlantopolis* assemblage zone) is an important and widespread biostratigraphic unit characterized by a distinctive spore and pollen flora. It is consistently associated with lower Turonian calcareous nannofossils on the Atlantic continental margin; these nannofossil assemblages are also present in pollen zone IV, in strata that encompass the *Sciponoceras gracile* zone and the lower part of the *Mytiloides labiatus* zone in the Gulf Coastal Plain at Dallas, Tex.

sediment of Hole 466 show the diversity of rock types that constitute the igneous basement. A major rock unit is middle Cretaceous limestone, chalk and minor chert that form the basal sedimentary unit. Some limestone samples, rich in organic carbon, reflect accumulation above the carbonate compensation depth (CCD) within a mid-water oxygen minimum zone. The organic-carbon-rich sediments probably were deposited on the submarine slopes of islands and banks that were at upper bathyal depths as Hess Rise crossed the wide equatorial divergence where increased upwelling and biogenic productivity contributed to high accumulation rates. The source of organic matter was mostly lipid-rich, autochthonous, marine organic matter.

Analyses of sediment samples from across the Cretaceous-Tertiary boundary at Site 465 show that there was a significant decrease in surface water temperature and biological productivity. An abrupt increase in transition metals and iridium suggest that an outside source, perhaps extraterrestrial, was the cause for many of the sudden oceanographic, geochemical, and biological changes at the boundary.

Volcanogenic sediments from Hess Rise and the mid-Pacific mountains, Deep Sea Drilling Project Leg 62

Vallier, T. L., and Jefferson, W. S., 1981, Deep Sea Drilling Project Initial Reports, v. 62, p. 545-557.

Volcanogenic sediments are most abundant in the Cretaceous sequences of the holes drilled during Deep Sea Drilling Project Leg 62. Volcanic contributions to the Cenozoic sequences are rare. Volumetrically significant volcanogenic sediments are in the Barremian-Aptian, upper Albian-lower Cenomanian, and Campanian-Maastrichtian intervals. The major volcanic events responsible for accumulation of Cretaceous volcanogenic sediments at Leg

62 sites probably were also responsible for volcanogenic components at other sites in the western Pacific, particularly on the Ontong-Java and Manihiki Plateaus and Horizon Guyot, and along the Line Island chain. Volcanism apparently was related both to the early formation of these rises and plateaus at mid-ocean ridges and to later intraplate tectonism.

Stratigraphy, sedimentation, and tectonic accretion of exotic terranes, southern Coast Ranges, California

Vedder, J. G., Howell, D. G., and McLean, Hugh, in Watkins, J. S., and Drakes, C. L., eds., 1983, Studies in continental margin geology: American Association of Petroleum Geologists Memoir 34, p. 471-496.

The southern Coast Ranges west of the San Andreas fault consist of two composite tectono-stratigraphic terranes. Paleomagnetic and geologic relations indicate that pre-early Eocene rocks in both terranes are allochthonous to the California region, and Late Cretaceous to early Eocene northward drift of 1,500 km is suspected. Basement rocks of the Salinian composite terrane are composed of middle Cretaceous granite plutons and older high-temperature meta-sedimentary rocks. The Salinian composite terrane is bordered on the west by the Sur-Obispo composite terrane, which includes a melange of the Franciscan assemblage (San Simeon terrane) that is structurally overlain by a Middle Jurassic ophiolite and Upper Jurassic and Cretaceous forearc basin strata (Stanley Mountain terrane). Along the east edge

of the Sur-Obispo composite terrane, an upper Campanian to lower Maastrichtian fluvio-deltaic sequence containing 102-m.y.-old to 126-m.y.-old granitic boulders lends credence to the postulated suturing of these two terranes in Late Cretaceous time. A regional unconformity that developed some time in the span of middle(?) Paleocene to early(?) Eocene time apparently crosses both terranes. We suggest that an allochthon composed of the Sur-Obispo and Salinian composite terranes, as well as other terranes, was accreted to the southern California region in latest Paleocene or earliest Eocene time. The hypothetical Santa Lucia-Orocopia allochthon (new name) represents the amalgamated composite of these mutually exotic terranes.

Igneous evolution of Hess Rise: petrologic evidence from DSDP Leg 62

Windom, K. E., Seifert, K. E., and Vallier, T. L., 1981, *Journal of Geophysical Research*, v. 86, no. B7, p. 6311-6322.

Igneous rock was recovered at three sites on Hess Rise, north-central Pacific Ocean, during Deep Sea Drilling Project leg 62: tholeiitic basalt at site 464 (northern Hess Rise), trachyte at site 465, and rounded clasts of alkalic basalt at site 466 (both on southern Hess Rise). The depths at which the igneous rocks from sites 464 and 465 were recovered correspond to strong acoustic reflectors, whereas the clasts from site 466 were recovered from within calcareous sediment. Although all the rocks are moderately to highly altered, petrographic and chemical studies, especially rare earth element determinations, provide data on the nature of these rocks. Data from these studies, combined with geophysical models of the evolution of the Pacific plate

during the Mesozoic, allow an interpretation of the formation of Hess Rise involving building of a volcanic platform by eruption of tholeiitic mid-oceanic ridge basalt caused by the breakup of a R-R-R-type triple junction during the middle Cretaceous. This period of platform building was accompanied by edifice building along the south edge of Hess Rise involving alkalic basalt and its differentiation products associated with a leaky transform fault. This interpretation agrees with proposed models for the origin of the tholeiitic parts of other oceanic plateaus but requires a different mechanism—namely, volcanism associated with leaky transform faults—to account for the alkalic rocks.

Geology of central Lake Michigan

Wold, R. J., Paull, R. A., Wolosin, C. A., and Friedel, R. J., 1981, *American Association of Petroleum Geologists Bulletin*, v. 65, no. 9, p. 1621-1632.

The geology beneath Lake Michigan between 43°00' and 44°00'N and between 86°30' and 87°40'W is interpreted from a synthesis of 1700 km of continuous seismic reflection profile data, bathymetry, grab samples, and onshore surface and subsurface information.

The continuous seismic reflection profiles and bathymetry provided information for maps of unconsolidated sediment thickness and Paleozoic bedrock topography. The map of unconsolidated sediment (primarily Pleistocene) shows thicknesses ranging from 180 m in a steep-walled, northeast-trending valley to less than 10 m over a mid-lake topographic high. This valley and the mid-lake high are the dominant topographic features developed on the gently eastward-dipping Paleozoic rocks along this part of the western flank of the Michigan basin.

Two structural-stratigraphic cross sections of the study area were constructed by utilizing a composite subsurface-surface section for eastern Wisconsin and two

control wells in western Michigan. The cross sections, grab samples previously described in the literature, the bedrock topographic map, and published maps were used to construct a Paleozoic geologic map for central Lake Michigan. Rocks from Middle Silurian through Early Mississippian age form subcrops beneath the study area, whereas rocks of Early Silurian, Ordovician, and Late Cambrian age are present at greater depth. The Upper Cambrian rocks unconformably overlie Precambrian igneous and metamorphic rocks.

The structural-stratigraphic cross sections also allow us to speculate about the petroleum potential beneath Lake Michigan. The possibility of oil occurrences within the Silurian is enhanced by major east-west facies changes, and other horizons with promise are present in Devonian and Ordovician rocks. Although Michigan and Wisconsin laws currently prohibit petroleum exploration in Lake Michigan, it is an area with future potential.

MARINE DEPOSITS AND SEDIMENTARY DYNAMICS

Ice rafting of fine-grained sediment, a sorting and transport mechanism, Beaufort Sea, Alaska

Barnes, P. W., Reimnitz, Erk, and Fox, Dennis, 1982, *Journal of Sedimentary Petrology*, v. 52, no. 2, p. 493-502.

The presence of turbid, sediment-rich fast ice in the Arctic is a major factor affecting transport of fine-grained sediment. Turbid ice was found to be present in a zone 10 to 20 km wide along the coast of the Beaufort Sea. Sediment concentrations observed in cores taken in seasonal fast ice ranged from 3 to more than 1,600 g/m³. Finely disseminated silt and clay-sized particles dominated, discoloring the upper segments of the cores in a layer up to 1 m thick. In almost all of the cores the uppermost 10 cm of ice was relatively less turbid, and the relief at the base of the turbid layer was 10 to 20 cm over distances of 1 to 2 m. Observers have documented the widespread, sporadic occurrence of sediment-rich fast ice in both the Beaufort and Bering Seas. The known sources and transport relations of suspended sediment did not explain this distribution of turbid ice.

The occurrence of sediment in only the upper part of

the seasonal fast ice indicates that sediment-rich ice forms early during ice growth. The most likely mechanism for the formation of sediment-laden ice and preferential sorting of fine sediments requires resuspension of nearshore bottom sediment during storms, accompanied by formation of frazil ice and subsequent lateral advection before the fast ice is stabilized.

We estimate that the sediment incorporated in the Beaufort ice canopy formed a significant proportion of the seasonal influx of terrigenous fine-grained sediment. The dominance of fine-grained sediment suggests that in the Arctic and sub-Arctic these size fractions may be ice rafted in greater volumes than the coarse fractions of traditionally recognized ice-rafted sediment. The incorporation and transport mechanism may be a significant factor in the transport of fine-grained sediments in the Arctic basin.

Temporal and spatial variations in suspended matter in continental shelf and slope waters off the north-eastern United States

Bothner, M. H., Parmenter C. M., and Milliman, J. D., 1981, *Estuarine, Coastal and Shelf Science*, v. 13, p. 213-234.

Seston in waters of Georges Bank originates primarily from biological production and from resuspension of bottom sediments. The concentrations of suspended matter observed on the central shoals are more influenced by storms than by seasonal changes. Winter storms produce highest concentrations of non-combustible material throughout the water column, and summer storms appear to increase biological production by mixing additional nutrients into the photic zone. On the south-east flank of the bank, in water depths between 80 and 200 m, the concentrations of total suspended matter and non-combustible material show little variation compared with the central shoals, and storm effects are far less noticeable.

Highest concentrations (15 mg l⁻¹) of suspended matter occur in bottom waters south of Nantucket Island after winter storms and appear to be primarily resuspended bottom sediment. Resuspended sediment is also common in near-bottom waters of the south-western Gulf of Maine, and occasionally near the intersection of the shelf/slope water mass front and the bottom.

Seasonal variations were observed in the distribution and species composition of phytoplankton. Coccoliths are predominant on the central bank during the winter, but during the spring and summer they are concentrated on the eastern flank at deeper depths.

Geochemical evidence for modern sediment accumulation on the continental shelf off southern New England

Bothner, M. H., Spiker, E. C., Johnson, P. P., Rendigs, R. R., and Aruscavage, P. J., 1981, *Journal of Sedimentary Petrology*, v. 51, no. 1, p. 281-292.

An area of fine-grained sediment approximately 170 km x 74 km in size, located in water depths between 60 m and 150 m, south of Martha's Vineyard, Mass., is a site of modern sediment deposition. The ¹⁴C ages systematically increase with sediment depth from about 1,300 years B.P. at the surface to 8,000-10,000 years B.P. at the depth of maximum core penetration. The old age for the surface sediments probably results from a combination of deposition of old carbon and faunal mixing. In the finest sediments, the sedimentation rates were approximately 130 cm/1,000 yrs when deposition began and have decreased to about 25 cm/1,000 yrs. The decreasing sedimentation rate reflects a diminishing source of fine sediments, which presumably came from the Georges Bank and Nantucket Shoals area.

Inventories of excess ²¹⁰Pb in undisturbed cores average 70 dpm/cm² (disintegrations per minute per square centimeter), more than two times higher than the flux of ²¹⁰Pb from the atmosphere and from ²²⁶Ra decay in the

overlying water. This additional influx of ²¹⁰Pb either must be with new fine-grained sediment material or from solutions that are stripped of their ²¹⁰Pb by particulates in the bottom nepheloid layer. Stable Pb concentrations in surface sediments are about 28 ppm, as much as two times higher than concentrations at depth.

The high accumulation rates, ²¹⁰Pb inventories, and trace-metal profiles imply that this area is a modern sink for fine-grained sediments and for pollutants associated with particulate matter in the water column. To our knowledge, this is the only site of present-day natural deposition on the Continental Shelf off the eastern United States, exclusive of the Gulf of Maine. Because the net currents on the outer half of this Continental Shelf flow from northeast to southwest, this fine-grained deposit may receive its sediments and possible contaminants from the Nantucket Shoals and Georges Bank regions.

Depositional sequences in clastic continental slope deposits, Gulf of Mexico

Bouma, A. H., 1981, *Geo-Marine Letters*, v. 1, p. 115-121.

Tertiary and Quaternary sediments, overlying diapiric older Tertiary shales and Louann Salt on the continental slope in the western Gulf of Mexico, show cyclicity based on seismic-reflection patterns. A set of indistinct parallel reflections or an acoustically semi-transparent zone, normally overlapping onto diapiric flanks, alternates with a set of distinct parallel reflections that drape the sea bottom. The indistinct

reflections represent deposits emplaced by bottom transport during a lowering of sea level. Sea level rise and high stand are characterized by hemipelagic sediments that form blanket-type deposits. Differential sediment loading causes diapiric activity that may reach maximum upward velocities when sea level rises.

Low frequency current and bottom-pressure variability

Brink, K. K., Magnell, B. A., and Noble, M. A., in press, Chap. 4.5 in Backus, Dean, ed., *The Georges Bank Book*.

An attempt is made to summarize the present observational and theoretical understanding of low-frequency velocity and bottom pressure fluctuations over and around Georges Bank. We define the low-frequency band as the range of periods from about two to thirty days. Generally, the low-frequency current ellipses are oriented such that the strongest flow component tends to parallel the isobaths. Current fluctuations tend to be weakest over the Bank top, and stronger near the Bank edges. Although alongbank currents are often coherent with each other along a given flank of the Bank, Bank-wide coherence in currents is generally lacking. In contrast, bottom pressure fluctuations are extremely

coherent over the entire Gulf of Maine-Georges Bank region, and are clearly driven by local meteorological forcing. Wind-driven currents over the Bank appear to be related to this regional pressure response. Current and pressure variability is much greater in winter than summer, qualitatively in accord with seasonal changes in wind variability.

The few available theoretical models of the region deal primarily with wind-driving of current and pressure variability. Apparently, the regional models, which treat Georges Bank in its larger geographical setting, will prove the most successful to accounting for forced motions.

Recent observations of the mean circulation on Georges Bank

Butman, Bradford, Beardsley, R. C., Magnell, B. A., Frye, D., Vermersch, J. A., Schlitz, R., Limeburner, R., Wright, W. R., and Noble, M. A., 1982, *Journal of Physical Oceanography*, v. 12, no. 6, p. 569-591.

A clockwise circulation around Georges Bank was measured by means of moored current meters, aircraft-tracked surface drifters, and satellite-tracked drifters drogued at 10 m. The strongest flow was in a narrow jetlike current (30 cm s^{-1}) along the northern flank of the bank. The flow of shelf water on the southern flank was westward (20 cm s^{-1}) toward the Middle Atlantic Bight; some of this water

flowed northward through the eastern side of Great South Channel and recirculated around Georges Bank. The satellite-tracked drifters and the moored observations indicate that the circulation around the bank was not completely closed and considerable variability occurs in the trajectory of an individual water particle.

Measurements of storm-generated bottom stresses on the continental shelf

Cacchione, D. A., and Drake, D. E., 1982, *Journal of Geophysical Research*, v. 87, no. C3, p. 1952-1960.

Large values of bottom friction velocity, \bar{u}^* , and roughness length, \bar{z}_0 , determined from burst-averaged speed data taken on the continental shelf in outer Norton Sound, Alaska, with the GEOPROBE tripod during a storm in September 1977 are correlated with extremely large values of near-bottom concentration of total suspended particulate matter (TSM). Combined wind-driven and tidal currents exceeding 30 cm/s at 1 m above the bottom and intense oscillatory bottom currents with maxima above 45 cm/s were associated with the largest measured values of TSM at 2 m above the sea floor. The values of \bar{u}^* and \bar{z}_0 obtained from the 'law of the wall' velocity-depth relationship are diminished substantially throughout the storm period (average

reduction of 44%) when the turbulence-reducing effects of the vertical concentration gradient of TSM are considered. The form of the latter correction was adapted from Smith and McLean (1977a). Values of the mean \bar{u}^* computed from the theory of Grant and Madsen (1979), which predicts an enhanced shear stress due to nonlinear wave-current interactions, compare favorably with the \bar{u}^* values determined from the measured velocity profiles. The measured values of \bar{z}_0 , however, are considerably larger than any of the estimates based on (1) the actual scales of the physical roughness elements; (2) the apparent roughness of Grant and Madsen (1979); or (3) the thickness of the bed-load layer as formulated by Smith and McLean (1977a).

Rippled scour depressions on the inner continental shelf off central California

Cacchione, D. A., Drake, D. E., Grant, W. D., and Tate, G. B., in press, *Journal of Sedimentary Petrology*.

Side-scan sonar records taken during the recent Coastal Ocean Dynamics Experiment (CODE) show elongate, shore-normal rippled depressions of low relief on the inner conti-

mental shelf off central California between Bodega Bay and Point Arena. These features extend up to 2 kilometers from the coast into water depths to 65 meters. The proposed

mechanism for their generation is storm-generated bottom currents associated with coastal downwelling during the late fall and winter which scour the surficial fine sand sediment and expose the coarser sand substrate in the depressions. The zones of most intense erosion and the irregular spacing of the

features may be controlled by submerged rock ledges and other prominent coastal features. The large straight-crested ripples within the depressions (heights to 40 cm; wavelengths to 1.7 m) are probably formed by large-amplitude, long-period surface waves generated by winter storms.

Velocity and bottom-stress measurements in the bottom boundary layer, outer Norton Sound, Alaska

Cacchione, D. A., Drake, D. E., and Wiberg, Patricia, 1982, in Nelson, C. H., and Nio, S. D., eds., The northeastern Bering shelf: new perspectives of epicontinental shelf processes and depositional products: *Geologie en Mijnbouw*, v. 61, p. 71-78.

We have used long-term measurements of near-bottom velocities at four heights above the sea floor in Norton Sound, Alaska, to compute hourly values of shear velocity u^* , roughness z_0 , and bottom-drag coefficient c_D . Maximum sediment resuspension and transport, predicted for periods when the computed value of u^* exceeds a critical level, occur during peak tidal currents associated with spring tides. The fort-

nightly variation in u^* is correlated with a distinct nepheloid layer that intensifies and thickens during spring tides and diminishes and thins during neap tides. The passage of a storm near the end of the experiment caused significantly higher u^* values than those found during fair weather. We attribute these increases in u^* to stronger bottom currents and larger surface waves.

Submarine valleys in the northeastern Gulf of Alaska: characteristics and probable origin

Carlson, P. R., Bruns, T. R., Molnia, B. F., and Schwab, W. C., 1982, *Marine Geology*, v. 47, p. 217-242.

The continental shelf of northeastern Gulf of Alaska between Prince William Sound and Cross Sound is cut by at least eight major valleys. From west to east, these are Hinchinbrook Seavally, Egg Island Trough, Kayak Trough, Bering Trough, Pamplona Troughs, Yakutat Valley, Alsek Valley and Yakobi Valley. Evidence common to most of these troughs or valleys indicating that the present morphology is due to glacial processes includes: (1) a pre-Holocene sub-bottom erosional surface incised into the underlying lithified strata of the shelf; (2) U-shaped cross sections, both at the sea floor and at the pre-Holocene erosional surface; (3) concave longitudinal sections, commonly shoaling at the seaward end; (4) till-like sediments collected from the walls or outer shelf adjacent to the troughs; and (5) seismic stratig-

raphy that can be correlated with bottom samples indicative of glacially derived strata.

Depressions with tens of meters of relief are present on the pre-Holocene subbottom erosional surface beneath most of these valleys. These depressions have been partially filled by a seaward-thinning wedge of Holocene glacial flour (clayey silt) that is filling the valleys and blanketing the inner shelf at rates as high as 15 mm/yr (based on ^{210}Pb measurements). Although glaciation played a dominant role in the modern morphology of these sea valleys, structural features, including structurally controlled topographic highs on the shelf (e.g., Tarr Bank, Kayak Island, Pamplona Spur and Fairweather Ground) influence the flow directions of the glacial lobes.

Discrimination between subtidal and intertidal facies in Pleistocene deposits, Willapa Bay, Washington

Clifton, H. E., 1983, *Journal of Sedimentary Petrology*, v. 53, no. 2, p. 353-369.

Sea cliffs on the north, west, and south sides of Willapa Bay, Washington, present excellent exposures of Pleistocene estuary deposits. Analysis of these deposits and comparison of them with modern facies in Willapa Bay indicate that a primary key to their interpretation is the delineation of stillstand units—that is, shallowing-upwards bodies of sediment deposited at a particular stand of the sea. Once identified, these units provide a basis for studying both vertical sequences and lateral trends as well as identifying the effects of tectonic deformation.

To recognize a stillstand unit, one must infer the relative water depth represented by successive facies or deposits. This inference in turn requires a distinction between intertidal and subtidal facies. In the analysis of the Willapa Bay deposits, a set of criteria for this distinction, derived largely from characteristics of modern facies in the bay, proved useful.

Criteria for identifying deposits as subtidal include the presence of 1) abundant *Ostrea lurida* in growth position; 2)

units of included strata more than 2 m thick; (3) laterally persistent lag deposits; 4) laterally persistent thin layers of mud; 5) medium- to large-scale crossbedding; 6) directionally uniform crossbedding and ripple lamination; and 7) assemblages of predominantly concave-up shells and shell fragments. Of these criteria the first is diagnostic of subtidal facies; the others are characteristic but not necessarily diagnostic of this environment. In association, however, the characteristic features provide generally adequate evidence for the indicated facies.

Criteria for recognizing intertidal deposits include the presence of 1) root or rhizome structures; 2) evidence of runoff channels; 3) regular lamination characteristic of supratidal deposits; 4) supratidal bluff breccia; and 5) vertical sequences in which upper accretionary bank deposits underlie those of the tide flat, which in turn underlie supratidal deposits. Some of these (root or rhizome structures) are probably diagnostic of an intertidal facies; the others are characteristic of such a facies.

Spilled oil and infaunal activity—modification of burrowing behavior and redistribution of oil

Clifton, H. E., Kvenvolden, K. A., and Rapp, J. B., 1984, *Marine Environmental Research*, v. 11, p. 111-136.

A series of experiments in Willapa Bay, Washington, indicates the degree to which the presence of spilled oil

modifies the burrowing behavior of infauna and the extent to which the animals redistribute oil into intertidal sediment.

Small amounts of North Slope crude oil introduced at low tide directly into burrow openings (mostly made by the crustacean *Callianassa*) resulted in a limited and temporary reduction in the number of burrow openings. In contrast, a layer of oil-saturated sand 1 cm thick buried about 5 cm below the sediment surface sharply reduced the number of burrow openings. After a year, the few new burrows penetrated only the margins of the experimental plot, and bioturbation below the buried oil-saturated sand layer declined dramatically.

The experiments suggest that small amounts of oil temporarily stranded by tides in themselves have no long-range effect on burrowing behavior. The fauna, however, are capable of introducing measurable amounts of oil into the subsurface, where it is retained long after the rest of the

stranded oil has washed away. A buried layer of oil-saturated sand greatly reduces infaunal activity; the oil presents an effective barrier that can persist for years.

The oil incorporated into the sediment from burrow openings showed evidence of degradation after 7 months. In contrast, the layer of buried oil remained essentially undegraded after a period of two years, even though oil in lower concentrations above the layer was degraded after a period of one year. This variation in degree of degradation of the buried oil, as well as the heterogeneity of oil distribution wherever the oil has been incorporated from the surface, emphasizes the importance of careful sampling in any attempt to locate or monitor the presence of spilled oil in the substrate.

Stability of a very coarse-grained beach at Carmel, California

Dingler, J. R., 1981, *Marine Geology*, v. 44, p. 241-252.

Monastery Beach at Carmel, California, is a pocket beach composed of very coarse to granular sediment. In profile, the beach has a well-defined berm crest; a steep foreshore; and a gently sloping, barless offshore covered by large, long-crested oscillation ripples. Carmel Submarine Canyon heads a few hundred meters offshore of the beach, and San Jose Creek, a small ephemeral stream, ponds onshore of the central part of the berm. Wave conditions vary greatly during a year because the beach lies open to the Pacific Ocean for azimuths between 270°-322°N whence come a variety of wave types. Even with a variable wave climate, Monastery Beach has maintained a swell profile for almost three years.

Aperiodic beach surveys show that the beach responds little to seasonal changes in wave climate. Four survey lines maintained the same swell profile throughout the study

period. The fifth line maintained a stable profile only across the foreshore; the berm was twice artificially breached during storms to prevent upstream flooding along San Jose Creek. In comparison, Carmel Beach, a nearby beach composed of medium sand, commonly alternates between swell and storm profiles. The increased stability of Monastery Beach relative to Carmel Beach is attributed to two factors: grain size differences and location within Carmel Bay.

Rebuilding proceeded very slowly along the breached part of the berm at Monastery Beach. The probable cause of such a low recovery rate is that oscillation ripples trapped the sand that was carried offshore when San Jose Creek eroded the beach. The ripples, which are active under high-energy conditions, approach dormancy under low-energy conditions. Each ripple, therefore, acts like a reservoir, retaining sand during most swell conditions.

Sand movement into Carmel Submarine Canyon, California

Dingler, J. R., and Anima, R. J., 1982, in *Proceedings, 18th Coastal Engineering Conference, ASCE/Cape Town, South Africa*, p. 1268-1287.

Carmel Submarine Canyon heads in shallow water near Monastery Beach at the southeast corner of Carmel Bay, California, U.S.A. Very coarse sand, shaped into large oscillation ripples, covers the narrow shelf between the beach and the canyon; when this sand enters the canyon head, it lies at angles as great as the angle of repose. In some areas, these sand slopes show evidence of active grain flows in the form of downslope-coarsening, inversely graded deposits.

The results of a dyed-sand tracer study adjacent to the canyon show that sand moved canyonward during the summer of 1979. Initially the dyed sand, which had been shaped into an oscillation ripple in the center of a 20-m by 60-m grid, moved offshore en masse. After a few days, though, the dyed sand dispersed with the center of mass moving canyonward.

As wave-transported sand accumulates along the canyon rim, the upper slopes oversteepen, thereby causing

some of the sand to avalanche downslope. Systematic changes in sand levels along three lines of rods over 15 months document preferential deposition of sand along the upper slopes; the greatest change occurred at the top of the lines (12-15 m depth) and the least at the bottom (30-40 m). Greater accretion during the spring months than during the summer months probably reflects the more energetic spring-time wave climate.

Between October 1981 and October 1982, 5.7 m³ of sand was deposited per meter alongslope on the middle line, which gives a calculated depositional rate of approximately 500 m³/yr in the study area. Although we have monitored this area for over a year, we have not yet documented any large-scale events capable of flushing sand out of the canyon head. The only erosive event we have observed was a small grain flow we generated while digging on the slope.

Seasonal variation in sediment transport on the Russian River Shelf, California

Drake, D. E., and Cacchione, D. A., in press, *Continental Shelf Research*.

Near-bottom currents, light transmission and scattering, and bottom pressure were measured with GEOPROBE tripods and vector-averaging current meters during June 1979 to April 1980 on the central shelf 10 km west of the Russian River, California. The instruments were located on the mid-shelf mud belt composed of bimodal sandy clayey silts contributed principally by the Russian River. During the summer

season of persistent northwesterly, upwelling-favorable winds, the average and maximum current speeds 5 m above the bottom were 11 cm/s and 31 cm/s, respectively. The mean (subtidal) flow at 5 m above bottom was poleward and slightly offshore at about 6 cm/s. The strongest wave-generated bottom currents were about 10 cm/s, but oscillatory velocities 5 cm/s were infrequent. Suspended-matter

concentrations, derived from the optical data at 1.9 m above the bottom, ranged from 1 to 6 mg/l. The optical data show that the currents and waves were generally below threshold levels for sediment erosion through the summer. In contrast, during the fall and, particularly, the winter months, the average and maximum concentrations of suspended matter increased substantially. The increases were primarily caused by larger waves from distant storms and short intervals of strong currents associated with local storms and, secondarily, by the large seasonal flow of the Russian River. Wind-driven and wave-generated bottom currents were as large as 37 cm/s and 45 cm/s, respectively, during local storms in December 1979 and February 1980. Suspended-matter concentrations averaged about 7 mg/l during non-storm winter periods, but increased to nearly 150 mg/l during a December storm.

Bottom currents and sediment transport on San Pedro shelf, California

Drake, D. E., Cacchione, D. A., and Karl, H. A., in press, *Journal of Sedimentary Petrology*.

GEOPROBE tripods were used to measure bottom currents, pressure, and light transmission and scattering and to obtain time-series photographs of the sea floor at depths of 23 m and 67 m on San Pedro shelf between 18 April and 6 June 1978. The shallower tripod was located on a patch of relict medium sand and the deeper tripod was at the shelf edge on a mixed (modern and relict) silty, very fine sand.

Winds were light (8 m/s) with a mean direction from the southwest throughout the measurement period. Hourly-averaged currents one meter above the bottom never exceeded 21 cm/s, average speeds were about 5 cm/s at the 23 m site and 6.8 cm/s at 67 m, and the strongest, low-frequency currents were produced by the tides. The mean flow of bottom water was 3 cm/s at both GEOPROBE and was rather persistently southward (offshelf). Wave-generated bottom currents and bottom pressure variations were sampled at hourly intervals; average wave period and wave height were 12.8 s and 0.4 m, respectively, at the 23 m site. Wave orbital velocities ranged from about 5 to 30 cm/s at 23 m and from 2 to 9 cm/s at 67 m.

An Arctic kelp community in the Alaskan Beaufort Sea

Dunton, K. H., Reimnitz, Erk, and Schonberg, Susan, 1982, *Arctic*, v. 35, no. 4, p. 465-484.

The discovery of the "Boulder Patch", an area of cobbles and boulders with attached kelp and invertebrate life, is reported from Stefansson Sound, near Prudhoe Bay, Alaska. Geophysical surveys using side-scan sonar and low-frequency recording fathometers reveal that cobbles and boulders occur in patches of various sizes and densities. Despite a seasonal influx of sediments, the Boulder Patch is a nondepositional environment. Physical disruption of cobbles and boulders by deep draft ice is minimal due to offshore islands and shoals which restrict the passage of large ice floes into Stefansson Sound. The apparent absence of similar concentrations of rocks with attached biota along the Alaskan Beaufort Sea coast is explained by the scarcity of rocks in areas protected from ice abrasion and with no net sediment deposition. In Stefansson Sound, the rocks provide a substratum for a diverse assortment of invertebrates and several species of algae.

Bioturbation in a dysaerobic, bathyal basin: California Borderland

Edwards, B. D., in press, in Curran, H. A., ed., *Biogenic structures: their use in interpreting depositional environments: Society of Economic Paleontologists and Mineralogists Special Publication*.

Oxygen-deficient waters at the bathyal depths of the Santa Cruz Basin in the California Continental Borderland

Estimates of suspended-matter flux near the bottom show that the local winter storms, which had a combined duration of about 12 days, could account for 30-50% of the total annual suspended-sediment transport at the mid-shelf site. Although intervals of large swell from distant storms were at times superimposed on southward advective currents, the major sediment-transport events were caused by strong southerly winds that produced poleward bottom currents with a significant offshore component. The primary aspects of the distribution of modern sediments on this shelf are in good agreement with the observed poleward transport. However, a large accumulation of mud on the central shelf to the south of the Russian River may be supplied by particles settling from wind-driven surface plumes during the winter and spring seasons.

Bottom photographs at 67 m show that the relatively sluggish tide-generated and mean currents were below threshold velocity for the silty, very fine sand throughout the observational period. Threshold depth for wave rippling of very fine sand averaged about 28 m with a range from about 12 m to 50 m. Wave-generated currents were the only currents that exceeded threshold levels. The wave currents maintained relatively high concentrations of sediment in suspension near the bottom over the inner shelf (25 m) and this material (principally silt and clay) was transported offshore by the weak mean flow. Between about 20 m and 35 m 50-70% of this material was deposited as the bottom orbital velocities decreased to sub-threshold values (10-15 cm/s). The observed movement of fine sediment across the inner shelf can account for a portion of the mud content of the modern silty sands on the central shelf and on the outer shelf. However, it is clear that the sand fractions, which constitute 70% of the central shelf substrate, must be transported during high energy winter storms.

Recolonization by the biota was minimal on twelve boulders denuded and then left undisturbed for a three-year period. Sedimentation and grazing activity appear to be the major factors inhibiting recolonization. Linear growth in the kelp, *Laminaria solidungula*, is greatest in winter and early spring when nutrients are available for new tissue growth. The plant draws on stored food reserves to complete over 90% of its annual linear growth during the nine months of darkness under a turbid ice canopy. These reserves are accumulated by photosynthetic activity during the preceding summer. The total carbon contribution made by kelp in Stefansson Sound under these conditions is about 146×10^9 g yr⁻¹ or $7 \text{ g m}^{-2} \text{ yr}^{-1}$. A small percentage of this carbon is consumed directly by herbivores, but its importance to other organisms is not known and is under investigation.

provide harsh conditions for marine life. A feeding strategy approach is used for descriptions of the life habits (i.e., the

organism's motility and its living position with respect to the substrate) of benthic fauna intended to provide insight into how these organisms disrupt slope and basin floor sediment. Washes of sediment recovered by box corers show that the basin supports a surprisingly high density and diversity of benthic macrofauna. In contrast, however, biogenic sedimentary structures preserved in the sediment are low in density and diversity. Furthermore, bottom photographs taken at 117 stations reveal a biogenically produced microhummocky topography with few resolvable biogenic traces.

Recognizable biogenic traces are of three main classes: tracks and trails, depressions, and fecal matter. Echinoderms, the most abundant epifauna on the slope and adjacent basin floor, produce most of the large tracks and trails. Significantly, because of the soft, soupy nature of the surficial bathyal sediment, many tracks and trails there are less distinct than similar markings found in abyssal depths. Depressions made by asteroids, regular echinoids, and bottom dwelling fish are most common at moderate depths (800 m).

Bottom-water observations in the Vema fracture zone

Eitrem, S. L., Biscaye, P. E., and Jacobs, S. S., 1983, *Journal of Geophysical Research*, v. 88, no. C4, p. 2609-2614.

The Vema fracture zone trough, at 11°N between 41° and 45°E, is open to the west at the 5000-m level but is silled at the 4650-m level on the east where it intersects the axis of the Mid-Atlantic Ridge. The trough is filled with Antarctic Bottom Water (AABW) with a potential temperature of 1.32°C and salinity of 34.82 ppt. The bottom water is thermally well mixed in a nearly homogeneous layer about 700 m thick. The great thickness of this bottom layer, as compared with the bottom-water structure of the western Atlantic basin, may result from enhanced mixing induced by topographic constriction at the west end of the fracture zone trough. A benthic thermocline, with potential temperature

A characteristic circular depression made by a feeding, tubulose polychaete is restricted to the lowermost slope and the adjacent basin floor. Holothurian fecal strands dominate the feces types that can be seen in bottom photographs. These holothurian feces take the clothes-line form common to the abyss.

Open burrows are common in bottom photographs but are scarce in box core slabs. Photography and X-ray radiography of box-core sediment slabs reveal relatively homogeneous, burrow-mottled sediment. The paucity of distinct biogenic structures results from a lack of sediment density contrast for radiography and from the thixotropic response of the sediment to biogenic disturbance. Traces at the sediment-water boundary and within the sediment have poor preservation potential. Sediment from silled bathyal environments similar to the Santa Cruz Basin will probably come to appear in the rock record as homogeneously mottled and bioturbated mudstones with few preserved biogenic structures.

gradients of about 1.2 mdeg m⁻¹, is associated with an abrupt increase in turbidity with depth at about 1200 m above bottom. A transitional layer of more moderate temperature gradients, about 0.4 mdeg m⁻¹, lies between the benthic thermocline above and the AABW below. The AABW layer whose depth-averaged suspended particulate concentrations range from 8 to 19 g L⁻¹, is consistently higher in turbidity than the overlying waters. At the eastern end of the trough, 140 m below sill depth, very low, northeastward current velocities, with maximums of 3 cm s⁻¹, were recorded for an 11-day period.

Seismic facies of shelfedge deposits, U.S. Pacific continental margin

Field, M. E., Carlson, P. R., and Hall, R. K., 1983, in Stanley, D. J., and Moore, G. T., eds., *The Shelfbreak: critical interface on continental margins*: Society of Economic Paleontologists and Mineralogists Special Publication No. 33, p. 299-313.

Pacific-style continental margins, such as that of western North America, are marked by large contrasts in the type of shelfedge sedimentary deposits and the processes that form them. The Pacific shelves of the United States are generally much narrower than the Atlantic shelves, and the source areas exhibit more relief. The greater relief of Pacific coast source terranes results in a relatively high rate of sedimentation in humid areas and fluctuating (areally and seasonally) sedimentation patterns and rates in semiarid areas. Sediment shed from the adjacent landmass is discharged, generally seasonally, onto the Pacific Continental Shelf at point sources. Many of the sediment sources of the northwestern United States and southern Alaska feed directly onto swell- and storm-dominated shelves. On such narrow unprotected shelves, sediment has a short residence time in

submarine deltaic deposits before being remobilized and dispersed to outer-shelf and upper-slope environments.

Through study of high-resolution seismic-reflection profiles, we have identified four principal types of shelfedge deposits: (1) starved, (2) draped, (3) prograded, and (4) upbuilt and outbuilt. Each type of shelfedge deposit results from a characteristic balance between sedimentation rate and distributive energy (waves and currents) and is, therefore, characterized by distinctive seismic facies and bedding patterns. A special type, the cut-and-fill shelfedge, and a composite type consisting of two or more of the main depositional styles supplement the four principal types of shelfedge. Incorporated within each of these facies, especially on the upper slope, are chaotic deposits formed by slumps or slides, which are common along tectonically active margins.

Earthquake-induced sediment failures on a 0.25° slope, Klamath River delta, California

Field, M. E., Gardner, J. V., Jennings, A. E., and Edwards, B. D., 1982, *Geology*, v. 10, p. 542-546.

On November 8, 1980, a major earthquake (magnitude 6.5 to 7.2) occurred 60 km off the coast of northern California. A survey of the area using high-resolution seismic-reflection and side-scan sonar equipment revealed the presence of extensive sediment failure and flows in a zone about 1 km wide and 20 km long that trends parallel to the shelf on

the very gently sloping (0.25°) Klamath River delta. The failure zone is marked by a well-defined terrace that slopes seaward at about 0.02° and a prominent 1- to 2-m high, seaward-facing toe scarp on the outer margin of the terrace. This toe scarp is sinuous, appears to be nearly continuous for a distance of 20 km, and closely parallels the 60-m

isobath. Evidence indicates that the toe scarp is the terminus of lateral spreads and lobes of sediment flows. Side-scan sonar records show evidence of gas vents and small (10 x 3 x 0.5 m high) pressure ridges formed seaward of and parallel to the sediment flow scarp. Indicators of liquefaction (sand

boils and collapse craters) are present on the sediment flow terrace. Extensive sediment failure occurred on a sea-floor slope of less than 0.25° , and we can unequivocally pinpoint the cause as an earthquake of known location, magnitude, and time.

Sand waves on an epicontinental shelf: northern Bering Sea

Field, M. E., Nelson, C. H., Cacchione, D. A., and Drake, D. E., 1981, *Marine Geology*, v. 42, p. 233-258.

Sand waves and current ripples occupy the crests and flanks of a series of large linear sand ridges (20 km x 5 km x 10 m high) lying in an open-marine setting in the northern Bering Sea. The sand wave area, which lies west of Seward Peninsula and southeast of Bering Strait, is exposed to the strong continuous flow of coastal water northward toward Bering Strait. A hierarchy of three sizes of superimposed bedforms, all facing northward, was observed in successive cruises in 1976 and 1977. Large sand waves (height 2 m; spacing 200 m) have smaller sand waves (height 1 m; spacing 20 m) lying at a small oblique angle on their stoss slopes. The smaller sand waves in turn have linguoid ripples on their stoss slopes.

Repeated studies of the sand wave fields were made both years with high-resolution seismic-reflection profiles, side-scan sonographs, underwater photographs, current-meter stations, vibracores, and suspended-sediment samplers. Comparison of seismic and side-scan data collected along

profile lines run both years showed changes in sand wave shape that indicate significant bedload transport within the year. Gouge marks made in sediment by keels of floating ice also showed significantly different patterns each year, further documenting modification to the bottom by sediment transport.

During calm sea conditions in 1977, underwater video and camera observations showed formation and active migration of linguoid and straight-crested current ripples. Current speeds 1 m above the bottom were between 20 and 30 cm/s. Maximum current velocities and sand wave migration apparently occur when strong southwesterly winds enhance the steady northerly flow of coastal water. Many cross-stratified sand bodies in the geologic record are interpreted as having formed in a tidal- or storm-dominated setting. This study provides an example of formation and migration of large bedforms by the interaction of storms with strong uniform coastal currents in an open-marine setting.

A climate-related oxidizing event in deep-sea sediment from the Bering Sea

Gardner, J. V., Dean, W. E., Klise, D. H., and Baldauf, J. G., 1982, *Quaternary Research*, v. 18, p. 91-107.

Many cores from the deep basins of the Bering Sea have a thin oxidized zone within otherwise reduced sediment. This oxidized zone began to form about 6000 yr ago and represents an interval of about 3200 yr. Mineralogically, the oxidized and reduced sediments are similar, but chemically they differ. Concentrations of Fe and C are lower, and concentrations of Mn, Ba, Co, Mo, and Ni are higher in the oxidized than in the reduced sediment. Mn is enriched about 10-fold in the oxidized zone relative to its concentration in the reduced sediment, Mo about threefold, and Ba, Co, and Ni about twofold. These data suggest that the oxidized zone developed diagenetically as the result of the balance between the flux of organic matter and the available dissolved oxygen in bottom and interstitial waters.

We propose that the Bering Sea was substantially ice covered when global glacial conditions prevailed. During the transition to global interglacial conditions, seasonal melt-

water from thawing sea ice formed a lens of fresh water that decreased organic productivity. During the winter seasons, however, sea ice reformed and caused downwelling of dense, oxygen-rich waters to recharge bottom waters. The combination of lower organic productivity and more oxygen-rich bottom water allowed oxidized sediment to accumulate. Once full interglacial conditions were established, the volume of sea ice produced was insufficient to affect either productivity or the supply of dissolved oxygen and so bottom conditions again became reducing.

Similar events probably occurred during the onset of global glacial conditions, and similar oxidized layers probably formed at these times. Such oxidized zones are highly unstable, however, in a reducing environment and, once buried beyond the influence of bacterial and infaunal activities, are depleted of their available oxygen and converted to reduced sediment.

Sedimentology and geochemistry of surface sediments, outer continental shelf, southern Bering Sea

Gardner, J. V., Dean, W. E., and Vallier, T. L., 1980, *Marine Geology*, v. 35, p. 299-329.

Present-day sediment dynamics, combined with lowerings of sea level during the Pleistocene, have created a mixture of sediments on the outer continental shelf of the southern Bering Sea that was derived from the Alaskan Mainland, the Aleutian Islands, and the Pribilof ridge. Concentrations of finer-grained, higher-organic sediments in the region of the St. George basin have further modified regional distribution patterns of sediment composition.

Q-mode factor analysis of 58 variables related to sediment size and composition—including content of major, minor, and trace elements, heavy and light minerals, and clay minerals—reveals three dominant associations of sediment:

(1) The most significant contribution, forming a coarse-grained sediment scattered over most of the shelf

consists of felsic sediment derived from the generally quartz-rich rocks of the Alaskan mainland. This sediment contains relatively high concentrations of Si, Ba, Rb, quartz, garnet, epidote, metamorphic rock fragments, potassium feldspar, and illite.

(2) The next most important group, superimposed on the felsic group consists of andesitic sediment derived from the Aleutian Islands. This more mafic sediment contains relatively high concentrations of Na, Ca, Ti, Sr, V, Mn, Cu, Fe, Al, Co, Zn, Y, Yb, Ga; volcanic rock fragments, glass, clinopyroxene, smectite, and vermiculite.

(3) A local group of basaltic sediment, derived from rocks of the Pribilof Islands, is a subgroup of the Aleutian andesite group. Accumulation of fine-grained sediment in St.

George basin has created a sediment group containing relatively high concentrations of C, S, U, Li, B, Zr, Ga, Hg, silt, and clay.

Sediment of the Aleutian andesite group exhibits a strong gradient, or "plume", with concentrations decreasing away from Unimak Pass and toward St. George basin. The absence of present-day currents sufficient to move even clay-

size material as well as the presence of Bering submarine canyon between the Aleutian Islands and the outer continental shelf and slope, indicates that Holocene sediment dynamics cannot be used to explain the observed distribution of surface sediment derived from the Aleutian Islands. We suggest that this pattern is relict and resulted from sediment dynamics during lower sea levels of the Pleistocene.

Sedimentary processes on the Iberian continental margin viewed by long-range side-scan sonar. Part 1: Gulf of Cadiz

Gardner, J. V., and Kidd, R. B., 1983, *Oceanologica Acta*, v. 6, no. 3, p. 245-254.

A long-range side-scan sonar (Gloria) survey of the central and western Gulf of Cadiz reveals fields of sediment waves in water depths ranging from less than 2000 to over 4000 m. The sediment waves in water depths less than 2000 m have an average amplitude of 23 m and an average wavelength of 1892 m. These bedforms appear to be related directly to Mediterranean outflow. Sediment waves in water depths greater than 2000 m are different in size from those shallower than 2000 m; they have average wave heights of 8 m and average wavelengths of 1121 m. These bedforms are probably not related to Mediterranean outflow, but rather are

the result of a proposed eastern boundary current that appears to flow along the Northwest African margin, into the Gulf of Cadiz, and along the Western Iberian margin.

Submarine canyon systems show the development of gulleys and dendritic-like drainage systems in the upper portions of the canyons. The floors of the canyons appear to have large blocks of material scattered along axis. The lower regions of the canyons merge onto the Seine and Horseshoe abyssal plains with no apparent development of fans, distributary channels, levees, etc.

Geological interpretation of cone penetrometer tests in Norton Sound, Alaska

Hampton, M. A., Lee, H. J., and Beard, R. M., in press, *Geo-Marine Letters*.

In situ cone-penetrometer tests at 11 stations in Norton Sound complement previous studies of geologic processes and provide geotechnical data for an analysis of sediment response to loading. Assessment of the penetrometer records shows that various geologic factors influence penetration resistance. On the Yukon prodelta, penetration

resistance increases with the level of storm-wave or ice loading. In central and eastern Norton Sound, thermogenic and biogenic gas, as well as variations in sediment texture and composition, effect a wide range of resistance to penetration.

Geology and geochemistry of gas-charged sediment on Kodiak Shelf, Alaska

Hampton, M. A., and Kvenvolden, K. A., 1981, *Geo-Marine Letter*, v. 1, p. 141-147.

Methane concentrations in some sediment cores from the Kodiak Shelf and adjacent continental slope increase with depth by three or four orders of magnitude and exceed the solubility in water at ambient conditions. Acoustic anomalies in seismic-reflection records imply that methane-rich sediment is widespread. Molecular composition of hydrocarbon

gases and isotopic composition of methane indicate gas formation by shallow biogenic processes. Stratigraphic positions of acoustic anomalies in Quaternary glacial and post-transgressive sediments suggest that these units are likely sources of gas. A seep along the extension of a fault may be gas venting from a deeper thermogenic source.

Geochemical indices of fine sediment transport, northwest Gulf of Mexico

Holmes, C. W., 1982, *Journal of Sedimentary Petrology*, v. 52, no. 1, p. 307-321.

The ^{210}Pb distribution, the clay mineralogy distribution, and the distribution of three trace metals, barium, lead, and manganese, in the sediments of the south Texas shelf are related to the dynamics of the sedimentary transport process. ^{210}Pb , whose concentration is time dependent, defines three loci of recent sediment accumulations. In addition, the variation of ^{210}Pb activity at the sediment-water interface delineates areas of terrestrial sedimentation from hemipelagic sedimentation.

The clay mineralogy composition of the bottom and suspended sediments assists in defining the origin of the persistent nepheloid layer and bottom sediment.

Barium, a major element used in drilling mud, tags

sediment movement from areas of hydrocarbon exploration. Lead concentrations, anthropogenically introduced from urban areas, tag the sediment derived from the metropolitan complexes of coastal Texas. Manganese, because of diagenic mobilization, is concentrated in areas of very slow sediment accumulation.

The distribution of these geochemical properties of the sediment are in direct response to the sediment regime of the shelf. Based on this data, a model of sediment transport and deposition which relates currents, wind, tides, sediment flux, and precipitation has been formulated. This model differs from the "advective" transport or convergent current schemes previously proposed for this shelf.

¹⁸O variations in the Halimeda of Virgin Islands sands: evidence of cool water in the northeast Caribbean, late Holocene

Holmes, C. W., 1983, *Journal of Sedimentary Petrology*, v. 53, no. 2, p. 429-438.

Halimeda segments separated from carbonate sands on the Virgin Islands platform have ¹⁸O versus PDB isotopic values ranging from -0.3‰ to -1.3‰ (x = -0.9‰). Modern Halimeda segments from the same area have a measured ¹⁸O ranging from -2.0‰ to -2.5‰ PDB (x = -2.15‰), and the carbonate skeleton appears to have formed in isotopic equilibrium with the oceanic waters on the platform. Biologic and geochemical data indicate that the

sand deposits have accumulated under physical and chemical conditions similar to the modern shelf environment. ¹⁴C data suggest that the sand was deposited over an approximate 5800-year span, centering about 4000 years B.P. The average isotopic difference of 1.25‰ between the Holocene and modern carbonate indicates that the late Holocene Halimeda lived in waters approximately 4° cooler than the present.

Stratification styles in eolian sandstones: some Pennsylvanian to Jurassic examples from the western interior U.S.A.

Hunter, R. E., 1981, in Etheridge, F. G., and Flores, R. M., eds., *Recent and ancient nonmarine depositional environments: models for exploration*: Society of Economic Paleontologists and Mineralogists Special Publication No. 31, p. 315-329.

Most of the basic types of stratification that occur in modern dune sands have been identified in Pennsylvanian to Jurassic crossbedded sandstones of the western interior United States that are generally considered eolian. The most common types are sandflow cross-stratification (formed by the avalanching of sand down slipfaces), subcritically climbing translant stratification (formed by wind ripples), and grainfall lamination (formed by the settling out of grains in zones of flow separation). A common type of stratification formed by poorly understood processes on damp or ponded interdune flats is characterized by irregular small-scale waviness.

Identification of the basic types of stratification in a

sand body has several uses. Eolian and subaqueous sands may be distinguished by certain types of stratification, especially by the types occurring in climbing-ripple structures. More sophisticated paleocurrent determinations can be made when the type of stratification is known. Knowledge of the type of stratification can be used to estimate the initial porosity; such porosity estimates help in the analysis of sand compaction and pre-lithification deformation. The occurrence and distribution of the basic types of stratification are useful clues in interpreting dune size, dune morphology, dune orientation relative to the wind direction, and the reasons for the typically low dip angles of eolian cross-strata in the lower parts of sets.

Cyclic deposits and hummocky cross-stratification of probable storm origin in Upper Cretaceous rocks of the Cape Sebastian area, southwestern Oregon

Hunter, R. E., and Clifton, H. E., 1982, *Journal of Sedimentary Petrology*, v. 52, no. 1, p. 127-143.

Cyclic deposits containing hummocky cross-stratification occur in the upper part of the Cape Sebastian Sandstone of Bourgeois (1980), a shallow marine transgressive sandstone of Late Cretaceous age on the southern Oregon coast. The cycles average 1.6 m in thickness and consist, where complete, of a lower hummocky cross-stratified sandstone, a middle planar- and ripple-bedded sandstone with a shale bed in its middle part, and an upper bioturbated sandstone. Noteworthy features of the hummocky cross-stratification include the presence of depositional domes in addition to scoured depressions, the absence of significant bedform migration, and the presence of a small proportion of dip angles greater than the angle of repose (34°) in addition to the large proportion of low (15°) dip angles.

The lower, stratified, fining-upward part of the cycle (up to the top of the shale bed) is interpreted as having accumulated under conditions of initially great but gradually decreasing current velocity and deposition rate. The currents probably had a strong oscillatory component, and the depositional event is inferred to have been a storm. The part of the planar- and ripple-bedded sandstone above the shale bed was probably deposited during relatively fair weather after the storm but before re-establishment of a normal benthic fauna. The bioturbated sandstone is interpreted to have been deposited during fair weather or during minor storms separated by long intervals of fair weather.

Interpreting cyclic crossbedding, with an example from the Navajo Sandstone

Hunter, R. E., and Rubin, D. M., 1983, in Brookfield, M. E., and Ahlbrandt, T. S., eds., *Eolian sediments and processes*: Amsterdam, The Netherlands, Elsevier Science Publishers, p. 429-454.

A set of crossbeds may be composed of cyclic bundles defined by repetitions of structural, textural, or mineralogic features. The bounding surfaces of an individual cycle may be concordant with the crossbedding within the cycle or may be erosional and discordant, in which case the crossbedding is compound as well as cyclic. Both concordant and compound cyclic crossbedding can be produced by either of two processes: fluctuations in some flow parameter, especially flow direction, or the migration of bedforms over the lee slope of

a larger bedform on which they are superimposed. Distinguishing these two possible causes of cyclic crossbedding is by no means simple. Fluctuating-flow cycles can best be recognized by structural features arising from reversals in the alongslope or across-slope component of flow. Superimposed-bedforms cycles can best be recognized by features proving that part of one cycle formed contemporaneously with part of another cycle (that is, by evidence that the cycles are climbing translant strata), but such features are seldom

present. In the absence of such features, superimposed-bedform cycles can be recognized by features that arise from the superimposed bedforms being shorter in crest length than the larger bedform, trending at an angle to the larger bedform through at least part of their extent, or persisting while migrating for considerable distances over the lee slope of the larger bedform.

By using such criteria, we found what we interpret to be cycles of both fluctuating-flow and superimposed-bedform origin in the Navajo Sandstone. The cycles of fluctuating-flow origin include both the concordant types first described by Stokes (1964) and compound crossbedding. The

superimposed-bedform cycles are described in an accompanying paper (Rubin and Hunter, this volume). From considerations of the distinctness, regularity in structure and thickness, and scale of the cycles, we strongly support Stokes' (1964) interpretation of the cyclicity as annual. This interpretation should eventually prove valuable for making more sophisticated interpretations of the dynamics of the Navajo dunes, but the problems of why cyclicity is well developed only in some sets of crossbeds and of why the cyclicity takes at least two distinct forms need to be solved before the full potential of Stokes' (1964) insight is realized.

Processes controlling the characteristics of the surficial sand sheet, U.S. Atlantic outer continental shelf

Knebel, H. J., 1981, *Marine Geology*, v. 42, p. 349-368.

A review of recent data on the velocity of bottom currents, the frequency of bottom-sediment movement, the kinds and amounts of suspended sediments in near-bottom waters, and the acoustic and sedimentary features of sub-bottom strata indicates that the characteristics of the ubiquitous sand sheet on the Atlantic outer continental shelf of the United States have been controlled by a variety of past and present processes. Although these processes collectively have had a widespread effect on the characteristics of the sand sheet, the relative importance of each process changes geographically. On Georges Bank, late Pleistocene glaciations along with modern tidal currents and the regional circu-

lation pattern have played a dominant role. On the Middle Atlantic shelf, ancestral rivers, former near-shore processes, and modern wind- and wave-generated currents are important factors. On the South Atlantic shelf, the sediments reflect subaerial weathering, erosion or nondeposition over or near hardgrounds, and the production of biogenic carbonate. Other processes such as the movement of water masses, bioturbation, and bottom fishing probably have affected the sediments in all areas. A knowledge of the various factors affecting the sand sheet is fundamental to an understanding of its general geologic history and to the paleoenvironmental interpretation of ancient sand strata.

Sedimentary framework of the Potomac River estuary, Maryland

Knebel, H. J., Martin, E. A., Glenn, J. L., and Needell, S. W., 1981, *Geological Society of America Bulletin*, pt. 1, v. 92, p. 578-589.

Analyses of seismic-reflection profiles, sediment cores, grab samples, and side-scan sonar records, along with previously collected borehole data, reveal the characteristics, distribution, and geologic history of the shallow strata beneath the Potomac River estuary. The lowermost strata are sediments of the Chesapeake Group (lower Miocene to lower Pleistocene) that crop out on land near the shore but are buried as much as 40 m below the floor of the estuary. The top of these sediments is an erosional unconformity that outlines the Wisconsinan valley of the Potomac River. This valley has a sinuous trend, a flat bottom, a relief of 15 to 34 m, and axial depths of 34 to 54 m below present sea level. During the Holocene transgression of sea level, the ancestral valley was filled with as much as 40 m of sandy and silty, fluvial-to-shallow estuarine sediments. The fill became the

substrate for oyster bars in the upper reach and now forms most marginal slopes of the estuary. Since sea level approached its present position (2,000 to 3,000 yr ago), the main channel has become the locus of deposition for watery, gray to black clay or silty clay, and waves and currents have eroded the heterogeneous Quaternary sediments along the margins, leaving winnowed brown sand on shallow shoreline flats. Pb-210 analyses indicate that modern mud is accumulating at rates ranging from 0.16 to 1.80 cm/yr, being lowest near the mouth and increasing toward the head of the estuary. This trend reflects an increased accumulation of fine-grained fluvial sediments near the turbidity maximum, similar to that found in nearby Chesapeake Bay. The present annual accumulation of mud is about 1.54 million metric tons; the cumulative mass is 406 million metric tons.

Modern sedimentary environments on the Rhode Island inner shelf, off the eastern United States

Knebel, H. J., Needell, S. W., and O'Hara, C. J., 1982, *Marine Geology*, v. 49, p. 241-256.

Analyses of side-scan sonar records along with previously published bathymetric, textural and subbottom data reveal the sedimentary environments on the inner Continental Shelf south of Narragansett Bay, Rhode Island. The bottom topography in this area is characterized by a broad central depression bordered by shallow, irregular sea floor on the north and east and by a discontinuous, curvilinear ridge on the south and west.

Four distinct environments were identified:

(1) Pre-Mesozoic coastal rocks are exposed on the sea floor at isolated locations near the shore (water depths 32 m). These exposures have pronounced, irregular topographic relief and produce blotchy patterns on side-scan sonographs.

(2) Glacial moraine deposits form the discontinuous offshore ridge. These deposits have hummocky sea-floor relief, are covered by lag gravel and boulders, and appear as predominantly black (strongly reflective) patterns on the side-scan records.

(3) Over most of the shallow, irregular bottom in the northeast, on the flanks of the morainal ridge, and atop bathymetric highs, the sea floor is characterized as a mosaic of light and dark patches and lineations. The dark (more reflective) zones are areas of coarse sands and megaripples (wavelengths = 0.8-1.2 m) that either have no detectable relief or are slightly depressed relative to surrounding (light) areas of finer-grained sands.

(4) Smooth beds that produce nearly featureless patterns on the sonographs occupy the broad central bathymetric depression as well as smaller depressions north and east of Block Island. Within the broad depression, sonographs having practically no shading indicate a central zone of modern sandy silt, whereas records having moderate tonality define a peripheral belt of silty sand.

The sedimentary environments that are outlined range

from erosional or nondepositional (bedrock, glacial moraine) to depositional (featureless beds), and include areas that may reflect a combination of erosional and depositional processes (textural patchiness). The distribution and characteristics of the environments reveal the general post-glacial sedimentary history of this area and provide a guide to future utilization of the shelf surface.

Bulk density and shear strength of several deep-sea calcareous sediments

Lee, H. J., 1982, in Demars, K. R., and Chaney, R. C., eds., *Geotechnical properties, behavior, and performance of calcareous soils: American Society for Testing and Materials, STP 777*, p. 54-78.

Deep-sea calcareous sediment commonly consists of chemically active, fragile, biologically derived sand- or silt-size carbonate particles combined with terrigenous silt and clay and biologically derived opaline silica. The shearing strength of these sediments depends on whether the noncarbonate matrix or a carbonate framework dominates and on the physical nature of the noncarbonate matrix. A model based on relations between bulk density and carbonate content is developed to delineate three types of behavior: matrix dominant, transition, and carbonate-framework dominant. The model is quantitatively evaluated using vane shear, bulk density, grain density, carbonate content, and triaxial shear strength measurements from four studies of deep-sea calcareous sediments. The divisions between the three

behavior types are found to be determined primarily by the character of the noncarbonate matrix. The presence or absence of opaline silica in the noncarbonate fraction has the strongest influence and is related to the overall sedimentary environment. Vane shearing strength increases with carbonate content through the transition and carbonate-framework-dominant zones. It is independent of carbonate content in the matrix-dominant zone. This trend may be masked by coring disturbance if only the results of laboratory analyses as opposed to *in situ* tests are considered. The cause of the strength increase with carbonate content may be the granular nature of the carbonate particles (mechanical) or interparticle cementation (chemical).

Geotechnical analysis of a submarine slump, Eureka, California

Lee, H. J., Edwards, B. D., and Field, M. E., 1981, 13th Annual Offshore Technology Conference, Proceedings, p. 53-65.

A large submarine slump covers more than 150 km² of a gentle (1°) slope offshore of Eureka, Calif. We have conducted a detailed geologic and geotechnical investigation of the slump and the surrounding area to delineate the geometry of the slump, determine its cause, and quantitatively evaluate the sediment properties that led to the failure. Our study included an effort to test procedures for using short-core samples in such an evaluation. Cyclic and static triaxial and one-dimensional consolidation tests were performed on gravity-core samples from both within and outside the slump; all

samples showed some degree of overconsolidation. We used a normalized-strength-parameter approach to estimate the strength at the failure surface below the level of sampling. A stability analysis based on a pseudo static infinite-slope model shows the slump probably to be earthquake induced. This analysis also gave values of the sediment parameters leading to failure at the slump site and to stability at surrounding sites. Owing to the complex variation in sediment properties, subtle changes in properties may determine the stability or failure of the sediment mass.

Heavy-mineral distribution in modern and ancient bay deposits, Willapa Bay, Washington, U.S.A.

Luepke, Gretchen, and Clifton, H. E., 1983, *Sedimentary Geology*, v. 35, p. 233-247.

Analysis of heavy-mineral distribution in modern sediments of Willapa Bay, Washington, indicates a dominance of two mineralogic assemblages, one with approximately equivalent amounts of hornblende, orthopyroxene and clinopyroxene, the other dominated by clinopyroxene. The hornblende-orthopyroxene-clinopyroxene suite is derived from the Columbia River, which discharges into the ocean a short distance south of the bay. The clinopyroxene suite is restricted in modern sediments to sands in rivers flowing into the bay from the east. The heavy-mineral distributions suggest that sand discharged from the Columbia River, borne north by longshore transport, and carried into the bay by tidal currents accounts for most of the sand within the interior of Willapa Bay.

Three heavy-mineral assemblages are present in the surrounding Pleistocene deposits; two of these are identical to the modern assemblages described above. These heavy-mineral assemblages reflect the relative influence of tidal

and fluvial processes on the Late Pleistocene deposits; their relative influences are consistent with those inferred on the basis of sedimentary structures and stratigraphic relations in about two-thirds of the samples examined. The anomalies can be explained by recycling of sand from older deposits. The persistence of the two heavy-mineral assemblages suggests that the pattern of estuarine sedimentation in Late Pleistocene deposits closely resembled that of the modern bay.

The third heavy-mineral suite, dominated by epidote, occurs in a few older Pleistocene units. On the north side of the bay, the association of this site with southwest-directed foresets in crossbedded gravel indicates derivation from the northeast, perhaps from an area of glacial outwash. The presence of this suite in ancient estuarine sands exposed on the east side of the bay suggests that input from this northerly source may have intermittently dominated bay deposition in the past.

Active diapirism and slope steepening, northern Gulf of Mexico continental slope

Martin, R. G., and Bouma, A. H., 1982, *Marine Geotechnology*, v. 5, no. 1, p. 63-91.

Large diapiric and nondiapiric masses of Jurassic salt and Tertiary shale underlie the northern Gulf of Mexico continental slope and adjacent outer continental shelf. These masses show evidence of being structurally active at present and in the very recent geologic past. Local steepening of the sea floor in response to the vertical growth of these structures is a serious concern to those involved in the site selection and the construction of future oil and gas production and transportation facilities in this frontier petroleum province.

The seabed of the northern Gulf slope is hummocky and consists of many hillocks, knolls, and ridges interspersed by topographic depressions and canyon systems. Topographic highs and lows relate respectively to vertical diapiric growth and to withdrawal of large volumes of salt and shale. Topographic highs vary considerably in shape and size, but all have very limited areas of nearly flat sea floor. Intraslope topographic lows consist of three principal types: (1) remnants of submarine canyons blocked by diapiric uplift that terminated active downslope sediment transport common during stages of low sea level; (2) closed depressions formed by subsidence in response to salt and shale withdrawal and flow into surrounding diapiric uplifts; and (3) small collapse basins formed by faulting in strata arched over structural crests of diapirs.

Distribution patterns of both diapiric features and sediment accumulations on the slope are the result of the complex relationship that exists between sediment loading and diapirism. Diapiric activity is proportional to the thick-

ness of salt or unconsolidated shale available for mobilization, and to the sedimentary load distribution on these highly plastic deposits. Variations in overburden load, in turn, are dependent on rates, volumes, and bulk densities of depositional influx; proximity to sources of supply, erosion, and distribution of sediments; and topographic control of sediment accumulation. Sediment capture in diapirically controlled interdomal basins and canyon systems localizes overburden load, thus inducing further diapiric growth, and complex structural and stratigraphic patterns are induced throughout the continental slope region.

Drill cores in the slope province indicate that most of the slope sediments are fine-grained muds; appreciable quantities of sand-size sediment are present principally in canyon axes. Turbidite sand layers drilled on a topographic high adjacent to the Gyre Basin reflect uplift far above their original deposition level, and calculations yield rates of uplift that average 2 to 4 m per 100 years. Seismic reflection profiles provide considerable evidence of "fresh" slumps and erosional surfaces on the flanks of many topographic highs not yet blanketed by a veneer of young sediments. This evidence thus supports our conclusion that the present continental slope region of the northern Gulf of Mexico is undergoing active diapirism and consequent slope steepening. Because most of the sediment on the flanks of diapiric structures consists of underconsolidated muds, slumping will take place regularly in response to further diapiric movement.

Ancestral head of Wilmington Canyon

McGregor, B. A., 1981, *Geology*, v. 9, p. 254-257.

A 12-channel seismic-reflection survey over parts of the head of Wilmington Canyon and the surrounding shelf revealed four major buried valleys and many small channels. The data indicate that the ancestral Delaware River valley was the most recent of a series of valleys to enter the canyon from the west. The head of Wilmington Canyon probably was eroded and then filled at various times from late Miocene to

late Pleistocene. Thick sedimentary sequences indicate a sediment supply from both the north and west. A large buried valley entering the canyon from the north was not mapped with the data presented here, but it is possible that such a valley exists. This is one of the first documentations of the long history of erosion of the United States east coast canyons.

Sediment failure and sedimentary framework of the Wilmington geotechnical corridor, U.S. Atlantic continental margin

McGregor, B. A., and Bennett, R. H., 1981, *Sedimentary Geology*, v. 30, p. 213-234.

Seaward of New Jersey and the Baltimore Canyon Trough, a 7500 km² corridor across the continental margin was studied in detail using geotechnical and geophysical techniques. The objective of the study was to identify the sedimentary pattern and bottom processes which have occurred and are active on the continental margin. Delineation of a mid-Pliocene unconformity, present throughout most of the corridor, permits an evaluation of the Quaternary sedimentation pattern and its variability. Sediment failure characterized by large slide blocks and thin layer slide deposits was found on the continental slope and rise within the

Quaternary sediments. Spencer and Wilmington Submarine Canyons have been active in channeling large volumes of sediment to the lower slope and rise. An increase in sediment thickness near Wilmington Canyon indicates the importance and activity of the Delaware Bay drainage system during the Pleistocene. Although both Spencer and Wilmington are as old as late Tertiary, the Wilmington Valley on the lower slope and rise is a recent topographic feature. Based on geophysical data the numerous valleys that dissect the continental slope and rise appear to be active periodically in the seaward transport of sediment to the deep sea.

Wilmington Submarine Canyon: a marine fluvial-like system

McGregor, B. A., Stubblefield, W. L., Ryan, W. B. F., and Twichell, D. C., 1982, *Geology*, v. 10, p. 27-30.

Midrange sidescan sonar data (swath width = 5 km) show that a system of gullies and small channels feeds into large submarine canyons on the Middle Atlantic Continental Slope of the United States. The surveyed canyons all have relatively flat floors, but they have different channel morphologies. Wilmington Canyon has a meandering channel that

extends down the Continental Slope and across the Continental Rise, whereas two canyons south of Wilmington Canyon have straight channels that trend directly downslope onto the rise. The morphology of these submarine canyon systems is remarkably similar to that of terrestrial fluvial systems.

Erosional channels on the shoreface of Nauset Beach, Cape Cod, Massachusetts

Needell, S. W., Dillon, W. P., and Knebel, H. J., 1982, *Geo-Marine Letters*, v. 2, p. 61-64.

Many channels (1 to 3 m relief) are located offshore of Nauset Beach, Cape Cod, Massachusetts, in water 4 to 18 m deep. The channels are oblique to the shoreline, are spaced approximately 260 m apart, and deepen seaward. The southern flank of each channel is rippled whereas the northern flank and interchannel areas are smooth. The origin of the

channels is unknown. They probably formed by erosion of the shoreface, perhaps by rip-current circulation during storm conditions or by rip-current circulation under quiet conditions. The channels may control current flow and thereby maintain themselves even though formative conditions may no longer exist.

Late Pleistocene-Holocene transgressive sedimentation in deltaic and non-deltaic areas of the northeastern Bering epicontinental shelf

Nelson, C. H., 1982, in Nelson, C. H., and Nio, S. D., eds., *The northeastern Bering shelf: new perspectives of epicontinental shelf processes and depositional products: Geologie en Mijnbouw* 61, p. 5-18.

The distribution of late Pleistocene and Holocene surface sediments on the northern Bering Seafloor is patchy and dependent upon locations of seafloor bedrock and pre-late Pleistocene glacial debris, late Holocene river sediment influx, and modern strong bottom currents. Seafloor vibracores and high-resolution profiles record two different sedimentary environments in the northern Bering shelf: late Pleistocene-Holocene shoreline transgression (16,000 years BP) in Chirikov Basin, and Holocene deposition from the Yukon River in Norton Sound.

Lag gravels remain exposed on the margins of Chirikov Basin where the transgression of the late Pleistocene-Holocene shoreline reworked pre-Quaternary bedrock and Pleistocene glacial moraines. In central Chirikov Basin, the transgressive deposits cover Pleistocene limnic peaty mud of

emergent shelf deposition. In places, a few centimeter-thick basal transgressive facies of pebbly medium to fine sand is left above which is a widespread sheet of thin (1 m) inner-shelf fine-sand facies. Water circulation patterns have inhibited deposition of Holocene Yukon River silt over transgressive sand and lag gravels of Chirikov Basin.

About 10,000 BP, a rapid marine transgression caused the deposition of a basal nearshore facies of thick storm-sand layers in marine silt over the Pleistocene freshwater peaty mud of Norton Sound. This has been covered by an offshore bioturbated silt.

A younger progradation of thick storm-sand layers and Holocene brackish-water silt (up to 14 m) in southern Norton Sound has been deposited since a shift of the active Yukon Delta into its present position about 2,500 BP.

Modern shallow-water graded sand layers from storm surges, Bering shelf: A mimic of Bouma sequences and turbidite systems

Nelson, C. H., 1982, *Journal of Sedimentary Petrology*, v. 52, no. 2, p. 537-545.

A sequence of graded sand layers, interbedded with mud, extends offshore over 100 km from the Yukon Delta shoreline across the flat, shallow (20 depth) epicontinental shelf of the northern Bering Sea, Alaska. Proximal graded sand beds on the delta-front platform near the shoreline are coarser (2-3), thicker (10 to 20 cm), and contain more complete vertical sequences of sedimentary structures than distal beds. The inshore graded vertical sequence of structures from the base to the top of individual sand layers includes plane-parallel lamination (S_b), cross lamination (S_c), plane-parallel lamination (S_d), and mud (S_e) analogous to the Bouma T_{a-e} turbidite sequence. Structures vary between interchannel platform deposits with complete S_b - S_e sequences and channel-floor sands that are all trough cross-laminated. Distally, storm-sand layers change to thin (1 to 5 cm) silt beds that contain flat and ripple-drift lamination

($S_{c-e,de}$), are commonly bioturbated, and are associated with shell and pebble lags from storm-wave reworking.

The sequence of graded sands appears to be related to the major storm surges that occur every several years. The major storms increase the average 10-m water depth in southern Norton Sound as much as 5 m and cause fluctuations in pore pressure from wave cyclic loading that may liquefy the upper 2 to 3 m of sediment. Storm-associated bottom currents, possibly dominated by rapidly waning ebb flow, transport the liquefied inshore sand far offshore (100 km). Such shallow-water graded layers off lobate deltas may be distinguished from similar deep-water turbidites by: 1) the predominance of trough cross-lamination, perhaps resulting from wave oscillation effects, in the proximal part of the system, and 2) gradation to common shallow marine fossils, bioturbation, and storm lag layers in distal areas.

Interplay of physical and biological sedimentary structures of the Bering continental shelf

Nelson, C. H., Rowland, Robert W., Stoker, Sam W., and Larsen, Bradley R., 1981 in Hood, G. W. and Calder, J. A., eds., *The eastern Bering shelf: its oceanography and resources*, v. 2: Seattle, Washington, University of Washington Press, p. 1265-1296.

Distinctive Holocene transgressive sand and post-transgressive mud with attendant physical and biological structures occur on the shallow (60 m) shelf of the northern Bering Sea. Thin gravel lag layers, formed during the Holocene shoreline transgression, veneer exposed glacial moraines. Epifaunal species dominate these relict gravel areas and cause little disruption of physical structures. Some relict submerged beach ridges contain faint rippling that probably is caused by modern current reworking. Well-sorted

medium sand on exposed shoal crests is reworked by the sand dollar and tellinid clam communities. Buried thin layers of transgressive beach sand and gravel retain rare original medium-scale cross-lamination and flat lamination that have been intensively bioturbated. A thin layer of an offshore fine-grained sand facies that was deposited by the Holocene transgression remains unburied by modern mud in central Chirikov Basin. Primarily because of ampeliscid amphipod bioturbation, this facies has no physical structures.

Post-transgressive silty mud from the Yukon River blankets the shallow (20 m) areas of Norton Sound. In places the silty mud contains thin beds of shells and pebbles and thin sand interbeds and lenses that exhibit ripples and small-scale flat and cross-lamination. These coarse-grained interbeds are interpreted to be storm layers formed by modern storm waves and storm-surge currents. Physical sedimentary structures are well preserved only near the delta fringe; there the frequency of physical reworking is highest, the potential for preservation by a high rate of deposition is greatest, and the

inhibition of bioturbation by low salinity is most severe. At greater distances from shore, infaunal deposit-feeding bivalves, polychaete worms, and small amphipods cause progressively greater disruption of bedforms in prodelta mud. Almost all modern physical structures have been destroyed at water depths greater than 25 m. As a result the following sequence of storm deposits is characteristic of profiles extending away from the delta: thick (5 cm) storm-sand layers, thin storm-sand layers, isolated and bioturbated sand lenses, faint bioturbated shell and pebble beds.

Wind-current coupling on the southern flank of Georges Bank: variation with season and frequency

Noble, Marlene, Butman, Bradford, and Wembush, Mark, in press, *Journal of Physical Oceanography*.

Comparison of several years of current observations on the southern flank of Georges Bank with nearby wind data show that the wind-current coupling is primarily between longshelf wind stress and longshelf current. The strongest wind-current coupling occurs in winter, when the water column is homogeneous. The weakest coupling is in late summer and early fall, when the water column is highly stratified. The coherence and transfer coefficient between longshelf wind and longshelf current is highest for periods between 100 and 300 hours, decreasing both for longer periods (out to 1344 hours) and shorter periods (down to 60 hours).

Models of the wind-current coupling predict a small current response at high frequencies and a smaller response when the water column is stratified. The observations also indicate that the wind-driven currents on Georges Bank are strongly controlled by friction. The near-surface current moves to the right of wind stress and there is a spring-neap modulation of the wind-current transfer coefficient caused by the modulation of the bottom stress associated with the spring-neap tidal cycle. The longshelf current is linearly related to wind stress and responds almost symmetrically to wind forcing.

On the longshelf structure and dynamics of subtidal currents on the eastern United States continental shelf

Noble, M. A., Butman, Bradford, and Williams, Edward, 1983, *Journal of Physical Oceanography*, v. 13, no. 12, p. 2125-2147.

Strong correlations were observed among subtidal longshelf currents from the Middle Atlantic Bight (MAB) to the Georges Bank region, a distance spanning 615 km. The longshelf current consisted predominantly of wind-forced motions and freely propagating events, which together accounted for 75%-90% of the longshelf current energy. Much stronger longshelf currents were observed in the MAB than on Georges Bank. The MAB/Georges Bank energy ratio for wind-forced currents on the 60-m isobath was 20. The ratio for freely propagating events was 3. The magnitudes of many of the terms in the vertically integrated, wind-driven momentum equations were estimated from observations of

current, pressure, and surface stress, and from calculations bottom stress. The cross-shelf momentum balance was geostrophic. Surface and bottom stresses, the longshelf pressure gradient, and the Coriolis force on the cross-shelf flow were important terms in the longshelf momentum balance. An analytic model of wind-forced current, which incorporated the significant force balances, accounted for the longshelf variation in wind-forced currents. Bottom-drag and bottom resistance coefficients estimated from current and bottom stress records had ranges of $4-8 \times 10^{-3}$ and 0.07-0.20 cm/s, respectively.

Quaternary development of channels, levees, and lobes on middle Laurentian fan

Normark, W. R., Piper, D. J. W., and Stow, D. A. V., 1983, *American Association of Petroleum Geologists Bulletin*, v. 67, no. 9, p. 1400-1409.

Seismic reflection profiles from the middle Laurentian fan show that the western fan valley has an abrupt eastward (leftward) hook at its terminus. The right-hand levee of this valley has been built across an older depositional surface in which numerous south-trending channels developed before the abrupt bend formed. This older channeled surface probably represents a complex depositional lobe deposit. Eastward deflection of turbidity-current flow occurred after debris-flow or slide deposits partly obstructed the valley near its termination or after aggradation of the lobe deposits. This deflection produced an abrupt change in the valley trend.

Through time, the eastward-growing part of the levee has migrated northward toward the axis of the channel; this northward migration confines turbidity-current flow against the levee of another valley immediately upfan.

This study documents progradation of muddy facies over sandy lobes thus providing conditions for an effective seal for any hydrocarbons accumulated in the lobe sands. Updip migration of hydrocarbons through valley-fill sands that are contiguous with the lobes could be blocked locally by thick debris-flow units or by fine-grained turbidite fill in abandoned channels.

Pleistocene stratigraphy of Nantucket, Martha's Vineyard, the Elizabeth Islands, and Cape Cod, Massachusetts

Oldale, R. N., 1981, in Larson, G. J., and Stone, R. D., eds., *Late Wisconsinan glaciation of New England*: Dubuque, Kendall/Hunt, p. 1-34.

Pleistocene strata of late Wisconsinan age have been identified on Cape Cod. Pre-Wisconsinan deposits are also

exposed on Nantucket and Martha's Vineyard. At Sankaty Head on Nantucket, stratified drift and till of presumed

Illinoian age lie below marine beds. Two tills and an interglacial deposit on Martha's Vineyard are also thought to be Illinoian or older. The marine beds at Sankaty Head are of Sangamonian age and make up two units. The lower unit, including the lower part of the Sankaty Sand, represents a marine transgression when the sea was considerably warmer than present. The upper unit, which consists mostly of the upper part of the Sankaty Sand, represents a marine transgression when the sea was colder than present. The marine beds may correlate with the pre-Wisconsinan marine deposits of Long Island.

Involutions in the upper part of the Sankaty Sand and an unconformity distinguished by a lag of wind-cut stones represent a cold subaerial climate during the onset of early or late Wisconsinan glaciation. Drift of early Wisconsinan age on Martha's Vineyard is represented in large part by till and is

probably equivalent to the early Wisconsinan Montauk Till member of the Manhasset Formation of Long Island. Deposits of the middle Wisconsinan interstadial period are absent but may be represented by wood and shell fragments in the upper Wisconsinan drift.

The late-Wisconsinan glacier formed the coastal end moraines, broad outwash plains, and the ice-contact features that now characterize Cape Cod and the islands. The moraines are largely glaciotectonic and morphostratigraphically equivalent to the late Wisconsinan end moraines of Rhode Island, Connecticut, and Long Island. Upper Wisconsinan drift units on Nantucket and Martha's Vineyard are probably time synchronous and were formed before the drift on Cape Cod. Relative ages of the drift units on Cape Cod demonstrate the progressive retreat of the glacial lobes from west to east.

Regional significance of pre-Wisconsinan till from Nantucket Island, Massachusetts

Oldale, R. N., and Eskenasy, D. M., 1983, *Quaternary Research*, v. 19, p. 302-311.

A major pre-Wisconsinan glacial event is the only possible source of the lower till on Nantucket Island, Massachusetts. The till occurs near the late Wisconsinan drift border and below fossiliferous marine beds of oxygen-isotope stage 5 (Sangamonian) age. It is considered to be Illinoian in age, but the evidence is tenuous. The till is correlated with

the lower till of New England, and its presence supports the view that the New England upper and lower tills represent two glaciations. The pre-Wisconsinan (lower) till in New England may correlate with older tills elsewhere in the northeastern United States and in southeastern Canada that are considered to be early Wisconsinan or older in age.

Stratigraphy, structure, absolute age, and paleontology of the upper Pleistocene deposits at Sankaty Head, Nantucket Island, Massachusetts

Oldale, R. N., Valentine, P. C., Cronin, T. M., Spiker, E. C., Blackwelder, B. W., Belknap, D. F., Wehmiller, J. F., and Szabo, B. J., 1982, *Geology*, v. 10, p. 246-252.

The Sankaty Head cliff of Nantucket Island, Massachusetts, exposes drift of at least two glaciations and interglacial marine deposits. Radiocarbon, amino-acid-racemization, and uranium-thorium analyses were used to determine the absolute ages of the beds. The results indicate that (1) the Sankaty Sand correlates with oxygen-isotope stage 5 (Sangamonian), (2) the underlying drift is older than stage 5 (Illinoian or older), and (3) the overlying drift is Wisconsinan in

age. Ostracodes and molluscs within the Sankaty Sand indicate that the marine climate during deposition of the lower part was somewhat warmer than the present climate off Sankaty Head and that the marine climate during the deposition of the upper part was as cold as or somewhat colder than the present climate. The paleoenvironmental data support a stage 5 (Sangamonian) age for the marine deposits.

Evidence for a postglacial low relative sea-level stand in the drowned delta of the Merrimack River, western Gulf of Maine

Oldale, R. N., Wommack, L. E., and Whitney, A. B., 1983, *Quaternary Research*, v. 19, p. 325-336.

A submerged delta of the Merrimack River, located offshore between Cape Ann, Massachusetts, and the New Hampshire border, indicates a postglacial low relative sea-level stand of about -47 m. The low stand is inferred to date to 10,500 yr B.P., but a lack of age control makes this as-

signment uncertain. A curve based on a late Wisconsinan, high relative sea-level stand of +32 m at 13,000 yr B.P., a low stand of -47 m at 10,500 yr B.P., and younger radiocarbon dates related to sea-level rise indicates an early postglacial crustal rise of at least 5 m per century.

Turbidite deposition patterns and flow characteristics, Navy Submarine Fan, California borderland

Piper, David J. W., and Normark, William R., 1983, *Sedimentology*, v. 30, p. 681-694

The late Pleistocene and Holocene stratigraphy of Navy Fan¹⁴ is mapped in detail from more than 100 cores. Thirteen ¹⁴C dates of plant detritus and of organic-rich mud beds show that a marked change in sediment supply from sandy to muddy turbidites occurred between 9000 and 12,000 years ago. They also confirm the correlation of several individual depositional units. The sediment dispersal pattern is primarily controlled by basin configuration and fan morphology, particularly the geometry of distributary

channels, which show abrupt 60° bends related to the Pleistocene history of lobe progradation. The Holocene turbidity currents are depositing on, and modifying only slightly, a relict Pleistocene morphology.

The uppermost turbidite is a thin sand to mud bed on the upper-fan valley levees and on parts of the mid-fan. Most of its sediment volume is in a mud bed on the lower fan and basin plain downslope from a sharp bend in the mid-fan distributary system. Little sediment occurs farther

downstream within this distributary system. It appears that most of the turbidity current overtopped the levee at the channel bend, a process referred to as flow stripping. The muddy upperpart of the flow continued straight down to the basin plain. The residual more sandy base of the flow in the distributary channel was not thick enough to maintain itself as gradient decreased and the channel opened out on to the mid-fan lobe.

Flow stripping may occur in any turbidity current that is thick relative to channel depth and that flows in a channel with sharp bends. Where thick sandy currents are stripped,

levee and mid-fan erosion may occur, but the residual current in the channel will lose much of its power and deposit rapidly. In thick muddy currents, progressive overflow of mud will cause less deceleration of the residual channelised current. Thus both size and sand-to-mud ratio of turbidity currents feeding a fan are important factors controlling morphologic features and depositional areas on fans. The size-frequency variation for different types of turbidity currents is estimated from the literature and related to the evolution of fan morphology.

Environmental implications of test-to-substrate attachment among some modern sublittoral foraminifera

Poag, C. W., 1982, *Geological Society of America Bulletin*, v. 93, p. 252-258.

Topographic highs on the outer continental shelf of New Jersey are sites for the concentration of three species of attached calcareous benthic foraminifera. Elphidium subarcticum Cushman, normally considered a vagrant species, cements itself by an organic film to one or more quartz grains. Webbinella concava (Williamson) attaches to quartz grains by secreting a flange-like calcite skirt at one side of its globuline test. Vasiglobulina reticulata n. sp. has evolved the most elaborate system of attachment: numerous closely

spaced spines connect the globuline test to a thin calcite lamina, which is in turn cemented to quartz grains.

The attachment mode of these species suggests that the added weight of the quartz grains may reduce displacement during the periodic resuspension of the shelf sediments by longshore and tidal current motion. The distribution of living populations of these species corroborates sedimentological inferences that little or no modern deposition takes place on the sampled topographic highs.

Living foraminifers of West Flower Garden Bank, northernmost coral reef in the Gulf of Mexico

Poag, C. W., and Tresslar, R. C., 1981, *Micropaleontology*, v. 27, no. 1, p. 31-70.

Living benthic foraminifers representing 73 genera and 104 species were collected from sediments and hard substrates sampled on the submerged coral reef and biostrome at West Flower Garden Bank, on the outer Texas-Louisiana Continental Shelf. Three habitat associations can be recognized: (1) association of abundant sediment-dwelling species; (2) association of abundant species dwelling on hard substrates; and (3) association dwelling in abundance both in the sediments and on hard substrates. Only 16 (15%) of the West Flower Garden Bank species are endemic to the Gulf of Mexico; 85 (82%) occur elsewhere in the Caribbean, and 54

(52%) also occur in the tropical Indo-Pacific. Thirty-one species (29%) are reported herein for the first time from the Gulf of Mexico, and 12 additional species (12%) are reported for the first time from the northwestern Gulf. Fifteen other species (14%) appear to be undescribed in previous literature. Many of the newly reported species are abundant at West Flower Garden Bank, and several other species known only sparsely from other Gulf and Caribbean reefs are important constituents of the West Flower Garden Bank foraminiferal community. These results emphasize the value of direct sampling techniques that recover hard reef substrates.

Dynamic ice-wallow relief of northern Alaska's nearshore

Reimnitz, Erk, and Kempema, Edward, 1982, *Journal of Sedimentary Petrology*, v. 52, no. 2, p. 451-461.

Contour maps with 0.5-m depth interval were prepared for a small area seaward of Reindeer Island, a barrier island in the Beaufort Sea, Alaska, by repeated surveys with very accurate navigation and very close trackline spacing. The maps reveal numerous closed depressions and mounds about 50 to 100 m in diameter and 2 to 3 m in relief, presumably related to grounded ice floes common in the area year round. Some of the features were obliterated over the course of three seasons while new ones formed. Although the depressions resemble kettles, they are formed by very different mechanisms. We believe that these bedforms represent erosion and deposition cause by: a) intensified flow

around stationary ice floes serving as obstacles and b) pulsating currents generated by vertical oscillations or rocking motions of grounded floes in a seaway. Because sediment transport occurs around the ice, not where it directly touches the sea floor, the depressions are much larger than the base of the acting floes.

Ice-wallow bedforms, although not found everywhere, are characteristic of arctic nearshore regions with non-cohesive sediments, and most likely occur in other ice-stressed coastal environments in differing degrees. The bedforms studied here are highly active and must be considered in planning nearshore construction activities.

High rates of bedload transport measured from infilling rate of large strudel-scour craters in the Beaufort Sea, Alaska

Reimnitz, Erk, and Kempema, E. W., 1983, *Continental Shelf Research*, v. 1, no. 3, p. 237-251.

Strudel scours are craters in the seafloor as much as 25 m wide and 6 m deep, that are excavated by vertical drainage flow during the yearly spring flooding of vast

reaches of shorefast ice surrounding arctic deltas; they form at a rate of about $2.5 \text{ km}^2 \text{ y}^{-1}$. We monitored two such craters in the Beaufort Sea and found that in relatively

unprotected sites they fill in by deposition from bedload in 2 to 3 years. Net westward sediment transport results in sand layers dipping at the angle of repose westward into the strudel-scour crater, whereas the west wall of the crater remains steep to vertical. At the bottom the crater traps almost all bedload: sand, pebbles and organic detritus. As infilling progresses, the materials are increasingly winnowed, and bypassing must occur. Over a 20 m wide sector, an exposed strudel scour trapped 360 m^3 of bedload during two seasons; this infilling represents a bedload transport rate of $9\text{ m}^3\text{ y}^{-1}\text{ m}^{-1}$. This rate should be applicable to a 4.5-km wide zone with equal exposure and similar or shallower depth. Within this zone, the transport rate is $40,500\text{ m}^3\text{ y}^{-1}$, similar to estimated longshore transport rates on local barrier beaches. Based on the established rate of cut and fill, all the delta-

front deposits should consist of strudel-scour fill. Vibracores typically show dipping interbedded sand and lenses of organic material draped over steep erosional contacts, and an absence of horizontal continuity of strata—criteria that should uniquely identify high-latitude deltaic deposits. Given a short 2- to 3-year lifespan, most strudel scours seen in surveys must be old and partially filled. The same holds true for ice gouges and other depressions not adjusted to summer waves and currents, and therefore such features recorded events of only the past few years. In view of such high rates of bottom reworking of the shallow shelf, any human activities causing turbidity, such as dredging, would have little effect on the environment. However, huge amounts of transitory material trapped by long causeways planned for offshore development would result in major changes in the environment.

Surficial geologic studies of the continental slope in the northern Baltimore Canyon Trough area—techniques and findings

Robb, J. M., Hampson, J. C., Jr., and Kirby, J. R., 1982, Offshore Technology Conference Proceedings, v. 1, p. 39-59.

Since 1978, the U.S. Geological Survey has been conducting a study of the Atlantic Continental Slope between Lindenkohl and South Toms Canyons, offshore New Jersey, to determine the nature of potential geological hazards to hydrocarbon exploration and exploitation. The study has progressed from characterization of the near-surface stratigraphy, using single-channel seismic-reflection data and piston cores, to detailed geomorphological studies using midrange sidescan-sonar coverage, and finally to targeted observations from deep-diving submersible. The seismic-reflection data and cores have shown that unconsolidated Pleistocene sediments as much as 400-m thick cover the upper and mid slope, and that identifiable slump or slide features occupy only a small part of the slope area mapped. Much of the slope is mantled by a veneer of fine-grained Holocene sediment. We inferred that the slope topography is largely relict from late Pleistocene or early Holocene time and that present conditions of geomorphic change are probably quiescent. Subsequently acquired sonographs from a deep-towed sidescan-sonar system having a 5 km swath show such

features as a debris field at the mouth of South Toms Canyon, oddly shaped features on the mid and lower slope suggestive of slump or slide origin, and areas of an enigmatic pattern of downslope-trending "stripes". Most recently, four dives in DSRV ALVIN during July 1981 on the area of Tertiary outcrops of the lower slope revealed 10-m -high talus blocks at the base of the slope, cliffs and steep-walled valleys having as much as 40 m relief, control of cliff surfaces and the shapes of valleys by sets of joints, occurrences of elastic dikes, and sets of parallel, $4\text{- to }12\text{-m}$ -deep furrows (probably erosional) spaced $20\text{-}50\text{ m}$ apart in Eocene calcareous claystone at the mouth of Berkeley Canyon. In some places, the smaller scale topography of the lower slope appears fresh; some planar surfaces are unboored by organisms or scoured, and some of the talus fragments on the upper rise appear to be recent. However, a thin cover of fine-grained flocculent sediment on horizontal surfaces implies that present-day activity is either not vigorous or is intermittent. Nevertheless, canyons and valley talwegs should probably be viewed with caution if considered for structure sites.

Geomorphology and sediment stability of a segment of the U.S. Continental Slope off New Jersey

Robb, J. M., Hampson, J. C., Jr., and Twichell, D. C., 1981, *Science*, v. 211, p. 935-937.

The morphology of complex deposits of Pleistocene sediments covering the upper continental slope between Lindenkohl Canyon and South Toms Canyon results from both depositional and erosional processes. Small slump or slide

features were detected primarily on the flanks of canyons or valleys and were observed to occur only within Pleistocene-aged sediments. Eocene to Miocene sediments are exposed over much of the mid- and lower slope in this area.

Furrowed outcrops of Eocene chalk on the lower continental slope offshore New Jersey

Robb, J. M., Kirby, J. R., Hampson, J. C., Jr., Gibson, P. R., and Hecker, Barbara, 1983, *Geology*, v. 11, no. , p. 182-186.

A sea bottom of middle Eocene calcareous claystone cut by downslope-trending furrows was observed during an *Alvin* dive to the mouth of Berkeley Canyon on the continental slope off New Jersey. The furrows are $10\text{ to }50\text{ m}$ apart, $4\text{ to }13\text{ m}$ deep, linear, and nearly parallel in water depths of $2,000\text{ m}$. They have steep walls and flat floors $3\text{ to }5\text{ m}$ wide, of fine-grained sediment. Mid-range sidescan-sonar images show that similarly furrowed surfaces are found

on nearby areas of the lower continental slope, not associated with canyons. The furrows are overlain in places by Pleistocene sediments. Although they show evidence of erosional origin, they do not appear to be related to observed structures, and their straight, parallel pattern is not well understood. A general cover of flocculent unconsolidated sediments implies that bottom-current erosion is not active now.

Bedform climbing in theory and nature

Rubin, D. M., and Hunter, R. E., 1982, *Sedimentology*, v. 29, p. 121-138.

When bedforms migrate during deposition, they move upward (climb) with respect to the generalized sediment surface. Sediment deposited on each lee slope and not eroded during the passage of a following trough is left behind as a cross-stratified bed. Because sediment is thus transferred from bedforms to underlying strata, bedforms must decrease in cross-sectional area or in number, or both, unless sediment lost from bedforms during deposition is replaced with sediment transported from outside the depositional area. Where sediment is transported solely by downcurrent migration of two-dimensional bedforms, the mean thickness of cross-stratified beds is equal to the decrease in bedform

cross-sectional area divided by the migration distance over which that size decrease occurs; where bedforms migrate more than one spacing while depositing cross-strata, bed thickness is only a fraction of bedform height.

Equations that describe this depositional process explain the downcurrent decrease in size of tidal sand waves in St. Andrew Bay, Florida, and the downwind decrease in size of transverse aeolian dunes on the Oregon coast. Using the same concepts, dunes that deposited the Navajo, De Chelly, and Entrada Sandstones are calculated to have had mean heights between several tens and several hundreds of metres.

Sea-floor-mounted rotating side-scan sonar for making time-lapse sonographs

Rubin, D. M., McCulloch, D. S., and Hill, H. R., 1983, *Continental Shelf Research*, v. 1, no. 3, p. 295-301.

A rotating side-scan sonar system was designed to make time-lapse sonographs of a circular area of the sea floor. To construct the system, the transducers of a commercial side-scan system (frequency 105 kHz; pulse length 0.1 ms; horizontal beam width 1°; vertical beam width 20°; beam depressed 10° with respect to horizontal) were mounted 2 m above the sea floor on a vertical shaft that had a rotation speed of 0.5 rpm.

The radially collected sonar images are recorded linearly on a standard side-scan recorder. To convert the linear record to a radial record, the original moving record is photographed through a slit by a rotating camera, exposing a circular image on film.

Records that are collected with this system offer several advantages over records that are collected with towed systems. Bottom features are presented in nearly true plan geometry, and transducer yaw, pitch, and roll are eliminated. Most importantly, repeated observations can be made from a single point, and bedform movements of 50 cm can be measured. In quiet seas the maximum useful range of the system varies from 30 m (for mapping ripples) to 200 m (for mapping 10-m wavelength sand waves to 450 m or more (for mapping gravel patches).

Geotechnical analyses of submarine landslides in glacial marine sediment, northeast Gulf of Alaska

Schwab, W. C., and Lee, H. J., in Molnia, B. F., ed., *Glacial-marine sedimentation*, New York, Plenum Press, p. 145-184.

Glaciation is the most important process contributing sediment to the northeast Gulf of Alaska. Large sediment failures within the Holocene glacial-marine sediment of the continental shelf have been identified on slopes as gentle as 0.5°. The major offshore processes responsible for sediment failure in the Gulf of Alaska are earthquake and storm wave loading coupled with cyclic shear strength degradation. A normalized soil parameter (NSP) approach can yield shear strength parameters that are somewhat independent of coring disturbance by normalizing these parameters by appropriate consolidation stresses. The NSP approach also appears capable of aiding in the extrapolation of surficial sediment properties to the subsurface. Laboratory tests using the NSP approach, supplemented with in-place vane shear data, reveal

that for these glacial-marine sediments, clayey silt with a natural water content between 35% and 45% is most susceptible to cyclic loading. Cores that contain more of this susceptible clayey silt roughly correlate with locations of sediment failure features. A simplified analysis shows that in water depths shallower than 35 m, maximum storm waves would produce shearing stresses greater than stresses induced by maximum earthquakes. In deeper water, earthquakes would produce greater stresses. Differences in failure morphology are difficult to relate to advanced geotechnical parameters but likely relate to observed variations in plasticity, slope angle, water depth, or variations in consolidation state.

Evolution of a classic sand ridge field: Maryland sector, North American inner shelf

Swift, D. J. P., and Field, M. E., 1981, *Sedimentology*, v. 28, p. 461-482.

The ridge and swale topography of the Middle Atlantic Bight is best developed on the Delaware-Maryland inner shelf. Here sand ridges can be seen in all stages of formation. Several aspects of the ridge field are pertinent to the problem of ridge genesis. The first is ridge morphology. There is a systematic morphologic change from shoreface ridges through nearshore ridges to offshore ridges, which reflects the changing hydraulic regime. As successively more seaward ridges are examined, maximum side slope decreases, the ratio of maximum seaward slope to maximum landward slope decreases, and the cross-sectional area increases.

These changes in ridge morphology with depth and distance from shore appear to be equivalent to the morphologic changes experienced by a single ridge during the course of the Holocene transgression.

A second aspect is the change in bottom sediment characteristics that accompanies these large-scale morphologic changes. Megaripples, sand waves and mud lenses appear in the troughs between nearshore and offshore ridges. These changes indicate that the storm flows which maintain ridges are less frequently experienced in the deeper sector, and that the role of high frequency wave surge

becomes less important relative to the role of the mean flow component in shaping the sea-floor.

A third aspect is the systematic relationship of grain size to topography. Grain size is 90° out of phase with topography, so that the coarsest sand lies between the axis of the landward trough and the ridge crest, while the finest sand lies between the ridge crest and the axis of the seaward trough. This relationship is characteristic of large-scale bedforms.

Finally, flow was measured and transport calculated on the same ridge during a one-month period (November 1976). Threshold was exceeded only during storm events. Mean transport was southerly and a little seaward with respect to both the ridge crest and the shoreline. These flow measurements are in conformity with the pattern of smaller

bedforms. A 43-year time series of bathymetric change for this ridge reveals a systematic pattern of landward flank erosion, seaward flank deposition, and seaward crest migration.

Sand ridges are considered the consequence of constructive feedback between an initial topography and the resulting distribution of bottom shear stress. The relationship between grain size and topography supports this model, but does not account directly for the oblique angle of the ridge with respect to the coastline. This feature may be due to a more rapid alongshore migration rate of the inshore edge of the ridge than the offshore edge, and the relationship between this migration rate, and the rate of shoreface retreat.

Bedform distribution and inferred sand transport on Georges Bank, United States Atlantic continental shelf

Twichell, D. C., 1983, *Sedimentology*, v. 30, p. 695-710.

Four bedform provinces have been identified on Georges Bank using sidescan-sonar and echo-sounding techniques: large sand waves superimpose on sand ridges, small sand waves, megaripples, and featureless seafloor. The large sand waves and sand ridges are found on the bank crest where surface tidal currents are strongest. Areas of small sand waves and megaripples, formed where tidal currents are moderate in strength, border the area of large sand waves to the north and south. Featureless seafloor is found farthest from the bank crest where surface tidal currents are weakest.

Sand-wave asymmetry and surface-sediment texture have been used to infer bedload transport paths on Georges Bank. In the large sand-wave area, bedforms indicate a clockwise transport around each of the linear north-west-

striking sand ridges with slight convergence of the sand waves on the ridge crests. This transport pattern implies erosion from the troughs and accumulation on the sand ridges. The asymmetry of the small sand waves along the south side of Georges Bank indicates that sand is also transported southward away from the linear sand ridges on top of the bank. Although the asymmetry of megaripples could not be determined, the occurrence of megaripples between the small sand-wave province and areas of featureless seafloor suggests a decreasing effectiveness of sand transport away from the bank crest. This sand dispersal pattern is further supported by the surface sediments which become progressively finer to the north and SW away from the crest of Georges Bank.

Morphology and processes associated with the accumulation of the fine-grained sediment deposit on the southern New England shelf

Twichell, D. C., McClennen, C. E., and Butman, Bradford, 1981, *Journal of Sedimentary Petrology*, v. 51, no. 1, p. 269-280.

A 13,000 km² area of the southern New England Continental Shelf which is covered by anomalously fine-grained sediment has been surveyed by means of high resolution, seismic-reflection and side-scan sonar techniques to map its morphology and structure, and a near bottom instrument system contributed to understanding present activity of the deposit. Seismic-reflection profiles show that the fine-grained deposit, which is as much as 13 m thick, has accumulated during the last transgression because it rests on a reflector that is geomorphically similar to and continuous with the Holocene transgressive sand sheet still exposed on the shelf to the west. The ridge and swale topography comprising the sand sheet on the shelf off New Jersey and Long Island are relict in origin as these same features are

found buried under the fine sediment deposit. Southwestward migrating megaripples observed on the sonographs in the eastern part of the deposit are evidence that sediment is still actively accumulating in this area. In the western part of the deposit, where surface sediment is composed of silt plus clay, evidence of present sediment mobility consists of changes in the near-bottom, suspended-matter concentrations primarily associated with storms. Nantucket Shoals and Georges Bank are thought to be the sources for the fine-textured sediment. Storms and strong tidal currents in these shoal areas may still erode available fine-grained material, which then is transported westward by the mean drift to the southern New England Shelf, where a comparatively tranquil environment permits deposition of the fine material.

Morphology, distribution, and development of submarine canyons on the United States Atlantic continental slope between Hudson and Baltimore Canyons

Twichell, D. C., and Roberts, D. G., 1982, *Geology*, v. 10, p. 408-412.

The distribution and morphology of submarine canyons off the eastern United States between Hudson and Baltimore Canyons have been mapped by long-range sidescan sonar. In this area canyons are numerous, and their spacing correlates with overall slope gradient; they are absent where the gradient is less than 3°, are 2 to 10 km apart where the gradient is 3° to 5°, and are 1.5 to 4 km apart where the gradient exceeds 6°. Canyons range from straight to sinuous; those

having sinuous axes indent the edge of the continental shelf and appear to be older than those that head on the upper slope and have straighter axes. A difference in canyon age would suggest that canyons are initiated on the continental slope and only with greater age erode headward to indent the shelf. Shallow gullies on the middle and upper slope parts of the canyon walls suggest that submarine erosion has been a major process in a recent phase of canyon development.

Barrier island shorelines: an assessment of their genesis and evolution

Williams, S. J., 1982, Florida Shore and Beach Association, Proceedings, 26th Annual Meeting, p. 188-199.

Barrier beaches comprise nearly 50 percent of the shore along the Atlantic and Gulf coasts and afford protection to wetlands and mainland areas by blocking storm waves and associated surge flooding. In addition to providing natural protection, barrier beaches are also an important recreation resource for half of the United States population, and increasingly are sites for long-term development. Because of increasing use and because most barriers are dynamic features, better understanding is needed of their origins and evolutionary history.

Barriers formed near the borders of Continental Shelf areas some 20,000 years ago when glaciers covered much of the land and sea level was approximately 130 meters below its present level. With climate warming, glacial melting brought sea levels to within several meters of the present level by 5000 years ago. During that time barrier migration by inlet filling and storm overwash processes was a dominant process. In the past 5000 years sea level has risen slowly or oscillated slightly in response to natural warming and cooling cycles of the climate. Widely spaced tide gauge data show a net rise in relative sea level for the past century, but possible

man-induced climate change make reliable predictions for the 21st century uncertain.

In 1980, CERC initiated a research program to increase and refine the basic knowledge about barrier island processes. The program consists of four substudies: (1) A cooperative effort between CERC and NOAA-NOS is underway to compile and publish a series of high quality shoreline change maps that will show and discuss historic movements of shoreline positions. (2) Coring and mapping of several pristine Virginia barrier environments, as well as several southern New Jersey developed barriers are in progress which will yield information on their three-dimensional framework and stratigraphy. (3) Changes in sea level elevation in the past have been primary agents affecting barrier processes. Sea level changes for the recent past are being studied in an attempt to predict likely future changes. (4) Naturally occurring minerals on the seafloor and beaches are being used as tracers to identify sediment sources and sinks on Atlantic barriers. Results from these studies will be used to refine sediment budget calculations for engineering works affecting littoral processes.

FORMATION OF MARINE ENERGY AND MINERAL DEPOSITS

Geothermal system at 21°N, East Pacific Rise: Physical limits on geothermal fluid and role of adiabatic expansion

Bischoff, J. L., 1981, *Science*, v. 208, p. 1465-1467.

Pressure-volume-temperature relations for water at the depth of the magma chamber at 21°N on the East Pacific Rise suggest that the maximum subsurface temperature of the geothermal fluid is about 420°C. Both the chemistry of the discharging fluid and thermal balance considerations indicate that the effective water/rock ratios in the geothermal system are between 7 and 16. Such low ratios preclude

effective metal transport at temperatures below 350°C, but metal solubilization at 400°C and above is effective even at such low ratios. It is proposed that the 420°C fluid ascends essentially adiabatically and in the process expands, cools, and precipitates metal sulfides within the upper few hundred meters of the sea floor and on the sea floor itself.

The aluminosilicate fraction of North Pacific manganese nodules

Bischoff, J. L., Piper, D. Z., and Leong, Kam, 1981, *Geochimica et Cosmochimica Acta*, v. 45, p. 2047-2063.

Nine nodules collected from throughout the deep North Pacific were analyzed for their mineralogy and major-element composition before and after leaching with Chester-Hughes solution. Data indicate that the mineral phillipsite accounts for the major part (75%) of the aluminosilicate fraction of all nodules. It is suggested that formation of

phillipsite takes place on growing nodule surfaces coupled with the oxidation of absorbed manganous ion. All the nodules could be described as ternary mixtures of amorphous iron fraction (Fe-Ti-P), manganese oxide fraction (Mn-Mg-Cu-Ni), and phillipsite fraction (Al-Si-K-Na), these fractions accounting for 96% of the variability of the chemical composition.

Geochemistry and economic potential of massive sulfide deposits from the eastern Pacific Ocean

Bischoff, J. L., Rosenbauer, R. J., Aruseavage, P. J., Baedeker, P. A., and Crock, J. G., in press, *Economic Geology*.

Bulk chemical analyses were performed for major and minor elements using a variety of techniques on a suite of 9 samples of sea floor massive sulfide deposits from 21°N EPR, Juan de Fuca Ridge and Galapagos Rift. Results indicate that deposits at 21°N and Juan de Fuca are very similar despite a geographic separation of 2300 km and are composed primarily of Zn, Fe, and S, with important minor concentrations of Ag, As, Cd and Ge. The Galapagos Rift massive sulfide is primarily Fe, Cu and S and with important minor contents of only Co and Mo. Au is low, ranging from below detection up to 0.17 ppm. Pt group metals are very low, and average about 0.001 ppm. Consideration of enrichment factors and relative metal abundance suggests that MORB is

a sufficient source for all the metals enriched in the sea floor deposits.

The economically important metals for the 21°N and Juan de Fuca deposits are primarily Zn and Ag (97%), with potential by-products of Cu, Cd and possibly, Ge. For the Galapagos Rift, the primary value is with Cu (86%) with potential by-products of Co and Mo. The Galapagos Rift deposit is similar to, but contains about twice the Cu content, of typical ore from the Skouriotisa mine of the Troodos complex of Cyprus. The grade of the 21°N/Juan de Fuca deposits is 4 times greater than that of the Galapagos Rift and about twice that of prime deep-sea manganese nodules.

Marine gas hydrates—II: Geophysical evidence

Dillon, W. P., and Paull, C. K., 1983, in Cox, J. L., *Natural gas hydrates: properties, occurrences, and recovery*: Boston, Mass., Butterworth Publishers, p. 73-90.

Hydrates of natural gases occur in marine sediments to depths of several hundreds of meters below the sea floor. The base of the layer in which the hydrates are stable occurs at a phase boundary that is dominantly influenced by the downward increase of temperatures. Because the temperature gradient is fairly constant within a small geographic area, the depth of gas hydrate instability is also quite constant. The base of the gas hydrate layer can be observed in seismic reflection profiles in which echoes from sound-reflecting layers are used to study subbottom geological structures. Echoes are observed from the base of the gas hydrate-cemented surface layer because gas hydrate cemen-

tation significantly increases the sound velocity of the sediments. The attendant drop in velocity at the base of the gas hydrate-cemented section generates reflection of sound. Gas hydrate reflections, known as bottom-simulating reflectors (BSR's), have been observed widely in continental margin sediments where enough gas is present to allow formation of the hydrate. The BSR is especially well developed off South Carolina in the Blake Ridge. The gas hydrates may not represent sources of gas themselves, at least in the immediate future. However, they may create seals beneath which free gas could be trapped, and some of our studies of seismic signatures and velocities seem to present evidence for this.

Observations on Cretaceous abyssal hills in the northeast Pacific

Eittrheim, S. L., Piper, D. Z., Chezar, Henry, Jones, D. R., and Kaneps, A., in press, *Marine Geology*.

An abyssal hills area of 50 km x 60 km in the northeast Pacific was studied using bottom transponder navigation, closely spaced survey lines, and long-traverse oblique photography. The block-faulted north-south hills are bounded by scarps, commonly with 40° slopes. On these steep scarps sedimentation is inhibited and pillow basalts often crop out. An ash layer of high acoustic reflectivity at about 7 m sub-bottom depth blankets the area. This ash occurs in multiple beds altered to phillipsite and is highly consolidated. A 24 m.y. age for the ash is based on ichthyolith dates from

samples in the overlying sediments. Acoustically transparent Neogene sediments above the ash are thickest in trough bottoms and are absent or thin on steep slopes. These Neogene sediments are composed of pale-brown pelagic clays of illite, quartz, smectite, chlorite, and kaolinite. Dark-brown pelagic clays, rich in smectite and amorphous iron oxides, underlie the Neogene surficial sediments. Manganese nodules cover the bottom in varying percentages. The nodules are most abundant near basement outcrops and where the sub-bottom ash layer is absent.

Organic geochemistry in the Deep Sea Drilling Project

Kvenvolden, K. A., 1981, in Warne, J. E., Douglas, R. G., and Winterer, E. L., eds., *The Deep Sea Drilling Project: a decade of progress: Society of Economic Paleontologists and Mineralogists Special Publication No. 32*, p. 227-249.

Since the beginning of the Deep Sea Drilling Project (DSDP) in 1968 and extending through 1975, organic geochemical studies have been undertaken on about 2300 samples recovered on Legs 1 through 44 from sediments beneath the ocean floors. These studies have provided fundamental information regarding the distribution of carbon in oceanic sediments and have yielded a better understanding of the processes that alter and transform organic matter in the marine environment.

Beginning with Leg 38 organic geochemists have been included as members of the scientific staffs of those legs of particular organic geochemical interest. They have advised operations personnel on matters concerning potential hazards, such as drilling into significant accumulations of oil and gas, and have collected samples for the scientific community. The shipboard organic geochemical laboratory is equipped with sophisticated instrumentation to provide those measurements helpful in advising the drilling operation.

Since Leg 15, samples for organic geochemical studies have been maintained at -18°C at the DSDP sample repository at the Scripps Institution of Oceanography, La Jolla, California. Samples are distributed to the scientific commu-

nity, but at least one quarter of all cores is retained for possible future studies.

Organic geochemical studies generally relate to one of these topic areas: (1) petroleum potential/source rock evaluation, (2) thermal history and gradients, (3) diagenesis, (4) gas hydrates, (5) novel geochemical fossils, (6) sources of organic materials, (7) paleo-depositional environments, and (8) geochronology.

Much of the organic geochemical work on hydrocarbons and kerogen has been directed to the potential of sediments as sources of petroleum. The organic matter found thus far during drilling is dominantly of terrestrial origin and thermally immature, but much of the organic matter could be a potential source of petroleum (mainly gas) if buried more deeply.

Three new technologies will help advance organic geochemical knowledge of ocean sediments: (1) pressure core barrel for evaluation of gas hydrates, (2) hydraulic piston core to study in detail sources and early diagenesis of organic matter, and (3) riser for the study of late diagenesis and catagenesis.

Hydrates of natural gas in continental margins

Kvenvolden, K. A., and Barnard, L. A., 1983, in Watkins, J. S., and Drake, C. L., eds., *Studies in continental margin geology: American Association of Petroleum Geologists Memoir 34*, p. 631-640.

Natural gas hydrates in continental margin sediment can be inferred from the widespread occurrence of an anomalous seismic reflector which coincides with the predicted transition boundary at the base of the gas hydrate zone. Direct evidence of gas hydrates is provided by visual observations of sediments from the landward wall of the Mid-America Trench off Mexico and Guatemala, from the Blake Outer Ridge off the southeastern United States, and from the Black Sea in the U.S.S.R. Where solid gas hydrates have been sampled, the gas is composed mainly of methane accompanied by CO₂ and low concentrations of ethane and hydrocarbons of higher molecular weight. The molecular and isotopic composition of hydrocarbons indicates that most of the methane is

of biological origin. The gas was probably produced by the bacterial alteration of organic matter buried in the sediment. Organic carbon contents of the sediment containing sampled gas hydrates are higher than the average organic carbon content of marine sediments. The main economic importance of gas hydrates may reside in their ability to serve as a cap under which free gas can collect. To be producible, however, such trapped gas must occur in porous and permeable reservoirs. Although gas hydrates are common along continental margins, the degree to which they are associated with significant reservoirs remains to be investigated.

Geochemistry of natural-gas hydrates in oceanic sediment

Kvenvolden, K. A., Barnard, L. A., Brooks, J. M., and Wiesenburg, D. A., 1983, in Bjory, M., and others, eds., *Advances in organic geochemistry, 1981: New York, John Wiley and Sons, Ltd.*, p. 422-430.

The occurrence of natural-gas hydrates in oceanic sediment has been indicated by both geophysical and geochemical evidence. The geophysical evidence consists mainly

of the appearance of a seismic reflection that mimics the bathymetry of the sea floor, commonly follows a predictable pressure-temperature surface, and lies between 100 and 1100

m below the bottom at water depths that usually exceed 500 m. This bottom-simulating reflector, which may mark the base of the zone of gas hydrates, has been observed in outer continental margins in all of the major oceans. The geochemical evidence for gas hydrates in oceanic sediment comes principally from Deep Sea Drilling Project Legs 66 (Mid-America Trench off southern Mexico), 67 (Mid-America Trench off Guatemala), and, particularly, 76 (Blake Ridge off southeastern United States). Cores recovered at sites on these three legs contained frothing sediment with ice-like properties that released mainly methane and small amounts (less than 1 per cent) of ethane and hydrocarbon gases of higher molecular weight, and carbon dioxide. Large methane to ethane ratios indicate that the methane is dominantly biogenic and not thermogenic. At one site on Leg 76 the carbon-isotopic contents of methane range from -88 to -67 permil relative to the Peedee belemnite standard (PDB); such values support the contention that the methane is biogenic.

Thermogenic hydrocarbons in unconsolidated sediment of Eel River basin, offshore northern California

Kvenvolden, K. A., and Field, M. E., 1981, American Association of Petroleum Geologists Bulletin, v. 65, no. 9, p. 1642-1646.

Thermally produced hydrocarbons were recovered from unconsolidated sediment ponded within a bathymetric depression on the surface of a shale diapir in the offshore Eel River Basin of northern California. Evidence that the hydrocarbons are thermogenic consists of the following: (1) very high concentrations of hydrocarbon gases, particularly ethane through butanes (C_2-C_4); (2) methane having a carbon isotopic composition (relative to the PDB standard) of -43 and -44 per mil; (3) presence of gasoline-range (C_{5+}) hydrocar-

Experiments conducted on Leg 76 confirmed the presence of marine gas hydrates. The molecular distribution of hydrocarbon gases in the decomposition products of one sediment sample that appeared to contain gas hydrates suggested that gas hydrates of Structure I and some Structure II had been formed. Methane, ethane, propane, and isobutane were present in measurable quantities, but *n*-butane and higher molecular weight hydrocarbon gases that cannot fit inside either of the gas hydrate structures were present only in trace amounts. The volume of gas released during decomposition of the sample was about twenty times the volume of pore fluid and indicated that gas hydrate was present because more gas was present than could be dissolved in the pore fluid. These observations also suggest the gas-hydrate structures are only partially filled. Finally, experiments on cores obtained with a pressure-core barrel showed that during degassing at constant temperature the pressure release followed a pattern tentatively suggestive of gas hydrates.

bons; and (4) presence of a complex mixture of heavy hydrocarbons (C_{15+}) with *n*-alkanes having a petroleumlike distribution. This mixture of gaseous and liquid hydrocarbons likely originated deep within the basin and migrated to the surface through fractures and faults developed during the emplacement of the diapir. The presence of thermogenic hydrocarbons in unconsolidated surface sediment indicates that conditions for petroleum generation have existed within this offshore basin.

Manganese-phosphorite deposits of the Blake Plateau

Manheim, F. T., Popenoe, Peter, Siapno, W., and Lane, C., 1982, in Halbach, P., and Winter, P., eds., Marine mineral deposits: New research results and economic prospects: Essen, Verlag Gluckauf GmbH, Band 6, p. 9-44.

The Blake Plateau is a submarine extension of the middle Atlantic segment of the North American continent, extending from Florida to South Carolina (Fig. 1). It is bounded by the continental shelf, and the continental slope, including the Blake Spur and its associated steep escarpment. It narrows northward to the Cape Hatteras region, and southward toward the Florida Straits and Bahama Islands Platform. Much of the Plateau is swept by the Gulf Stream. As will be discussed later, this phenomenon is critical for the development of significant phosphorite and ferromanganese oxide deposits in the area.

Ferromanganese nodules and slabs were first reported in 1885 by Sir John Murray in dredgings from the Coast Survey steamer Blake (Bartlett, 1883). Subsequent development of knowledge of hard mineral resources on the Blake Plateau is summarized by Manheim et al (1980) in a paper

principally directed to the phosphorite deposits on the Blake Plateau. The Blake Plateau superficially resembles certain other ocean plateau areas, Chatham Rise (Cullen, 1978), the Campbell Plateau off New Zealand (Summerhayes, 1967), the Agulhas Bank (Summerhayes, 1973), and the Manihiki Plateau in the South Central Pacific (Heezen, et al, 1966; Baturin, 1979). All of these plateaus have been reported to contain phosphorite substrates, and some, such as the Manihiki Plateau and Agulhas Bank also demonstrate development of manganese crusts. Smaller mini plateau formations around Florida are the Miami and Pourtales Terraces (Gorsline and Milligan, 1963; Gomberg, 1976; Mullins and Neumann, 1979; and W. S. Burnett, oral communication). The latter two sites also have phosphorites and relatively minor manganese crust formations.

Active hydrothermal vents and sulfide deposits on the southern Juan de Fuca ridge

Normark, W. R., Morton, J. I., Koski, R. A., Clague, D. A., and Delaney, J. R., 1983, Geology, v. 11, p. 158-163.

Massive-sulfide deposits rich in zinc and silver were recovered from the Juan de Fuca Ridge 500 km west of Oregon in September 1981. The samples recovered are composed largely of zinc sulfide, with lesser amounts of iron, lead, and copper sulfide. Most of the deposits occur at a series of hydrothermal vents within a relatively continuous depression in the center of a smooth 1 km wide valley along

the ridge axis. The depression appears to be formed by collapse of a lava lake possibly modified by extensional faulting. The axial valley floor outside the depression is underlain by fresh, glassy, ferrobasalt sheet and lobate flows. Two types of sulfide-mineral deposits were dredged from one of the hydrothermal vents: (1) angular slabs of dark-gray zinc sulfide; and (2) subrounded fragments of

porous light-gray zinc sulfide. The samples contain fresh sphalerite, zoned wurtzite, pyrite, and minor amounts of marcasite, galena, and chalcopyrite-cubanite. The spreading rate of the Juan de Fuca Ridge and the composition of the

sulfide samples are generally similar to the East Pacific Rise lat 21°N site; however, the texture and geologic setting of the sulfide deposits are significantly different.

OTHER

LORAN-C latitude-longitude conversion at sea: programming considerations

McCullough, J. R., Irwin, B. J., and Bowles, R. M., 1982, Wild Goose Association, Proceedings of Eleventh Technical Symposium, October 1982, p. 42-75.

To aid programmers of LORAN-C latitude-longitude conversion, we:

1. Provide reference to the literature.
2. Compare digital "processings-noise" for several arc-length methods.
3. Discuss some practical aspects of overland signal propagation (ASF) modeling for offshore navigation.

Comparisons are made of the precision of arc-length routines as computer precision is reduced. Overland propagation delays (ASF's) are discussed and illustrated with observations from offshore New England. Present practice of LORAN-C error budget modeling is then reviewed with the suggestion that additional terms be considered in future modeling. Finally, some detailed numeric examples are provided to help with new computer program checkout.

